Mode of Action and Resistance Mechanism of Griselimycin

Dissertation

zur Erlangung des Grades

des Doktors der Naturwissenschaften

der Naturwissenschaftlich-Technischen Fakultät III

Chemie, Pharmazie, Bio- und Werkstoffwissenschaften

der Universität des Saarlandes

von

Angela Kling

Saarbrücken

2015

Tag des Kolloquiums:	27.01.2016
Dekan:	Prof. Dr.-Ing. Dirk Bähre
1. Berichterstatter:	Prof. Dr. Rolf Müller
2. Berichterstatter:	Prof. Dr. Manfred J. Schmitt
Vorsitz:	Prof. Dr. Andriy Luzhetskyy
Akad. Mitarbeiter:	Dr. Jens Neunzig

Diese Arbeit entstand unter Anleitung von Prof. Dr. Rolf Müller in der Fachrichtung 8.2 Pharmazeutische Biotechnologie der Naturwissenschaftlich-Technischen Fakultät III der Universität des Saarlandes von Oktober 2011 bis Oktober 2015.

für Stephan

ZUSAMMENFASSUNG

Tuberkulose ist eine weltweit verbreitete Infektionskrankheit, die im Jahr 2013 geschätzte 1.5 Millionen Tote zur Folge hatte. Die Behandlung der Tuberkulose wird zudem durch die Entstehung und Verbreitung von arzneimittelresistenten Erregern (*Mycobacterium tuberculosis*) erschwert.

Griselimycin und Methylgriselimycin sind Naturstoffe, die von Streptomyceten produziert werden und Aktivität gegen arzneimittelresistente *Mycobacterium tuberculosis* zeigen. Cyclohexylgriselimycin ist ein synthetisches Griselimycin-Analogon mit einer Cyclohexyl-Substitution und verbesserten pharmakokinetischen Eigenschaften. In der vorliegenden Studie wurden der Wirkmechanismus und der Resistenzmechanismus von Griselimycinen in Mykobakterien und der Eigenresistenzmechanismus gegen Griselimycine in dem Griselimycin-Produzenten *Streptomyces caelicus* aufgeklärt. Griselimycine wirken bakterizid auf Mykobakterien, indem sie die Bindung der replikativen DNA-Polymerase an die beta Untereinheit der DNA-Polymerase (die sogenannte DNA-Klammer) verhindern und dadurch die DNA Replikation blockieren. Eine Resistenz gegen Griselimycin in Mykobakterien wird durch eine Amplifikation des Target-Proteins vermittelt. Die Resistenz ist jedoch reversibel, erfolgt mit nur geringer Resistenzfrequenz und geht mit einem erheblichen Fitness-Verlust einher. Die Eigenresistenz gegen Griselimycine in *Streptomyces caelicus* wird durch ein zusätzliches Analogon der DNA-Klammer vermittelt, das im Gegensatz zu der konventionellen DNA-Klammer aus *Streptomyces caelicus* Griselimycine mit einer um 3 - 4 Zehnerpotenzen geringeren Affinität bindet.

ABSTRACT

Tuberculosis is a global infectious disease that caused an estimated 1.5 million deaths in 2013. The treatment of tuberculosis is additionally complicated by the emergence and spread of drug-resistant pathogens (*Mycobacterium tuberculosis*).

Griselimycin and methylgriselimycin are natural compounds produced by Streptomycetes which exhibit activity against drug-resistant *Mycobacterium tuberculosis*. Cyclohexylgriselimycin is a synthetic analog of griselimycin that contains a cyclohexyl substitution and exhibits improved pharmacokinetic properties. In the present study the mode of action and the resistance mechanism of griselimycins in mycobacteria and the self-resistance mechanism against griselimycins in the griselimycin producer *Streptomyces caelicus* were elucidated. Griselimycins exhibit bactericidal activity against mycobacteria by inhibiting the interaction of the replicative DNA polymerase with the DNA polymerase beta subunit (the so-called sliding clamp) and thereby blocking the DNA replication. Griselimycin resistance in mycobacteria is mediated by target amplification. However, resistance is reversible and occurs with only low resistance frequency, and is accompanied by a considerable fitness loss. The self-resistance against griselimycins in *Streptomyces caelicus* is mediated by an additional analog of the sliding clamp, which in contrast to the conventional sliding clamp of *Streptomyces caelicus* binds griselimycins with a 3 – 4 orders of magnitude lower affinity.

TABLE OF CONTENTS

1 INTRODUCTION

1.1 TUBERCULOSIS

Tuberculosis (TB) is caused by a set of closely related mycobacteria that belong to the *Mycobacterium tuberculosis* complex (MTBC). The MTBC includes the human-associated pathogens *M. tuberculosis* and *M. africanum* and several animal-infecting mycobacteria (*M. bovis*, *M. microti*, *M. pinnipedii* and *M. caprae*).[1,2] Apart from the MTBC, there are two other categories of pathogenic mycobacteria. These are *M. leprae*, the causative agent of leprosy, and the nontuberculous mycobacteria (NTM) (also called mycobacteria other than tuberculosis (MOTT), atypical mycobacteria or environmental mycobacteria) such as *M. abscessus, M. intracellulare*, *M. avium, M. ulcerans* or *M. kansasii*. The NTM can also cause mycobacterioses in humans, but mostly in patients with immunodeficiency or other predisposing conditions (e.g. chronic pulmonary diseases).[3]

TB is an infectious disease that typically affects the lungs (pulmonary TB) but can also attack other sites (extrapulmonary TB), including larynx, lymph nodes, pleura, brain, kidneys, bones or joints. TB is transmitted through the air by persons who have active pulmonary or laryngeal TB. Infection occurs after inhalation of tubercle bacilli that reach the alveoli of the lungs (Figure 1-1). These bacilli are ingested by alveolar macrophages where most of them are eradicated. However, *M. tuberculosis* is an intracellular pathogen with the ability to persist in the early phagosomal compartment and thereby evade the immune system. Thus, the microbes can exist in the host without causing apparent symptoms (latent TB infection). In healthy people infection with tubercle bacilli often causes no symptoms, but regrowth of the bacilli or insufficient control of the bacilli by the immune system can lead to disease outbreak (active TB disease). Symptoms of active TB include weight loss, cough, fever and bloody mucus.[4,5,6]

The causative agent and the infectious nature of TB were demonstrated in the 19th century by Robert Koch and Jean-Antoine Villemin, respectively. In the mid 19th century sanatoria for the isolation of TB patients were established and patients were treated by extended bed rest and improved nutrition. In the late 19th and early 20th centuries surgical procedures were widely used for TB treatment. In 1921, the vaccine called Bacillus Calmette-Guerin (BCG) was introduced. In 1943, chemotherapy of TB was initiated with the discovery of streptomycin. In the following years other antituberculotic drugs were introduced, such as

para-aminosalicylic acid (1949), isoniazid (1952), pyrazinamide (1954), cycloserine (1955), ethambutol (1962) and rifampicin (1963). Monotherapy with streptomycin caused remarkable reduction in patient mortality, but also led to frequent emergence of resistant mutants. The observation that the combined administration of streptomycin with isoniazid or *para*-aminosalicylic acid reduced the incidence of resistance was the basis of the current drug combination regimen for the treatment of TB.[7,8]

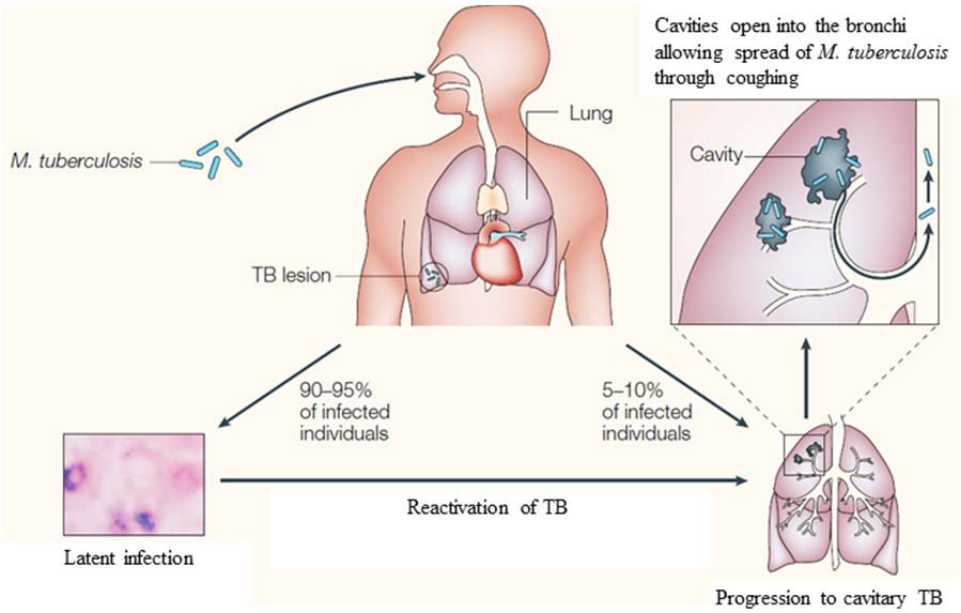

Figure 1-1: TB is spread by aerosols and an infection can be established with or without a visible primary lesion anywhere in the lungs. In 90 - 95 % of the individuals the infection remains latent but the bacilli can be reactivated when an individual is immunosuppressed. In 5 -10 % of the individuals there is a progressive disease development. Pulmonary cavities and extracellular growth of *M. tuberculosis* in cavities can lead to opening of cavities into the bronchi and spread of TB during coughing (modified from reference 9).

Since in 1993 the world health organization (WHO) declared TB as a global public health emergency, the global TB disease burden is slowly declining through effective diagnosis and treatment. The TB incidence rate fell at an average of 1.5 % per year between 2000 and 2013. Since 1990 the TB mortality and prevalence rates fell by 45 % and 41 %, respectively (Figure 1-2). However, the death toll is still high and TB is the second most common cause of death from an infectious disease worldwide (after the human immunodeficiency virus, HIV). Globally, an estimated 9 million people developed TB in 2013 and 1.5 million people died from this disease (including 360,000 HIV-positive TB cases). The proportion of incident TB cases varies widely among countries and ranges from 56 % and 29 % in Asia and the African region, respectively, to 4 % in the European region.[4,10]

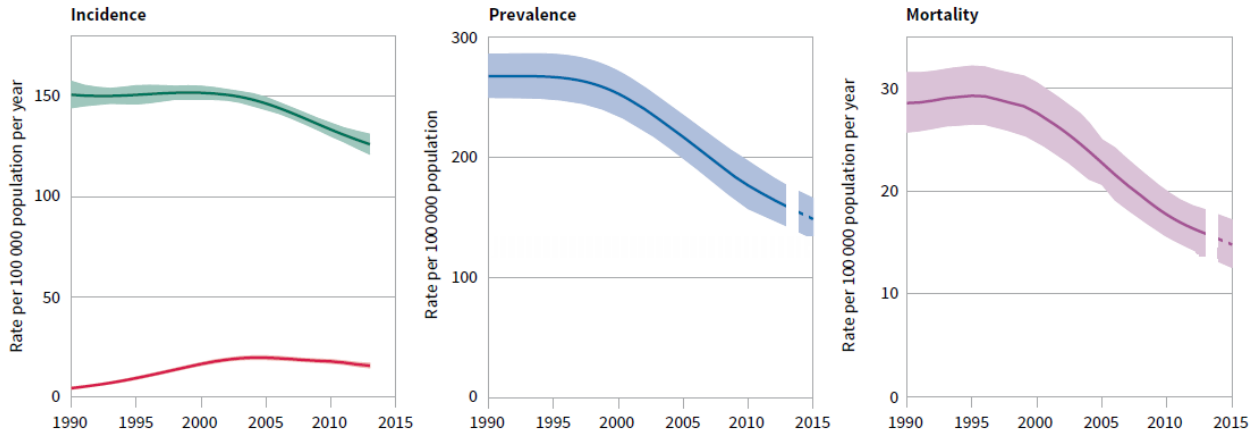

Figure 1-2: TB incidence, prevalence and mortality from 1990 to 2013. Incidence: number of new and relapse cases per year, prevalence: number of cases at a given timepoint, mortality: number of deaths per year. Left: Global trend in estimated TB incidence rate (green: TB incidences including HIV-positive TB cases, red: incidences of HIV-positive TB). Centre and right: Global trends in estimated TB prevalence and mortality (excluding HIV positive cases) rates 1990 - 2013 with forecast rates 2014 - 2015. Shaded areas indicate uncertainty bands (modified from reference 10).

Control of TB is further complicated by drug-resistant TB (DR-TB). Drug-resistant TB can result from transmission of drug resistant organisms (primary DR-TB) or can be acquired during TB treatment (secondary DR-TB). Multidrug-resistant TB (MDR-TB) is caused by *M. tuberculosis* with resistance to the most effective first-line anti-TB drugs isoniazid and rifampicin. Extensively drug resistant TB (XDR-TB) is caused by *M. tuberculosis* with resistance to the first-line drugs isoniazid and rifampicin plus resistance to any fluoroquinolone and a second-line injectable drug (Table 1-1). Moreover, totally drug resistant TB (TDR-TB) with resistance to all tested drugs was reported from four different countries.[11] Since 2009 an increase in the number of notified cases of MDR-TB has been evident. In 2013, an estimated 3.5 % new and 20.5 % previously treated TB cases worldwide were MDR-TB. An estimated 9 % of the MDR-TB cases were XDR- TB.[4,10]

Anti-TB drugs are classified into five groups depending on their efficacy, potency, drug class and experience of application (Table 1-1). The first-line anti-TB drugs (group 1 drugs) are currently recommended for the treatment of drug-susceptible TB. The second-line anti-TB drugs (group 2, 3 and 4 drugs) are used for the treatment of drug-resistant TB. Third-line anti-TB drugs (group 5 drugs) are also used for the treatment of drug-resistant TB but have unclear efficacy.[12]

Table 1-1: Classification of anti-TB drugs. Group 2 drugs comprise injectable aminoglycosides (STM, KM, AMK) and injectable polypeptides (CM, VIM). Group 3 drugs comprise oral and injectable fluoroquinolones. Group 4 drugs comprise oral drugs (modified from reference 12).

First-line anti-TB drugs		
Group 1 drugs		
Isoniazid (H, INH)		
Rifampicin (R, RIF)		
Rifapentine (P, RPT)		
Pyrazinamide (Z, PZA)		
Ethambutol (E, EMB)		
Second-line anti TB drugs		
Group 2 drugs	Group 3 drugs	Group 4 drugs
Streptomycin (S, STM)	Ciprofloxacin (CFX)	*para*-aminosalicylic acid (PAS)
Kanamycin (KM)	Levofloxacin (LFX)	Cycloserine (DCS)
Amikacin (AMK)	Moxifloxacin (MFX)	Terizidone (TRD)
Capreomycin (CM)	Ofloxacin (OFX)	Ethionamide (ETH)
Viomycin (VIM)	Gatifloxacin (GFX)	Prothionamide (PTH)
		Thioacetazone (THZ)
Third-line anti TB drugs		
Group 5 drugs		
Clofazimine (CFZ)		
Linezolid (LZD)		
Amoxicillin plus clavulanate (AMX/CLV)		
Imipenem plus cilastatin (IPM/CLN)		
Clarithromycin (CLR)		

The current standard treatment for drug-susceptible TB is a six-months regimen with an intensive phase of RIF, INH, EMB and PZA for 2 months followed by a continuation phase of RIF and INH for 4 months. This regimen is highly efficacious, with cure rates of more than 85 % in HIV-negative patients. However, the long duration and the toxic side effects of the current treatment affect patient compliance, which in turn contributes to the emergence and spread of drug-resistant TB. Treatment of latent TB, which is important to control TB, especially in regions with high HIV prevalence rates, also requires long treatment periods (up to 9 months with INH). Treatment of drug-resistant TB requires longer (at least 20 months) and more expensive treatment with second- and third-line anti-TB drugs and is associated with multiple side-effects and low cure rates. Furthermore, some anti-TB drugs significantly interact with cytochrome (CYP) P450 enzymes that are involved in the metabolism of several antiretroviral agents, which challenges TB therapy for HIV-positive patients. The main goals in the development of new regimens are thus to shorten and simplify the treatment of

drug-sensitive and latent TB infections, to improve efficacy and tolerability of the treatment of drug-resistant TB and to improve treatment of patients co-infected with HIV. The ideal drug thus exhibits a novel mechanism of action and no cross-resistance with current drugs to minimize the probability of pre-existing resistance, no significant CYP P450-mediated drug-drug interactions to allow effective co-administration with antiretroviral agents, a pharmacokinetic profile that supports once daily or less frequent dosing, and an optimal safety and tolerability profile.[10,13]

Currently, there are 7 new or repurposed anti-TB drugs in various stages of clinical development (Figure 1-3). All these drugs except for RPT exert a novel mechanism of action and are active against drug-susceptible and drug-resistant TB. TBA-354 is a drug in phase I of development that belongs to the nitroimidazole class and is developed by the TB Alliance.[14] In phase II there are currently 4 drugs, sutezolid (SZD, PNU-100480), SQ109, RPT and levofloxacin (LFX). SZD belongs to the class of oxazolidinones and is developed by Pfizer.[15] SQ109 belongs to the class of ethylenediamines and is developed by Sequella.[16] RPT is a synthetic rifamycin derivative and is evaluated by Sanofi-Aventis in collaboration with the centers for disease control and prevention (CDC) for the treatment of drug-susceptible TB.[17] LFX is a fluoroquinolone which is currently tested for the best dose for the treatment of MDR-TB by the CDC and the national institute of allergy and infectious diseases (NIAID). Two drugs are in phase III of development, bedaquiline (sirturo, TMC207, R207910) and delamanid (OPC-67683). Bedaquiline belongs to the class of diarylquinolines and is developed by Janssen.[18] Delamanid is a nitro-dihydro-imidazooxazole and is developed by Otsuka Pharmacuetical Co. Ltd. Delamanid and bedaquiline received conditional approval for the treatment of MDR-TB in 2013 as the first novel TB drugs in the last 40 years.[19]

Furthermore, two new TB drug regimens that are composed of repurposed drugs and new chemical entities are in clinical development, whereby the entire regimen and not a single drug is the unit of development. The BPaZ regimen is comprised of bedaquiline (B), pretomanid (Pa, PA-824) and pyrazinamide (Z) and has the potential to cure TB in 3 months. The PaMZ regimen is composed of pretomanid (Pa), moxifloxacine (M) and pyrazinamide (Z) and has the potential to cure drug-susceptible and some forms of drug-resistant TB in 4 months and is compatible with antiretroviral agents. Both regimens are developed by the TB Alliance.[20,21]

Additionally, 15 TB vaccine candidates are currently in clinical trials. For the development of new TB vaccines two approaches have been used: Either the development of vaccines superior to BCG to replace it or the development of a new vaccine that is given to adults to supplement the BCG vaccination given in childhood to prolong protection against TB disease. BCG is a live attenuated strain of *M. bovis* and the vaccination with BCG protects against severe forms of TB in children (meningeal and miliary TB). However, the estimated efficacy of the BCG vaccination in preventing pulmonary TB in adults varies from 0 to 80 % .and is therefore estimated to have a low impact in limiting TB spread. BCG is also not recommended for use in HIV-positive children, due to the risk of disseminated BCG disease. The current vaccine candidates include recombinant BCGs, attenuated *M. tuberculosis* strains, recombinant vector vaccines, protein-adjuvant combinations and mycobacterial extracts which either prevent infection or primary progression to disease.[10,22,23]

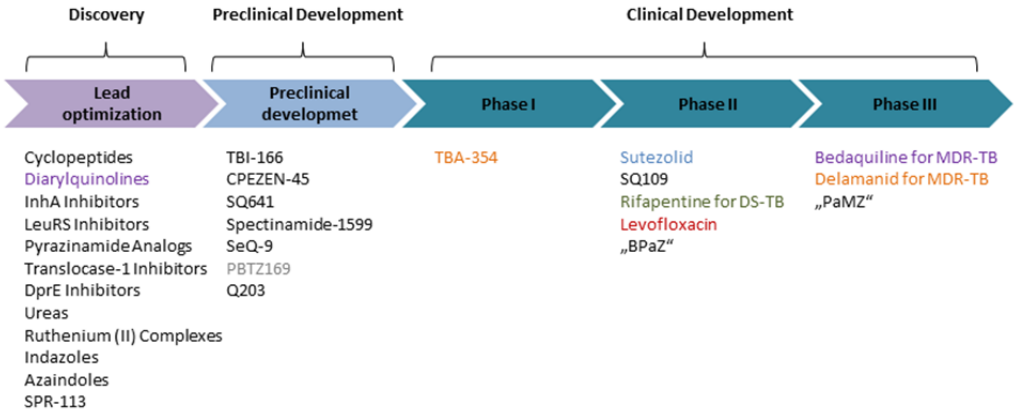

Figure 1-3: Anti-TB agents currently in discovery or development. Chemical classes: fluoroquinolone (red), rifamycin (green), oxazolidinone (blue), nitroimidazole (orange), diarylquinoline (purple), benzothiazinone (grey). “BPaZ”: Regimen consisting of bedaquiline, pretomanid and pyrazinamide, “PaMZ”: Regimen consisting of pretomanid, moxifloxacin and pyrazinamide (modified from the Working Group on New Drugs (WGND) Portfolio website from August 2015, http://www.newtbdrugs.org/pipeline-discovery.php).

1.2 Mechanisims of action of antitubercular drugs

For the treatment of active pulmonary TB, the most common form of TB, drugs must be transported from the blood compartment to pulmonary lesions, enter granulomas and diffuse into the necrotic foci (caseous necrosis) of the tuberculous infection, penetrate and accumulate in immune cells including subcellular organelles such as the phagolysosome, permeate the lipid-rich cell envelope of *M. tuberculosis* and finally reach their molecular target at adequate

concentrations for the required time (Figure 1-4). Additionally, mycobacterial subpopulations in a dormant or persistent state are present. Persister cells are characterized by a nonheritable tolerance to antimicrobial agents. Dormant bacteria (or nonreplicating bacteria) are in a stable but reversible nonreplicating state which is characterized by low metabolic activity and by resistance to antimicrobial agents. Dormant and persister cells underlie latent infections and post-treatment relapses, however, the molecular mechanisms are poorly understood.[24] No single drug currently available can reach and eradicate all mycobacterial subpopulations emphasizing the need for combination therapies.

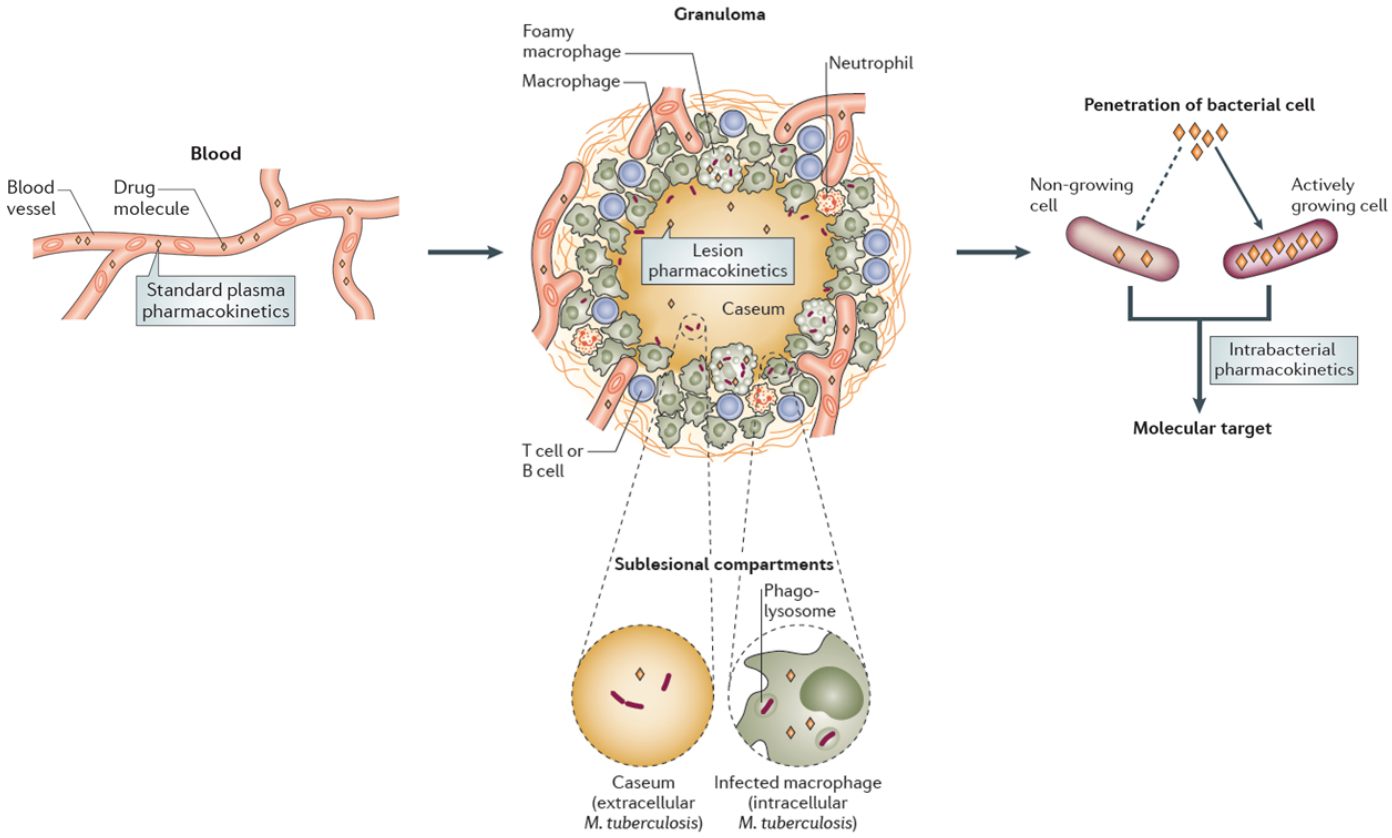

Figure 1-4: To reach their targets anti-TB drugs travel from the blood compartment into the interstitial space of granulomas and then penetrate and accumulate in immune cells, including within subcellular organelles (such as the phagolysosome) where intracellular bacilli can reside. In necrotic granulomas and cavities drugs must diffuse through caseum in the absence of vascularization and active transport system to reach extracellular bacilli. Different lesion compartments can harbor bacterial populations in different metabolic and physiological states (e.g. slowly-replicating or non-replicating bacilli), which can result in alterations in bacterial cell wall structure and transport mechansims which also influence the permeability of the pathogen. Finally, drugs must permeate the pathogen to reach their molecular target (modified from reference 24).

The rational combination of drugs for the treatment of TB can be based on pharmacokinetic and pharmakodynamic factors to achieve complementary activity, with the intention to reach all bacterial subpopulations or an improved effect or duration of action.[25] Drug combinations are pharmacodynamically synergistic, additive or antagonistic, if the effect is greater than, equal to or less than the sum of the effect of the combined drugs.[26] An example is the synergistic effect of erythromycin in combination with penicillin. The effect of erythromycin, which inhibits bacterial protein synthesis, is enhanced by penicillin, which weakens the bacterial cell wall by inhibiting peptidoglycan synthesis and thereby facilitates penetration of erythromycin into bacterial cells. However, the initial drug regimens for the treatment of TB were rather defined by what was available in the mid 20th century and new drugs were then tested with older drugs until the current standard TB treatment was defined. Meanwhile further anti-TB drugs are available for which the pharmacodynamic characteristics and in part also the pharmacokinetic characteristics were described. Therefore, in the following sections the known pharmacodynamic characteristics of the first-, second- and third- line anti-TB drugs and of the new anti-TB drugs (Figure 1-5) currently in clinical phases are described. As described below, these anti-TB drugs are partially synthetically derived and partially natural products or derivatives thereof. About half of the anti-TB drug classes inhibit cell wall synthesis and several others inhibit translation. Additional drug classes act on transcription, trans-translation, DNA synthesis or target the folate pathway or the energy metabolism.

Rifampicin (RIF) and the cyclopentyl derivative **rifapentine (RPT)** belong to the class of rifamycins and are semisynthetic derivatives of rifamycin B (which is produced by *Amycolatopsis rifamycinica*).[27] RPT shows a longer half-life than RIF, which allows less frequent dosing. Rifamycins inhibit RNA synthesis by targeting the DNA-dependent RNA polymerase (RNAP).[28] Thererby, rifamycins bind to the β-subunit of RNAP within the DNA/RNA channel and sterically block the extension of the RNA chain.[29] RIF and RPT are broad-spectrum antibiotics with bactericidal activity and a MIC of 0.1-0.4 and 0.031 μg/mL, respectively, against *M. tuberculosis*.[30] Both are active against intracellular (in human macrophages) and moderately active against dormant *M. tuberculosis*.[31,32,33]

Isoniazid (INH) is a synthetic derivative of isonicotinic acid. INH is a prodrug and is activated by the mycobacterial catalase-peroxidase hemoprotein (KatG), which usually protects against host phagocyte peroxides.[34,35] KatG catalyzes the peroxidation of INH into active INH-NADH (isonicotinic acyl-NADH) adducts. INH-NADH complexes inhibit cell

wall synthesis by targeting the enoyl acyl carrier protein reductase InhA, a component of the fatty acid synthase II system and essential for the synthesis of fatty acids including mycolic acids. Additionally, INH metabolites have been reported to block multiple cellular pathways including nucleic acid synthesis and NAD metabolism.[36,37,38,39] INH is a narrow-spectrum agent that exerts bactericidal activity on fast replicating mycobacteria and bacteriostatic activity on slow growing mycobacteria, and is thus used to treat latent TB. It shows a MIC of 0.025 μg/mL against *M. tuberculosis*.[30] It is also active against intracellular mycobacteria (in human macrophages), but has no activity on dormant mycobacteria.[40]

Pyrazinamide (PZA) is a synthetic analog of nicotinamide and structurally related to INH. PZA is a prodrug and is converted to pyrazinoic acid (POA) by the pyrazinamidase (PZase), which usually converts nicotinamide to nicotinic acid in *M. tuberculosis*. POA is then excreted by a weak efflux pump and converted to the protonated pyrazinoic acid (HPOA) if the extracellular pH is acidic. The uncharged HPOA can permeate the membrane and re-enter the bacilli, explaining the requirement of acidic pH for PZA activity.[41] Fatty acid synthase I has been proposed as a target of PZA on the basis of studies with the derivative 5-Cl-PZA[42], but recent studies have shown that fatty acid synthase I is indeed inhibited by 5-Cl-PZA but not by PZA.[43] Recently, it was reported that PZA inhibits trans-translation (but not canonical translation) of *M. tuberculosis* by targeting the 30S ribosomal protein S1 (RpsA).[44] PZA is a narrow-spectrum agent that exerts bacteriostatic activity, but can show bactericidal activity against replicating *M. tuberculosis*. For PZA MICs between 6-50 μg/mL at pH 5.5 are reported against *M. tuberculosis*.[30,45] PZA is not active on intracellular bacilli[46] but is preferentially active on dormant bacilli, probably due to slow metabolism and efflux of old cells, and is thus effective in therapy shortening and reducing relapse.[47,48]

Ethambutol (EMB) and **SQ109** are synthetic compounds that belong to the class of ethylenediamines.[16] EMB inhibits cell wall synthesis by targeting the arabinosyl transferases A and B, which are homologous enzymes responsible for the polymerization of the arabinan (from arabinose) of the arabinogalactan of the mycobacterial cell wall.[49] Additionally, EMB was shown to block other cellular pathways such as RNA metabolism, mycolic acid transport and phospholipid synthesis.[36] SQ109 inhibits cell wall synthesis by interfering with the incorporation of mycolic acids, most likely by targeting the putative trehalose monomycolate transporter (MmpL3) and preventing translocation of trehalose monomycolate across the membrane.[16] EMB and SQ109 are narrow-spectrum agents with MIC values of 0.5 and 0.35

µg/mL, respectively, against *M. tuberculosis*. EMB exerts bacteriostatic activity against actively growing bacilli and is active against intracellular bacilli (in human macrophages) but not against dormant bacilli.[30,31] SQ109 exerts bactericidal activity, is also active against intracellular bacilli (in murine macrophages) and is assumed to be active on dormant bacilli.[50]

The aminoglycosides **streptomycin (STM)** and **kanamycin (KM)** are natural products produced by *Streptomyces griseus* and *Streptomyces kanamyceticus*, respectively. **Amikacin (AMK)** is a semisynthetic analog of KM. Aminoglycosides inhibit protein biosynthesis by binding the A site of the 16S rRNA in the 30S ribosomal subunit and blocking peptide elongation. Additionally, the interaction between aminoglycosides and 16S rRNA can induce protein mistranslation through incorporation of improper amino acids and lead to incorporation of mistranslated proteins into the membrane and by this to altered membrane permeability and integrity.[51,52] Aminoglycosides are broad-spectrum antibiotics, most of them are bactericidal (STM has no bactericidal activity).[30] The MIC of STM, KM and AMK are 1, 2 and 0.5-1 µg/mL, respectively, against *M. tuberculosis*. Aminoglycosides are poorly active against dormant and intracellular bacilli, this is presumed to depend on the accumulation of aminoglycosides in the lysosomal host cells compartment and pH related inactivation.[53,54]

The tuberactinomycins **viomycin (VIM)** and **capreomycin (CM)** are cyclic peptides produced by *Streptomyces vinaceus* and *Streptomyces capreolus*, respectively.[55,56] Tuberactinomycins inhibit protein synthesis by binding to the ribosome between the 16S rRNA of the 30S ribosomal subunit and the 23S rRNA of the 50S ribosomal subunits, thereby stabilizing the peptidyl-tRNA at the ribosome and blocking ribosome translocation during peptide elongation.[57] CM and VIM are broad-spectrum antibiotics that exert bactericidal activity with a MIC of 2 and 2-4 µg/mL, respectively, against *M. tuberculosis*. CM is active against dormant but poorly active against intracellular bacilli.[40,58,110]

The fluoroquinolones **ciprofloxacin (CPX)**, **levofloxacin (LFX)**, **moxifloxacin (MFX)**, **ofloxacin (OFX)** and **gatifloxacin (GFX)** are synthetic derivatives of nalidixic acid (a byproduct of the synthesis of quinine, a natural compound of cinchona tree).[59,60] Fluoroquinolones inhibit DNA synthesis by forming drug-enzyme-DNA complexes (by intercalating into the DNA at nicks introduced by topoisomerases) and interact with topoisomerase II (gyrase) or topoisomerase IV subunits (in *M. tuberculosis* there is no evidence for topoisomerase IV homologs).[61,62] This traps the topoisomerases on the cleaved

DNA, prevents strand rejoining and induces DNA double-strand breaks and stalled replication forks.[52] Additionally, the DNA damage induces the bacterial stress response (SOS response). Fluoroquinolones are broad-spectrum agents, exert bactericidal activity and are active against dormant bacteria.[30,63] The MICs of CFX, LFX, MFX, OFX and GFX against *M. tuberculosis* are 0.5, 0.35, 0.177, 0.71 and 0.125 µg/mL, respectively.[30] MFX, OFX, GFX and LFX show moderate activity against intracellular (in murine or human macrophages) bacilli, CFX shows no activity on intracellular bacilli due to mammalian cell efflux.[64,65]

***Para*-aminosalicylic acid (PAS)** is a synthetic analog of salicylic acid (naturally produced in willow tree).[66] PAS inhibits the folate pathway that generates tetrahydrofolate (THF), which leads to THF depletion and growth arrest.[67] THF is involved in the amino acid and nucleic acid metabolism, including the synthesis of formylmethionyl tRNA, which is responsible for protein synthesis initiation. PAS acts as a prodrug, it is a substrate analog of the folate precursor *para*-aminobenzoic acid and is activated by enzymes of the folate pathway. PAS is converted to hydroxyl-dihydropteroate and subsequently to hydroxyl-dihydrofolate by dihydropteroate synthase and dihydrofolate synthase, respectively. Hydroxyl-dihydrofolate finally inhibits dihydrofolate reductase (DHFR), possibly by mimicking the DHFR substrate dihydrofolate, which is assumed to result in THF depletion and impaired protein synthesis.[67] PAS is a narrow-spectrum agent with bacteriostatic activity and a MIC of 0.4 µM (~0.06 µg/mL) against *M. tuberculosis*.[30,68] PAS is not active against intracellular bacteria.[69]

Cycloserine (DCS) is a synthetic analog of D-alanine. **Terizidone (TRD)** is a DCS analog composed of two DCS molecules. Alanine analogs inhibit cell wall synthesis by blocking the alanine racemase (which converts L-alanine to D-alanine) and the D-alanine-D-alanine ligase, which are both required for the synthesis of peptidoglycan. DCS is a broad-spectrum agent with bacteriostatic activity and a MIC of 25 µg/mL against *M. tuberculosis*.[70,71], and activity against intracellular (in human macrophages) *M. tuberculosis.*[40]

The thioamides **ethionamide (ETH)** and **prothionamide (PTH)** are analogs of INH. ETH is a prodrug and is activated by the flavin monooxygenase ethA, by oxidation to its corresponding *S*-oxide and subsequently to 2-ethyl-4-amidopyridine.[72] Like INH, ETH and PTH inhibit cell wall synthesis by targeting InhA.[34,73] ETH and PTH are narrow-spectrum agents that exert bactericidal activity. ETH shows a MIC of 0.25 µg/mL against *M. tuberculosis* and is active against intracellular bacilli.[30]

Thioacetazone (THZ) is a synthetic compound of the class of thiosemicarbazoles. THZ is a prodrug and is, similar to ETH, activated by the monoxygenase EthA by *S*-oxidation of its thiocarbonyl moiety.[74] THZ inhibits cell wall synthesis by blocking the β-hydroxyacyl ACP dehydratase HadABC of the fatty acid synthase II required mycolic acid synthesis.[75] Additionally, THZ was proposed to inhibit mycolic acid methyltransferases and cyclopropane mycolic acid synthases, which introduce cyclopropane rings at mycolic acid precursors.[76] THZ is a narrow-spectrum agent with poor bactericidal activity and a MIC between 0.08 - 1.2 µg/mL against *M. tuberculosis.*[77,78], and poor activity against dormant cells.[79]

Linezolid (LZD) and the novel compound **sutezolid (SZD)** (a thiomorpholinyl analog) are synthetic compounds that belong to the oxazolidinone class.[80] Oxazolidinones inhibit protein synthesis by binding to the A-site at the 23S rRNA of the 50S ribosomal subunit and blocking peptide bond formation between the A- and P-site tRNAs.[15,81,82,83] LZD and SZD show a MIC of 0.25 and <0.05 µg/mL against *M. tuberculosis*.[30,84] Oxazolidinones are broad-spectrum agents that exert bacteriostatic activity against actively replicating *M. tuberculosis* but bactericidal activity against dormant cells and are also active against intracellular bacilli.

TBA-354, **delamanid** and **pretomanid** are synthetic compounds of the nitroimidazol class. Nitroimidazoles are prodrugs that are activated by reduction of the aromatic nitro group (pretomanid and delamanid are activated by the F_{420}-deazaflavin-dependent nitroreductase Ddn), whereby the reduction potential lies beyond that of the eukaryotic aerobic redox system.[14,85,86]. Delamanid inhibits cell wall synthesis by blocking mycolic acid biosynthesis. Pretomanid inhibits cell wall biosynthesis by blocking mycolic acid synthesis, and it inhibits protein biosynthesis.[87] Additionally, upon activation of nitroimidazoles reactive nitrogen species including nitric oxide (NO) are formed, which could react with cytochromes and interfere with ATP homeostasis under hypoxic nonreplicating conditions. The mechanism of action of TBA-354 is not fully understood, but it is assumed to be similar to pretomanid.[14] TBA-354, pretomanid and delamanid are narrow-spectrum agents with MICs of 0.006, 0.04 and 0.002 µM (~ 0.002, 0.014, 0.001 µg/mL) against *M. tuberculosis*, respectively,[14,30] and exert bactericidal activity against replicating and dormant *M. tuberculosis.*[14,30] Delamanid is also active against intracellular (in human macrophages) *M. tuberculosis*.[30]

Clofazimine (CFZ) belongs to the class of riminophenazines and is a derivative of diploicin (a natural product from the lichen *Buellia canescens*).[88] CFZ is a prodrug that is activated by

reduction by NADH dehydrogenase and subsequent oxidation by O_2 and concomitant release of reactive oxygen species.[89] The exact mechanism of CFZ remains to be elucidated, but the outer membrane was proposed as main site of action.[90] CFZ is a broad-spectrum agent with bacteriostatic activity and a MIC of 0.1 µg/mL against *M. tuberculosis*. CFZ is active against dormant and intracellular (in murine macrophages) bacilli.[91]

Bedaquiline is a synthetic compound of the diarylquinoline class. It interferes with the energy metabolism by targeting the ATP synthase.[92] It binds to subunit c of the ATP synthase and blocks conformational changes associated with proton flow and ATP synthesis. Bedaquiline is a narrow-spectrum agent with bactericidal activity and a MIC of 0.06 µg/mL against *M. tuberculosis*, and it is active on dormant and intracellular (in murine macrophages) bacilli.[93]

Clarithromycin (CLR) is a macrolide antibiotic and is a derivative of erythromycin (which is produced by *Streptomyces erythreus*) .[94] Macrolides inhibit protein synthesis by binding to the ribosome at the V-domain of the 23S rRNA of the 50S subunit and blocking trans-peptidation and translocation.[95] CLR is a broad-spectrum agent with bacteriostatic activity and a MIC of 16 µg/mL against *M. tuberculosis*.[96,97] CLR is active against dormant[98] and moderately active against intracellular (in human macrophages) *M. tuberculosis*.[96]

Amoxicillin (AMX) and **imipenem (IPM)** belong to the class of β-lactams and are semisynthetic derivatives of penicillin (produced by molds of the genus *Penicillium*) and thienamycin (produced by *Streptomyces* spp.), respectively.[99,100] β-lactam antibiotics inhibit cell wall synthesis by targeting D,D-cross-linking transpeptidases (the penicillin-binding proteins) responsible for crosslinking peptidoglycan units.[52] Thereby β-lactams block transpeptidases by acting as substrate analogs for the terminal D-alanyl-D-alanine dipeptide of peptidoglycan. AMX is administered in combination with **clavulanate (CLV)** to counteract AMX resistance.[101] CLV inhibits the β-lactamase which hydrolyses AMX and causes AMX resistance. IPM is administered in combination with **cilastatin (CLN)**, to counteract IPM degradation.[102] CLN inhibits the human dehydropeptidase responsible for imipenem degradation. AMX and IPM are broad-spectrum agents with bactericidal activity and MICs of 64 and 4 µg/mL, respectively, against *M. tuberculosis*.[103] Co-administration of AMX with CLV reduces the MIC to 1 µg/mL. AMX and IMP are not active against dormant bacilli but are active against intracellular (in murine macrophages) bacilli.[104,105]

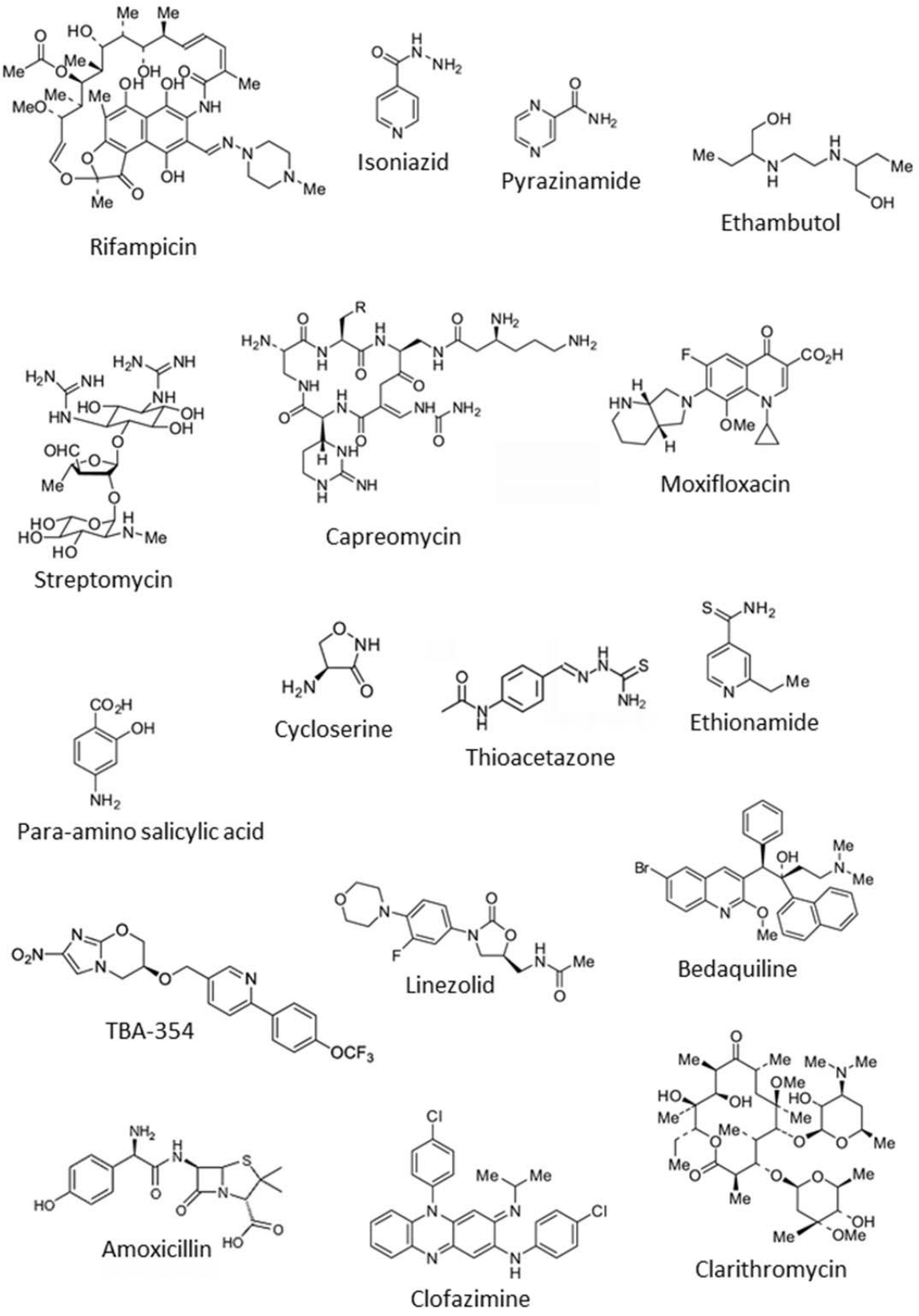

Figure 1-5: Structures of selected anti-TB drugs from the described drug classes.[14,30]

1.3 RESISTANCE IN MYCOBACTERIA

The evidence of antibiotic resistance genes in metagenomes of ancient sediments indicated that antibiotic resistance is a natural phenomenon.[106,107] The rise and spread of antibiotic resistance is further promoted by the selection pressure caused by the frequent use of antibiotics in human and animal health and agriculture.[108] Antibiotic resistance in bacteria can be mediated by inherent structural or functional characteristics (i.e. intrinsic resistance determinants) - such as the absence of a susceptible target of a specific antibiotic or the presence of an outer membrane which cannot be crossed by different antibiotics- or antibiotic resistance can be acquired by bacteria via chromosomal mutations or horizontal gene transfer. On a molecular level, antibiotic resistance is usually mediated by one of the following mechanisms: The prevention of access of an antibiotic to the molecular target by a reduced permeability of the membrane or an increased efflux of the antibiotic, the introduction of changes in antibiotic targets or prodrug-activating enzymes by mutations (in the target gene) or by direct modifications (e.g. by methylation) to prevent efficient antibiotic binding, or the inactivation of antibiotics by enzyme-catalysed modifications (e.g. by hydrolysis or by transfer of a chemical group to prevent binding to its target protein due to steric hindrances).[109]

Mycobacteria exhibit an intrinsic drug resistance against several antibiotics, which limits the number of usable drugs and which has been attributed to the low permeability of the waxy cell wall and to efflux mechanisms.[110] The acquirement of drug resistance by mycobacteria occurs via genetic or via phenotypic alterations.[25] Phenotypic drug resistance (or drug tolerance) is non-heritable and reversible, and includes metabolic and physiological adaptions.[111] For example, the cell wall inhibitor INH acts on actively replicating bacilli, whereby dormant bacilli are phenotypically resistant to INH.[31,112] Genetic drug resistance, on the other hand, is heritable and usually arises through horizontal gene transfer, genome rearrangements (such as gene acquisition, duplication and deletion) or chromosomal mutations. However, for the MTBC horizontal gene transfer had not been evidenced. [11,108] Genetic drug resistance in mycobacteria is mostly conferred by chromosomal mutations that affect the structure or the regulation of the expression of an antibiotic target or of pro-drug activating enzymes.[113] Furthermore, genome rearrangements were reported not only to contribute to resistance evolution but also to the speciation of mycobacteria and the evolution

of new gene functions.[11] Recently also large-scale duplications, which were generally thought to be absent in MTBC, were reported for *M. tuberculosis*.[11]

Compared to the slow mutation rate, *M. tuberculosis* shows a relatively rapid rate of drug resistance development, whereby the reason for the relatively rapid emergence of drug resistance remains elusive.[11,115] On the other hand, the limitation of the intrinsic mutation rate was shown to reduce drug resistance evolution, as prevention of SOS response induction by blocking LexA cleavage in *E. coli* inhibited resistance acquisition against CPX and RIF[114] and as deletion of the error-prone DNA polymerase DnaE2 in *M. tuberculosis* reduced the rate of RIF resistance development.[116] The estimated mutation rate for actively replicating *M. tuberculosis* is about 2 x 10^{-10} and 2 x 10^{-8} mutations per cell division for RIF and INH, respectively, and is related to errors during replication.[11,115] The estimated mutation rate for dormant bacilli in latent TB is similar, but is assumed to be related to oxidative damage in the host rather than to replication errors.[11] However, the intrinsic mutation rate varies between different strains of the MTBC, which was attributed to genetic variations affecting DNA replication, recombination and repair. This implies that different strains of the MTBC carry different risks for acquiring drug resistance and that the mutation rate could be altered. The mutation rate can for example be influenced by error-prone DNA replication or by inaccurate DNA mismatch repair (caused by mutations affecting DNA repair and replication fidelity) or by the induction of low fidelity polymerases upon activation of the bacterial SOS response.[116]

Natural evolution of antibiotic resistance is inevitable, however, antibiotic resistance is accompanied by the co-evolution of natural antibiotic molecules that target essential bacterial targets. One approach to respond to antibiotic resistance is the identification of those essential bacterial targets and of their according pre-existing mechanisms of resistance, which can then aid the design of improved semi-synthetic derivatives of these natural antibiotic molecules that may evade many resistance mechanisms. This approach was already successful in the design of different generations of antibiotics as in the case of fluoroquinolone antibiotics.[117] Another approach to overcome drug resistance is the combined treatment with different antibiotic drugs. The rational combination of drugs can be based on the synergistic action of the drugs or on the collateral sensitivity of bacteria to different antibiotics.[118] For example, the combination of β-lactam antibiotics and β-lactamase inhibitors, such as amoxicillin and clavulanate, results in a synergistic effect, which is based on the mechanism of resistance to amoxicillin and the mechanism of action of clavulunate (clavulanate inhibits the degradation

of amoxicillin by inhibition of β-lactamases as described below). However, the combination of two drugs that target the same molecular target or the same metabolic pathway may result in a synergistic effect but may also promote resistance mutations that support resistance to both drugs. Futhermore, collateral sensitivity occurs, when resistance or adaptive mutations caused by one drug increase the sensitivity to another drug. For example, aminoglycosides cause mutations in the *cpx* locus that affect the membrane potential (i.e. a reduction in the proton-motive force across the inner membrane), which is assumed to diminish the activity of proton-motive force dependent efflux pumps (such as the AcrAB transporter), which in turn leads to hypersensitivity to other antibiotics such as chloramphenicol.[119] Notably, chloramphenicol resistance is associated with upregulation of the AcrAB transporter. In addition, mutations conferring resistance to amikacin were reported to be counterselected by chloramphenicol.[118]

Since the introduction of new drugs is invariably followed by the emergence of resistance, it was recently suggested to link the elucidation of resistance mechanisms against novel antibiotics to the drug approval process (and possibly also the elucidation of resistance mechanisms of old antibiotics included in new regimens), to enable the development of appropriate drug-susceptibility testing assays and to the tailoring of treatment regimens.[120] This is particularly feasible in the case of TB, as resistance for the MTBC arises exclusively by chromosomal changes but not by horizontal genes transfer. Treatment regimens could thus be tailored with respect to the intrinsic resistance mechanisms of MTBC species and with respect to the acquired resistance mechanisms against drugs. For example resistance against bedaquiline is associated with the upregulation of the MmpL5 efflux pump which also confers cross-resistance to clofazimine, so that regimens that contain both drugs may have to be reconsidered. An example where the intrinsic resistance should be considered is *M. canettii*, which is intrinsically resistant to pyrazinamide and might also be intrinsically resistant to pretomanid, so that the PaMZ regimen currently in phase 3 clinical trials (Figure 1-3) might lead to monotherapy of *M. canettii* infections.

In the following sections the known resistance mechanisms, which could provide a basis for the rational design of drug regimens, of the first-, second- and third- line anti-TB drugs and of the new anti-TB drugs currently in clinical phases are described. Given informations are related to *M. tuberculosis*, if not otherwise stated. In addition to the described resistance

mechanisms, for almost all compounds additional or unidentified resistance mutations were observed, which suggest alternative resistance mechanisms that remain unclear.

Resistance to the rifamycins **rifampicin** and **rifapentine** is primarily associated with mutations in the molecular target, the β-subunit of the DNA-dependent RNA polymerase, which arise by single point mutations in the *rpoB* gene.[36,121] These mutations lead to substitutions of amino acids with compact side chains to such with larger side chains and thereby to prevention of access of the rifamycin molecule.[122,123] The frequency of acquired RIF resistance was determined to be ~10^{-8} at 1 µg/mL RIF for *M. tuberculosis.*[124]

Resistance to **isoniazid** is mostly attributed to mutations in the activating catalase-peroxidase KatG which arise by single point mutations, insertions or deletions in the *katG* gene.[36] This affects the ability to activate the INH prodrug, whereby the level of INH resistance depends on the type of mutation.[36] The most commonly observed serine to threonine substitution at residue 315 of KatG results in a narrowed heme access channel that prevents access of INH to the oxidizing site and is associated with high-level INH resistance.[35] INH resistance is also attributed with mutations in the target enzyme InhA that affect the affinity for NADH or with mutations in the *inhA* promoter region that result in InhA overexpression, which are associated with lower level resistance. Mutations in *ndh* (NADH dehydrogenase) that could result in an increased NADH/NAD ratio were also observed in INH resistant isolates. The frequency of acquired INH resistance was determined to be ~10^{-6} at 1 µg/mL INH for *M. tuberculosis.*[124]

Resistance to **pyrazinamide** is primarily associated with mutations in the activating enzyme PZase which arise by single point mutations, insertions and deletions in the *pncA* gene or its promoter region. The intrinsic resistance to mycobacteria (e.g. *M. bovis*) against PZA is likewise attributed to genetic variations in the *pncA* gene. The frequency of acquired PZA resistance was determined to be ~10^{-5} at 100 µg/mL PZA for *M. tuberculosis*.[125]

Resistance to the ethylenediamine **ethambutol** is associated with mutations in the arabinosyl transferases A and B.[30,36] by mutations in the *embB* and *embA* genes. Thereby the EMB resistance level is higher for multiple mutations in the *emb* genes. The frequency of acquired EMB resistance was determined to be ~10^{-8} organisms at 16 µg/mL EMB for *M. tuberculosis*.[126] No resistant mutants could be generated for the novel ethylenediamine **SQ109**

so far, but mutants resistant to similar ethylenediamines that contain mutations in the putative trehalose monomycolate transporter MmpL3 showed some cross-resistance to SQ109.[50]

Resistance to the aminoglycosides **streptomycin**, **kanamycin** and **amikacin** is usually caused by mutations in the molecular target, the ribosome, which lead to alterations in the aminoglycoside binding site.[36] Thereby mutations occur mostly in the *rrs* gene that encodes 16S rRNA.[36,127] A majority of STM resistant isolates also contain mutations in the *rpsL* gene that encodes the ribosomal protein S12.[36] Some STM resistant isolates contain mutations in *gidB* encoding the 7-methylguanosine methyltransferase that specifically methylates the 16S rRNA at the STM binding site, which resulted in loss of this methylation and in low level resistance to STM. Additionally, aminoglycoside resistance is associated with mutations in the *cpx* locus.[128] The Cpx envelope stress response mediates adaption to envelope stresses at the inner membrane and is linked to changes in the membrane protein content and in proton motive driven transport. In addition, mutations in the promoter region of *eis*, which encodes an aminoglycoside acetyltransferase that inactivates many aminoglycosides by transfer of acetyl groups from acetyl-coenzyme A to an amino group of the aminoglycoside, resulted in *eis* overexpression and low-level KAN resistance.[127] The frequency of acquired resistance was determined to be ~10^{-8} at 4 µg/mL for STM and AMI for *M. tuberculosis*.[129]

Resistance to the tuberactinomycins **viomycin** and **capreomycin** is associated with target modification, as mutations in *tlyA* encoding a 2'-O-methyltransferase that methylates the tuberactinomycin binding sites at the 23S rRNA and the 16S rRNA, resulted in loss of this methylation and conferred resistance to CAP and VIO.[127,130] Additionally, mutations in *rrs* encoding the 16S rRNA conferred resistance to both aminoglycosides. The frequency of acquired CAP resistance was determined to be ~5x10^{-7} for *M. tuberculosis* at 10 µg/mL CAP.

Resistance to the fluoroquinolones **ciprofloxacin**, **levofloxacin**, **moxifloxacin**, **ofloxacin** and **gatifloxacin** is primarily attributed to modifications in molecular target, the DNA gyrase.[36] The resistance mutations are located at the fluoroquinolone binding site in *gyrA* and/or *gyrB*, wherby the resistance depends on position and number of amino acid substitutions.[131] The frequency of acquired CFX and OFX resistance was determined to be ~10^{-6} at 2 µg/mL for *M. tuberculosis*.[132]

Resistance to ***para*-aminosalicylic acid** is associated with mutations in the thymidylate synthase A, which result in reduced activity of this enzyme. The thymidylate synthase A

consumes reduced folate and is thus involved in regulation of intracellular folate levels, however the precise resistance mechanism remains unclear.[133] Some PAS resistant isolates also contained mutations in the PAS activating dihydrofolate synthase.[134] The frequency of acquired PAS resistance was determined to be ~10^{-7} at 4 µg/mL for *M. tuberculosis*.

The resistance mechanism to the alanine analogs **cycloserine** and **terizidone** has not been identified. However, overexpression of the genes encoding the molecular targets, the alanine racemase and the D-alanine-D-alanine ligase, confers resistance to DCS in *M. smegmatis*.[135]

Resistance to the thionamides **ethionamid** and **prothionamide** is attributed to modifications of the activating enzyme or the target enzyme or their regulation, as ETH resistant isolates mostly contained mutations in *ethA* encoding the activating enzyme, in *ethR* encoding the regulator of *ethA*, in *inhA* encoding the target enzyme or in the *inhA* promoter.[136] Few ETH resistant isolates contained mutations in *mshA* encoding a glycosyltransferase involved in the mycothiol biosynthesis, thereby resistance is assumed to be mediated by a defect in ETH activation.[137] For mutants with mutations in *inhA* a cross-resistance to INH was observed.[30]

Resistance to **thioacetazone** is attributed to target amplification, as overexpression of the *hadABC* operon resulted in resistance to THZ.[138] Additionally, mutations in *ethA*, encoding the activating enzyme were associated with THZ resistance. Loss of function mutations in *mma4*, encoding a cyclopropyl mycolic acid synthetase that was recently suggested to be a THZ target, also led to THZ resistance. The frequency of acquired THZ resistance was determined to be ~4x10^{-6} at 2 µg/mL for *M. tuberculosis*.

Resistance to **oxazolidinones** is associated with target modification, as LZD resistant mutants contained mutations in the *rrl* gene encoding the 23S rRNA.[139] Additionally, resistant mutants contained mutations in *rplC* encoding the ribosomal L3 protein of the 50S subunit, suggesting this ribosomal protein as additional target. The frequency of acquired LZD resistance was determined to be ~10^{-8} at 8 µg/mL LZD for *M. tuberculosis*.

Resistance to **nitroimidazoles** is attributed to impaired prodrug activation, as resistance to pretomanid is associated with mutations in enzymes involved in biosynthesis of the electron carrier coenzyme F_{420} (such as the activating enzyme Ddn that is capable of directly reducing pretomanid, the F_{420}-dependent glucose-6-phosphate dehydrogenase that recycles coenzyme F_{420} to the reduced form, or the FO synthase that is essential for F_{420} coenzyme synthesis).[140]

The frequency of acquired resistance was determined to be ~$3x10^{-7}$ at 0.025 µM (~0.01 µg/mL) for TBA-354 and ~$6.5x10^{-7}$ at 2 µg/mL for pretomanid for *M. tuberculosis*.[14,141]

Resistance to **clofazimine** is associated with loss of function mutations in *rv678* encoding a transcriptional repressor, which led to upregulation of the *mmpl5* gene encoding a multi-substrate efflux pump.[143] This resulted in partial resistance to CFZ, suggesting that CFZ may be a substrate for this efflux pump.

Resistance to **bedaquiline** is attributed to target modification, as drug resistant mutants contained mutations in *atpE* encoding the c subunit of the ATP synthase.[142] Additionally, CFZ resistant mutants with a mutation resulting in upregulation of the efflux pump MmpL5 showed partial cross-resistance to bedaquiline, suggesting that bedaquiline is a substrate for this efflux pump.[143] The frequency of acquired bedaquiline resistance was determined to be ~$5x10^{-8}$ at 8 times MIC (~0.24 µg/mL bedaquiline) for *M. tuberculosis*.

Resistance to **clarithromycin** is associated with target modification, as methylation of the 23S rRNA by the methyltransferase ErmMT results in loss of drug binding.[30,97] ErmMT is thereby induced by CLR.[144] The 16S rRNA adenine dimethyltransferase KsgA was also associated with CLR resistance, although methylation of the 23S rRNA by KsgA has not been described yet.

Resistance to **β-lactam antibiotics** is primarily attributed to enzymatic β-lactam inactivation by β–lactamases, which mainly inactivate β–lactams by hydrolyzing the amide group of the β–lactam ring. [145,146] In addition, nonclassical L,D-cross-linking transpeptidases recently have been identified in *M. tuberculosis* (and other Gram-positive organisms) that are resistant to β-lactam antibiotics. In addition, β-lactam resistance in *M. tuberculosis* is associated with low cell envelope permeability, low penicillin-binding protein binding affinity, and efflux pumps (as an ABC-transporter encoded by *rv0194* and the MmpL5 transporter were found to be upregulated upon β-lactam exposure).

1.4 GRISELIMYCINS

In addition to the above described anti-TB drugs in clinical development, several agents are in discovery and preclinical development for the treatment of TB. Griselimycins are

cyclopeptides, which were recently added to the TB drug pipeline and are developed by Sanofi and the TB Alliance (Figure 1-3, "cyclopeptides").

Griselimycin (GM) (initially named 11072 RP) and methylgriselimycin (MGM) are natural products that are synthesized non-ribosomally by *Streptomyces* strains (*Streptomyces caelicus* and *Streptomyces griseus*).[147] GMs are cyclic peptides which are composed of ten amino acids, including non-coded *N*-methylamino acids and a D-amino acid (Figure 1-6).[148]

GM was discovered and characterized in the 1960s and its natural derivative MGM, which is naturally produced only in small amounts, was discovered in the 1970s. [149,150,151] GM was found to be active against drug-resistant *M. tuberculosis* and the first human studies were promising but revealed poor pharmacokinetic properties of GM, in particular a poor stability (i.e. a short half-life in plasma).[152,153] In the 1970s, after rifampicin became available, the studies on GMs were not further pursued. However, GMs were recently rediscovered in search of neglected antibiotics with promising antituberculosis activity and the studies to GMs were reinitiated. In order to find GM analogs with improved pharmacokinetic properties, structure-activity-relationship (SAR) studies with a library of synthetic GM derivatives were conducted. The SAR studies revealed that GM analogs with substitutents at position 8 of the molecule led to metabolically more stable compounds and that increasing lipophilicity resulted in increased potency. Finally, a synthetic GM analog with a cyclohexyl substitution at proline 8 (cyclohexylgriselimycin, CGM) was found to show optimized properties, such as improved pharmacokinetic properties (i.e. high oral bioavailability, moderate plasma clearance, a large volume of distribution and prolonged half-life in mice) and a limited potential for drug-drug interactions, and was chosen for further *in vivo* studies.[154] The *in vivo* studies revealed that CGM exerts bactericidal activity in mouse models of TB and, moreover, that combined administration of CGM with the first-line antituberculosis drugs RIF and PZA in mouse models of TB resulted in shortened treatment duration (mouse lung culture conversion after only 8 weeks) compared to the TB standard treatment in the same mouse models.

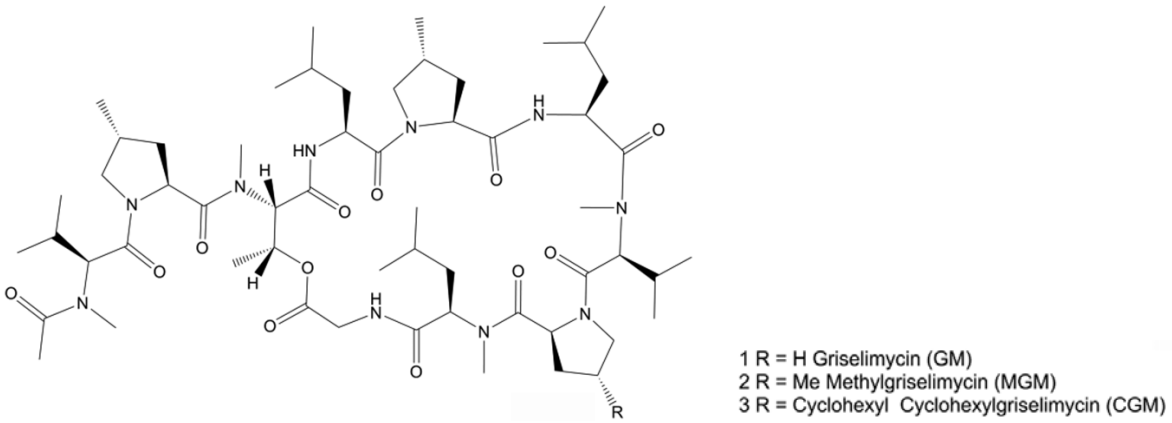

Figure 1-6: Chemical structure of GMs. Griselimycin: R = H, $C_{57}H_{96}N_{10}O_{12}$, MW 1113.7; Methylgriselimycin: R = methyl, $C_{58}H_{98}N_{10}O_{12}$, MW 1127.7; Cyclohexylgriselimycin: R = cyclohexyl, $C_{63}H_{106}N_{10}O_{12}$, MW 1195.8. GMs are composed of ten amino acids in the following order: L-*N*-methylvaline (MeVal) which is *N*-acetylated, L-trans-4-methylproline (MePro), L-*N*-methylthreonine (MeThr), L-leucine (Leu), L-trans-4-methylproline, L-leucine, L-*N*-methylvaline, L-proline (Pro), D-*N*-methylleucine (D-MeLeu), glycine (Gly).[154]

1.5 OUTLINE OF THE DISSERTATION

The aim of the present work was the elucidation of the mechanism of action and of the resistance mechanism of griselimycins and in addition, the elucidation of the self-resistance mechanism in the griselimycin producer strain.

The self-resistance mechanism of the griselimycin producer *Streptomyces caelicus* was investigated by examination of the griselimycin biosynthetic gene cluster. It was found out that an additional homolog of the DNA polymerase beta subunit (sliding clamp), which is encoded by a gene (*griR*) located in the griselimycin biosynthetic gene cluster, serves as self-resistance determinant of the griselimycin producer *S. caelicus*. The interaction of the natural compounds griselimycin and methylgriselimycin and of the synthetic compound cyclohexylgriselimycin (which was synthesized at Sanofi-Aventis LGCR/Chemistry) with the purified sliding clamps of *S. caelicus* (i.e. the conventional sliding clamp DnaN and the additional sliding clamp homolog GriR) were characterized by surface plasmon resonance (SPR) analyses and isothermal titration calorimetry (ITC) to gain further insights into the self-resistance mechanism. The self-resistance mechanism against griselimycins was investigated at the Helmholtz Institute for Pharmaceutical Research Saarland (HIPS) and is described in chapters 3.1 and 4.1.

Griselimycins were characterized and compared at the HIPS regarding their antibacterial spectrum and cyclohexylgriselimycin was further characterized with respect to the activity on *M. tuberculosis in vitro* and *in vivo* at the Sanofi-Aventis Infectious Disease Therapeutic Strategic Unit and the Johns Hopkins University School of Medicine, respectively. Based on the griselimycin self-resistance determinant, the sliding clamp was assumed to be the molecular target of griselimycins in mycobacteria and the interaction of griselimycins with different purified sliding clamps was characterized by surface plasmon resonance (SPR) at the HIPS and by analysis of the crystal structures at the Helmholtz Centre of Infection Research (HZI). Eventually, the impact of griselimycin on the bacterial replication was examined at the HIPS by investigation of the binding of the replicative DNA polymerase to the mycobacterial sliding clamp by an SPR based inhibition assay and by analysis of the induction of DNA damage. The characterization of the activity and investigation of the mechanism of action of griselimycins are described in chapters 3.2 and 4.2.

The mechanism of resistance of mycobacteria against griselimycins was characterized by generation of resistant mycobacteria and subsequent comparative genome analysis, therefore griselimycin resistant *M. smegmatis* were generated *in vitro* at the HIPS and cyclohexylgriselimycin resistant *M. tuberculosis* were generated *in vivo* at the John Hopkins University School of Medicine. The griselimycin resistance was further characterized at the HIPS regarding resistance reversibility, resistance frequency, and induced fitness costs. The investigation of the mechanism of resistance to griselimycins is described in chapters 3.3 and 4.3.

2 MATERIALS AND METHODS

2.1 MATERIALS

2.1.1 COMPOUNDS

Griselimycin and its derivatives methylgriselimycin and cyclohexylgriselimycin were kindly provided by Dr. Armin Bauer (Sanofi-Aventis Deutschland GmbH, Frankfurt a. M.).

2.1.2 CHEMICALS

All chemicals were of reagent grade quality and were obtained from commercial sources.

2.1.3 OTHER REAGENTS

Table 2-1: Other reagents.

Reagent	**Manufacturer**
Proteinase K from *Tritirachium album*	Sigma-Aldrich
Ribonuclease A	Carl Roth GmbH
Lysozyme	Carl Roth GmbH
DMSO	Sigma-Aldrich
miRNeasy mini Kit	Quiagen
RevertAid reverse transcriptase	Thermo Scientific
Dynamo Colorflash SYBR green qPCR kit	Biozym
Restriction enzymes	Fermentas
T4-DNA-ligase	New England Biolabs
Phenol/chloroform/isoamylalcohol	Carl Roth GmbH
CPD-Star (Chemiluminescent substrate)	Roche
DIGEasyHyb	Roche

2.1.4 BUFFERS AND MEDIA

All media and buffers were prepared in distilled water unless otherwise noted and sterilized by autoclaving or sterile filtration.

Table 2-2: Media.

Medium	**Ingredients**	**Concentration**
GYM Medium (pH 7.2)	Glucose	0.4 %
	Yeast extract	0.4 %
	Malt extract	1 %
Mannitol soy agar (MS) (prepared with tap water)	Mannitol	2 %
	Soya flour	2 %
	Agar	1.5 %
Tryptic soy broth (TSB) (pH 7.3)	Peptone casein	1.7 %
	Peptone soymeal	0.3 %
	Glucose	0.25 %
	NaCl	0.5 %
	K_2HPO_4	0.25
Middlebrook 7H9 medium	Bacto Middlebrook 7H10 medium (Difco)	19.7 %
	Glycerol	2 mL/L
	Glucose	0.25 %
	Middlebrook albumin-dextrose-catalase enrichment (0.5 % bovine albumin fraction V, 0.2 % Dextrose, 0.004% beef catalase, 0.085 % NaCl)	10 %
ZYM 5052 medium	N-Z-amine (tryptone)	1 %
	Yeast extract	0.5 %
	K_2HPO_4	25 mM
	NaH_2PO_4 x H_2O	25 mM
	NH_4Cl	50 mM
	Na_2SO_4 x 10 H_2O	5 mM
	Glycerol (100%)	0.5 %
	Glucose	0.05 %
	α-Lactose	0.2 %
	$FeCl_3$ x 6 H_2O	10 mM
	$CaCl_2$ x 2 H_2O	4 mM
	$MnCl_2$ x 4 H_2O	2 mM
	$ZnSO_4$ x 7 H_2O	2 mM
	$CoCl_2$ x 6 H_2O	0.4 mM
	$CuCl_2$ x 2 H_2O	0.4 mM
	$NiSO_4$ x 6 H_2O	0.4 mM
	Na_2MoO_4 x 2 H_2O	0.4 mM
	Na_2SeO_3	0.4 mM
	H_3BO_3	0.4 mM
	$MgSO_4$ x 7 H_2O	2 mM

LB medium (pH 7.0)	Trypton	1 %
	NaCl	0.5 %
	Yeast extract	0.5 %
MYC medium (pH 7.0)	Phytone Peptone	1 %
	Glucose	1 %
	HEPES	50 mM
R2L medium (pH 7.2)	TES	25 mM
	$CaCl_2$ x $2H_2O$	0.3 %
	Casamino acids	0.01 %
	Glucose	1 %
	Yeast extract	0.5 %
	K_2SO_4	0.025 %
	Mannitol	7.3 %
	$MgCl_2$	1 %
	Low melt point agarose	0.7 %
Müller Hinton broth (BD Difco)	Beef extract	0.2 %
	Acid digest of Casein	1.75 %
	Starch	0.15 %

Table 2-3: Buffers.

Buffer	**Ingredient**	**Concentration**
Sodium acetate coupling buffer (pH 4, 4.5, 5 or 5.5)	Acetic acid	1 mM
	Sodium hydroxide	(for pH adjustment)
Maleate coupling buffer (pH 6, 6.5 or 7)	Maleic acid	1 mM
	Sodium hydroxide	(for pH adjustment)
HBS-EP buffer	HEPES	10 mM
	Sodium chloride	150 mM
	EDTA	3 mM
	Tween-20	0.05 %
GTE buffer (pH 8.0)	Glucose	50 mM
	Tris base	025 mM
	EDTA	10 mM
	Tween-80	0.1 %
Denaturation buffer	Sodium hydroxide	500 mM
	Sodium chloride	1500 mM
Neutralization buffer	Tris-HCl (pH 7.5)	0.5 M
	Sodium chloride	3000 mM
20 x SSC buffer	Sodium chloride	3000 mM
	Sodium citrate	300 mM

2 x washing buffer	SSC buffer	2 x
	Sodium dodecyl sulfate (SDS)	0.1 %
0.5 x washing buffer	SSC buffer	0.5 x
	Sodium dodecyl sulfate (SDS)	0.1 %
Dig1 buffer (pH 7.5)	Sodium chloride	150 mM
	Maleic acid	100 mM
	Sodium hydroxide	(for pH adjustment, ca 8 g)
Dig 2 buffer (pH 7.5)	Sodium chloride	150 mM
	Maleic acid	100 mM
	Tween-20	0.3 %
Dig3 buffer (pH 9.5)	Tris base	100 mM
	Sodium chloride	100 mM
	Sodium hydroxide	(for pH adjustment)

2.1.5 MICROORGANISMS AND CELL LINES

All microorganisms were obtained from the DSMZ (Deutsche Sammlung von Mikroorganismen und Zellkulturen GmbH) and the ATCC (American Type Culture Collection) or were part of the internal strain collection. *Staphylococcus aureus* strain Newman[155] was obtained from PD Dr. Markus Bischoff, Saarland University Hospital, Homburg. *Pseudomonas aeruginosa* strain PAO1 was obtained from Prof. Dr. Susanne Häußler, Helmholtz Centre for Infection Research/, Braunschweig/Twincore, Hannover.

Table 2-4: Microorganisms.

Strain	**Source**
Acinetobacter baumannii	DSMZ No. 30008
Burkholderia cenocepacia	DSMZ No. 16553
Chromobacterium violaceum	DSMZ No. 30191
Escherichia coli	DSMZ No. 1116
Escherichia coli (TolC-deficient strain)	Internal strain collection
Escherichia coli K12 DH10B	Internal strain collection
Escherichia coli HS996	Internal strain collection
Escherichia coli BL21 (DE3)	Internal strain collection
Klebsiella pneumoniae	DSMZ No. 30104
Pseudomonas aeruginosa PAO1	Internal strain collection
Bacillus subtilis	DSMZ No. 10
Corynebacterium glutamicum	DSMZ No. 20300

Enterococcus faecium	DSMZ No. 20477
Micrococcus luteus	DSMZ No. 1790
Mycobacterium bovis BCG	DSMZ No. 43990
Mycobacterium smegmatis mc^2155	ATCC No. 700084
Nocardia asteroides	DSMZ No. 43757
Staphylococcus aureus Newman	Internal strain collection
Staphylococcus aureus, methicillin-resistant	DSMZ No. 11822
Staphylococcus carnosus	DSMZ No. 20501
Streptococcus pneumoniae	DSMZ No. 20566
Streptomyces caelicus	DSMZ No. 40835
Streptomyces coelicolor A3(2)	Internal strain collection
Candida albicans	DSMZ No. 1665
Wickerhamomyces anomalus	DSMZ No. 6766
Mucor hiemalis	DSMZ No. 2656

All mammalian cell lines were were obtained from the DSMZ (Deutsche Sammlung von Mikroorganismen und Zellkulturen GmbH) or were part of the internal cell collection. The RAW264.7 cell line was obtained from Prof. Dr. Alexandra K. Kiemer, Saarland University, Saarbrücken.

Table 2-5: Cell lines.

Cell line	**Species**	**Type**
CHO-K1	Chinese hamster	Ovary
L929	Mouse	Fibroblast
RAW264.7	Mouse	Leukemic macrophage

2.1.6 PLASMIDS

For cloning and expression of *dnaN* genes the pJET1.2 cloning vector and expression constructs based on a modified pCOLADuet-1 vector were used. The pCOLADuet-1 vector contains a Strep-tag II sequence and a TEV protease site. The *dnaN* genes were inserted into the pCOLADuet-1 vector using primers (Table 2-7) with introduced *PstI/NdeI* restriction sites for *S. caelicus griR* and the *NotI/NdeI* restriction sites for all other *dnaN* genes (*M. smegmatis, M. tuberculosis, S. caelicus dnaN, E. coli*).

Table 2-6: Plasmids.

Plasmid	Replicon	Selection marker
pJET1.2::*dnaN*-Ms	*dnaN M. smegmatis* mc^{2}155	Ampicillin
pCOLADuet-1::*dnaN*-Ms	*dnaN M. smegmatis* mc^{2}155	Kanamycin
pJET1.2::*dnaN*-Mtb	*dnaN M. tuberculosis* H37Rv	Ampicillin
pCOLADuet-1::*dnaN*-Mtb	*dnaN M. tuberculosis* H37Rv	Kanamycin
pJET1.2::*dnaN*-Sc	*dnaN S. caelicus*	Ampicillin
pCOLADuet-1::*dnaN*-Sc	*dnaN S. caelicus*	Kanamycin
pJET1.2::*girR*-Sc	*griR S. caelicus*	Ampicillin
pCOLADuet-1::*griR*-Sc	*griR S. caelicus*	Kanamycin
pJET1.2::*dnaN*-Ec	*dnaN E. coli* K12 DH10B	Ampicillin
pCOLADuet-1::*dnaN*-Ec	*dnaN E. coli* K12 DH10B	Kanamycin

2.1.7 OLIGONUCLEOTIDES

Table 2-7: Oligonucleotides for gene amplification.

Primer	Sequence (5‘-3‘ direction, restriction sites underlined)	Restriction enzyme	Organism
dnaN-Mtb_NotI_fwd	GCGGCCGCATGGACGCGGCTACGACAAGAGTTG	NotI	*M. tuberculosis* H37Rv
dnaN-Mtb_NdeI_rev	CCATATGTCAGCCCGGCAACCGAACCGG	NdeI	*M. tuberculosis* H37Rv
dnaN-Sc_PstI_fwd	GGGCTGCAGATGAAGATCCGGGTGG	PstI	*S. caelicus*
dnaN-Sc_NdeI_rev	CCATATGTCAGCCGCTCAGACGCACCGG	NdeI	*S. caelicus*
griR-Sc_NotI_fwd	GCGGCCGCATGCGGTTTCAGGTCGAGCGGG	NotI	*S. caelicus*
griR-Sc_NdeI_rev	CCATATGTCACCGATGGAACCGTACAGGCATG	NdeI	*S. caelicus*
dnaN-Ms_BamHI_fwd	GGACGGATCCGTGGCGACGACGACGGCTGG	BamHI	*M. smegmatis* mc^{2}155
dnaN-Ms_NotI_rev	CCGGCGGCCGCTCAGCCCGGAAGCCGCACC	NdeI	*M. smegmatis* mc^{2}155
dnaN-Ec_NotI_fwd	AAGAATGCGGCCGCATGAAATTTACCGTAGAACGTG	NotI	*E. coli* K12 DH10B
dnaN-Ec_KpnI_rev	GGGGTACCTTACAGTCTCATTGGCATGACAAC	KpnI	*E. coli* K12 DH10B

Table 2-8: Oligonucleotides for expression analyses.

Primer	**Sequence (5‘-3‘ direction)**	**Gene**	**Organism**
*dnaN*_fwd	CTTGAAGTTTCGCGTCGTCC	*dnaN*	*M. smegmatis* mc^2155
*dnaN*_rev	CGATTTCAGCGCTCACCTTG	*dnaN*	*M. smegmatis* mc^2155
*recA*_fwd	GAGTTCGACATCCTCTACGG	*recA*	*M. smegmatis* mc^2155
*recA*_rev	CTTCTTCTCGATCTCGTTGGC	*recA*	*M. smegmatis* mc^2155
*lexA*_fwd	CACCATCCTCGAGGTCATC	*lexA*	*M. smegmatis* mc^2155
*lexA*_rev	GATACCCCTTGCGTTCGAG	*lexA*	*M. smegmatis* mc^2155
*dnaE2*_fwd	CAGGTTCTACGACGGGATG	*dnaE2*	*M. smegmatis* mc^2155
*dnaE2*_rev	GCTTGAACCACGACGAGTAG	*dnaE2*	*M. smegmatis* mc^2155
*dnaB*_fwd	GAGCACGATGTCTACGACG	*dnaB*	*M. smegmatis* mc^2155
*dnaB*_rev	CAAGGATGATGTCGGCTTC	*dnaB*	*M. smegmatis* mc^2155
*16S*_fwd	TCACGAACAACGCGACAAACC	16S rRNA	*M. smegmatis* mc^2155
*16S*_rev	GTATGTGCAGAAGAAGGACCG	16S rRNA	*M. smegmatis* mc^2155

2.1.8 PROTEINS AND PEPTIDES

The human sliding clamp equivalent (PCNA) was ordered as glycosylated protein with a His_6-tag from Prospec-Tany Technogene Ltd., Israel. The peptide containing the internal DnaN binding site from DnaE of *M. smegmatis* (amino acid sequence: KAEAMGQFDLFG) was ordered as HPLC-purified peptide from Bio-Synthesis Inc. (Lewisville, Texas).

2.1.9 TECHNICAL EQUIPMENT AND CONSUMABLES

Table 2-9: Equipment.

Description	**Type**	**Manufacturer**
Surface plasmon resonance (SPR)	X100	Biacore, GE Healthcare
Isothermal calorimetry (ITC)	MicroCal ITC200	Microcal Inc., GE Healthcare
Plate readers	Infinite 200 Pro	Tecan Group Ltd.
Protein purification system	Äkta purifier system	GE Healthcare
UV-Vis spectrophotometer	NanoDrop 2000c	Thermo Scienticfic
Electroporator	Eporator	Eppendorf
PCR cycler	Mastercycler	Eppendorf
qPCR cycler	Peqstar 96Q	Peqlab
Beadmill	Fastprep-24	MP biomedicals
French press	French press	Thermo Electron

Table 2-10: Consumables.

Description	Type	Manufacturer
SPR chips	CM5	Biacore, GE Healthcare
SPR vials	Plastic Vials and Caps,Ø 11 mm Plastic Vials, Ø 15 mm	Biacore, GE Healthcare
SPR amine coupling kit		Biacore, GE Healthcare
96-well plates	96 Well, clear, flat bottom, sterile	Sarstedt AG & Co.

2.2 METHODS

The methods chapter was previously published in the original publication (see chapter 7, page 121), except for sections 2.2.2, 2.2.6 and 2.2.11 and parts of sections 2.2.5 and 2.2.13. Methods marked with an asterisk * were applied by collaborators. Methods marked with an asterisk in brackets (*) were applied partly by collaborators and partly by the author (as listed on page 122).

2.2.1 OVEREXPRESSION OF GRIR

* To achieve heterologous expression of *griR* in the GM sensitive *S. coelicolor* A3(2), the gene was subcloned into the *E. coli/Streptomyces* integrative shuttle vector pSET152[156]. The vector was first equipped with a polylinker harboring the *PermE** promoter from plasmid pUWL201[157] by ligating the corresponding 370 bp *PvuI/PciI* fragment with pSET152 hydrolysed with the same enzymes, resulting in plasmid pSET152- *PermE**. Oligonucleotides Gri32 (5'- TCT GGA TCC AGC CAC CTC ATG GAA CTC- 3', BamHI site underlined) and Gri33 (5'- GAA CTC CAG CTG GAC GTG CAG CAA GCC ATC-3', PvuII site underlined) were used to amplify the *griR* gene from the GM producing *Streptomyces caelicus* DSM-40835 using Phusion polymerase (Biozym) according to the manufacturer's protocol. The PCR product was subsequently hydrolyzed with *PvuII/BamHI* and ligated into pSET152-*PermE** (linearized with *EcoRV/BamHI*), resulting in plasmid pGri17. Both, the empty vector and pGri17 were transformed into *S. coelicolor* A3(2) by triparental conjugation according to standard procedures.[156] The resulting transformants, *S. coelicolor*::pSET152-*PermE** and *S. coelicolor*::pGri17, were selected and cultivated on MS medium (44) supplemented with 60 µg/mL apramycin (MS-Apra) at 30 °C. Integration of the pSET152 derivatives into the chromosomal ϕC31 phage attachment site was verified by PCR analysis.

2.2.2 CLONING OF DNAN

(*) The genomic DNA of *M. smegmatis* mc^2155, *S. caelicus* and *E. coli* K12 DH10B was prepared by an enzymatic procedure as previously described[158] with minor modifications. Cells from 5 mL cultures were resuspended in GTE buffer (50 mM glucose, 25 mM Tris, 10

mM EDTA, pH 8.0) containing 0.1% (*v/v*) Tween-80 and 2 mg/mL lysozyme and kept at 37°C for 3.5 h. The cell suspensions were then mixed with SDS-activated Proteinase K (2 mg/mL) and incubated for 2 h at 55 °C prior to the addition of 1 mg/mL RNase A and further incubation for 30 min at 37 °C. DNA isolation was performed by standard phenol-chloroform extraction, and DNA was spooled out after the addition of 300 mM NaOAc (pH 4.8) and 2.5 volumes of cold ethanol. DNA was washed with 70 % ethanol and finally dissolved in 10 mM Tris-HCl (pH 8.0). DNA concentration and purity was determined with a NanoDrop spectrophotometer. The genomic DNA of *M. tuberculosis* H37Rv was kindly provided by Prof. Dr. Franz Bange, Hannover Medical School. The *dnaN* genes were isolated from the genomic DNA by PCR using Taq polymerase according to the manufacturer's instructions. The resulting PCR products were ligated into the pJET1.2 cloning vector (Thermo Scientific) according to the manufacturer's instructions. The expression constructs were based on a modified pCOLADuet-1. The pJET1.2-dnaN construct and the modified pCOLADuet-1 expression construct were treated with appropriate restriction enzymes (PstI/NdeI for *S. caelicus dnaN* and NotI/NdeI for all other *dnaNs*) and the resulting *dnaN* fragment was ligated into the modified pCOLA-Duet-1 vector using T4-DNA-ligase (New England Biolabs) according to the manufacturer's instructions. For amplification, the different *dnaN* containing pJET1.2 and pCOLADuet-1 constructs were transformed into electrocompetenc *E. coli* HS996 by electroporation (1250 V, Eppendorf Eporator).

2.2.3 PROTEIN EXPRESSION AND PURIFICATION

(*) For protein expression the *dnaN* genes were heterologously expressed in *E. coli* BL21 (DE3) as fusion proteins consisting of full-length DnaN with N-terminal Strep-tag II and TEV-protease recognition site from a modified pCOLADuet-1 construct. The cells were grown in ZYM-5052 auto-inducing medium[159] at 20 °C for 20-24 h. The cell pellets were resuspended in Tris-HCl (pH 7.5, 20 mM)/NaCl (150 mM) and lysed by sonication. The proteins were isolated from the supernatant after centrifugation using a self-packed 10 mL column with Strep-Tactin Superflow High Capacity (IBA) and eluted from the column with a single step of 5 mM D-desthiobiotin. The affinity tag was cleaved off with TEV protease (1:50 mg/mg) at 4 °C overnight. The *M. smegmatis* protein was further purified by anion exchange with a MonoQ 10/10 column (GE Healthcare) using a linear gradient from 0 to 1 M NaCl in Tris-HCl (pH 7.5, 20 mM), while this step was omitted for the other proteins. Gel filtration was carried out as final polishing step with a HiPrep Superdex 200 16/60 GL column (GE Healthcare) in the storage buffer (20 mM Tris-HCl (pH 7.5)/20% glycerol for the *E. coli* DnaN and in 20 mM Tris-HCl (pH 7.5)/NaCl 150 mM for all other DnaN proteins). Chromatographic steps were carried out on an Äkta Purifier system (GE Healthcare). The samples were analyzed by SDS-PAGE (12%), and protein concentrations were determined from the absorbances at 280 nm using the NanoDrop device with the theoretical molare extinction coefficients as calculated by Protparam[160].

2.2.4 MIC DETERMINATION

(*) All microorganisms were obtained from the DSMZ and the ATCC or were part of the internal strain collection. MIC values for *M. bovis* were determined in 5 mL cultures (37 °C, 250 rpm, 3 weeks), and all other MIC values were determined in microdilution assays[161]. Overnight cultures were diluted in the appropriate growth medium to achieve a final inoculum of 10^4-10^6 CFU/mL. Yeasts and molds were grown in Myc medium (1 % phytone peptone, 1 % glucose, 50 mM HEPES, pH 7.0); *Streptococcus* species in tryptic soy broth (TSB: 1.7 % peptone casein, 0.3 % peptone soymeal, 0.25 % glucose, 0.5 % NaCl, 0.25 % K_2HPO_4; pH 7.3); and mycobacteria species in Middlebrook 7H9 medium supplemented with 10 % (*v/v*) Middlebrook albumin-dextrose-catalase enrichment and 2 mL/L glycerol. All other listed bacteria were grown in Müller-Hinton broth. Serial dilutions of compounds were prepared as duplicates in sterile 96-well plates. The cell suspension was added and microorganisms were grown on a microplate shaker (750 rpm, 30-37 °C, 18-48 h), except *S. pneumonia*, which was grown at non-shaking conditions (37 °C, 5% CO_2, 18 h). For cross-resistance evaluation, wild-type *M. smegmatis* mc^2155 was cultured in supplemented 7H9 broth for 3 days, and *M. smegmatis* mc^2155-Mt50.7 (GM resistant mutant) was cultured in the presence of 25 µg/mL GM for 4 days. Both cultures were diluted to approximately 10^6 CFU/mL for microdilution experiments. Growth inhibition was assessed by visual inspection in two independent experiments, and the MIC was defined as the lowest concentration of compound that inhibited visible growth. MIC values for *Streptomyces spp.* were determined by microbroth dilution in solid medium. A serial dilution of drugs was prepared in R2L medium (25 mM TES, 0.3% $CaCl_2 \times 2\ H_2O$, 0.01% casamino acids, 1% glucose, 0.5% yeast extract, 0.025% K_2SO_4, 7.3% mannitol, 1% $MgCl_2$, 0.7% low melting point agarose; pH 7.2) as duplicates in sterile 96-well plates. After solidification of the medium, 10 µl of a fresh spore suspension in 20% glycerol (2×10^7 CFU/ml) was added per well and the plates were incubated for 5 d at 28 °C. Growth inhibition was assessed by visual inspection in two independent experiments, and the MIC was defined as the lowest concentration of compound that inhibited visible growth.

2.2.5 SPR ANALYSES

Surface plasmon resonance (SPR) analyses were performed on a Biacore X100 system (GE Healthcare). All proteins were immobilized on a CM5 sensor chip (Biacore) by standard amine coupling. The sliding clamps (DnaN) of *M. smegmatis*, *M. tuberculosis*, *E. coli* and *S. caelicus* and GriR of *S. caelicus* were heterologously expressed as described above, diluted to 15, 20, 20, 50 and 25 µg/mL in 10 mM sodium acetate buffer (pH 5.0, 4.5, 5.5, 4.5 and 4.5), respectively, and immobilized for 100 to 200 sec so that the chip was finally loaded with protein at densities of around 800, 800, 4,000, 2,000 and 2,000 response units (RU), respectively. The human sliding clamp (PCNA) was ordered as glycosylated protein with a His_6-tag from Prospec (pro-303), diluted to 40 µg/mL in sodium acetate buffer (pH 5.5, 10 mM) and immobilized for 250 sec so that the chip was finally loaded with protein at a density of around 2700 RU. All measurements were performed in triplicate. Increasing concentrations of GM, MGM and CGM were injected over the sliding clamp proteins (*M. smegmatis* DnaN: 2, 4, 8, 16 and 32 nM; *M. tuberculosis* DnaN: 1, 2, 4, 8 and 16 nM; *E. coli* DnaN: 0.125, 0.250, 0.5, 1 and 2 µM; *S. caelicus* GriR: 1.5, 3.1, 6.3, 12.5 and 25 µM; *S. caelicus* DnaN: 2,

4, 8, 16 and 32 nM). Binding interactions were monitored at 25 °C with a flow rate of 30 µl min^{-1} in HBS-EP/1% DMSO as running buffer. The theoretical maximal RU (Rmax) was determined as follows: R_{max} = molecular weight $(MW)_{Analyte}$ (Da) ÷ MW_{Ligand} (Da) × immobilized ligand density (RU) × stoichiometric ratio (number of binding sites per ligand). The MW values for the *E. coli*, *M. tuberculosis*, *M. smegmatis* DnaN and *S. caelicus* DnaN and *S. caelicus* GriR proteins are 43,252, 41,652, 42,113 and 39,790 and 40,333 Da, respectively. The MW of the human PCNA is 29,794 Da. The MW values for GM, MGM and CGM are 1113.7, 1127.7 and 1195.8 Da, respectively. The stoichiometric ratio for all interactions was assumed to be 1. The resulting sensorgrams were double-referenced and solvent corrected, and the K_D values were calculated from the response data fitted to a model (the classical Langmuir binding model) with assumption of one GM binding site per sliding clamp monomer or from steady-state affinity analyses, using the Biacore X100 evaluation software 2.0.1. For SPR based inhibition assays, *M. smegmatis* DnaN was diluted to 20 µg/mL in 10 mM sodium acetate buffer (pH 5.0) and immobilized as described above, so that the chips were finally loaded with densities of around 1,500 RU. Measurements were performed in triplicate and with three independently prepared chips. HPLC-purified peptide containing the internal DnaN binding site from DnaE of *M. smegmatis* (amino acid sequence: KAEAMGQFDLFG) was ordered from Bio-Synthesis Inc. (Lewisville, Texas). For evaluation of the inhibition of the interaction of the *M. smegmatis* DnaE peptide with the *M. smegmatis* DnaN, 50 µM of the internal peptide was injected over untreated DnaN and over GM-saturated DnaN that was prepared by pre-injection of 200 nM GM. The resulting sensorgrams were double-referenced and solvent corrected, and the inhibition of the interaction was analyzed by comparison of the binding level achieved with untreated and with GM-saturated DnaN.

2.2.6 ITC ANALYSES

Isothermal titration calorimetry analyses were performed on a MicroCal ITC200 titration system (MicroCal Inc., GE Healthcare). The *E. coli* DnaN protein was stored in buffer containing 20 mM Tris-HCl (pH 7.5)/20 % glycerol and all other DnaN proteins were stored in buffer containing 20 mM Tris-HCl (pH 7.5)/ 150 mM NaCl/ 10% glycerol. Griselimycin was dissolved in DMSO and diluted in the according protein storage buffer resulting in a final DMSO concentration between 1 and 2 % DMSO. Before start of the experiment between 1 and 2 % DMSO were added to the protein solutions to match the protein buffer with the ligand (griselimycin) buffer. The reference cell was loaded with degassed water. The sample cell was rinsed (3x) with buffer and then filled with 0.1 mM protein solution. The syringe was rinsed with buffer and then loaded with GM in 10fold excess to the protein (i.e. 1 mM GM). Experiments were performed at 25°C by one pre-injection (0.8 µL, 1.6 s) followed by 18 injections (2 µL, 4 s) with 180 seconds spacing time between injections and with a stirring speed of 500-1000 rpm. Heat signals were corrected for the heats of dilution by substracting the final baseline comprised of small peaks of the same size. The raw data was fitted to a theoretical titration curve using the Origin7 sofware provided by the manufacturer. Thereby the stoichiometric ratio for all interactions was assumed to be 1. Thermodynamic parameters

were calculated from $\Delta G = \Delta H - T\Delta S = RT\ln K_A = -RT\ln K_D$ (ΔG (kcal mol^{-1}): Gibbs free energy, ΔH (kcal mol^{-1}): enthalpy, ΔS (cal mol^{-1} deg): entropy, T (K) = absolute termperature, R (gas constant) = 1,987 cal mol^{-1} K^{-1}).

2.2.7 X-RAY CRYSTALLOGRAPHY

* Crystallization trials were set up at room temperature with a HoneyBee 961 crystallization robot (Digilab Genomic Solutions) in Intelli 96-3 plates (Art Robbins Instruments) with 200 nL protein solution at different concentrations and 200 nL reservoir solution. A crystal from a GM containing *M. smegmatis* DnaN sample (2.5 mg/mL protein, 1.25 mM GM, 1.25 % (*v/v*) DMSO) that was obtained in 370 mM $MgCl_2$, 7.33 % (*v/v*) Glycerol, 25.6 % (*w/v*) Jeffamine M-2070, 100 mM Tris-HCl pH 8.56 was cryoprotected by quick-soaking in the reservoir solution with added 10 % (*v/v*) glycerol, and a dataset was recorded at the beamline P11 at PETRA III, DESY, Hamburg, Germany. A crystal of *M. smegmatis* DnaN containing CGM (5 mg/mL protein, 2.5 mM CGM, 2.5 % (*v/v*) DMSO) has been obtained in 200 mM $MgCl_2$, 16.3 % (*v/v*) glycerol, 12.2% (*w/v*) PEG 3350, 100 mM Tris-HCl pH 7.44, and a dataset was recorded at the beamline X06DA at the Swiss Light Source, Paul Scherrer Institute, Villigen, Switzerland. A crystal from a GM containing *M. tuberculosis* DnaN sample (5 mg/mL protein, 2.5 mM GM, 2.5 % (*v/v*) DMSO) was obtained in 21.2 % (w/v) PEG 3000, 100 mM Tris- HCl pH 7.67. For a CGM containing *M. tuberculosis* DnaN sample (5 mg/mL protein, 2.5 mM CGM, 2.5 % (*v/v*) DMSO), a crystal was obtained in 333 mM $CaCl_2$, 144 mM Lithium acetate, 11.7 % (*w/v*) PEG 8000, 100 mM HEPES-NaOH pH 7.58. Both *M. tuberculosis* DnaN crystals were cryoprotected by quick-soaking in the reservoir solution with added 10 % (*v/v*) (2R,3R)-butane-2,3-diol, and datasets were recorded at the beamline 14.1 at BESSY II, Berlin, Germany. All datasets were recorded at a temperature of 100 K at a wavelength of λ = 1.0 Å. The datasets were processed using the Autoproc[162] toolbox (Global Phasing) executing XDS[163], Pointless[164] and Aimless[165]. High resolution cutoffs of 2.13 Å for the GM and 2.31 Å for the CGM containing datasets of *M. smegmatis* DnaN and 2.17 Å for the GM and 1.93 Å for the CGM containing *M. tuberculosis* protein were determined based on CC1/2[166] and I/σI values (Table 6-1). Molecular replacement was carried out using Phaser[167] from the Phenix suite[168] with the crystal structure of *M. tuberculosis* sliding clamp (PDB: 3P16)[169], 77% sequence identity to *M. smegmatis* DnaN). The structural models were built using Coot[170] and crystallographic refinement was performed with Phenix.refine[171] including TLS-refinement. In all crystal structures, GM and CGM were modelled with an occupancy of 1.0. Figures of crystal structures were prepared using PyMOL Molecular Graphics System Version 1.7.2.0. Electrostatic surface potentials were calculated using APBS[172]. Ligand interaction diagrams were generated with Ligplot+[173]

2.2.8 SEQUENCE AND PHYLOGENY ANALYSES

(*) Genome sequencing of wild-type and GM resistant *M. smegmatis* strains was performed using paired-end Illumina technology. Resulting short reads (110 bp) were mapped to the reference genomic sequence available from GenBank (accession number NC_008596) by Geneious software[174] under “low sensitivity” settings. The resulting assembly file was

exported and later analyzed for the presence of single nucleotide polymorphisms and small indel rearrangements by GATK toolkit[175]. Sequence data of the wild-type and GM resistant *M. tuberculosis* strains were obtained with paired-end Illumina technology (250 bp) and subsequently analyzed in the same way, using the genomic sequence of *M. tuberculosis* H37Rv as a reference (accession number NC_000962). Alignment of whole genomes of reference and mutant strains was done by MAUVE 2.3.1[176]. Start and end of amplified chromosomal regions were determined by analyzing localizations of clustered micro-heterogeneities within aligned sequencing data in Geneious software. Multiple amplification events of different sizes were discerned with the help of their variable sequencing read coverage. The approximate copy number of the amplicons was determined by the ratio of the mean sequencing read coverage of the amplicon divided by the mean sequencing read coverage of the bacterial chromosome. The total size of the amplified region was determined by the amplicon unit size multiplied by the amplicon copy number in case of one amplicon type. In cases of variable amplicon lengths, this was repeated for each amplicon type, and the products were then added. Mean sequencing read coverage was calculated in Geneious software. Protein homology analyses were performed using BLAST[177] and Geneious software. Sequence data of DnaN homologs were obtained from the NCBI protein database. The *in silico* search for potential secondary metabolite biosynthesis gene clusters was performed using the software antismash[178] (antibiotics and secondary metabolite analysis shell). Phylogenetic trees were generated from protein sequence alignments using Geneious software and MrBayes[179] program version 3.2.1.

2.2.9 TIME-KILL CURVE *M. TUBERCULOSIS*

* Frozen stocks of *M. tuberculosis* strain H37Rv were thawed and used to start cultures in early logarithmic growth in Middlebrook 7H9 broth supplemented with 10 % (*v/v*) OADC, 0.4 % (*v/v*) glycerol and 0.05 % (*v/v*) Tween-80, at a density of 5×10^5 CFU/mL, as confirmed by quantitative plate counts. Compounds were solubilized and diluted in pure DMSO (to a final DMSO concentration of 1 %). These cultures were exposed to a range of compound concentrations or to a 1 % DMSO non-compound containing control in 125 mL Erlenmeyer flasks (25 mL/flask) for 14 days at 37 °C under shaking conditions. On days 2, 4, 7, 10 and 14, samples (500 µL) were taken for quantitative CFU plate counts. In order to prevent drug carry-over, samples were washed once by centrifugation at 14,000 × g for 10 min, resuspending the bacterial pellet in PBS. The washed suspensions were serially diluted in PBS and plated onto antibiotic-free 7H10 agar plates supplemented with OADC. After 21 days of incubation at 37 °C and 5 % CO_2, CFU counts were determined. Log_{10} CFUs were plotted against time in days to obtain time-kill curves.

2.2.10 MIC DETERMINATION *M. TUBERCULOSIS*

* Minimum inhibitory concentrations (MICs) of test compounds for *M. tuberculosis* strains were determined as described.[180] Rifampicin (RIF) and isoniazid (INH) were used as positive controls. Compound stock solutions, as well as dilutions, were prepared in DMSO. Compound dilutions or DMSO only (2 µL) were added to 100 µL Middlebrook 7H12 broth

(Middlebrook 7H9 broth containing 0.1 % w/v casitone, 5.6 µg/mL palmitic acid, 5 mg/mL bovine serum albumin, 4 µg/mL catalase). *M. tuberculosis* (100 µL of 10^5 CFU/mL culture in 7H12 broth) was added in 96-well microplates (black viewplates), yielding a final testing volume of 200 µL. The plates were incubated at 37 °C and 5 % CO_2 in plastic bags. On the sixth day of incubation, 50 µL of Alamar Blue (Promega) with 5 % v/v Tween-80 were added to each well; plates were then incubated at 37 °C for 16-24 h, and fluorescence of the wells was measured (λ_{ex} = 530 nm, λ_{em} = 590 nm). The MIC_{80} was defined as the lowest concentration affecting an 80 % reduction in fluorescence relative to the signal for the no drug control. For the determination of MICs against *M. tuberculosis* in macrophages, RAW264.7 murine macrophage-like cells (American Type Culture Collection [ATCC] #TIB-71) were grown at 37 °C with 5 % CO_2 in RAW medium (Dulbecco's modified Eagle medium supplemented with 10 % fetal calf serum, 4 mM L-glutamine and 1 mM sodium pyruvate). Macrophages were seeded the day of the infection and separated into two flasks. One flask was used as the non-infected control. Green fluorescent protein (GFP)-expressing *M. tuberculosis* H37Rv were cultured for 6 days at 37 °C in Middlebrook 7H9 medium supplemented with 10 % (*v/v*) oleic acid-albumin-dextrose-catalase (OADC), 0.4 % (*v/v*) glycerol and 0.05 % (*v/v*) Tween80. All mycobacteria were used at late log phase to inoculate the second flask containing the RAW264.7 cells. Cells were infected in batch at a multiplicity of infection of 2 and incubated for 2 h at 37 °C with weak agitation. Cells were then washed twice with RAW medium to remove extracellular bacteria. The infected cells were added, at a concentration of 10^5 infected cells/well, to 96-wells plates (clear bottom black poly-D-lysine coated) containing the compounds to be tested. Uninfected and infected compound-free controls were included in the plates. INH and amikacin were used as positive and negative references, respectively. Plates were incubated for 4 days at 37 °C and 5 % CO_2. Infection was stopped by fixation of wells with 4 % paraformaldehyde for 30 min at room temperature. The infected macrophages were stained with Cell Mask Blue (Invitrogen) diluted (1/5,000) in PBS/0.1 % (*v/v*) Triton for 15 min at room temperature. The plates were washed with PBS prior to image acquisition. Images were recorded on an automated fluorescent microscope Cellomics ArrayScan VTI HCS reader (Thermo). Each image was processed using the SpotDetector V3 BioApplication. The number of objects acquired per well was fixed (3,000 macrophages). Images contained two channels: one for the cell nuclei (Ch1; blue channel, Hoechst) and one for GFP-expressing M. tuberculosis (Ch2; green channel, FITC). For each well the intensity of green fluorescence per cell was recorded. This value was used to calculate the percent inhibition. The MIC_{80} was defined as the lowest drug concentration affecting signal inhibition of 80 % relative to the signal for the high control.

2.2.11 MTT VIABILITY ASSAY

Cells were seeded into 96-well plates (Corning CellBind) with 10^4 cells/well in 180 µl medium supplemented with 10 % FBS (F12 medium for CHO-K1 cells, RPMI 1640 medium for L929 cells, DMEM medium for RAW264.7 cells) and incubated for 2 h at 37 °C and 5 % CO_2 and afterwards treated solvent control or with compounds in serial dilution. After incubation for 5 days, 50 µg/ml per well MTT (thiazolyl blue tetrazolium bromide) in PBS

was added and the cells were incubated for 1-3 h at 37°C.[181] The supernatant was discarded, the cells were washed with 100 µl PBS and 100 µl 2-propanol/10 M HCl (250:1) were added to dissolve the formazan granules. The absorbance of the reduced MTT at 570 nm was measured using a microplate reader (Infinite 200 Pro, Tecan Group Ltd.) and the the fraction of viable cells was determined relative to the respective solvent control. IC_{50} values were determined by sigmoidal curve fitting (dose-response analysis) using Origin6.1G.

2.2.12 MICRONUCLEI GENOTOXICITY TEST

* Chinese hamster ovary (CHO-K1) cells were maintained in 90 % Ham's F12 medium with 10 % heat-inactivated fetal bovine serum at 37 °C and 5 % CO_2. For genotoxicity studies the cells were seeded at 5×10^3 cells/well in black 96-well plates (with optical bottom) and allowed to adhere for 1d prior to the addition of compound. GM, MGM, CGM and mitomycin C (positive control) were added to a final concentration of 10 µM (GMs) and 100 ng/ml (mitomycin C). The cells were treated for 48 h, washed twice with PBS (pH 7.4) and fixed using AcO/MeOH (1:1, -20°C) for 10 min at room temperature. After repeated washing with PBS, nuclei were stained with 5 µg/mL Hoechst33342 in PBS for 15 min at room temperature protected from light. After washing the samples were imaged (200x magnification) on an automated microscope (Pathway855, BD Biosciences) with an appropriate filter set. All samples were prepared and analyzed as triplicates in two independent experiments.

2.2.13 GENE EXPRESSION ANALYSIS

For the analysis of the SOS response induction *M. smegmatis* mc^2155 cells were cultured in Middlebrook 7H9 medium supplemented with 10 % Middlebrook albumin-dextrose-catalase enrichment and 2 mL/L glycerol. In the early logarithmic phase cultures were treated with 1 µg/mL GM and further cultivated over a period of 10 h. Samples were taken from three independent GM exposed cultures at 0, 2.5, 5 and 10 hours and from one unexposed culture at time point zero as a reference and immediately frozen in liquid nitrogen and stored at -80°C. Cells were lysed using a FastPrep-24 homogenizer and microtubes with Lysing Matrix D (MP Biomedicals). The RNA was extracted using the miRNeasy mini kit (Qiagen). The RNA was quantified using the NanoDrop 2000c spectrophotometer. The cDNA was synthesized using the RevertAid reverse transcriptase (Thermo Scientific) according to the manufacturer's protocol. Quantification of gene expression was conducted on a peqSTAR96Q thermal cycler (Peqlab) using 1:100 diluted cDNA and primer pairs for *recA* (forward primer: 5' – GAG TTC GAC ATC CTC TAC GG – 3', reverse primer: 5' – CTT CTT CTC GAT CTC GTT GGC – 3'), *lexA* (forward primer: 5' – CAC CAT CCT CGA GGT CAT C – 3', reverse primer: 5' – GAT ACC CCT TGC GTT CGA G – 3'), *dnaE2* (forward primer: 5' – CAG GTT CTA CGA CGG GAT G – 3', reverse primer: 5' – GCT TGA ACC ACG ACG AGT AG – 3'), *dnaB* (forward primer: 5' – GAG CAC GAT GTC TAC GAC G – 3', reverse primer: 5' – CAA GGA TGA TGT CGG CTT C– 3'), and the 16S rRNA (forward primer: 5' – TCA CGA ACA ACG CGA CAA ACC – 3', reverse primer:5' – GTA TGT GCA GAA GAA GGA CCG – 3'). Target genes were amplified using the Dynamo Colorflash SYBR green qPCR kit (Biozym) in 10 µL reaction mixtures according to the manufacturer's

protocol. Each measurement was performed in triplicate and from three independent cultures, including a control without reverse transcriptase for each sample. Relative gene expression was calculated using the $2^{-\Delta\Delta Ct}$ method, normalizing all genes to the 16S rRNA gene, which is considered to be constant under stress conditions. All gene expression levels were referenced to the according gene of an untreated control sample. For the analysis of the influence of the *dnaN* promoter mutation on the *dnaN* gene expression level *M. smegmatis* mc^2155 WT and GM resistant *M. smegmatis* mutant 1.GM2.5 were cultivated in Middlebrook 7H9 medium supplemented with 10 % Middlebrook albumin-dextrose-catalase enrichment and 2 mL/L glycerol without and with 2.5 µg/mL GM, respectively. In the mid-logarithmic phase cultures were harvested by centrifugation and immediately frozen in liquid nitrogen and stored at -80°C. The cells were lysed and the RNA was extracted, quantified and reverse transcribed as described above. Quantification and evaluation of gene expression was conducted as described above using primer pairs for *dnaN* (forward primer: 5' – CTT GAA GTT TCG CGT CGT CC– 3', reverse primer: 5' – CGA TTT CAG CGC TCA CCT TG– 3') and 16S rRNA (see primer sequences above).

2.2.14 SELECTION OF GM-RESISTANT BACTERIA *IN VITRO*

GM resistant *M. smegmatis* mc^2155 were selected *in vitro* by stepwise increasing the concentration of GM (2.5, 5, 10, 20, 40 µg/mL) and inoculation of resistant colonies obtained on agar plates in liquid medium in an iterative process. In total, ten independent mutants were generated in five sequential steps. Genomic DNA from all five steps and the retrospective wild-type parent colonies of five independent mutants was prepared by an enzymatic procedure as described in section 2.2.2. In order to determine the frequency of spontaneous resistance to GM, log-phase bacterial cell suspensions were adjusted in supplemented Middlebrook 7H9 broth to a final concentration of 3.5×10^{10} CFU/mL and streaked out on five replicate Middlebrook 7H10 agar plates (supplemented with Middlebrook OADC enrichment and 2 mL/L glycerol) containing GM at either two or five times the MIC. In addition, several dilutions of the *M. smegmatis* mc^2155 culture were streaked out on plates containing no antibiotic. After 9 days, frequencies of resistance were determined by dividing the CFUs on GM-containing plates by the number of CFUs on GM-free plates. In order to analyze the fitness cost of GM mutants, the initial wild-type $1.GM_0$, and mutants $1.GM_{40}$, $1.GM_{40\rightarrow 0}$ and mutant $1.GM_5$ were inoculated in 60 mL supplemented Middlebrook 7H9 broth with zero, 40, zero or 5 µg/mL GM, respectively, and bacterial growth was monitored over five days by continuous sample drawing of 100 to 400 µL and measurement of the optical density at 600 nm in microcuvettes. Morphological changes of *M. smegmatis* cells induced by prolonged GM exposure were analyzed by light microscopy of cells. Genomic analyses of resistant and wild-type *M. smegmatis* mc^2155 cells were performed as described in section 2.2.8.

2.2.15 SELECTION OF CGM-RESISTANT BACTERIA *IN VIVO*

* To select for CGM-resistant bacteria in vivo, six-week-old nude mice (purchased from Charles River Wilmington, MA, USA) were infected with 3-3.5 $\log_{10}$ CFU by aerosol

infection with *M. tuberculosis H37Rv*, and treatment (monotherapy with either CGM at 100 mg/kg or with INH at 5 mg/kg) was initiated 2 weeks after infection and administered daily (5 days per week, Monday-Friday) by oral gavage for 12 weeks. All animals were cared for in strict accordance with the guidelines of and the protocols approved by the University's Animal Care and Use Committee (Protocol MO10M59). CGM was prepared as a suspension in 0.6 % methylcellulose with 0.5% Tween80. Groups of 3-4 mice were sacrificed after 4, 8 and 12 weeks of treatment for determination of lung CFU counts, and homogenates were directly plated on plain and drug-containing 7H11 selective agar plates (INH: 0.1 µg/mL; CGM: 0.125 and 0.25 µg/mL). The MIC values of isolated CFUs obtained at Day 0 (pre-treatment) and at Week 12 for INH and CGM were determined using the indirect agar proportion method as previously described (41), using the following concentrations (µg/mL): INH, 0.012, 0.025, 0.05, 0.125, 0.25, 0.5 and 1.0; CGM, 0.015, 0.03, 0.06, 0.125, 0.25, 0.5, 1.0, 2.0, 4.0 and 8.0. Drug susceptibility testing of CGM-resistant *M. tuberculosis* was also assessed by the indirect agar proportion method for the following drugs (breakpoint concentrations): isoniazid (0.2 µg/mL), rifampin (1.0 µg/mL), moxifloxacin (0.5 µg/mL) and streptomycin (1.0 µg/mL). Genomic analyses of resistant and wild-type *M. tuberculosis* H37Rv cells were performed as described in section 2.2.8.

2.2.16 SOUTHERN BLOTTING

Southern blot hybridization was performed according to standard protocols.[182] Briefly, 10 µg genomic DNA of each sample was digested with EcoRI for 8 hours and separated by agarose gelelectrophoresis. The gel was incubated in 250 mM HCl for 15 min, afterwards 2 times in denaturation buffer for 15 min each time, afterwards 2 times in neutralization buffer for 15 min each time and finally in 20xSSC buffer. The genomic DNA was blotted on a nylon membrane (Roche) over night. The membrane was washed in 0.4 M NaOH for 1 min and afterwards in 0.25 M Tris-HCl (pH 7.5) and afterwards dried at 80°C for 2 hours. The probe was generated by PCR using genomic DNA as template (forward primer 5' – CAA GGT GAG CGC TGA AAT CG-3', reverse primer 5'-ATG GCC TCG GCG AAC AGA TC – 3') together with DIG-labeled dNTP, purified using the a kit for PCR clean up (Macherey-Nagel) and denaturated for 10 min at 100°C and chilled on ice. The probe (2 µg) was mixed with DIGEasyHyb (Roche), incubated at 37 °C over night and mixed with DigEasyHyb solution (Roche). The probe containing solution was incubated with the membrane at 42 °C over night for hybridization. The membrane was washed 2 times with 2 x washing buffer for 20 min at room temperature and afterwards 2 times with 0.5 x washing buffer for 20 min at 58 °C and finally with blocking reagent (Roche) for 1 hour at room temperature. The membrane was incubated with anti-digoxigenin-antibody in blocking buffer for 30 min, afterwards washed with Dig1 buffer 2 times for 15 min, afterwards rinsed with Dig2 buffer and finally incubated in Dig3 buffer for 2-5 min. Reactions were detected using the chemiluminescent reagent CPD-Star (Roche). Chemiluminescence signals were detected using the Fusion FX7 system (Vilber Lourmat), and images were processed regarding brightness and contrast using the corresponding software FusionCapt Advance FX7 16.06 (Vilber Lourmat).

3 RESULTS

3.1 SELF-RESISTANCE TO GRISELIMYCINS IN *STREPTOMYCES CAELICUS*

To evaluate if the *griR* gene located in the GM cluster is responsible for the GM self-resistance in *S. caelicus*, *griR* was transferred into the GM sensitive *S. coelicolor* and the GM susceptibility was tested in comparison to the wildtype strain and the empty vector control (Table 3-1). As a result, the *S. coelicolor* wildtype and the *S. coelicolor* containing the empty vector were both sensitive to GM and MGM (MIC: 7 µg/mL for GM and MGM for both strains) whereby the *S. coelicolor* overexpressing *griR* was resistant to GM and MGM (MIC: > 55 µg/mL for GM and MGM). All three *S. coelicolor* strains (the wildtype, the empty vector control and the *griR* overexpressing strain) were not sensitive to CGM, which might be a matter of solubility of CGM in solid medium (susceptibility testing for organisms other than *Streptomyces* was performed in liquid media).

Table 3-1: GM susceptibility of *S. coelicolor* wildtype and *S. coelicolor* with the *griR* containing vector (pGri17) and the empty vector (pSET-PermE*) (modified from reference 154).

Organism	MIC (µg/mL)		
	GM	MGM	CGM
Streptomyces coelicolor A3(2)	7.0	7.0	>55
Streptomyces coelicolor::pSET-*PermE** (empty vector)	7.0	7.0	>55
Streptomyces coelicolor::pGri17 (*griR*-expressing)	>55	>55	>55

The sequence and the gene context of the *dnaN* genes were examined to confirm that the *dnaN* genes were correctly classified as the conventional and the additional *dnaN* gene of *S. caelicus*. The *dnaN* gene is usually surrounded by *dnaA*, *recF* and *gyrB,* and this was also observed for *dnaN* of *S. caelicus* (Figure 3-1). In contrast, *griR* of *S. caelicus* is surrounded by genes of the GM biosynthesis cluster (Figure 3-2) and was therefore classified as the additional *dnaN* homolog.

The amino acid sequences of the conventional sliding clamp (DnaN) and of the additional sliding clamp (GriR) of the GM producing *S. caelicus* show 51 % amino acid identity to each other (Figure 3-3). For comparison, the sliding clamp sequences of other *Streptomyces* strains with published genome sequences were also analyzed. Several other *Streptomyces* genomes

also show signs of second homologs of *dnaN* genes. Thereby the conventional DnaN is designated as DnaN1 and the additional DnaN is designated as DnaN2. From the compared *Streptomyces* strains the DnaN1 proteins show amino acid similarities of < 54 % to other DnaN2 proteins and similarities of > 89 % to other DnaN1 proteins and cluster in one branch of the according phylogenetic tree (Figure 3-4, Figure 6-1, Table 6-2). In contrast, the amino acid similarities of the different DnaN2 genes range between 35 - 99 % to each other. Except for the *S. caelicus* GriR, none of the *Streptomyces* DnaN2 genes was found to be located inside of a secondary metabolite biosynthetic gene cluster, as predicted by antismash[178] (a software for the identification and analysis of secondary metabolite biosynthesis gene clusters in the genome of bacteria and fungi).

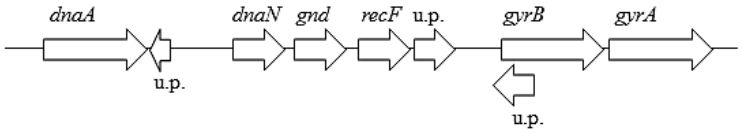

Figure 3-1: Gene environment of the *dnaN* gene of *Streptomyces caelicus* DSM40835. u.p.: uncharacterized protein. DnaA: chromosomal replication initiator protein. DnaN: DNA polymerase III subunit beta. Gnd: 6-phosphogluconate dehydrogenase., RecF: DNA recombination protein. GyrB: DNA gyrase subunit B. GyrA: DNA gyrase subunit A.

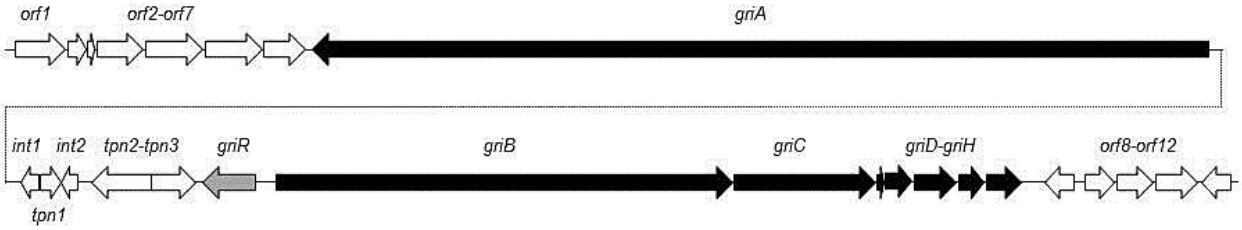

Figure 3-2: GM biosynthesis gencluster of *S. caelicus* DSM40835.[147] Orf1, Orf12: XRE family transcriptional regulators, Orf2, Orf3, Orf4, Orf9, Orf10: Hypothetical proteins, Orf5: Amino acid permease, Orf6: Glutamine synthetase, Orf7: Phosphotransferase enzyme family, GriA, GriB, GriC: Nonribosomal peptide synthetase, Int1, Int2: Integrase catalytic regions, Tnp1, Tnp2, Tnp3: Transposases, GriR: DNA polymerase III beta subunit, GriD: MbtH-like protein, GriE: Leucine hydroxylase, GriF: Alcohol dehydrogenase, GriG, Alpha/beta hydrolase, GriH: Oxidoreductase, Orf8: Pyridoxamine 5'-phosphate oxidase family protein, Orf11: Amidohydrolase family protein.[154]

Figure 3-3: Alignment of the amino acid sequences of the conventional sliding clamp (DnaN) and the additional sliding clamp (GriR) of the GM producing strain *Streptomyces caelicus* DSM40835. The sliding clamps show 51 % similarity to each other.

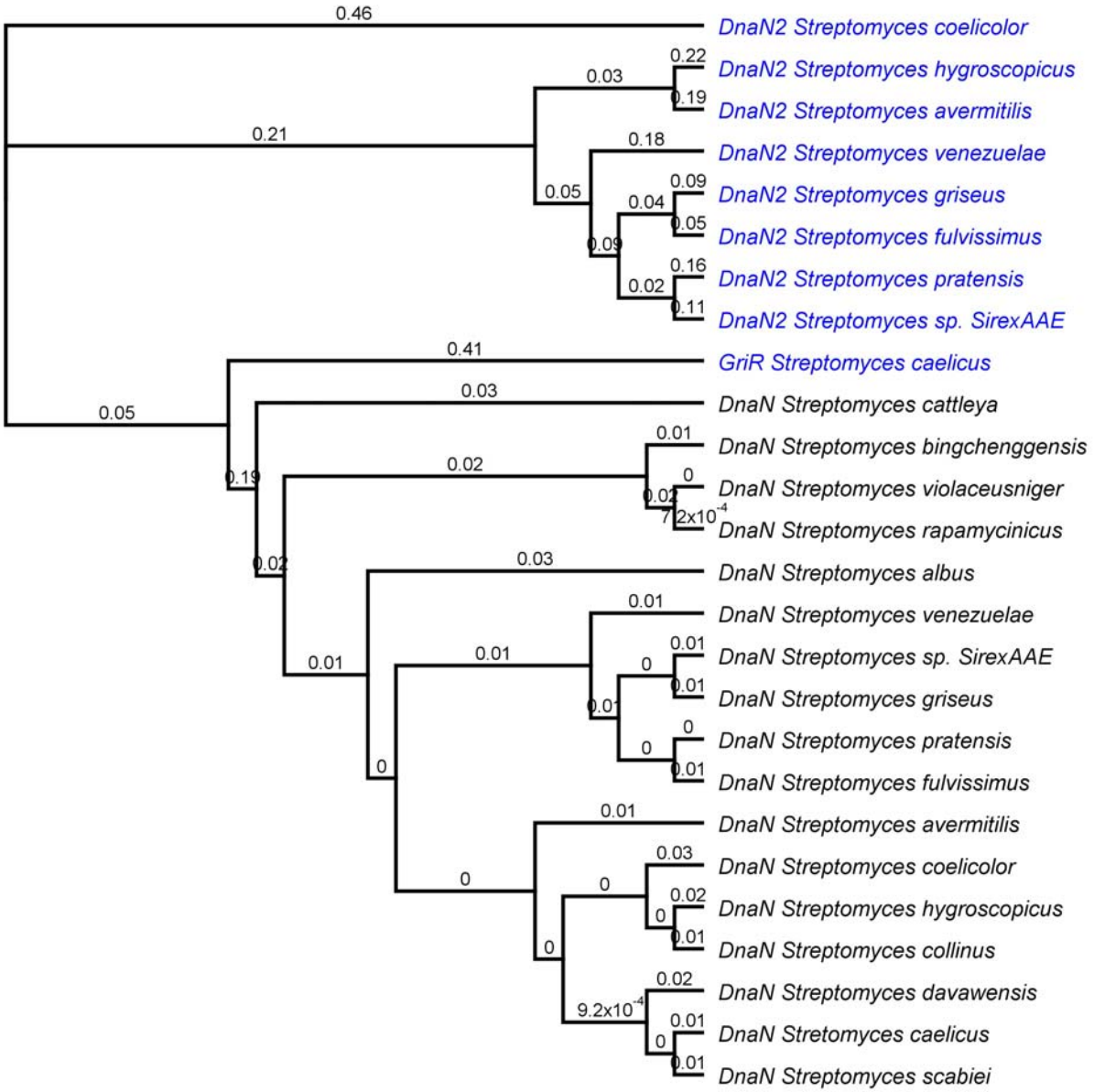

Figure 3-4: Phylogenetic tree (derived by the tree builder method implemented in the geneious software and based on the alignment in Figure 6-1) of amino acid sequences of DnaN1 and DnaN2 of different *Streptomyces* strains with available genome sequences including DnaN and GriR of *S. caelicus*. Second DnaN copies (DnaN2) are marked in blue. Evolutionary distances (substitutions/site) are indicated on each branch of the tree. GeneInfo Identifier (gi) numbers of the sequences used in this analysis are as follows: DnaN *S. coelicolor A3(2)*, 21222286; DnaN *S. griseus*, 182437494; DnaN *S. albus*, 478689546; DnaN *S. avermitilis*, 29830860; DnaN *S. bingchenggensis*, 374988140; DnaN *S. cattelya*, 386356756; DnaN *S. collinus Tu*, 529226638; DnaN *S. davawensis JCM*, 471324000; DnaN *S. fulvissimus*, 488611034; DnaN *S. hygroscopicus TL01*, 474983487; DnaN *S. pratensis*, 357412382; DnaN *S. rapamycinicus*, 557687913; DnaN *S. scabiei*, 290959003; DnaN2 *S. coelicolor* A3(2), 695227561; DnaN2 *S. griseus*, 182437190; DnaN2 *S. hygroscopicus* TL01, 474984464; DnaN2 *S. pratensis*, 357412572; DnaN2 *S. sp. SirexAAE*, 345000616; DnaN2 *S. venezuelae*, 408680935.

The binding of GMs to DnaN of *S. caelicus* was examined by surface plasmon resonance (SPR) spectroscopy (Figure 3-5, Table 3-2). Therefore, the DnaN of *S. caelicus* was immobilized to a sensor chip by standard amine coupling and increasing concentrations of GM, MGM and CGM were injected over the chip. As a result, significant interactions of GM, MGM and CGM with the *S. caelicus* DnaN were observed. GMs bind to the *S. caelicus* DnaN with high affinity with equilibrium dissociation constants (K_D) in the picomolar range (K_D GM: 3.2 x 10^{-10} M, K_D MGM: 4.2 x 10^{-10} M, K_D CGM: 0.1 x 10^{-10} M) and dissociate slowly from the DnaN protein, as indicated by low dissociation rate constants (k_d) and high dissociative half-lifes ($t_{1/2}$) (GM: k_d: 2.2 x 10^{-3} s^{-1} and $t_{1/2}$: 349 s, MGM: k_d: 1.6 x 10^{-3} s^{-1} and $t_{1/2}$: 465 s, CGM: k_d: 8.3 x 10^{-3} s^{-1} and $t_{1/2}$: 85 s). GM, MGM and CGM bind to *S. caelicus* DnaN with association rate constants (k_a) of 7.0 x 10^6 $M^{-1}s^{-1}$, 3.8 x 10^6 $M^{-1}s^{-1}$ and 7.8 x 10^6 $M^{-1}s^{-1}$, respectively. The kinetic profile of GM, MGM and CGM is similar, whereby the dissociation rate of CGM is somewhat slower.

To analyze if GMs also bind to the resistance protein GriR of *S. caelicus*, SPR based binding analyses were also performed with GriR (Figure 3-6). As a result, binding was also observed to *S. caelicus* GriR, but with lower affinity with equilibrium dissociation constants in the micromolar range (K_D GM: 5.8 x 10^{-6} M, K_D MGM 6.6 x 10^{-6} M and K_D CGM: 6.5 x 10^{-6} M). The association to and dissociation from the GriR protein by GMs was too fast to reliably determine the association and dissociation rate constants. K_D values were therefore determined by steady state affinity analyses from the dependence of steady-state binding levels on analyte concentrations.

Table 3-2: Kinetic parameters of the interaction of GMs with DnaN and GriR of *S. caelicus* as determined by surface plasmon resonance (SPR) spectroscopy. For interactions with *S. caelicus* DnaN, the K_D values were determined from the ratio between the kinetic rate constants (k_a/k_d); the dissociative half-life $t_{1/2}$ was calculated by $\ln 2/k_d$. For interactions with *S. caelicus* GriR the K_D values were determined by steady-state affinity analyses due to the fast on- and off-rates of the interactions. Data represent the mean and the standard deviation (SD) from three independent experiments. n.a.: not applicable. The kinetic parameters of the interaction with GriR were previously published in reference 154.

Interactants		K_D (M)	k_a ($M^{-1}s^{-1}$)	k_d (s^{-1})	$t_{1/2}$ (s)
Protein	Compound	[SD]	[SD]	[SD]	[SD]
$DnaN_{S.\ caelicus}$	GM	3.2×10^{-10}	7.0×10^{6}	2.2×10^{-3}	349
		$[1.6 \times 10^{-11}]$	$[2.3 \times 10^{6}]$	$[7.4 \times 10^{-4}]$	[123]
	MGM	4.2×10^{-10}	3.8×10^{6}	1.6×10^{-3}	465
		$[7.8 \times 10^{-11}]$	$[6.3 \times 10^{5}]$	$[4.4 \times 10^{-4}]$	[145]
	CGM	1.1×10^{-9}	7.8×10^{6}	8.3×10^{-3}	85
		$[5.0 \times 10^{-11}]$	$[1.2 \times 10^{6}]$	$[1.2 \times 10^{-3}]$	[12]
$GriR_{S.\ caelicus}$	GM	5.8×10^{-6}	n.a.	n.a.	n.a.
		$[1.4 \times 10^{-6}]$			
	MGM	6.6×10^{-6}	n.a.	n.a.	n.a.
		$[6.8 \times 10^{-7}]$			
	CGM	6.5×10^{-6}	n.a.	n.a.	n.a.
		$[3.2 \times 10^{-7}]$			

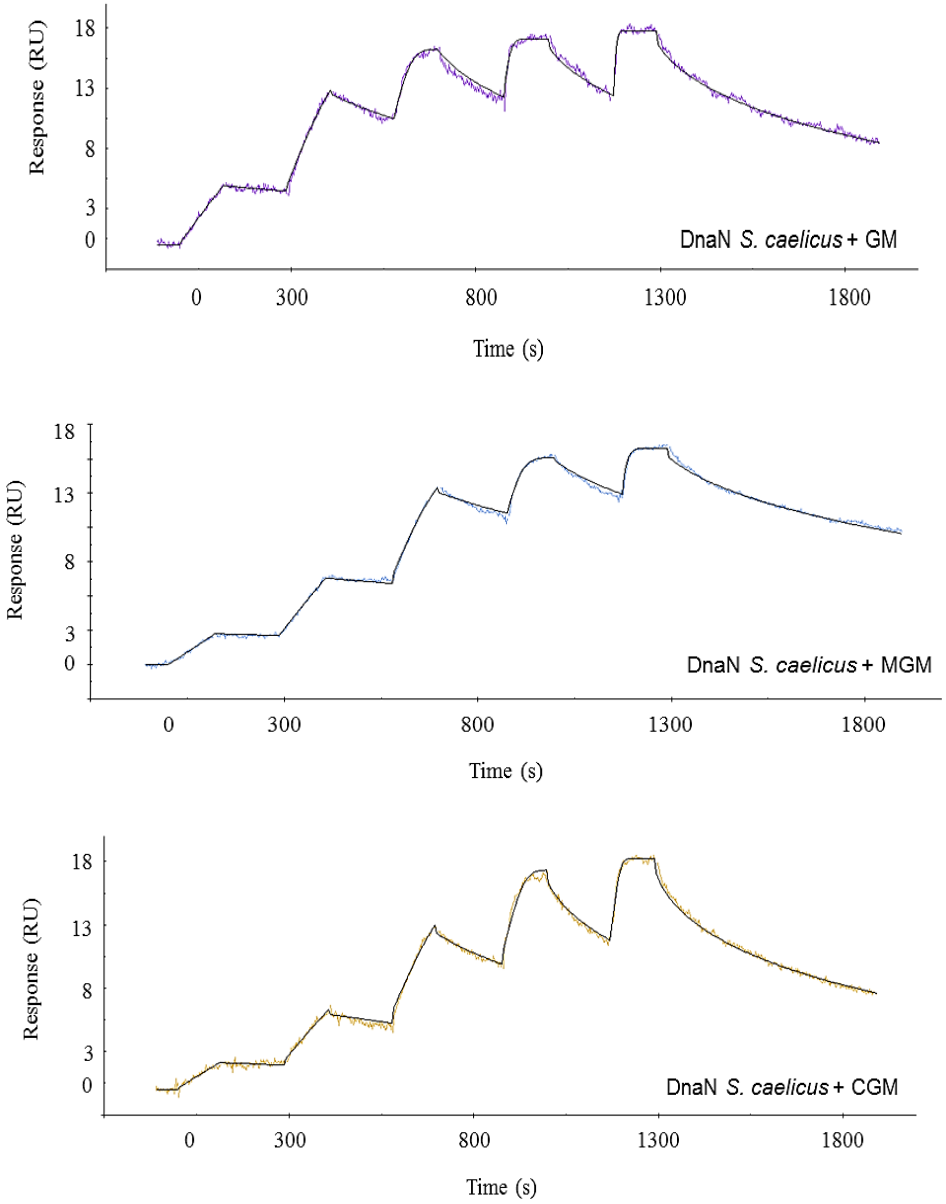

Figure 3-5: SPR sensorgrams of binding of GM (upper image), MGM (middle image) and CGM (lower image) to DnaN of *S. caelicus*. Shown are representative images from triplicate measurements.

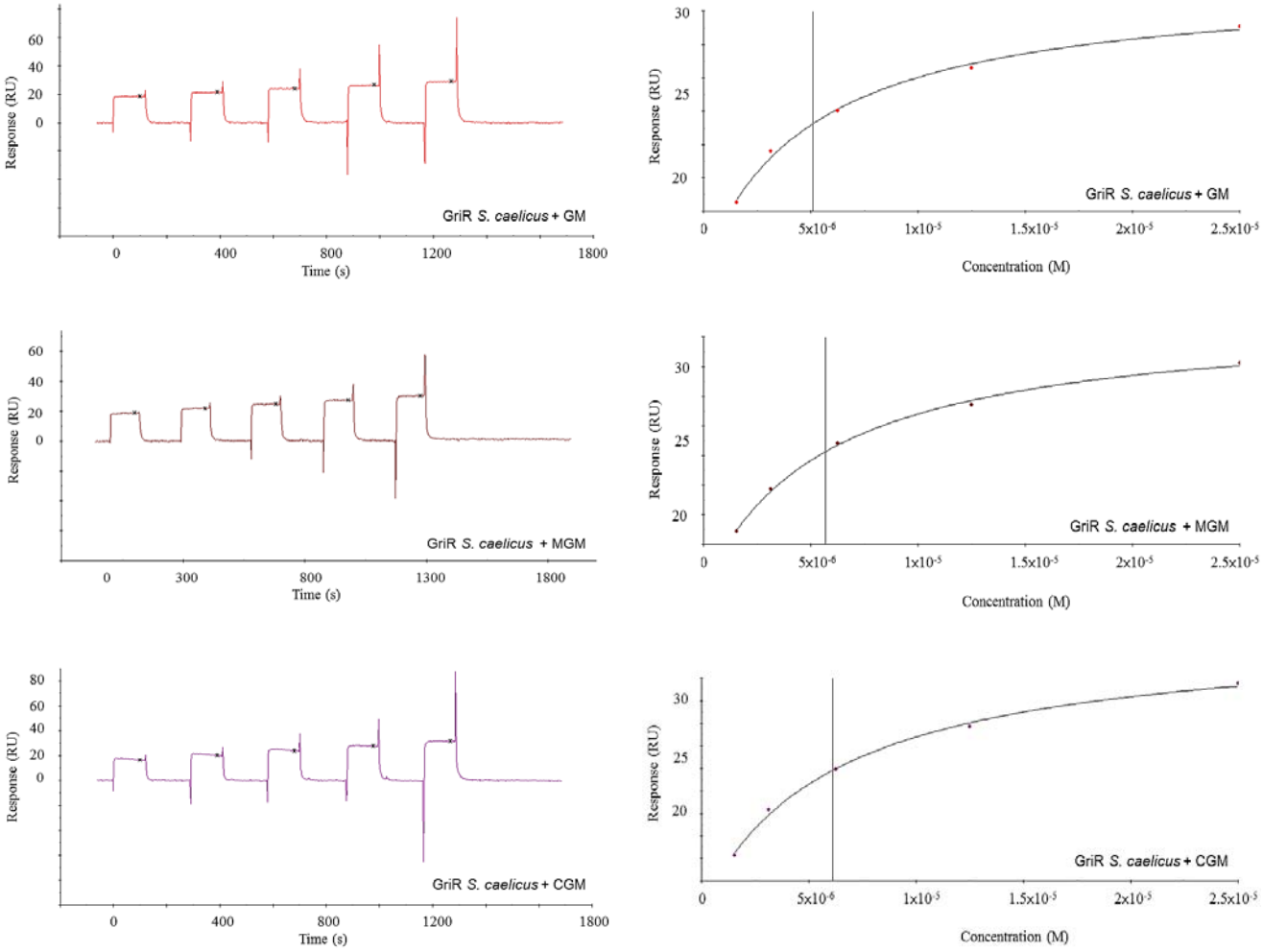

Figure 3-6: SPR sensorgrams (left images) and steady state analyses plots (right images) of binding of GM (upper images), MGM (middle images) and CGM (lower images) to GriR of *S. caelicus*. Shown are representative images from triplicate measurements (modified from reference 154).

Additionally, the interaction of GM with the *S. caelicus* DnaN and GriR was analyzed by isothermal titration calorimetry (ITC) measurements (Table 3-3, Figure 3-7, Figure 3-8). Due to solubility reasons, the ITC measurements were conducted with GM but not with MGM and CGM. The number of binding sites (n) was confirmed to be 1 for the interaction of GM with *S. caelicus* DnaN and GriR. For the binding of GM to GriR the equilibrium dissociation constant K_D was in the micromolar range (K_D = 2.0 x 10^{-6} M), which was in agreement with the K_D value determined by SPR, and the change in the Gibbs free energy of binding (ΔG) was -7.8 kcal mol^{-1} with an enthalpic contribution (ΔH) of -4.6 kcal mol^{-1} and an entropic contribution (-TΔS) of -3.2 kcal mol^{-1}. For the interaction of GM with DnaN the binding isotherm was too steep for reliable determination of affinity constants, therefore the K_D mean (3.2 x 10^{-10} M) determined by SPR measurements was used for the calculation of -TΔS and ΔG. However, this indicates a very small equilibrium dissociation constant, which is in agreement with the value determined by SPR. The change in the Gibbs free energy of binding (ΔG) reports on the affinity of an interaction and was accodingly smaller for the interaction of GM with DnaN (ΔG = -12.9) compared to that of the interaction of GM with GriR, with an enthalpic contribution (ΔH) of -7.3 kcal mol^{-1} and an entropic contribution (-TΔS) of -5.6 kcal mol^{-1}.

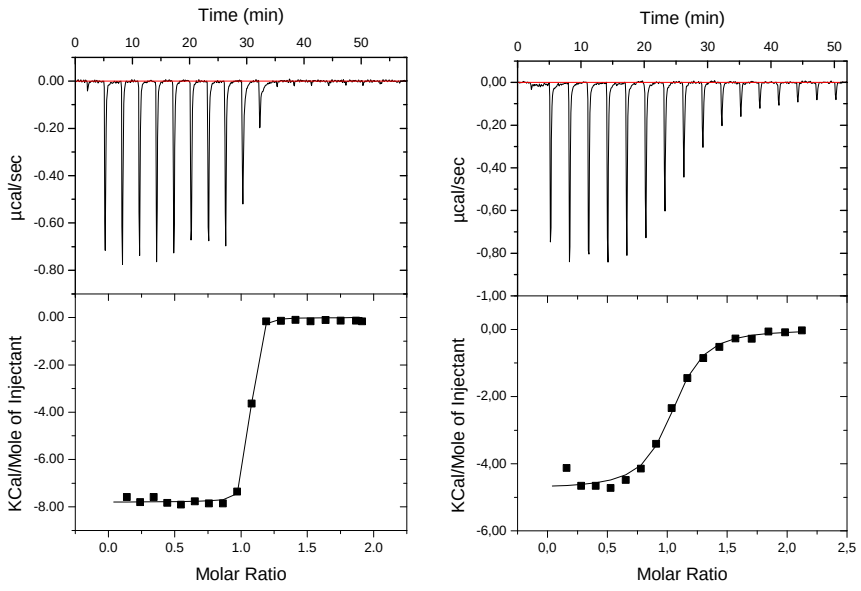

Figure 3-7: ITC binding isotherms of the interaction of GM with DnaN (left image) and GriR (right image) of *S. caelicus*. Shown are representative images from triplicate or quadruplicate measurements.

Table 3-3: Thermodynamic parameters of the interaction of GM with DnaN of *S. caelicus* or GriR of *S. caelicus* as determined by ITC. Given are the mean values and standard deviations (SD) from three independent measurements. ΔG was calculated from $\Delta G = RT\ln K_D$ (with R= 1.98 cal mol^{-1} K^{-1}) and -TΔS was calculated from ΔG=ΔH-TΔS with (T = 25°C = 298.15 K.) For DnaN of *S. caelicus* the curve was too steep for reliable determination of affinity constants and the values marked with an asterisk (*) are calculated using the K_D mean determined by SPR measurements (see Table 3-2) and no SD is given for values calculated from the K_D mean of the SPR analyses and other constants.

	S. caelicus DnaN	*S. caelicus* GriR
K_A (M^{-1}) [SD]	* $3.13x10^{9}$	$5.3x10^{5}$ [$6.2x10^{4}$]
K_D (M) [SD]	* $3.2x10^{-10}$	$2.0x10^{-6}$ [$2.1x10^{-7}$]
ΔH(kcal mol^{-1}) [SD]	-7.3 [0.3]	-4.6 [0.2]
ΔS (cal mol^{-1} deg^{-1}) [SD]	* 18.8 [1.0]	10.9 [0.4]
N (Sites) [SD]	1.1 [0.1]	1 [0.04]
−TΔS (kcal mol^{-1}) [SD]	* -5.6 [0.3]	-3.2 [-0.1]
ΔG (kcal mol^{-1}) [SD]	* -12.9	-7.8 [-0.1]

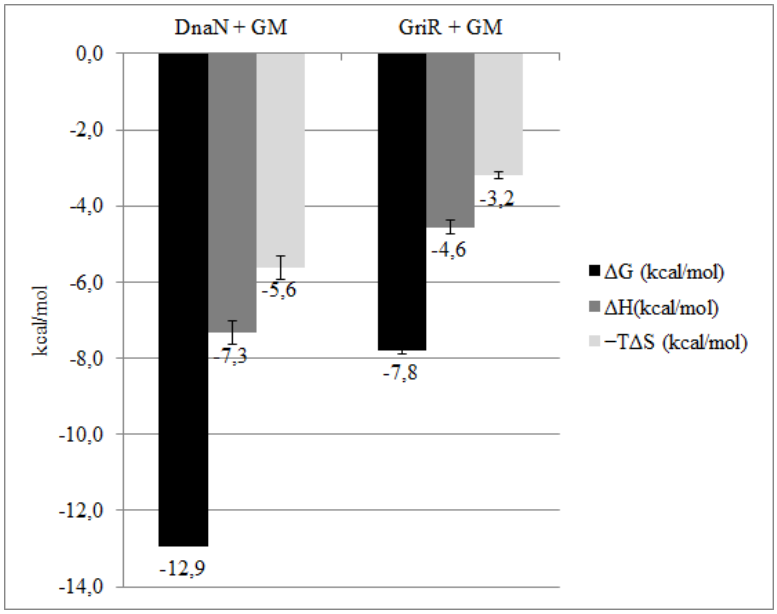

Figure 3-8: Binding signature plot illustrating the thermodynamic parameters (Table 3-3) of the interaction of GM with DnaN and GriR of *S. caelicus*.

3.2 MECHANISM OF ACTION OF GRISELIMYCINS

The activity of GM, MGM and CGM was tested against a panel of microorganisms, including several Gram-positive and Gram-negative bacteria and fungi (Table 3-4).

Table 3-4: Activity of GM, MGM and GGM against selected microorganisms. MIC: minimal inhibitory concentration (modified from reference 154).

Classification	Organism	MIC (µg/mL)		
		GM	MGM	CGM
Gram-negative	*Acinetobacter baumannii* DSM-30008	>70	>70	>70
	Burkholderia cenocepacia DSM-16553	>70	>70	>70
	Chromobacterium violaceum DSM-30191	>70	>70	>70
	Escherichia coli DSM-1116	>70	>70	>70
	Escherichia coli (TolC-deficient strain)	>70	>70	>70
	Klebsiella pneumoniae DSM-30104	>70	>70	>70
	Pseudomonas aeruginosa PAO1	>70	>70	>70
Gram-positive	*Bacillus subtilis* DSM-10	>70	>70	>70
	Corynebacterium glutamicum DSM-20300	0.1	0.1-0.3	0.6-1.2
	Enterococcus faecium DSM-20477	>70	>70	>70
	Micrococcus luteus DSM-1790	0.6	1.1	2.5
	Mycobacterium bovis BCG DSM-43990	0.5	0.4	0.3
	Mycobacterium smegmatis mc^2155	4.5	2.3	0.6
	Mycobacterium tuberculosis H37Rv	1	0.6	0.06
	Nocardia asteroides DSM-43757	35.6	18	4.9-9.9
	Staphylococcus aureus Newman	>70	>70	>70
	Staphylococcus aureus, methicillin-resistant DSM-11822	>70	>70	>70
	Staphylococcus carnosus DSM-20501	>70	>70	>70
	Streptococcus pneumoniae DSM-20566	>70	>70	>70
	Streptomyces coelicolor A3(2)	7.0	7.0	>55
Fungi	*Candida albicans* DSM-1665	>70	>70	>70
	Wickerhamomyces anomalus DSM-6766	>70	>70	>70
	Mucor hiemalis DSM-2656	>70	>70	>70

None of the tested Gram-negative or fungal microorganisms were susceptible to GMs. From the tested Gram-positive microorganisms only *Corynebacterium glutamicum*, *Micrococcus luteus*, *Mycobacterium smegmatis*, *Mycobacterium bovis*, *Nocardia asteroids* and *Streptomyces coelicolor* were susceptible. No susceptibility was detected for the other tested Gram-positive bacteria (*Bacillus subtilis*, *Enterococcus faecium*, *Staphylococcus aureus*, *Streptococcus pneumoniae*). Against *Nocardia* and the tested mycobacteria CGM showed the highest activity and GM showed the lowest activity. Against the other sensitive organisms (*Corynebacterium glutamicum*, *Micrococcus luteus* and *Streptomyces coelicolor*) GM showed the highest activity and CGM showed the lowest activity. For *S. coelicolor* no activity of up to 55 µg/mL CGM was detected. The activity of GM, MGM and CGM increased with increasing lipophilicity as indicated by the correlation of the distribution coefficient log D and the MIC (Table 3-5). However, the activity was not further improved for compounds displaying a log D > 6 (data not shown). Additionally, all three GMs were also active against intracellular *M. tuberculosis* (in murine macrophages) (Table 3-5).

Table 3-5: Activities (MIC) against *M. tuberculosis* H37Rv in liquid culture or in macrophages and lipophilicity (Log D) of GM, MGM, CGM. Log D: Distribution coefficient (modified from reference 154).

Optimization parameter	GM	MGM	CGM
MIC (µg/mL) for *M. tuberculosis* in liquid culture	1	0.6	0.06
MIC (µg/mL) for *M. tuberculosis* in macrophages	6.2	2.1	0.2
Log D	3.26	3.61	5.71

To determine if GMs exert bacteriostatic or bactericidal activity a time-kill curve of *M. tuberculosis* treated with CGM was recorded (Figure 3-9). CGM concentrations of the 0.75-fold MIC (0.045 µg/mL) led to a reduction of > 3 $\log_{10}$ units CFUs (colony forming units) in about 7 days, whereby the effect was enhanced by prolonged time and not by higher concentrations.

To examine the toxicity of GMs on mammalian cells, MTT assays with CHO-K1 (hamster ovary, epithelial-like), L929 (mouse fibroblast) and RAW264.7 (mouse leukaemic macrophage) cell lines were performed (Figure 3-11). GM and MGM showed no significant toxicity *in vitro* (IC_{50} > 100 µM) on all three tested cell lines. CGM showed moderate toxicity *in vitro* (with an IC_{50} of about 17 µM for CHO-K1, 15 µM for L929 and 11 µM for RAW264.7 cells). Additionally, the genotoxic effect of GMs was examined in a micronucleus

test with CHO-K1 cells (Figure 3-10). As a result, GMs did not induce any apparent genotoxicity or apoptotic cell death. In contrast, the reference drug mitomycin C induced a large number of micronuclei (μN) and some nuclei from late apoptotic cells (AN).

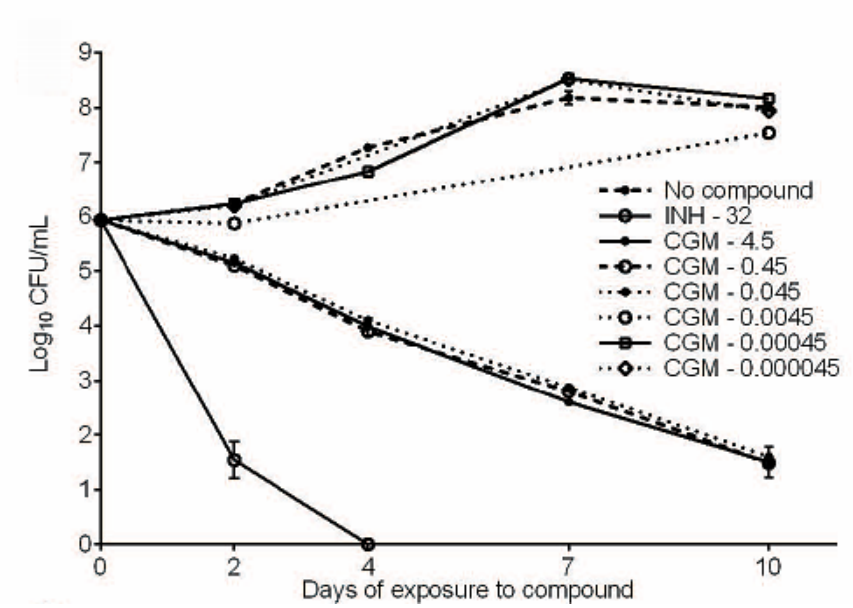

Figure 3-9: Activity of CGM against *M. tuberculosis in vitro* in 7H9 broth culture. The untreated and the INH treated controls are indicated for comparison. The number following the compound abbreviation indicates the concentration in μg/mL.[154]

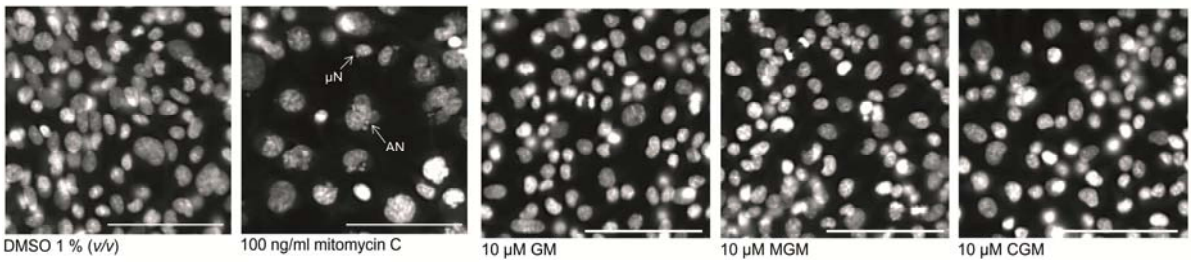

Figure 3-10: Micronucelus tests showing the effect of GMs on nuclei of CHO-K1 cells. Shown are representative images of Hoechst33342 stained nuclei. μN: micronuclei. AN: late apoptotic cells. Scale bars: 20 μM.[154]

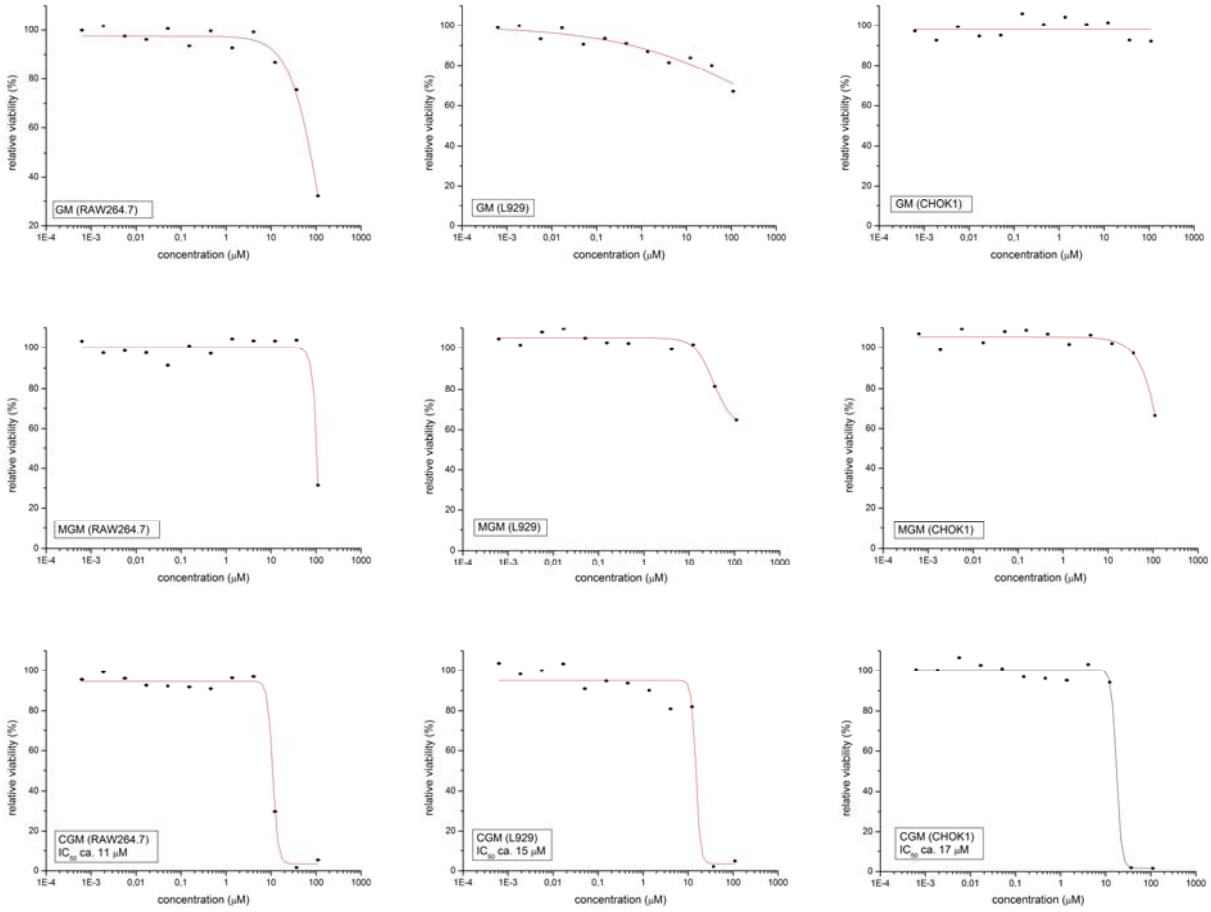

Figure 3-11: Toxicity of GMs on mammalian cells (CHO-K1, L929, RAW264.7). Represented are the means of duplicate measurement. The standard error is indicated but is too small to be visible in most cases. The IC_{50} for CGM is about 17 µM for CHO-K1 cells, about 15 µM for L929 cells and about 11 µM for RAW264.7 cells.

To further examine if the specific activity of GMs could result from different amino acid sequence similarities between different sliding clamps (as the sliding clamp represents the target of GMs in *S. caelicus*), the homology between the different sliding clamps was analysed *in silico* (Figure 3-12). As a result, the human and fungal sliding clamp analogs show low amino acid similarity (sequence identity < 12 %) to the microbial sliding clamps and the sliding clamps of Gram-positive organisms show higher sequence similarity to each other than to that of Gram-negative organisms and vice versa (Table 6-3). In the resulting phylogenetic tree (Figure 3-12) the sliding clamps of the analyzed Gram-negative and Gram-positive organisms accordingly cluster in separate branches of the tree. The sliding clamps of the GM sensitive microorganisms show a higher sequence similarity to each other than to sliding clamps of other organisms (as indicated by a lower number of substitutions per site in the phylogenetic tree) and accordingly cluster in a separate branch in the tree. The peptide

binding pockets of the sliding clamps of different microorganisms are shaped by about 20 amino acids[183,184] which also show different similarities for different microorganisms (Table 3-6). The peptide binding pockets of the sliding clamps of Gram-negative organisms show a sequence identity of 90 – 100 % to each other and a sequence identity of 35 – 60 % to the sliding clamps of Gram-positive organisms (Table 6-4). The peptide binding pockets of the sliding clamps of GM sensitive microorganisms show a sequence identity of 60 - 100 % to each other and a sequence identity of 45 – 60 % to other Gram-positive and of 35 – 55 % to other Gram-negative organisms (Table 6-4).

Table 3-6: Amino acids shaping the peptide binding pocket of different sliding clamps. The sliding clamps of GM sensitive strains and GM producing strains are indicated in bold; hydrophobic residues are indicated in grey; basic residues are indicated in blue; neutral residues are not coloured; subscripts indicate amino acid positions. GeneInfo Identifier (gi) numbers of the included DnaN amino acid sequences are as follows: *A. baumannii*, 213987621; *B. subtilis*, 16077070; *B. cenocepacia*, gi 206558824; *C. violaceum*, 34495457; *C. glutamicum*, 21322767; *E. faecium*, 389867185; *E. coli* DH10B, 169891038; *K. pneumonia*, 238897211; *M. luteus*, 239837780; *M. smegmatis* mc^{2}155, 118169404; *M. tuberculosis* H37Rv, 15607144; *N. asteroides* NBRC 15531, 549076545; *P. aeruginosa* PAO1, 9945820; 49240384; *S. aureus* Newman, 151220214; *S. carnosus*, 222422562; *S. pneumoniae*, 116077515; *S. coelicolor* A3(2), 21219691; *S. griseus*, 182437190.

Protein	Subsite 2 of the peptide binding site																Subsite 1 of the peptide binding site			
DnaN *E. coli*	R_{152}	Y_{154}	L_{155}	T_{172}	G_{174}	H_{175}	R_{176}	L_{177}	P_{242}	V_{247}	N_{320}	Y_{323}	V_{344}	S_{346}	V_{360}	V_{361}	M_{362}	P_{363}	M_{364}	R_{365}
DnaN *A. baumannii*	R_{156}	Y_{158}	L_{159}	T_{176}	G_{178}	H_{179}	R_{180}	L_{181}	P_{258}	V_{263}	N_{336}	Y_{339}	N_{360}	S_{362}	V_{376}	V_{377}	M_{378}	P_{379}	M_{380}	R_{381}
DnaN *B. cenocepacia*	R_{153}	Y_{155}	L_{156}	T_{173}	G_{175}	H_{176}	R_{177}	L_{178}	P_{244}	V_{249}	N_{322}	Y_{325}	S_{345}	S_{346}	V_{362}	V_{363}	M_{364}	P_{365}	M_{366}	R_{367}
DnaN *C. violaceum*	R_{155}	Y_{157}	L_{158}	T_{175}	G_{177}	H_{178}	R_{179}	L_{180}	P_{245}	V_{250}	N_{323}	Y_{326}	S_{347}	S_{348}	I_{363}	V_{364}	M_{365}	P_{366}	M_{367}	R_{368}
DnaN *K. pneumoniae*	R_{152}	Y_{154}	L_{155}	T_{172}	G_{174}	H_{175}	R_{176}	L_{177}	P_{242}	V_{247}	N_{320}	Y_{323}	V_{344}	S_{345}	V_{360}	V_{361}	M_{362}	P_{363}	M_{364}	R_{365}
DnaN *P. aeruginosa*	R_{152}	Y_{154}	L_{155}	T_{172}	G_{174}	H_{175}	R_{176}	L_{177}	P_{243}	V_{248}	N_{321}	Y_{324}	N_{345}	S_{346}	V_{361}	V_{362}	M_{363}	P_{364}	M_{365}	R_{366}
DnaN *B. subtilis*	R_{159}	I_{157}	L_{158}	T_{179}	S_{181}	H_{182}	R_{183}	L_{184}	P_{250}	L_{255}	S_{331}	Y_{334}	M_{355}	P_{356}	L_{371}	I_{372}	L_{373}	P_{374}	V_{375}	R_{376}
DnaN *S. aureus*	R_{160}	V_{162}	L_{163}	T_{180}	S_{182}	H_{183}	R_{184}	L_{185}	P_{250}	L_{255}	N_{330}	Y_{333}	M_{354}	P_{355}	L_{370}	I_{371}	L_{372}	P_{373}	I_{374}	R_{375}
DnaN *E. faecium*	R_{158}	I_{160}	L_{161}	T_{178}	S_{180}	H_{181}	R_{182}	L_{183}	P_{248}	L_{253}	N_{328}	Y_{331}	I_{352}	P_{353}	L_{369}	I_{370}	T_{371}	P_{372}	V_{373}	R_{374}
DnaN *S. pneumoniae*	R_{159}	I_{161}	L_{162}	T_{180}	S_{182}	H_{183}	R_{184}	L_{185}	P_{250}	L_{255}	N_{330}	Y_{333}	V_{354}	P_{355}	L_{371}	I_{372}	T_{373}	P_{374}	V_{375}	R_{376}
DnaN *M. luteus*	L_{152}	I_{154}	L_{155}	T_{172}	R_{174}	Y_{175}	R_{176}	L_{178}	P_{245}	L_{250}	N_{322}	Y_{325}	P_{346}	P_{347}	L_{367}	V_{368}	M_{369}	P_{370}	V_{371}	R_{372}
DnaN *S. coelicolor*	L_{149}	V_{151}	L_{152}	T_{169}	R_{171}	Y_{172}	R_{173}	F_{174}	P_{245}	L_{250}	N_{322}	F_{325}	T_{346}	P_{347}	L_{368}	I_{369}	M_{370}	P_{371}	V_{372}	R_{373}
DnaN2 *S. coelicolor*	L_{148}	T_{150}	L_{151}	T_{170}	R_{172}	Y_{173}	R_{174}	F_{175}	P_{243}	L_{248}	N_{322}	F_{325}	T_{346}	P_{347}	L_{364}	L_{365}	M_{366}	P_{367}	I_{368}	R_{369}
DnaN *S. griseus*	L_{149}	V_{151}	L_{152}	T_{169}	R_{171}	Y_{172}	R_{173}	F_{174}	P_{245}	L_{250}	N_{322}	F_{325}	T_{346}	P_{347}	L_{368}	I_{369}	M_{370}	P_{371}	V_{372}	R_{373}
DnaN *S. caelicus*	L_{149}	V_{151}	L_{152}	T_{169}	R_{171}	Y_{172}	R_{173}	F_{174}	P_{245}	L_{250}	N_{322}	F_{325}	T_{346}	P_{347}	L_{368}	I_{369}	M_{370}	P_{371}	V_{372}	R_{373}
GriR *S. caelicus*	L_{149}	V_{151}	L_{152}	T_{169}	R_{171}	Y_{172}	R_{173}	F_{174}	P_{242}	L_{247}	N_{319}	F_{322}	N_{343}	K_{344}	L_{365}	V_{366}	M_{367}	P_{368}	V_{369}	R_{370}
DnaN2 *S. griseus*	L_{155}	A_{157}	L_{158}	T_{175}	R_{177}	Y_{178}	R_{179}	Y_{180}	P_{246}	L_{251}	N_{325}	Y_{328}	G_{349}	R_{350}	L_{366}	L_{367}	M_{368}	S_{369}	V_{370}	K_{371}
DnaN *N. asteroides*	L_{149}	M_{151}	L_{152}	T_{169}	R_{171}	F_{172}	R_{173}	L_{174}	P_{246}	L_{251}	N_{323}	Y_{326}	S_{347}	P_{348}	L_{378}	L_{379}	M_{380}	P_{381}	V_{382}	R_{383}
DnaN *C. glutamicum*	L_{154}	M_{156}	L_{157}	T_{174}	R_{176}	F_{177}	R_{178}	L_{179}	P_{254}	L_{259}	N_{331}	Y_{334}	S_{355}	P_{356}	L_{386}	L_{387}	M_{388}	P_{389}	V_{390}	R_{391}
DnaN *M. tuberculosi*	L_{161}	M_{163}	L_{164}	T_{181}	R_{183}	F_{184}	R_{185}	L_{186}	P_{259}	L_{264}	N_{336}	Y_{339}	G_{350}	P_{351}	L_{394}	L_{395}	M_{396}	P_{397}	V_{398}	R_{399}
DnaN *M. smegmatis*	L_{159}	M_{161}	L_{162}	T_{179}	R_{181}	F_{182}	R_{183}	L_{184}	P_{257}	L_{262}	N_{334}	Y_{337}	S_{348}	P_{349}	L_{389}	L_{390}	M_{391}	P_{392}	V_{393}	R_{394}

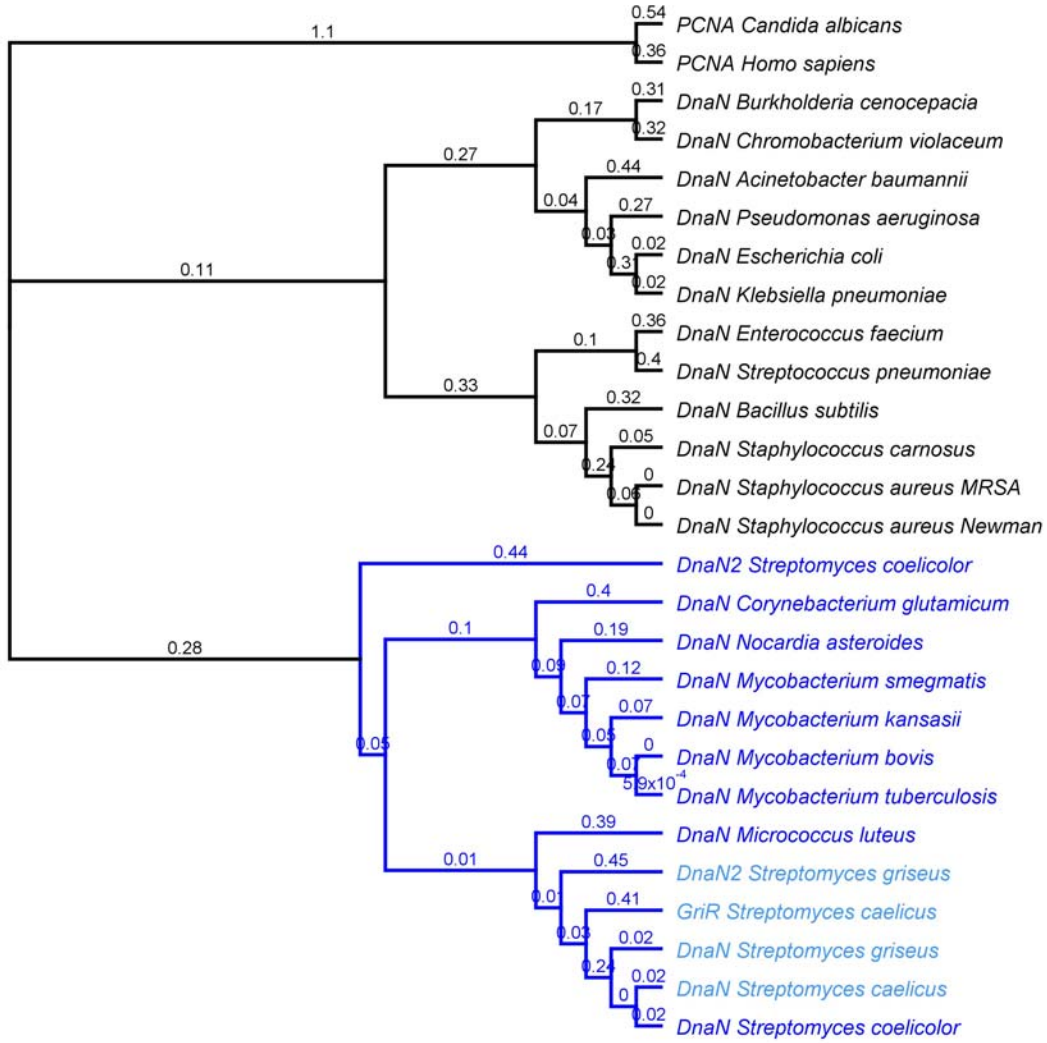

Figure 3-12: Phylogenetic tree of microbial sliding clamps, derived by Bayesian phylogeny estimation. Sliding clamps of GM sensitive strains are marked in blue, and GM producing strains are marked in light blue. Evolutionary distances (substitutions/site) are indicated on each branch of the tree. The human sliding clamp, PCNA, is used as outgroup. GeneInfo Identifier (gi) numbers of the sequences used in this analysis are as follows: *A. baumannii*, 213987621; *B. subtilis*, 16077070; *B. cenocepacia*, gi 206558824; *C. violaceum*, 34495457; *C. glutamicum*, 21322767; *E. faecium*, 389867185; *E. coli* DH10B, 169891038; *K. pneumonia*, 238897211; *M. luteus*, 239837780; *M. bovis* BCG, 224988385; *M. kansasii*, 240172092; *M. smegmatis* mc^2155, 118169404; *M. tuberculosis* H37Rv, 15607144; *N. asteroides* NBRC 15531, 549076545; *P. aeruginosa* PAO1, 9945820; *S. aureus* MRSA, 49240384; *S. aureus* Newman, 151220214; *S. carnosus*, 222422562; *S. pneumoniae*, 116077515; *S. coelicolor* A3(2), 21222286; DnaN2 *S. coelicolor* A3(2), 695227561; DnaN *S. griseus* 182437494, DnaN2 *S. griseus*, 182437190; *H. sapiens* PCNA, 49456555; *C. albicans* PCNA, 723213130. (Modified from reference 154).

To examine if GMs bind to the sliding clamps of GM susceptible organisms, binding of GMs to mycobacterial sliding clamps was analysed by SPR (Table 3-7, Figure 3-13). To further examine if GMs also bind to the sliding clamps of organisms not susceptible to GMs, the binding of GMs to the DnaN of *E.coli* was analysed (Table 3-7, Figure 3-14). Therefore the DnaNs of *M. smegmatis*, *M. tuberculosis* and *E. coli* were immobilized to a sensor chip by standard amine coupling and increasing concentrations of GMs were injected over the chip. As a result, significant interactions of GM, MGM and CGM with the DnaN of *M. smegmatis* and of *M. tuberculosis* were observed. All three GMs bind to both mycobacterial DnaNs with high affinity with similar equilibrium dissociation constants (K_D) in the picomolar range (*M. smegmatis*: GM: K_D 8.3 x 10^{-11} M, MGM: K_D 9.9 x 10^{-11} M, CGM: K_D 1.2 x 10^{-10} M; *M. tuberculosis*: GM: K_D 1.0 x 10^{-10} M, MGM: K_D 1.1 x 10^{-10} M, CGM K_D 2.0 x 10^{-10} M) and dissociate slowly from the DnaN proteins, as indicated by low dissociation rate constants (k_d) and high dissociative half-lifes ($t_{1/2}$). The dissociation rate constants are similar for all interactions but the dissociation is somewhat slower for the interaction of CGM with the mycobacterial DnaNs (*M. smegmatis*: GM: k_d 1.3 x 10^{-3} s^{-1} and $t_{1/2}$: 450 s, MGM: k_d 1.3 x 10^{-3} s^{-1} and $t_{1/2}$: 545 s, CGM: k_d 4.1 x 10^{-4} s^{-1} and $t_{1/2}$: 1998 s; *M. tuberculosis*: GM: k_d 8.4 x 10^{-4} s^{-1} and $t_{1/2}$:863 s, MGM: k_d 7.1 x 10^{-4} s^{-1} and $t_{1/2}$: 1080 s, CGM: k_d 4.7 x 10^{-4} s^{-1} and $t_{1/2}$: 1659 s). GM, MGM and CGM are recognized by the *M. smegmatis* DnaN with association rate constants (k_a) of 2.2 x 10^7 $M^{-1}s^{-1}$, 1.6 x 10^7 $M^{-1}s^{-1}$ and 4.5 x 10^6 $M^{-1}s^{-1}$, and by the *M. tuberculosis* DnaN with with association rate constants of 6.8 x 10^6 $M^{-1}s^{-1}$, 6.5 x 10^6 $M^{-1}s^{-1}$ and 2.6 x 10^6 $M^{-1}s^{-1}$, respectively.

Binding was also observed to *E. coli DnaN*, but with lower affinity compared to the mycobacterial DnaNs, with equilibrium dissociation constants that were all in the high nanomolar range (K_D GM: 6.5 x 10^{-7} M, K_D MGM 8.4 x 10^{-7} M and K_D CGM: 6.6 x 10^{-7} M). The association to and dissociation from the *E. coli* DnaN protein by GMs was too fast to reliably determine the association and dissociation rate constants. K_D values were therefore determined by steady state affinity analyses from the dependence of steady-state binding levels on analyte concentrations.

Table 3-7: Kinetic parameters of the interaction of GMs with DnaN of *M. smegmatis*, *M. tuberculosis* and *E. coli* as determined by surface plasmon resonance (SPR) spectroscopy. K_D values were determined from the ratio between the kinetic rate constants (k_a/k_d) for interactions with the *M. tuberculosis* and the *M. smegmatis* DnaN and from steady-state affinity analyses interactions with the *E. coli* DnaN due to the fast on- and off-rates.The dissociative half-life $t_{1/2}$ was calculated by $\ln 2/k_d$. Data represent the mean and the standard deviation (SD) from three independent experiments. n.a.: not applicable.[154]

Interactants		K_D (M)	k_a ($M^{-1}s^{-1}$)	k_d (s^{-1})	$t_{1/2}$ (s)
Protein	Compound	[SD]	[SD]	[SD]	[SD]
$DnaN_{M.\ smegmatis}$	GM	8.3×10^{-11}	2.2×10^{7}	1.9×10^{-3}	450
		$[3.9 \times 10^{-11}]$	$[5.4 \times 10^{5}]$	$[8.7 \times 10^{-4}]$	[160]
	MGM	9.9×10^{-11}	1.6×10^{7}	1.3×10^{-3}	545
		$[5.7 \times 10^{-11}]$	$[7.2 \times 10^{6}]$	$[2.7 \times 10^{-4}]$	[227]
	CGM	1.2×10^{-10}	4.5×10^{6}	4.1×10^{-4}	1998
		$[4.2 \times 10^{-11}]$	$[3.4 \times 10^{6}]$	$[1.7 \times 10^{-4}]$	[785]
$DnaN_{M.\ tuberculosis}$	GM	1.0×10^{-10}	6.8×10^{6}	8.4×10^{-4}	863
		$[8.1 \times 10^{-12}]$	$[2.5 \times 10^{6}]$	$[1.9 \times 10^{-4}]$	[183]
	MGM	1.1×10^{-10}	6.5×10^{6}	7.1×10^{-4}	1080
		$[1.1 \times 10^{-11}]$	$[2.1 \times 10^{6}]$	$[2.1 \times 10^{-4}]$	[361]
	CGM	2.0×10^{-10}	2.6×10^{6}	4.7×10^{-4}	1659
		$[7.9 \times 10^{-11}]$	$[7.8 \times 10^{5}]$	$[1.4 \times 10^{-4}]$	[643]
$DnaN_{E.\ coli}$	GM	6.5×10^{-7}	n.a.	n.a.	n.a.
		$[1.7 \times 10^{-8}]$			
	MGM	8.4×10^{-7}	n.a.	n.a.	n.a.
		$[6.0 \times 10^{-9}]$			
	CGM	6.6×10^{-7}	n.a.	n.a.	n.a.
		$[1.7 \times 10^{-8}]$			

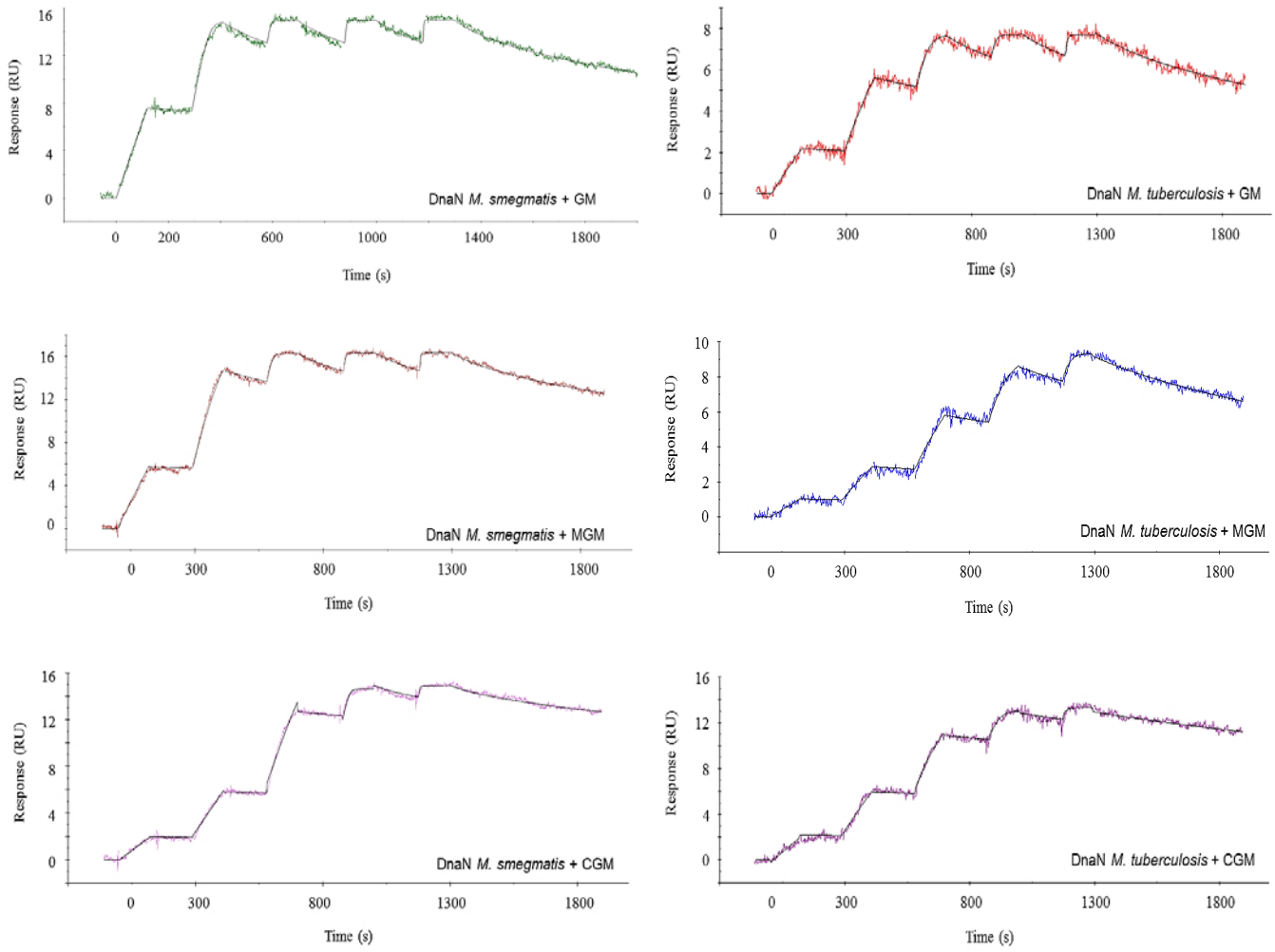

Figure 3-13: SPR sensorgrams of binding of GM (upper images), MGM (middle image) and CGM (lower images) to DnaN of *M. smegmatis* (left images) and *M. tuberculosis* (right images). Shown are representative images from triplicate measurements (modified from reference 154).

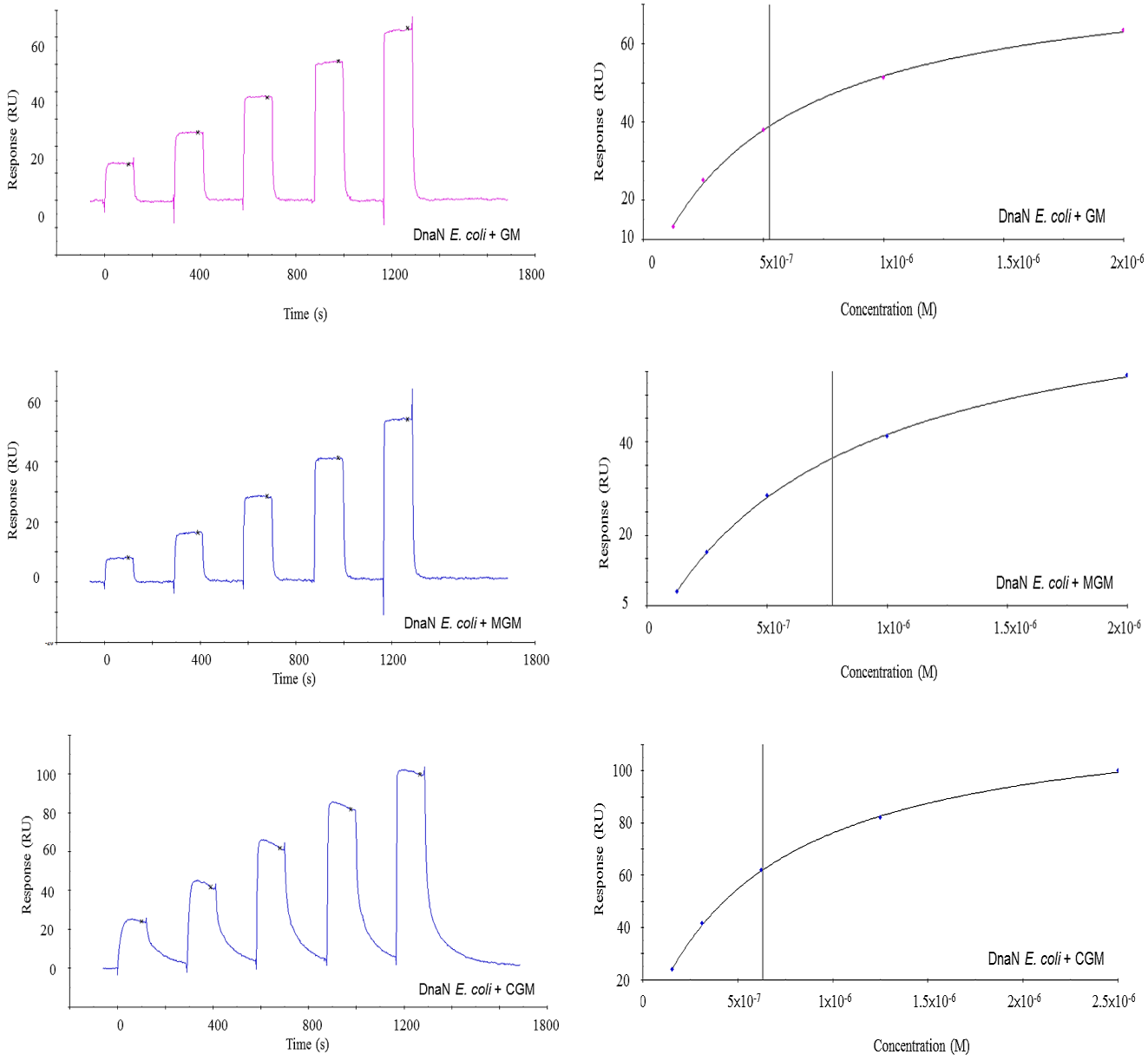

Figure 3-14: SPR sensorgrams (left images) and steady state analyses plots (right images) of binding of GM (upper images), MGM (middle images) and CGM (lower images) to DnaN of *E. coli*. Shown are representative images from triplicate measurements (modified from reference 154).

Additionally, the interaction of GM with the *E. coli* DnaN was analyzed by isothermal titration calorimetry (ITC) analyses (Table 3-8, Figure 3-15). For the binding of GM to the *E. coli* DnaN the equilibrium dissociation constant K_D was in the micromolar range (K_D = 2.6 x 10^{-7} M) and the change in the Gibbs free energy of binding (ΔG) was -9.0 kcal mol^{-1} with a enthalpic contribution (ΔH) of -3.2 kcal mol^{-1} and an entropic contribution (-TΔS) of -5.8 kcal mol^{-1}.

Table 3-8: Thermodynamic parameters of the interaction of GM with DnaN of *E. coli* as determined by ITC. Given are the mean and standard deviations (SD) from three independent measurements. ΔG was calculated from $\Delta G = RT\ln K_D$ (with R= 1.98 cal mol^{-1} K^{-1}) and -TΔS was calculated from ΔG=ΔH-TΔS with (T = 25°C = 298.15 K.)

	E.coli DnaN
K_A (M^{-1}) [SD]	4.2 x 10^6 [1.2 x 10^6]
K_D (M) [SD]	2.6 x 10^{-7} [7.8 x 10^{-8}]
ΔH(kcal mol^{-1}) [SD]	-3.2 [0.6]
ΔS (cal mol^{-1} deg^{-1}) [SD]	19.5 [2.3]
N (Sites) [SD]	1.1 [0.1]
−TΔS (kcal mol^{-1}) [SD]	-5.8 [0.7]
ΔG (kcal mol^{-1}) [SD]	-9.0 [0.2]

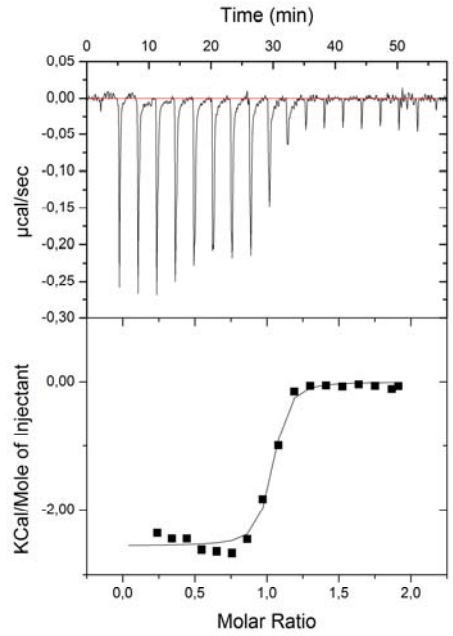

Figure 3-15: ITC binding isotherms of the interaction of GM with DnaN of *E. coli*. Shown is a representative image from triplicate measurements.

To further examine if GMs bind to the human sliding clamp analog, binding of GMs to the human PCNA was analysed by SPR (Figure 3-16). Therefore, the glycosylated human PCNA was immobilized to a sensor chip by standard amine coupling, increasing concentrations of GMs were injected over the chip and the interaction was analyzed in multicycle mode. No

specific interaction of GM, MGM and CGM with human sliding clamp was observed, as indicated by the low response signals upon injection of high concentrations of GM (up to 500 µM) compared to theoretical maximal response levels of around 100 RU (see section 2.2.5) and the lacking saturation upon injection of up to 500 µM GM.

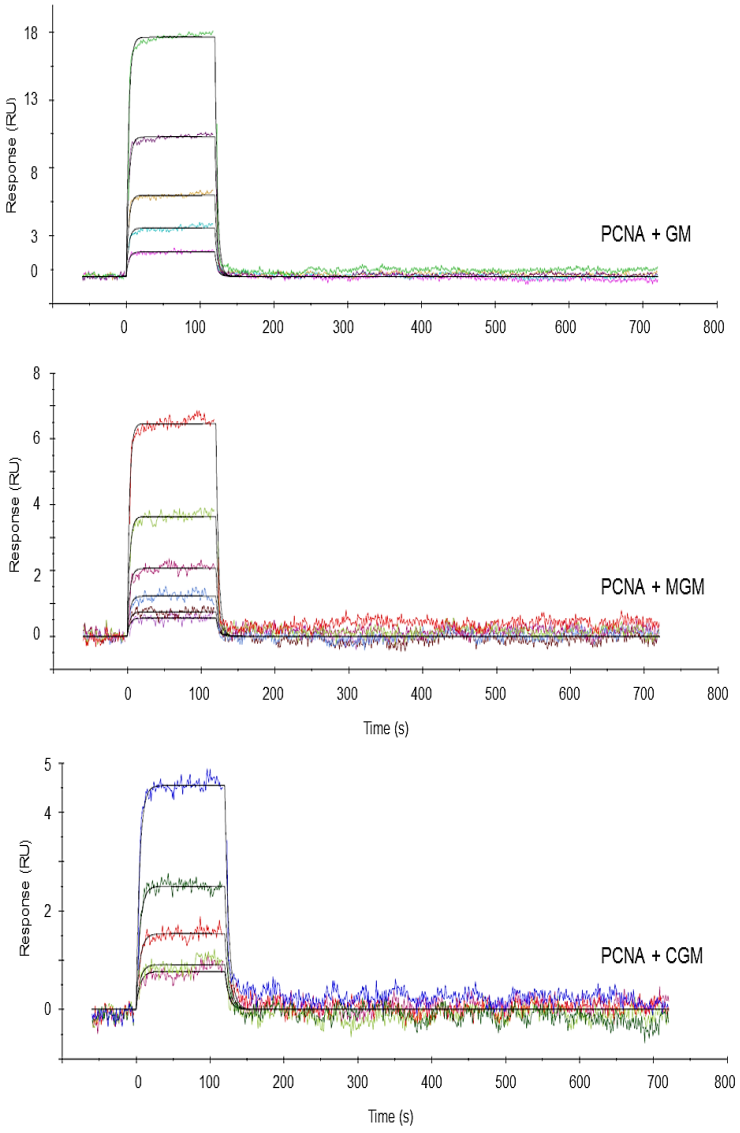

Figure 3-16: SPR sensorgrams of the binding analyses of GM (upper images), MGM (middle image) and CGM (lower images) and the human PCNA. Shown are representative images from triplicate measurements. Injected concentrations: GM: 500, 250, 125, 62.5, 31.25 µM; MGM: 200, 100, 50, 25, 12.5 µM; CGM: 100, 50, 25, 12.5, 6.25 µM.

Crystal structures of mycobacterial sliding clamps in complex with GM and CGM were solved by Dr. Peer Lukat to determine the binding site and the molecular interactions of GMs and DnaNs. The structures of the *M. smegmatis* DnaN with bound GM and CGM were refined

to resolutions of 2.1 and 2.3 Å, respectively (Table 6-1, Figure 6-3). The structures of the *M. tuberculosis* DnaN with bound GM and CGM were refined to resolutions of 2.2 and 1.9 Å, respectively. The crystal structures revealed that GMs bind to the peptide binding site of the DnaN dimer between domains II and III at each monomer (Figure 3-17) and thereby occupy subsite 1 and subsite 2 of the binding site.

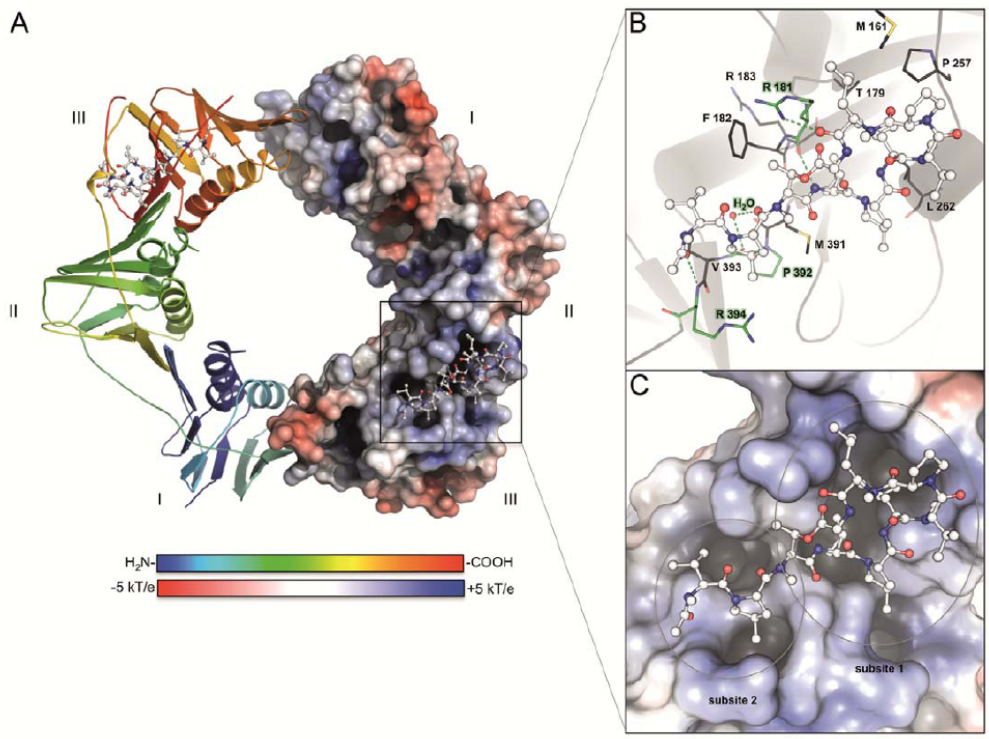

Figure 3-17: (A) Crystal structure of the *M. smegmatis* DnaN with bound GM. The cartoon representation of the left half of DnaN is colored from the N-terminus (blue) to the C-terminus (red). The second half of DnaN is shown as surface representation colored according to the electrostatic surface potential, ranging from –5 kT/e (red) to +5 kT/e (blue) (k, Boltzmann's constant; T, temperature; e, charge of an electron). (B) Interactions between the ligand and the protein.The residues involved in hydrophobic contacts with GM are represented as gray sticks. The residues also involved in hydrogen bonding with the ligand are represented as green sticks. Hydrogen bonds are indicated by dashed green lines. (C) The surface is colored according to the electrostatic surface potential. Both subsites of the binding pocket are indicated by circles.[154]

GMs bind to the DnaNs mainly via hydrophobic interactions and four hydrogen bond interactions (Figure 3-18). Two hydrogen bond interactions are formed with Arg181/Arg183 of *M. smegmatis*/*M. tuberculosis* (one with the backbone carbonyl oxygen and one with the guanidine moiety), the third hydrogen bond interaction is formed with Arg349/Arg399 (with the backbone amide nitrogen) of *M. smegmatis*/*M. tuberculosis* and the fourth hydrogen bond interaction is formed via a bridging water molecule with Pro392/Pro397 of *M. smegmatis*/*M.*

tuberculosis. The hydrogen bond interaction between GM and arginine183 of *M. tuberculosis* is also formed via a bridging water molecule.

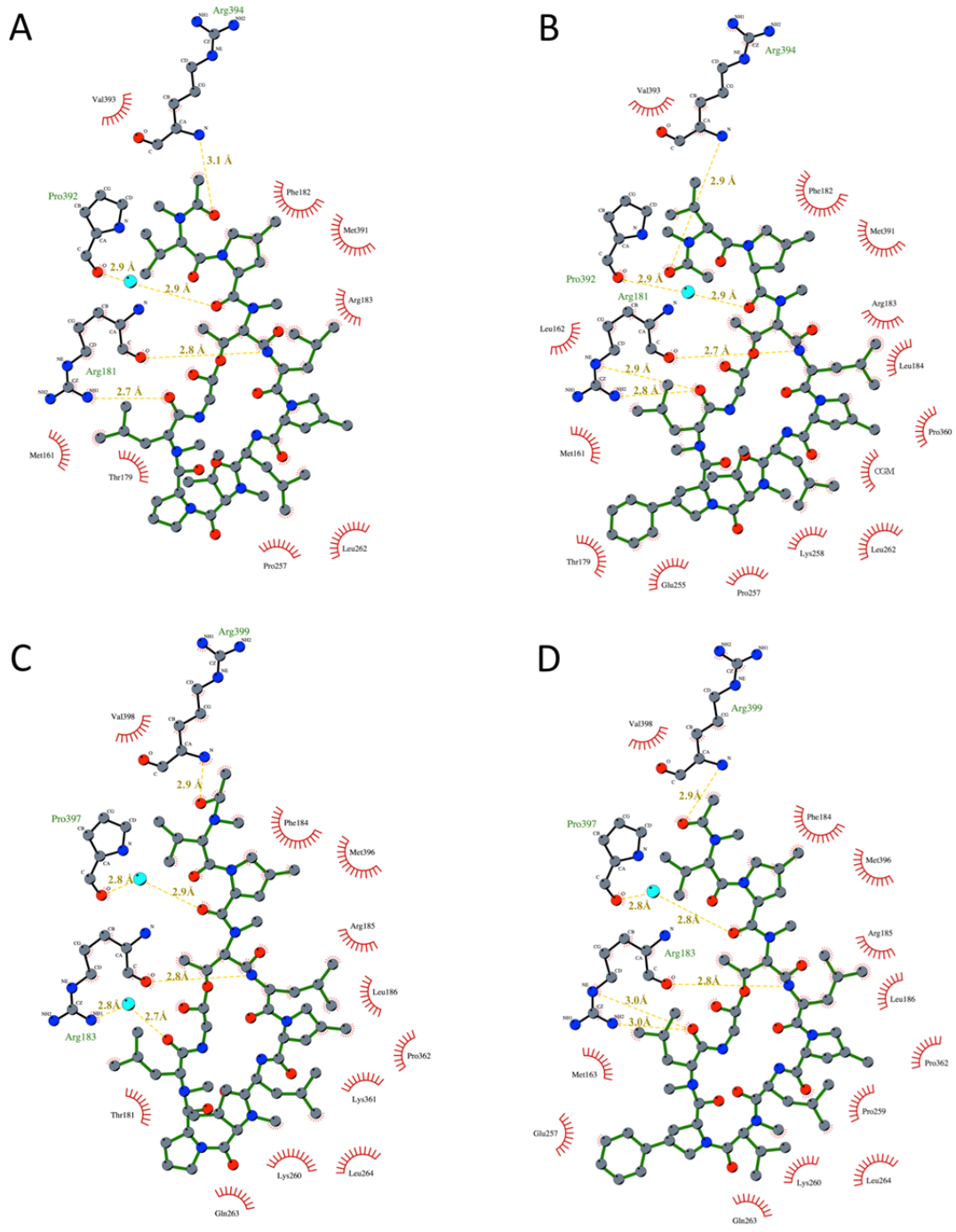

Figure 3-18: Ligand interaction diagrams for GM bound to *M. smegmatis* DnaN (A), CGM bound to *M. smegmatis* DnaN (B), GM bound to *M. tuberculosis* DnaN (C) and CGM bound to *M. tuberculosis* DnaN (D). GMs are depicted with green bonds, DnaN residues are depicted with black bonds, water molecules are depicted in cyan, hydrophobic interactions are depicted as red sparks, hydrogen bonds are depicted as yellow dashes and labelled with the according bond lengths.[154]

To examine if binding of GMs to the peptide binding site of the sliding clamp affects binding of the replicative DNA polymerase in mycobacteria, binding of a mycobacterial DNA polymerase III derived peptide that contains the sliding clamp binding motif was monitored by an SPR based inhibition assay in the presence and in the absence of GM. Therefore the DnaN of *M. smegmatis* was immobilized to a sensor chip by standard amine coupling. GM-saturated DnaN was prepared by injection of GM concentrations of 200 nM (corresponding to more than the the 2000-fold K_D value). A peptide derived from the *M. smegmatis* DNA polymerase III alpha (DnaE1) subunit containing the internal DnaN binding site, with the sequence KAEAMGQFDLFG (the putative DnaN binding motif is underlined) was injected over the chip with untreated or GM-saturated DnaN and binding was evaluated by comparison of the binding level achieved with untreated and with GM saturated DnaN. As a result the binding level was decreased by about half for the interaction of the internal DnaE1 peptide with GM-saturated DnaN compared to the binding level for the interaction with untreated DnaN, indicating an impaired interaction of the internal DnaE1 binding site in the presence of GM.

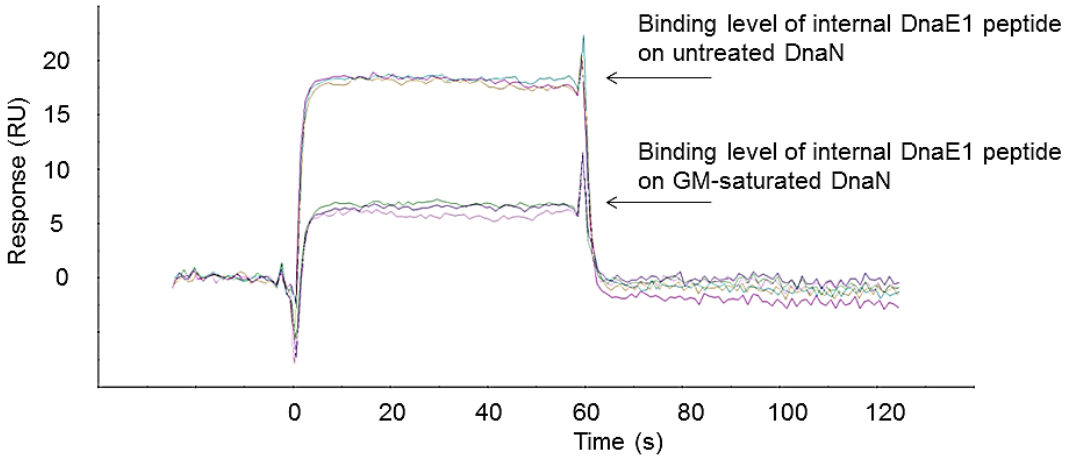

Figure 3-19: SPR based inhibition assay. Interaction of the DnaE1 peptide (KAEAMGQFDLFG), containing the internal DnaN binding motif of *M. smegmatis* DnaE1, with untreated and with GM-saturated *M. smegmatis* DnaN. In the sensorgram triplicate measurements are shown.[154]

The induction of the SOS response in *M. smegmatis* upon exposure to 1 µg/mL GM over 10 hours was monitored by the relative fold change in expression of *recA*, *lexA*, *dnaE2* and *dnaB* using quantitative PCR (qPCR). Therefore the expression level of all four reporter genes was analyzed at four timepoints (after 0, 2.5, 5, and 10 hours of GM exposure) in four independent cultures. Thereby two of the cultures (samples A) were cultivated for 26.5 hours and reached

an OD_{600} of about 0.7 and two of the cultures (samples B) were cultivated for 22 hours and reached an OD_{600} of about 0.5 before sampling was initiated (i.e. timepoint 0 h), and subsequent GM treatment was initiated 2.5 hours later (i.e. timepoint 2.5 h) (Table 3-9, Figure 3-20). The expression levels of *recA*, encoding the bacterial replicase and *lexA*, encoding a repressor protein responsible for regulating the expression of SOS genes, were increased over the whole observation period of 10 hours, with the highest level after 2.5 or 5 hours of GM treatment indicating an induction of the SOS response. The expression level of *dnaE2*, encoding a translesion polymerase, and *dnaB*, encoding a replicative helicase which are also DNA damage inducible, were also slightly increased with the highest level after 2.5 or 5 hours of GM treatment. For all four reporter genes samples A showed the highest expression level after 5 hours and samples B showed the highest expression level after 2.5 hours.

Table 3-9: Raw data of the relative fold change in expression of *recA*, *lexA*, *dnaE2* and *dnaB* in *M. smegmatis* after exposure to 1 µg/mL GM over 10 hours. The relative expression level was measured by qPCR and calculated by $2^{-\Delta\Delta Ct}$ and double referenced to the 16S rRNA expression level and the expression level of the according gene of an independent untreated sample. The values represent the mean of the relative gene expression level of two independent samples each measured in triplicate. The error bars indicate the standard deviation of the mean. Samples A (left images) were cultivated for 26.5 h and reached an OD_{600} of about 0.7 and samples B (right images) were cultivated for 22 h and reached an OD_{600} of about 0.5 before sampling was initiated (i.e. timepoint 0 h) and subsequent GM treatment was initiated 2.5 hours later (i.e. timepoint 2.5 h).

	Relative expression level [SD]							
time (h)	*recA* samples A	*recA* samples B	*lexA* samples A	*lexA* samples B	*dnaE2* samples A	*dnaE2* samples B	*dnaB* samples A	*dnaB* samples B
0	2.0 [0.3]	1.4 [0.2]	1.4 [0.3]	1.2 [0.1]	1.0 [0.2]	0.8 [0.01]	1.2 [0.3]	0.7 [0.2]
2.5	7.7 [1.0]	14.6 [4.3]	2.5 [0.1]	19.4 [7.7]	1.8 [0.8]	7.6 [2.1]	1.3 [0.2]	9.0 [0.8]
5	16.2 [1.5]	6.5 [0.9]	11.1 [5.0]	4.9 [0.6]	3.7 [0.1]	3.7 [0.6]	7.4 [2.1]	3.0 [0.8]
10	7.9 [0.7]	7.8[1.3]	2.6 [0.5]	4.3 [1.0]	3.1 [0.1]	1.4 [0.1]	2.9 [0.1]	1.5 [0.6]

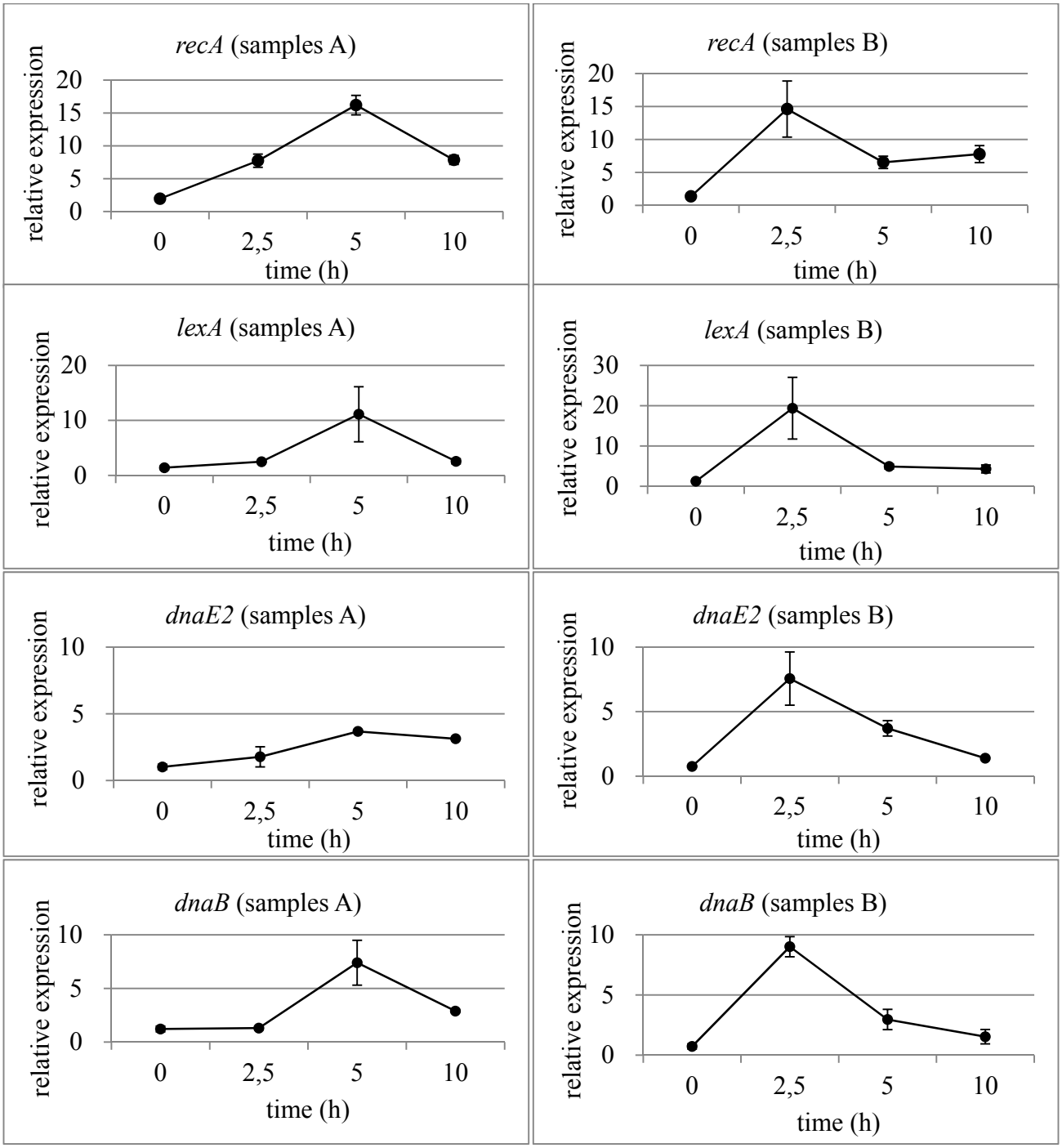

Figure 3-20: Analysis of SOS response induction. Relative fold change in expression of *recA*, *lexA*, *dnaE2* and *dnaB* in *M. smegmatis* after exposure to 1 µg/mL GM over 10 hours. The relative expression level was measured by qPCR and calculated by $2^{-\Delta\Delta Ct}$ and double referenced to the 16S rRNA expression level and the expression level of the according gene of an independent untreated sample. The values represent the mean of the relative gene expression level of two independent samples each measured in triplicate. Error bars indicate the standard deviation of the mean. Samples A were cultivated for 26.5 h and reached an OD_{600} of about 0.7 and samples B were cultivated for 22 h and reached an OD_{600} of about 0.5 before sampling was initiated (i.e. timepoint 0 h) and subsequent GM treatment was initiated 2.5 hours later (i.e. timepoint 2.5 h) (modified from referece 154).

3.3 GRISELIMYCIN RESISTANCE MECHANISM IN MYCOBACTERIA

To investigate the development of resistance against GM in *mycobacteria*, GM resistant *M. smegmatis* mc^2155 mutants were generated. Therefore ten independent *M. smegmatis* mc^2155 mutants were generated by exposure to increasing concentrations of GM (2.5, 5, 10, 20, 40 µg/mL) in five sequential steps. The frequency of spontaneous resistance to GM for *M. smegmatis* mc^2155 was determined to be 5×10^{-10} at a GM concentration of 10 µg/mL. It was observed that the GM resistant mutants exhibited an altered elongated cellular morphology (Figure 3-21).

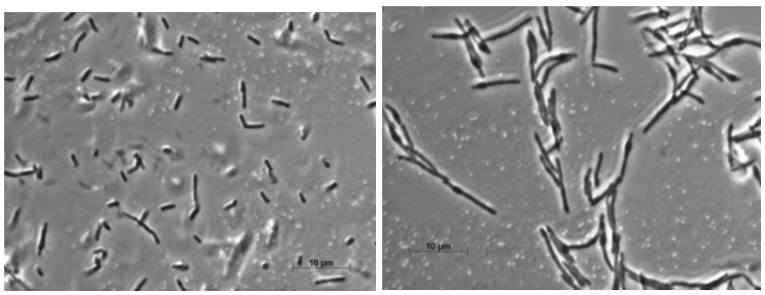

Figure 3-21: Phase contrast images of WT and GM resistant *M. smegmatis* cells. Scale bars, 10 µM.[154]

Cross-resistance testing of a GM resistant *M. smegmatis* mutant showed that GM resistant bacteria were cross-resistant to MGM and CGM but not to RIF or any other tested antibiotic (Table 3-10). Accordingly, *M. tuberculosis* strains with resistance against first- or second-line anti-TB drugs showed a similar MIC against CGM as the *M. tuberculosis* H37Rv wildtype strain (Table 3-11, Table 3-5).

Table 3-10: Cross resistance testing of GM resistant *M. smegmatis* mutant.[154]

Antimicrobial compound	MIC (µg/mL) for the following *M. smegmatis* strains	
	mc^2155 (GM susceptible)	$1.GM_{40}$ (GM resistant)
GM	5	80
MGM	2.5	40
CGM	0.6	5
Actinomycin D	16	16
Ampicillin	>320	>320
Ciprofloxacin	0.2	<0.2
Erythromycin	1.3	0.6
Kanamycin	<0.2	<0.2
Polymyxin B	2.5	2.5-5
Rifampicin	10	5-10
Tetracycline	0.2	0.2
Vancomycin	5	2.5

Table 3-11: Cross-resistance testing of CGM with *M. tuberculosis* strains mono-resistant to first- or second-line anti-TB drugs.[154] The MIC of *M. tuberculosis* H37Rv against CGM was 0.06 µg/mL (Table 3-5).

M. tuberculosis strain	Lineage	CGM MIC (µg/mL)
ATCC35822	H37Rv, isoniazid mono-resistant	0.056
ATCC35838	H37Rv, rifampicin mono-resistant	0.094
ATCC35827	H37Rv, kanamycin mono-resistant	0.087
ATCC35820	H37Rv, streptomycin mono-resistant	0.142
ATCC35826	H37Rv, cycloserine mono-resistant	0.051
rMOX	H37Rv, moxifloxacin mono-resistant	0.200

To further characterize the GM resistance mechanism, the genomic DNA of all five steps of five independent *M. smegmatis* mutants and the parental wildtypes was sequenced and compared. *In silico* analyses of the genomes of the wildtypes and the stepwise mutants revealed that GM resistant mutants contained one consistent single point mutation in the *dnaN* promoter region, an amplification of a chromosomal segment and several inconsistent mutations. In the present case the *dnaN* promoter mutation is regarded as a consistent mutation as this mutation occurs in all five independent mutants in the first mutant step (Table 3-12). However, this mutation is not maintained in all mutant steps of all five independent mutants. In contrast, the inconsistent mutations are mostly present only one of the five independent mutants but are passed to the subsequent mutant steps (Table 3-14).

All five independent GM resistant mutants contained an amplified chromosomal segment, as observed by *in silico* genome analyses, but the amplicons of different mutants varied in size from around 12 kb to around 28 kb (and consequently included a different number of genes) and evolved in different mutant steps during the selection process (Table 3-12, Table 3-13, Figure 3-22). Additionally, the amplicons of different steps of the mutants varied in copy number from 3 to 49 copies. The amplified chromosomal segment (amplicon) was confirmed by Southern blot for all steps of mutant 1 (Figure 3-23).

The first mutant steps of all five independent mutants contained a G-to-A transition mutation 115 bp upstream of the *dnaN* gene in the *dnaN* promoter region. The effect of this promoter mutation on the *dnaN* expression level was analyzed by qPCR (Figure 3-24, Table 3-16) using mutant $1.GM_{2.5}$, which is resistant against around 8 µg/mL GM but contains only the transition mutation in the *dnaN* promoter region and no amplification of a chromosomal segment, and mutant $1.GM_5$, which is resistant against around 16 µg/mL GM and contains the transition mutation in the *dnaN* promoter region as well as the amplification of a chromosomal segment containing the *dnaN* gene (Table 3-12). Compared to the wildtype the

dnaN expression level is increased around 5-fold in mutant 1.$GM_{2.5}$ and around 35-fold in mutant 1.GM_5, which indicates that the *dnaN* promoter mutation leads to an increase in the *dnaN* expression level and that the additional amplification further increases the *dnaN* expression level.

Determination of the MIC of all steps of the GM resistant mutants showed that the susceptibility of the stepwise mutants decreased with increasing amplicon copy number. Cultivation of GM mutants (1.GM_{40} and 9.GM_{40}) selected with 40 µg/mL GM in the absence of GM led to a decrease of the amplicon copy number together with an increase of the MIC.

A number of inconsistent mutations were also observed in GM resistant *M. smegmatis* mutants (Table 3-14, Table 3-15). Compared to the parental wildtypes, which were used for mutant selection, exposure to GM resulted in 0 to 8 mutations in each step during mutant selection. One mutation was present in two of the mutants (mutation 24 in mutant 7 and 9) and three different mutations affected the same gene (mutations 7, 8, and 9 in mutant 8, 4, and 9, respectively), all other mutations were present in only one of the five GM resistant mutants.

The situation was similar for CGM resistant *M. tuberculosis* mutants (Table 3-17, Figure 3-25). To select for CGM resistant mutants *in vivo,* nude mice were infected with 3-3.5 $\log_{10}$ CFU, after 2 weeks CGM monotherapy was initiated (100 mg/kg, once daily) and after 4 weeks of treatment CGM resistant isolates were selected and directly plated on plain and CGM (0.125 µg/mL) containing plates. The CGM resistant *M. tuberculosis* were around 15-30-fold less sensitive than the wildtype (CGM MIC of resistant *M. tuberculosis*: 1-2 µg/mL). Genome comparison of three resistant isolates revealed that CGM resistant *M. tuberculosis* mutants contained an approximately 5-fold amplification of a 10.3 kb chromosomal segment which contained the genes *dnaN*, *recF, gyrB* and *gyrA* as well as the *ori* region and a fraction of the *dnaA* gene.

Table 3-12: Genetic changes associated with the stepwise selection of GM resistant *M. smegmatis*. †Subscript indicates concentration of GM (µg/mL) used for stepwise mutant selection. Subscript 40→0 indicates that mutant selected under 40 µg/mL GM were grown in GM-free media for 2-4 days. *Percentage of sequencing reads with the 115 G > A point mutation in the *dnaN* promoter. **These mutants contained amplicons of different sizes and numbers (marked in grey) (modified from reference 154).

		Amplicon characteristics			
***M. smegmatis* mutant†**	**Promoter transition mutation (%)***	**Chromosomal segment (MSMEG locus tags)**	**Size (kb)**	**Copy number**	**GM MIC (µg/mL)**
Wild-type	0	No amplicon	---	---	4
1.$GM_{2.5}$	94	No amplicon	---	---	8
1.GM_{5}	99	6942 to 0006	12.054	4	16
1.GM_{10}	97	6942 to 0006	12.054	7	32
1.GM_{20}	100	6942 to 0006	12.054	8	64
1.GM_{40}	99	6942 to 0006	12.054	10	>64
1.$GM_{40\rightarrow0}$	98	6942 to 0006	12.054	9	64
4.$GM_{2.5}$	98	No amplicon	---	---	16
4.GM_{5}	98	No amplicon	---	---	16
4.GM_{10}	99	6941 to 0019	27.881	6	64
4.GM_{20}	97	6941 to 0019	27.881	9	64
4.GM_{40}	99	6941 to 0019	27.881	10	64
7.$GM_{2.5}$	95	No amplicon	---	---	8
7.GM_{5}	6	6940 to 0019	24.360	7	16
7.GM_{10}	16	6940 to 0019	24.360	11	32
7.GM_{20}**	79	6941 to 0002	6.414	8	64
		6940 to 0004	8.811	4	
		6940 to 0019	24.360	3	
7.GM_{40}	98	6940 to 0004	8.811	9	Poor growth
8.$GM_{2.5}$	18	6947 to 0018	19.228	3	16
8.GM_{5}	0	6947 to 0018	19.228	18	32
8.GM_{10}	0	6947 to 0018	19.228	30	32
8.GM_{20}	0	6947 to 0018	19.228	33	32
8.GM_{40}	0	6947 to 0018	19.228	49	Poor growth
9.$GM_{2.5}$**	23	6947 to 0004	5.228	2	8
		6936 to 0007	18.031	2	
9.GM_{5}**	33	Too variable	---	---	16
9.GM_{10}**	0	6940 to 0007	14.621	10	>64
		6945 to 0019	22.534	3	
9.GM_{20}	0	6940 to 0007	14.621	12	>64
9.GM_{40}	0	6940 to 0007	14.621	13	>64
9.$GM_{40\rightarrow0}$	0	6940 to 0007	14.621	4	32

Table 3-13: Genetic changes associated with *M. smegmatis* resistance to GM. Greater than symbol (>) indicates genetic change upstream of locus tag.[154]

Locus tag	Genetic change	Gene product and function
MSMEG_0001	Over-represented genomic region	DnaN: DNA polymerase III subunit beta (sliding clamp)
>MSMEG_0001	SNP: 115 G > A upstream of start codon	Non-coding region: putative regulatory function
MSMEG_0002	Over-represented genomic region	Gnd: 6-phosphogluconate dehydrogenase
MSMEG_0003	Over-represented genomic region	RecF: recombination protein F involved in DNA replication/repair
MSMEG_0004	Over-represented genomic region	hypothetical protein
MSMEG_0005	Over-represented genomic region	GyrB: DNA gyrase subunit B, negatively supercoils closed circular dsDNA during replication
MSMEG_0006	Over-represented genomic region	GyrA: DNA gyrase subunit A, negatively supercoils closed circular dsDNA during replication
MSMEG_0007	Over-represented genomic region	hypothetical protein
MSMEG_0008	Over-represented genomic region	tRNA-Ile
MSMEG_0009	Over-represented genomic region	hypothetical protein
MSMEG_0010	Over-represented genomic region	tRNA-Ala
MSMEG_0011	Over-represented genomic region	hypothetical protein with siderophore-interacting/FAD-binding domain
MSMEG_0012	Over-represented genomic region	FepD: ferric enterobactin transporter permease, iron complex transport system
MSMEG_0013	Over-represented genomic region	pseudogene, encodes ferric enterobactin transporter FepG but has a frame shift mutation
MSMEG_0014	Over-represented genomic region	formyl transferase
MSMEG_0015	Over-represented genomic region	FepC: ferric enterobactin transporter ATP-binding protein
MSMEG_0016	Over-represented genomic region	hypothetical protein
MSMEG_0017	Over-represented genomic region	ABC transporter permease
MSMEG_0018	Over-represented genomic region	ABC transporter permease
MSMEG_0019	Over-represented genomic region	amino acid adenylation protein
MSMEG_6936	Over-represented genomic region	hypothetical protein
MSMEG_6938	Over-represented genomic region	ParB-like partition proteins
MSMEG_6939	Over-represented genomic region	Soj family protein
MSMEG_6940	Over-represented genomic region	GidB: methyltransferase
MSMEG_6941	Over-represented genomic region	R3H domain-containing protein
MSMEG_6942	Over-represented genomic region	YidC: inner membrane protein translocase component
MSMEG_6944	Over-represented genomic region	hypothetical protein
MSMEG_6945	Over-represented genomic region	RnpA: ribonuclease P protein component
MSMEG_6946	Over-represented genomic region	RpmH: 50S ribosomal protein L34
MSMEG_6947	Over-represented genomic region	DnaA: chromosomal replication initiation protein

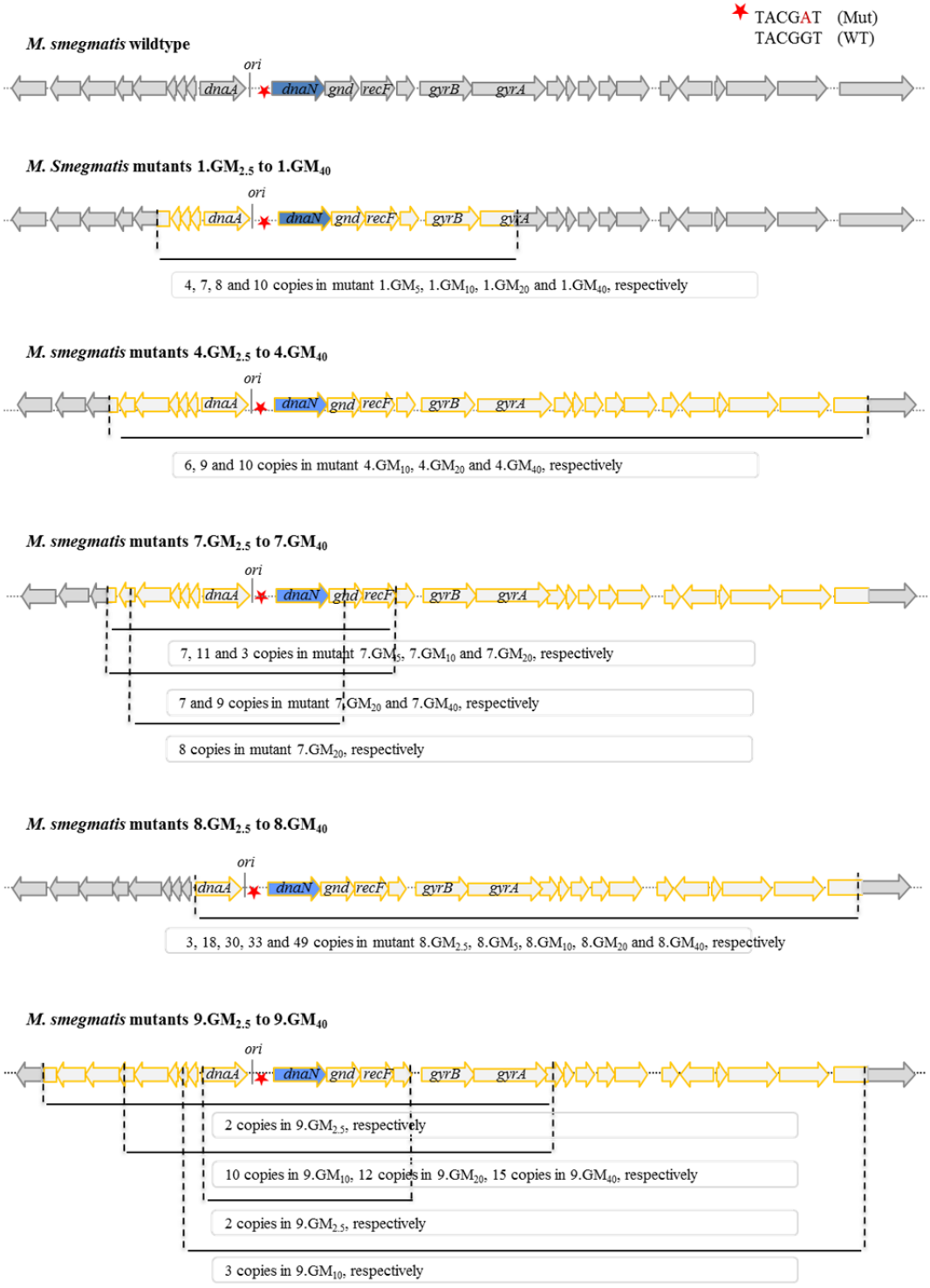

Figure 3-22: Overview of the genotype of all *M. smegmatis* mutants and the according mutant steps (see also Table 3-12 and Table 3-13). Depicted are the genetic changes of all analyzed GM mutants (1, 4, 7, 8, 9) that were acquired in the course of exposure to increasing concentrations GM in five steps (2.5, 5, 10, 20 and 40 µg/mL). The *ori* region is indicated. The *dnaN* gene is indicated in blue, the amplicon is indicated in yellow, the borderlines of the amplicons are indicated as dotted lines, the *dnaN* promoter region that contains the single point mutation is indicated as red star.[154]

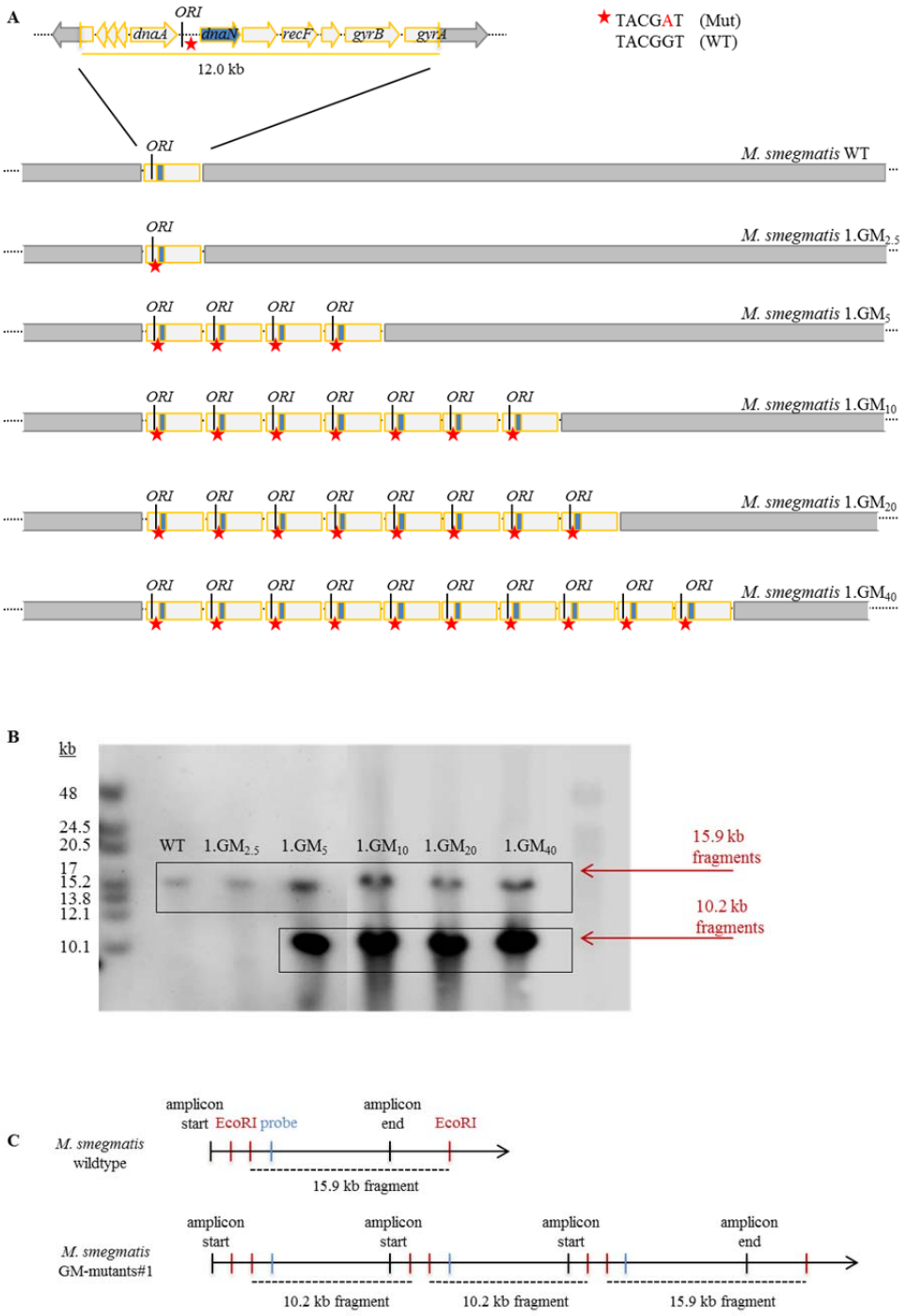

Figure 3-23: (A) Overview of the genetic changes associated with exposure to increasing concentrations GM for *M. smegmatis* mutants $1.GM_{2.5}$ to $1.GM_{40}$ (subscripts indicate GM concentration in µg/mL when the mutant was obtained). Red stars represent the G > A mutation in the *dnaN* promoter region 115 bp upstream of the *dnaN* gene. (B) Southern blot and (C) fragmentation pattern of *EcoRI*-digested genomic DNA of *M. smegmatis* WT and GM resistant mutants. *EcoRI* cuts downstream of the *dnaN* gene inside the amplicon and upstream of the *dnaN* gene outside the amplicon, resulting in a 15.9 kb fragment for samples without amplicons and 15.9 kb and 10.2 kb fragments for samples with amplicons. *EcoRI* restriction sites are indicated in red, the binding site of the probe (in the *dnaN* gene) is indicated in blue.[154]

Table 3-14: Inconsistent mutations (i.e. inconsistent single point mutations and other genomic rearrangements) observed in stepwise GM resistant mutants. Single point mutations that emerged during the course of exposure to stepwise increasing concentrations of GM compared to the wildtype are marked in black. The number of mutations newly added in each selection step is indicated in brackets after the mutant description and the GM concentration used for mutant selection is indicated as subscript, wherby subscript 0 indicates the parental wildtype. The description of the mutations is given in Table 3-15.

Mutation	*M. smegmatis* mc^{2}155																																	
	1.GM$_0$	1.GM$_{2.5}$ (3)	1.GM$_5$ (1)	1.GM$_{10}$ (0)	1.GM$_{20}$ (1)	1.GM$_{40}$ (2)	1.GM$_{40\text{-ohne}}$ (2)	4.GM$_0$	4.GM$_{2.5}$ (6)	4.GM$_5$ (0)	4.GM$_{10}$ (1)	4.GM$_{20}$ (0)	4.GM$_{40}$ (0)	7.GM$_0$	7.GM$_{2.5}$ (2)	7.GM$_5$ (3)	7.GM$_{10}$ (0)	7.GM$_{20}$ (6)	7.GM$_{40}$ (7)	8.GM$_0$	8.GM$_{2.5}$ (5)	8.GM$_5$ (4)	8.GM$_{10}$ (1)	8.GM$_{20}$ (0)	8.GM$_{40}$ (0)	9.GM$_0$	9.GM$_{2.5}$ (1)	9.GM$_5$ (0)	9.GM$_{10}$ (8)	9.GM$_{20}$ (0)	9.GM$_{40}$ (0)	9.GM$_{40\text{-ohne}}$ (0)
Mutation 1																			■															
Mutation 2																							■	■	■									
Mutation 3						■																												
Mutation 4																					■	■	■	■	■									
Mutation 5																■	■	■	■															
Mutation 6									■	■	■	■	■																					
Mutation 7																						■	■	■	■									
Mutation 8									■	■	■	■	■																					
Mutation 9																											■	■	■	■	■	■	■	
Mutation 10																		■	■															
Mutation 11																					■	■	■	■	■									
Mutation 12																■	■	■	■															
Mutation 13																													■	■	■	■	■	
Mutation 14																						■	■	■	■									
Mutation 15																													■	■	■	■	■	
Mutation 16					■	■	■																											
Mutation 17							■																											
Mutation 18																		■	■															
Mutation 19																			■															
Mutation 20																													■	■	■	■	■	
Mutation 21																			■															
Mutation 22		■	■	■	■	■	■																											
Mutation 23									■	■	■	■	■																					
Mutation 24																			■															
Mutation 25															■	■	■	■	■										■	■	■	■	■	
Mutation 26																													■	■	■	■	■	
Mutation 27									■	■	■	■	■																					
Mutation 28															■	■	■	■	■										■	■	■	■	■	
Mutation 29																		■	■															
Mutation 30																		■	■															
Mutation 31																■	■	■	■															
Mutation 32																			■															
Mutation 33																						■	■	■	■									
Mutation 34			■	■	■	■	■																											
Mutation 35									■	■	■	■	■																					
Mutation 36						■	■																											
Mutation 37																					■	■	■	■	■									
Mutation 38																					■	■	■	■	■									
Mutation 39																													■	■	■	■	■	
Mutation 40																		■	■															
Mutation 41		■	■	■	■	■	■																											
Mutation 42																													■	■	■	■	■	
Mutation 43		■	■	■	■	■	■																											
Mutation 44											■	■	■																					
Mutation 45																			■															
Mutation 46																						■	■	■	■									
Mutation 47									■	■	■	■	■																					
Mutation 48							■																											
Mutation 49																			■															
Mutation 50																		■	■															

Table 3-15: Description of inconsistent mutations (i.e. inconsistent single point mutations and other genomic rearrangements) observed in stepwise GM resistant mutants. Unspecified rearrangement denominates cases in which the nature of the mutation could not be determined.

Mutation	**Mutation description (position/ mutation description/ affected gene)**
Mutation 1	676,071/ G>A/ between MSMEG_0597 and MSMEG_0599
Mutation 2	721,883/ G>A, to STOP/ MSMEG_0639 (oligopeptide transport ATP-binding protein AppF)
Mutation 3	≈726,648/ deletion 1 bp/ MSMEG_0643 (extracellular solute-binding protein, family protein 5)
Mutation 4	≈886,316/ insertion 1 bp/ upstream MSMEG_0800 (hypothetical protein)
Mutation 5	951,614-951,622/ deletion 9 bp/ MSMEG_0868 (hypothetical protein)
Mutation 6	1,024,892-1,024,895/ unspecified rearrangement/ MSMEG_0946 (NAD dependent epimerase/dehydratase)
Mutation 7	1,038,906/ A>G/ upstream MSMEG_0965 (porin)
Mutation 8	1,039,243-1,039,247/ unspecified rearrangement/ MSMEG_0965(porin)
Mutation 9	≈1,039,306/ insertion 1 bp/ MSMEG_0965 (porin)
Mutation 10	1,040,482/ G>A/ 12 bp upstream MSMEG_0967(hypothetical protein)
Mutation 11	1,195,877/ G>T/ 35 bp upstream MSMEG_1134 (heat shock protein HtpX)
Mutation 12	≈1,280,802/ insertion 1 bp/ upstream MSMEG_1211 (Fatty acid desaturase)
Mutation 13	1,330,346/ T>G, V872G/ MSMEG_1252 (hypothetical protein)
Mutation 14	1,334,452-1,334,462/ unspecified rearrangement/ promoter MSMEG_1253(hypothetical protein)
Mutation 15	1,413,60/ C>A, V51F/ MSMEG_1317 (transcriptional regulator)
Mutation 16	1,437,811-1,437,814/ insertion 4 bp/ between MSMEG_1342 and MSMEG_1343
Mutation 17	1,664,020/ T>G, L394R/ MSMEG_1573 (carbohydrate kinase)
Mutation 18	1,905,775/ G>A, P120L/ MSMEG_1830 (FO 2-phospho-L-lactate transferase LPPG)
Mutation 19	1,974,89/ A>G, V182A/ MSMEG_1895 (HTH-type transcriptional regulator AlsR)
Mutation 20	1,996,866/ A>G, synonymous/ MSMEG_1913 and MSMEG_1914
Mutation 21	2,225,135/ T>C, T277A/ MSMEG_2150 (transposition helper protein)
Mutation 22	2,365,460-2,365,459/ unspecified rearrangement/ pseudogene area
Mutation 23	≈2,429,869/ insertion 1 bp/ pseudogene area
Mutation 24	2,478,682/ C>T/ MSMEG_2395 (D-alanyl-alanine synthetase A)
Mutation 25	2,600,364-2,600,365/ unspecified rearrangement/ pseudogene area
Mutation 26	2,717,606/ C>T, V151M/ MSMEG_2636 (LacI family transcriptional regulator)
Mutation 27	≈2,961,162/ deletion 1 bp/ MSMEG_2897 (hypothetical protein)
Mutation 28	3,407,191-3,407,193/ unspecified rearrangement/ MSMEG_3328 (hypothetical protein)
Mutation 29	3,413,575/ T>C, S162G/ MSMEG_3336 (hydrolase)
Mutation 30	3,512,112/ A>G, Q249R/ MSMEG_3442 (cyclohexadienyl dehydratase)
Mutation 31	3,529,047/ T>C, V711A/ MSMEG_3461 (catalase/peroxidase HPI)
Mutation 32	3,602,746/ C>G, G22A/ MSMEG_3541 (cytochrome C biogenesis protein transmembrane region)
Mutation 33	3,798,639/ G>A/ non-coding area
Mutation 34	deletion of ca. 95 genes between transposases MSMEG_3984 and MSMEG_4081
Mutation 35	4,179,311/ G>A, P488S/ MSMEG_4101 (ABC transporter substrate-binding protein)
Mutation 36	4,669,225-4,669,233/ unspecified rearrangement/ MSMEG_4576 (SpfH domain-containing protein)
Mutation 37	4,709,848-4,709,855/ insertion 1 bp/ between MSMEG_4625 and MSMEG_4626
Mutation 38	4,749,972-4,749,976/ insertion 1 bp/ MSMEG_4663 (protein lolB)
Mutation 39	5,215,424/ C>T, synonymous/ MSMEG_5118 (nudix hydrolase)
Mutation 40	5,303,249/ T>C, S394G/ MSMEG_5205 (hypothetical protein)
Mutation 41	5,458,577-5,458,579/ ACT>CCC/ non-coding area
Mutation 42	5,588,902/ C>T, synonymous/ MSMEG_5504 (hypothetical protein)
Mutation 43	5,680,625/ T>C, T469A/ MSMEG_5593 (pyruvate dehydrogenase)
Mutation 44	6,034,663 T>C, H308R/ MSMEG_5969 (hypothetical protein)
Mutation 45	6,046,066/ G>A, R435 to STOP/ MSMEG_5982 (UDP-glucose 6-dehydrogenase)
Mutation 46	6,130,265/ A>C, L97R/ MSMEG_6062 (Fe uptake system permease)
Mutation 47	6,216,852/ G>T, A324S/ MSMEG_6147 (hypothetical protein)
Mutation 48	6,393,894/ G>A, synonymous/ MSMEG_6326 (tRNA-Ser)
Mutation 49	6,694,493/ T>G, D456A/ MSMEG_6643(DNA-binding protein)
Mutation 50	6,755,312 T>C, V147A MSMEG_6705 (regulatory protein)

Table 3-16: *DnaN* expression level, promoter mutation, amplicon copy number and GM MIC of *M. smegmatis* wildtype and GM resistant mutants $1.GM_{2.5}$ and GM_5. Mutant $1.GM_{2.5}$ shows a MIC of about 8 µg/mL GM but contains only the transition mutation in the *dnaN* promoter region and no amplification of a chromosomal segment. Mutant $1.GM_5$ shows a MIC of about 16 µg/mL GM and contains the transition mutation in the *dnaN* promoter region as well as the amplification of a chromosomal segment containing the *dnaN* gene. The *dnaN* expression level is given as the mean of the relative gene expression level of three independent samples each measured in triplicate. The standard deviation (SD) of the mean is indicated in brackets.

M. smegmatis	Promoter mutation	Relative *dnaN* expression level [SD]	Amplicon copy number	GM MIC (µg/mL)
WT	no	1	1	4
$1.GM_{2.5}$	yes	5 [0,7]	1	8
$1.GM_5$	yes	34,7 [7,9]	4	16

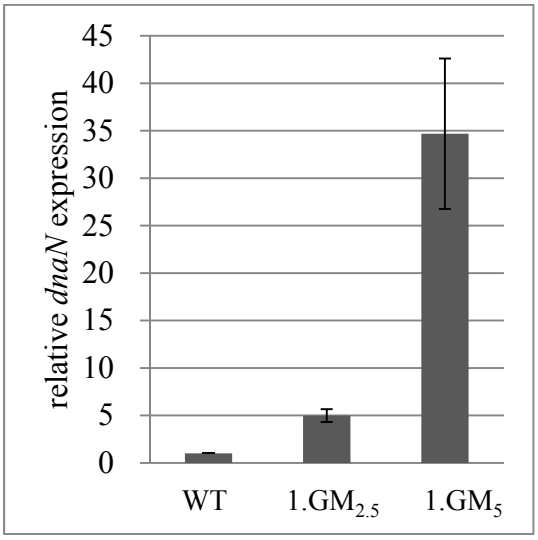

Figure 3-24: Relative fold change in expression of the *dnaN* expression level in *M. smegmatis* GM resistant mutants $1.GM_{2.5}$ and $1.GM_5$ compared to the parental *M. smegmatis* wildtype. Mutant $1.GM_{2.5}$ shows a MIC of about 8 µg/mL GM but contains only the transition mutation in the *dnaN* promoter region and no amplification of a chromosomal segment and mutant $1.GM_5$ shows a MIC of about 16 µg/mL GM and contains the transition mutation in the *dnaN* promoter region as well as the amplification of a chromosomal segment containing the *dnaN* gene (Table 3-16). The relative expression level was measured by qPCR and calculated by $2^{-\Delta\Delta Ct}$, and double referenced to the 16S rRNA expression level and the expression level of the wildtype. The bars represent the mean of the gene expression level (relative to the wildtype) of three independent samples each measured in triplicate. Error bars indicate the standard deviation of the mean.

Table 3-17: Genetic changes associated with *M. tuberculosis* resistance to CGM.[154]

Locus tag	Genetic change	Gene product and function
Rv0001	Over-represented genomic region	Pseudogene (partial *dnaA*, encoding the chromosomal replication initiation protein)
Rv0002	Over-represented genomic region	DnaN: DNA polymerase III subunit beta (sliding clamp)
Rv0003	Over-represented genomic region	RecF: recombination protein F involved in DNA replication/repair
Rv0004	Over-represented genomic region	Hypothetical protein
Rv0005	Over-represented genomic region	GyrB: DNA gyrase subunit B, negatively supercoils closed circular dsDNA during replication
Rv0006	Over-represented genomic region	GyrA: DNA gyrase subunit A, negatively supercoils closed circular dsDNA during replication
Rv0007	Over-represented genomic region	Pseudogene (partial possible conserved membrane protein)

Figure 3-25: Overview of the genetic changes of *M. tuberculosis* associated with CGM resistance. CGM resistance is acquired by approximately 5-fold amplification of a 10.3 kb chromosomal segment (amplicon), containing the *dnaN* gene (indicated in blue), several other genes (Table 3-17) and the *ori* site.[154]

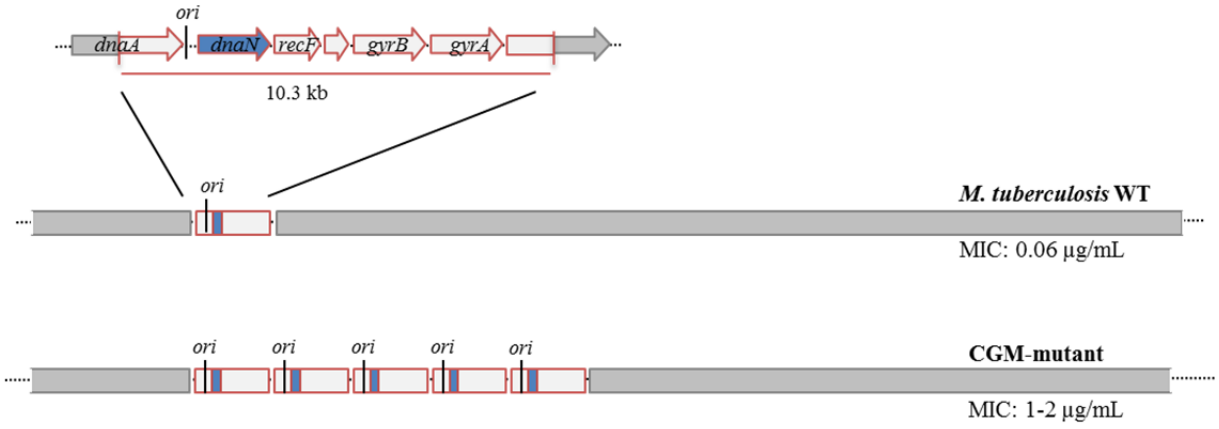

To characterize the fitness of GM resistant *M. smegmatis* mutants in comparison to the wildtype, growth curves for GM resistant mutants $1.GM_5$, $1.GM_{40}$ and $1.GM_{40\rightarrow0}$ and the parental wildtype ($1.GM_0$) were recorded. Mutant $1.GM_5$ was grown in the presence of 5 µg/mL GM. Mutant $1.GM_{40\rightarrow0}$ was grown without GM and mutant $1.GM_{40}$ was grown in the presence of 40 µg/mL GM, whereby both cultures were inoculated from the same pre-culture of mutant $1.GM_{40}$ grown with 40 µg/mL GM. As a result, GM resistant mutants showed a prolonged lag phase of growth and an overall reduction of the final cell density, indicating that acquisition of antibiotic resistance is associated with physiological costs for the mutants. Removal of GM (i.e. $1.GM_{40\rightarrow0}$) results in less retarded growth but no significant difference in the final cell density.

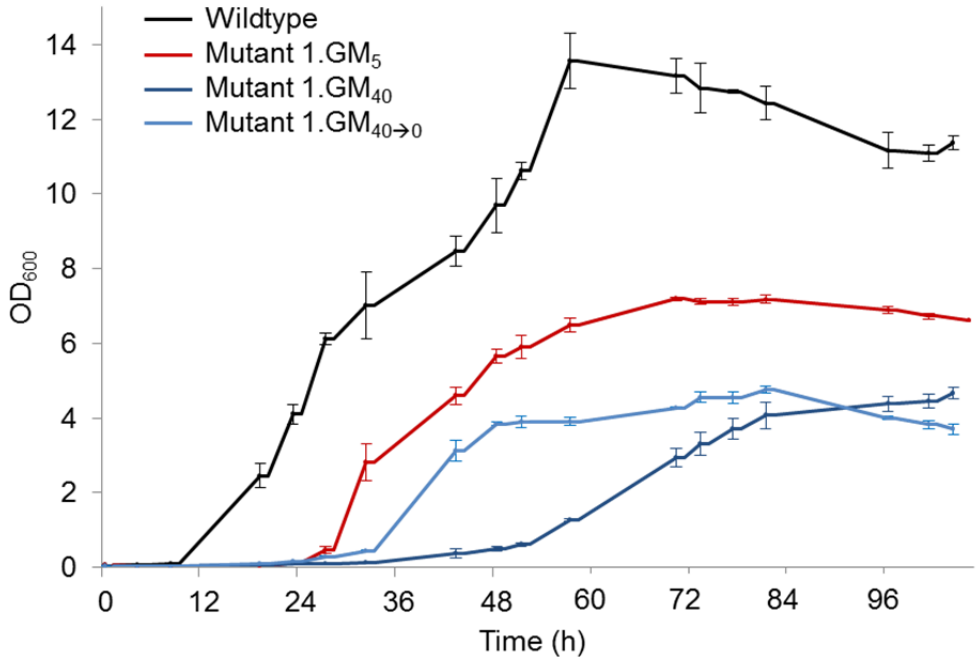

Figure 3-26: Growth curves of *M. smegmatis* wildtype ($1.GM_0$) and GM resistant mutants $1.GM_5$, $1.GM_{40}$ and $1.GM_{40\rightarrow0}$. Subscript indicates the GM concentration in µg/mL when mutant was obtained. Data points and error bars represent the mean and the standard deviation of three independent measurements, respectively.[154]

4 DISCUSSION

4.1 SELF-RESISTANCE TO GRISELIMYCINS IN *STREPTOMYCES CAELICUS*

The GM biosynthesis gene cluster of the GM producing strain *Streptomyces caelicus* contains, besides the genes involved in GM biosynthesis or regulation, an unusual gene that encodes for an additional homolog of the DNA polymerase III β subunit (Figure 3-2).[147] The conventional DNA polymerase β subunit is encoded by the *dnaN* gene and is also called sliding clamp or DnaN.

The sliding clamp is a subunit of the main replicative DNA polymerase (DNA polymerase III) and is structurally highly conserved among prokaryotes.[185] In bacteria, two DnaN polypeptide chains build a dimer, whereby each chain consists of three distinct domains. The eukaryotic sliding clamp equivalent PCNA (proliferating cell nuclear antigen) is also structurally highly conserved among eukaryotes, but is composed of three monomers that consist of two domains each and shows low sequence similarity to the bacterial sliding clamps. The sliding clamp forms a ring around the DNA and tethers the DNA polymerase to the DNA during replication and increases the processivity of the DNA polymerase. The inner surface of the sliding clamp shows a positive electrostatic potential that is assumed to favour association with acidic polynucleotide phosphates of the DNA backbone by unspecific contacts, so that the clamp can slide along the DNA.[186,187] The processivity is a measure of the number of nucleotides (nt) a polymerase is capable to incorporate before it dissociates from the template DNA. In the absence of the sliding clamp, the replicative polymerase of *E. coli* synthesizes DNA at a rate of about 10 nt/s with a processivity of 10 - 20 nt.[188] In complex with the sliding clamp the polymerase incorporates 1000 - 2000 nt at a rate of about 350 - 500 nt/s.

The additional sliding clamp homolog in the GM cluster of the GM producing strain *S. caelicus* was named GriR. GriR shows 51 % amino acid similarity to the conventional DnaN of *S. caelicus*. As GriR is located inside of the GM cluster but does not have any apparent function regarding GM synthesis, regulation, transport or similar, it was assumed that GriR may function as a resistance determinant for GM. Overexpression of the *griR* gene in the GM sensitive *S. coelicolor* indeed conferred GM resistance to *S. coelicolor*, which indicates that GriR functions as a self-resistance determinant in *S. caelicus*.

Most bacterial genomes carry a single copy of the *dnaN* gene.[189] However, several bacterial genomes carry more than one *dnaN* gene. Thereby the conventional *dnaN* gene is designated as *dnaN1* and the additional copy is designated as *dnaN2*. The *dnaN1* gene is usually located in a conserved gene environment next to *dnaA*, *recA* and *gyrB*. This was also observed for *dnaN1* of *S. caelicus* (Figure 3-1). In contrast, the additional homolog *griR* of *S. caelicus* is surrounded by genes of the GM biosynthesis cluster (Figure 3-2). Several other *Streptomyces* genomes also carry additional *dnaN* homologs, but these *dnaN2* genes are not located in a conserved gene environment and the function of DnaN2 remains unclear. Additionally, a sequence comparison of DnaN1 and DnaN2 proteins of several *Streptomyces* with available genome sequences showed that the DnaN1 proteins hold high sequence similarity to each other whereby the DnaN2 proteins hold less sequence similarity to each other (Figure 3-4, Figure 6-1, Table 6-2). The compared *Streptomyces* DnaN1 proteins show amino acid identities of > 89 % to each other and of < 54 % to other DnaN2 proteins, whereby the identities of the compared *Streptomyces* DnaN2 proteins range between 35 - 99 % to each other, so that the different DnaN2 proteins might have evolved for different reasons. As none of the compared *Streptomyces dnaN2* genes was predicted to be located inside of a biosynthetic gene cluster by the software antismash[178], there was no obvious indication that these *dnaN2* genes are involved in resistance to a secondary metabolite as in the case of *griR*. In addition, GM resistance is obviously not conferred by arbitrary additional DnaN copies, as *S. coelicolor* contains an additional DnaN copy but is sensitive to GM (Figure 3-4, Table 3-1). However, at least one copy of the sliding clamp is essential for cell viability. Knockout of all present *dnaN* copies is lethal, as was shown for *Bacillus anthracis*.[189] *B. anthracis* contains two *dnaN* genes whereby knockout of *dnaN1* led to a decreased growth rate and an increased mutation rate, whereby growth and mutation rate of a *dnaN2* knockout mutant were comparable to that of the wildtype. It is therefore assumed that DnaN2 functions less efficiently than DnaN1, with a lower replication and mismatch repair rate.

As self-resistance to GMs in *S. caelicus* is mediated by an additional sliding clamp homolog, it was examined if GMs bind directly to the conventional sliding clamp DnaN of *S. caelicus* and if resistance is possibly mediated by no or weak binding of GMs to the additional sliding clamp GriR. SPR analyses showed that GMs bind to both, the conventional DnaN of *S. caelicus* and the resistance conferring GriR of *S. caelicus* (Table 3-2, Figure 3-5, Figure 3-6). However, GMs bound to the DnaN of *S. caelicus* with a high affinity in the picomolar

range and showed a slow dissociation from the protein, whereby GMs bound to the resistance protein GriR of *S. caelicus* with lower affinity in the micromolar range and showed a fast dissociation from the protein, so that resistance to GMs is apparently conferred by the combination of a weaker affinity of GMs to GriR and a shorter duration of the interaction. Proteins (such as the replicative DNA polymerase) that interact with the sliding clamp in *S. caelicus* may show a higher affinity to GriR than GMs, so that GMs may be displaced from GriR by these proteins and allow GriR to resume its function. To examine possibe differences that could lead to the different affinities of GMs to the *S. caelicus* GriR and the *S. caelicus* DnaN, the thermodynamic profiles of these interactions were characterized by ITC (Table 3-3, Figure 3-7, Figure 3-8). However, the changes in binding enthalpy and in entropy were similar for both interactions. For the binding of GM to the *S. caelicus* DnaN, the entropic contribution ($-T\Delta S$) was somewhat more favorable than for the binding to GriR, whereby the relatively small favorable entropy change suggests no or minor conformational changes upon binding of GM and a favorable desolvation entropy change for both interactions. The enthalpic contribution (ΔH) to the binding of GM to the *S. caelicus* DnaN was also somewhat more favorable compared to that of the binding to GriR, which could result from additional bonds between GM and DnaN or steric clashes or non-complementary interactions between GM and GriR. This could cause different binding modes of GMs to GriR and DnaN of *S. caelicus* and by this the different affinities. To further examine possible differences in the binding modes, a model of the two *S. caelicus* sliding clamps was generated (Figure 4-1), with GMs bound to the common sliding clamp peptide binding site, which is also bound by the replicative polymerase and other sliding clamp interaction partners (since GMs were found to bind to this common peptide binding site of sliding clamps, see section 4.2). This model suggests that there is a lysin (K_{344}) in the peptide binding site of GriR in a position where a proline (P_{347}) is found in the *S. caelicus* DnaN, which could lead to steric hindraces and a different binding mode of GMs to GriR compared to DnaN of *S. caelicus*. The comparison of the amino acids shaping the sliding clamp peptide binding sites of GriR and DnaN of *S. caelicus* (Table 4-1) revealed that this lysine (K_{344}) represents the only conservative amino acid exchange in GriR compared to DnaN of *S. caelicus*. The additional sliding clamp DnaN2 of the second known GM producer *S. griseus* likewise shows a conservative amino acid exchange at this position (R_{350} in DnaN2 of *S. griseus* instead of P_{347} in DnaN of *S. caelicus* and *S. griseus*), whereby DnaN2 of *S. griseus* shows three additional conservative amino acid exchanges compared to DnaN of *S.caelicus* and *S. griseus*. Under the

assumption that DnaN2 also confers self-resistance to GMs in *S. griseus*, these amino acid exchanges might affect the affinity and the binding mode of GMs to *S. griseus* DnaN2 compared to *S. griseus* DnaN, by being involved in direct contacts to GMs, by inducing steric clashes, or by altering the overall hydrophobicity in the peptide binding site. However, one single amino acid exchange in the peptide binding site of the sliding clamp (e.g. P_{347} → K in DnaN *S. caelicus*) might be sufficient to affect the binding of GMs. The reason for the exchange of about 50 % of the amino acids in GriR compared to *S. caelicus* DnaN remains unclear, a fraction of the amino acid exchanges might be related to adaptions to additional contacts of sliding clamp interaction partners outside the peptide binding site (e.g. to compensate an impaired binding caused by amino acid exchanges in the peptide binding site) or to adaptions to specific processes other than the conventional replication (e.g. to bind more efficiently to enzymes involved in translesion synthesis). No second replicative DNA polymerase was found to be present in *S. caelicus* (or *S. griseus*), which could have evolved to bind more efficiently to GriR (or DnaN2), so that the peptide binding site of the GM resistance conferring sliding clamps presumably evolved in a way to prevent efficient binding of GMs but to still enable polymerase binding. The indication that GMs may bind to GriR and DnaN of *S. caelicus* with different binding modes suggests that the replicative DNA polymerase also may bind to the two sliding clamps with different binding modes and different affinities. A lower binding affinity of the replicative DNA polymerase to additional sliding clamp analogs could contribute to the decreased growth rate and increased mutation rate, which was observed upon knock out of the conventional sliding clamp DnaN (leaving only the additional sliding clamp DnaN2) in *B. anthracis*.[189]

Table 4-1: Amino acids shaping the peptide binding site of DnaN and GriR of *S. caelicus* and DnaN1 and DnaN2 of *S. griseus*. Hydrophobic residues are indicated in grey; basic residues are indicated in blue; neutral residues are not coloured; subscripts indicate amino acid positions.

Protein	Amino acids shaping the sliding clamp peptide binding site																			
DnaN *S. griseus*	L_{149}	V_{151}	L_{152}	T_{169}	R_{171}	Y_{172}	R_{173}	F_{174}	P_{245}	L_{250}	N_{322}	F_{325}	T_{346}	P_{347}	L_{368}	I_{369}	M_{370}	P_{371}	V_{372}	R_{373}
DnaN *S. caelicus*	L_{149}	V_{151}	L_{152}	T_{169}	R_{171}	Y_{172}	R_{173}	F_{174}	P_{245}	L_{250}	N_{322}	F_{325}	T_{346}	P_{347}	L_{368}	I_{369}	M_{370}	P_{371}	V_{372}	R_{373}
GriR *S. caelicus*	L_{149}	V_{151}	L_{152}	T_{169}	R_{171}	Y_{172}	R_{173}	F_{174}	P_{242}	L_{247}	N_{319}	F_{322}	N_{343}	K_{344}	L_{365}	V_{366}	M_{367}	P_{368}	V_{369}	R_{370}
DnaN2 *S. griseus*	L_{155}	A_{157}	L_{158}	T_{175}	R_{177}	Y_{178}	R_{179}	Y_{180}	P_{246}	L_{251}	N_{325}	Y_{328}	G_{349}	R_{350}	L_{366}	L_{367}	M_{368}	S_{369}	V_{370}	K_{371}

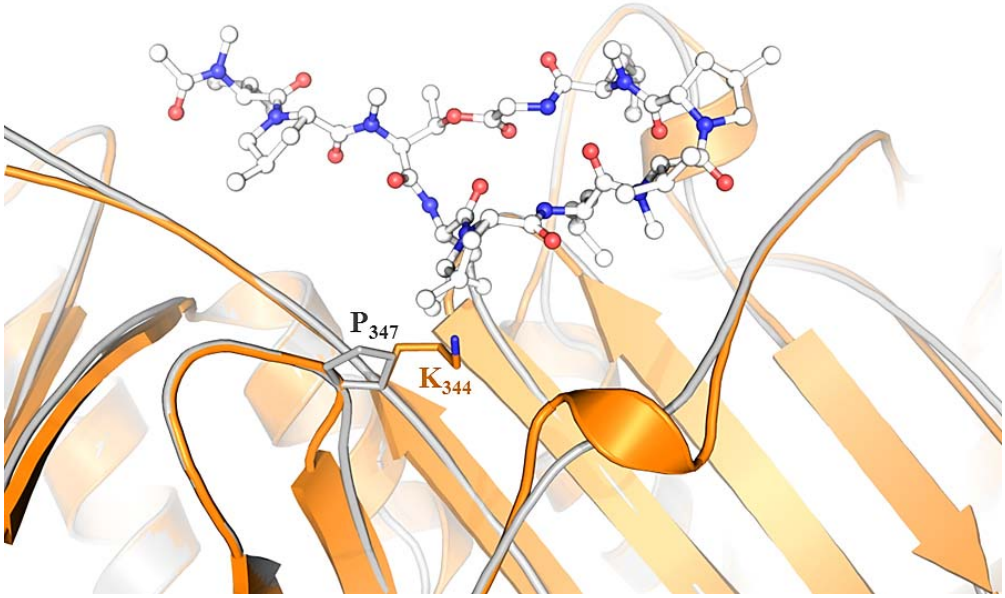

Figure 4-1: Model showing the superposition of GriR and DnaN of *S. caelicus* with GM bound to the common sliding clamp peptide binding site. Grey: preliminary crystal structure of DnaN *S. caelicus* with bound MGM (resolved by Dr. Peer Lukat); orange: homology model of GriR *S. caelicus* (based on the *S. caelicus* DnaN structure); white: MGM.

4.2 Mechanism of Action of Griselimycins

GMs are narrow-spectrum agents that are active against several microorganisms that belong to the *Actinomycetales* order (Table 3-4), which includes mycobacterial species. No susceptibility of Gram-negative or fungal microorganisms to GMs was detected. Against mycobacteria and *Nocardia*, CGM showed the highest activity and GM showed the lowest activity. This was in reverse for the other susceptible organisms. Against *Corynebacterium glutamicum*, *Micrococcus luteus* and *Streptomyces coelicolor* GM showed the highest and CGM showed the lowest activity. Additionally, GMs were also active on intracellular (in murine macrophages) mycobacteria (Table 3-5).

The difference in the potency of the GM derivatives presumably depends at least partly on the lipophilicity of the compounds (Log D (distribution coefficient) GM: 3.26, Log D MGM: 3.61, Log D CGM: 5.71). An enhanced activity of more liphophilic derivatives of other compound classes (e.g. derivatives of INH or fluoroquinolones) against mycobacteria was previously demonstrated. For example INH derivatives with attached hydrophobic hydrocarbon moieties were reported to show increased activity against *M. tuberculosis*

compared to INH itself.[190] However, the INH derivatives did not show increased potency on all tested *M. tuberculosis* isolates. Likewise, several CFX or LFX analogs with alkyl substitutions were described to be more active against *M. tuberculosis* compared to CFX or LFX itself.[191,192] The same CFX analogs did not show improved potency on other Gram-positive and Gram-negative bacteria and not on all tested mycobacterial species. However, regarding the LFX analogs, the compound with the highest lipophilicity was no necessarily the most potent one. Similar observations were made for GMs, the more lipophilic methyl and cyclohexyl substituted derivatives showed higher activity against mycobacteria and *Nocardia* but were less active against other Gram-positive bacteria. Additionally, the GM derivatives showed a differential improvement in potency for different mycobacteria. Compared to GM the potency of CGM was enhanced by a factor of about 16.7 for *M. tuberculosis* (MICs: GM 1 µg/mL, CGM 0.06 µg/mL), by a factor of about 7.5 for *M. smegmatis* (MICs: GM 4.5 µg/mL, CGM 0.6 µg/mL), and by a factor of about 1.7 for *M. bovis* (MICs: GM 0.5 µg/mL, CGM 0.3 µg/mL). GM derivatives with a lipophilicity (Log D) higher than that of CGM showed no further improvement in potency, possibly because they exceed the optimal lipophilicity. Compounds that exceed the optimal lipophilicity for cell permeability are assumed to remain trapped in the cell membrane.[193] The increased potency of more hydrophobic compounds against mycobacteria is assumed to depend on their ability to penetrate the bacterial cell wall as they could dissolve in the lipids of the outer cell wall layer. The cell envelope of mycobacteria is composed of a cytoplasmic membrane that is surrounded by an outer layer of peptidoglycan and arabinogalactan that is ligated with mycolic acids (Figure 4-2).[194] The outer cell wall layer is surrounded by a non-covalently linked capsule of proteins and polysaccharides and functions as exclusion barrier for many antibiotics.[195] For hydrophilic drugs the permeability of the cell wall is low but small hydrophilic antibiotics may enter mycobacterial cells via porins (as shown for β-lactams, chloramphenicol or norfloxacin).[196] Hydrophobic compounds such as GMs may traverse the cell wall by diffusion through the hydrophobic bilayer.[197] The different sensitivity levels of different mycobacterial species to hydrophobic compounds are assumed to depend on differences in the mycolic acid structure that may affect cell wall fluidity and permeability.[198] For mycobacterial species that are less sensitive to GMs a combination treatment with antibiotics, which can lead to an altered membrane permeability (such as aminoglycosides[50,51]) might thus be considered.

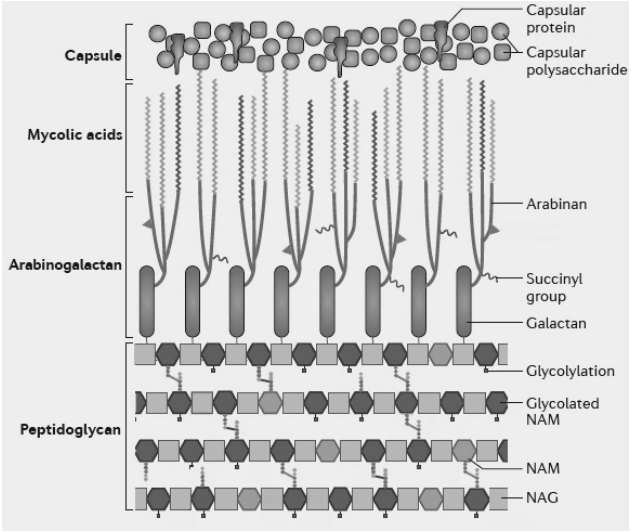

Figure 4-2: The mycobacterial cell wall is composed of peptidoglycan (comprised of the disacharide NAG-NAM), arabinogalactan and mycoblic acids. NAM, *N*-acetyl muramic acid; NAG, *N*-acetyl-glucosamine (modified from reference 194).

CGM exhibited bactericidal activity against *M. tuberculosis in vitro* and *in vivo*. By definition, bacteriostatic compounds prevent growth of bacteria (growth arrest in the stationary phase) and bactericidal compounds kill more that 99.9 % of the bacteria (i.e. the initial inoculum of 5 x 10^5 CFU is reduced by at least 3 $\log_{10}$ CFU).[199] A *M. tuberculosis* time-kill curve revealed a CFU reduction of > 3 $\log_{10}$ upon treatment with the 0.75-fold MIC of GM, whereby the effect was enhanced by time but not by concentration, indicating a time-dependent bactericidal effect of CGM on *M. tuberculosis in vitro* (Figure 3-9). A bactericidal effect of CGM was also observed *in vivo*.[154] In the acute mouse model of TB which is used to test the activity of compounds against actively multiplying bacteria, bacterial growth could be prevented upon treatment with 50 mg/kg/day (defining the minimal effective dose of CGM) and a decrease of the CFU count was observed upon treatment with 100 mg/kg/day (defining the minimal bactericidal dose of CGM). In the chronic mouse model of TB, which is used to test the antimicrobial activity of compounds against a stable nonreplicating bacterial population, treatment with 100 mg/kg/day resulted in a decrease in lung CFU counts.[154]

GM and MGM did not show significant toxicity and CGM showed a moderate toxicity *in vitro* on tested mammalian cells (hamster epithelial cells CHO-K1, mouse fibroblast cells L929 and mouse leukaemic macrophages RAW264.7) (Figure 3-11). Additionally, no overt adverse effects upon administration of CGM were observed in treated mice.[154] Since the sliding clamp is the target of GMs in *S. caelicus*, the binding of GMs to the human sliding

clamp analog PCNA and a possible genotoxic effect, which would present an obstacle for an antibiotic therapy with GMs, were also examined. A possible genotoxic effect could be caused by the inhibition of the binding of polymerases to PCNA, which could result in inefficient replication and DNA damage. However, no specific binding of GMs to the human PCNA was observed (Figure 3-16) and no apparent genotoxic effect was observed in a micronucleus test with CHO-K1 cells (Figure 3-10).

As GMs target the sliding clamp of the GM producer *S. caelicus*, it was assumed that GMs also target the sliding clamps of GM sensitive microorganisms. To further examine if the specific activity of GMs could at least partly depend on the homology of the sliding clamps of GM susceptible microorganisms, a homology analysis of the amino acid sequences of different sliding clamps was performed *in silico* (Figure 3-12). The homology analysis showed that the human and fungal sliding clamp analogs show low amino acid similarity (sequence identity < 12 %) to the microbial sliding clamps and that the sliding clamps of Gram-positive microorganisms show a higher sequence similarity to each other than to those of Gram-negative microorganisms (Table 6-3). The sliding clamps of Gram-negative and Gram-positive organisms correspondingly cluster in separate branches of the according phylogenetic tree (Figure 3-12). In addition, the sliding clamps of the GM susceptible organisms also cluster in a separate branch of the tree. As the sliding clamps of the GM sensitive organisms share a high amino acid similarity, GM susceptibility apparently correlates with the sliding clamp sequence similarity. Although sliding clamps of Gram-positive and Gram-negative organisms share low sequence similarity, they show a similar structure (Figure 4-3). Crystal structures of the *E. coli* and *M. tuberculosis* sliding clamps show that both sliding clamps are composed of two monomers that are comprised of three domains. In *E. coli* each domain consists of two α-helices inside of the ring and two β-sheets outside of the ring. In *M. tuberculosis* domain II shows the same organization and domains I and III contain only an additional short β-strand at the end of the first β–sheet, which does not lead to major structural differences compared to the *E. coli* sliding clamp.[200,201] The peptide binding pockets of the *E. coli* and *M. tuberculosis* sliding clamps were also reported not show major structural differences (as estimated by their C_α positions)[183], however, the about 20 amino acids shaping the sliding clamp peptide binding pockets[184,202] of different microorganisms show different similarities. The amino acids of the sliding clamp binding pockets of Gram-positiv organisms show a higher similarity to each other than to those of

Gram-negative organisms (and vice versa) (Table 3-6, Table 6-4). Thereby, the amino acids shaping the sliding clamp peptide binding sites of the analyzed Gram-negative organisms are mostly identical with a conservative amino acid variation in only one position. The amino acids shaping the sliding clamp peptide binding pockets of Gram-positive organisms show conservative exchanges at nine positions (plus few non-conservative exchanges), whereby seven of the nine conservative exchanges affect the sliding clamp peptide binding pockets of all or some of the GM sensistive organisms or GM producing strains, so that these differences could at least partly contribute to the sensitivity to GMs (Table 3-6).

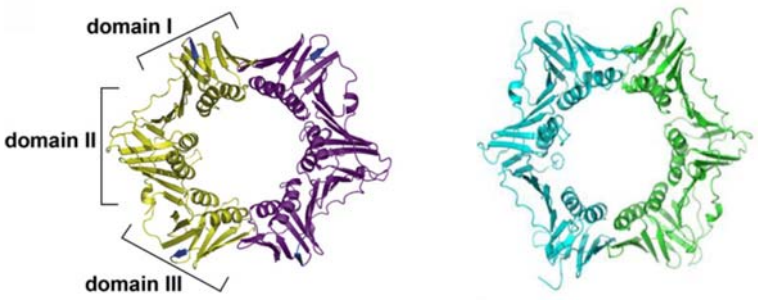

Figure 4-3: Structure of the sliding clamp of the Gram-positive organism *M. tuberculosis* (PDB: 4TR7) (left image) and the Gram-negative organism *E. coli* (PDB1: OK7) (right image). The additional short β-strands in the *M. tuberculosis* sliding clamp are indicated in blue (modified from references 201 and 183).

To analyse if GMs exert their activity by binding to the sliding clamp of GM susceptible organisms, binding of GMs to the purified sliding clamps of mycobacteria was examined by SPR. GM, MGM and CGM interact with the sliding clamps of *M. smegmatis* and *M. tuberculosis* similarly as with the *S. caelicus* DnaN, with a high affinity in the picomolar range and with a slow dissociation of GMs from the sliding clamps (Table 3-7, Figure 3-13). The kinetic profiles of the interaction of the three GMs with the mycobacterial DnaNs were similar, whereby the dissociation rate of CGM was somewhat slower. However, binding of GMs was also observed to the sliding clamp of *E. coli,* with an affinity in the high nanomolar range and with a fast dissociation from the protein (Table 3-13, Figure 3-14). The kinetic profile thus resembles rather that of the resistance protein GriR than that of the mycobacterial DnaNs (Figure 4-4). ITC measurements confirmed that GM binds to the *E. coli* DnaN with an affinity in the high nanomolar range with the expected stoichiometry of one GM per DnaN polypeptide chain. For the binding of GM to the *E. coli* DnaN the enthalpic contribution was higher than the entropic contribution ($-T\Delta S$ = -5.8 kcal mol^{-1}, ΔH = -3.2 kcal mol^{-1}), which was in reverse for the binding of GM to GriR or DnaN of *S. caelicus*, but the overall

thermodynamic profile was comparable to those of the *S. caelicus* DnaNs (i.e. negative changes in entropy and enthalpy in a similar range). The lacking activity of GMs against *E. coli* may thus result from the lower affinity and the faster dissociation compared to the interaction with the mycobacterial DnaNs, and from impaired penetration of GMs into Gram-negative cells. The SPR measurements showed that the association rate of all GMs is similar and sufficiently fast for the DnaN of *M. tuberculosis*, *M. smegmatis* and *S. caelicus* and even faster for GriR and the DnaN of *E. coli* (as is visible in the according sensorgrams), so that the uptake and the duration of the interaction may be the determining factors for the potency of GMs (Figure 4-4).

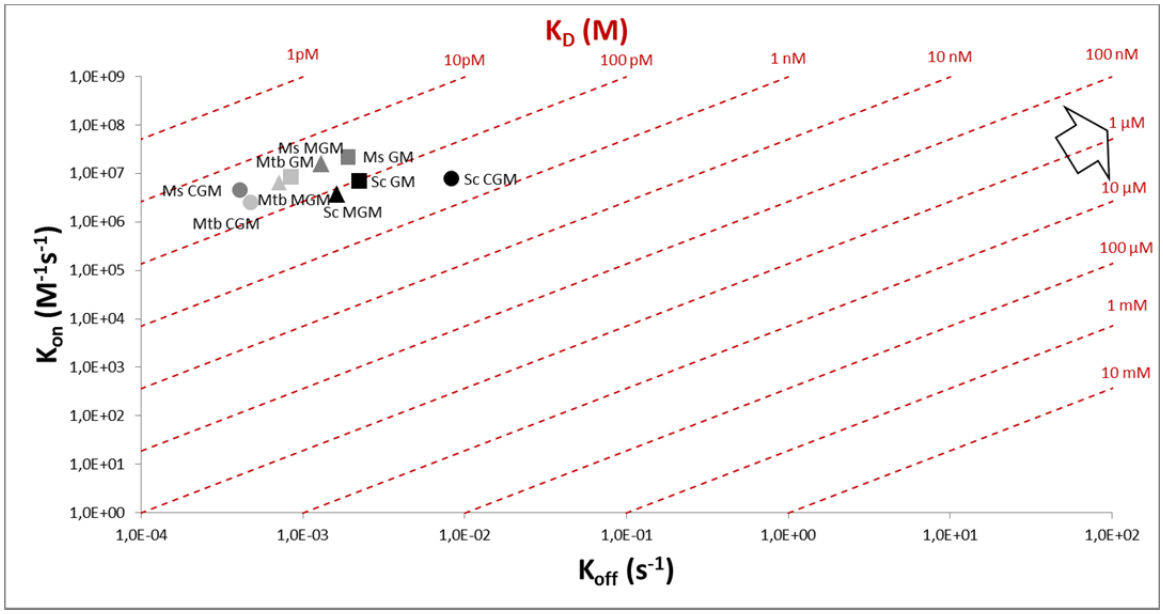

Figure 4-4: On-off rate plot for the interactions of GMs and the DnaNs of *M. smegmatis*, *M. tuberculosis* and *S. caelicus*. GM: rectangles, MGM: triangles, CGM: circles; Ms: *M. smegmatis* DnaN (dark grey), Mtb: *M. tuberculosis* DnaN (light grey), Sc: *S. caelicus* DnaN (black). K_D values are depicted and as red numbers and red dotted lines. The association (on-) and dissociation (off-) rates for the interaction of GMs with GriR and with DnaN of *E. coli* were too fast to be quantitatively determined and are indicated in a roughly schematic manner by a black arrow according to their measured K_D value and according to the fact that the on- and off- rates are higher than for the mycobacterial and *S. caelicus* DnaNs, as is visible in the sensorgrams.

To further characterize the binding site and the molecular interactions of GMs with the sliding clamps, crystal structures of the mycobacterial DnaNs with bound GM and CGM were solved. The crystal structures revealed that GMs indeed bind to the common sliding clamp peptide binding site of each polypeptide chain of the DnaN dimer (Figure 3-17), which is also responsible for binding of other proteins interacting with the sliding clamp. The peptide

binding site is a hydrophobic cleft that consists of two subsites, whereby subsite 1 is located between domains II and III of the sliding clamp and subsite 2 is located in domain III. In *E. coli* subsite 1 has a size of 8 Å x 10 Å and is 8.5 Å deep and subsite 2 has a size of 14 Å x 7.5 Å and is 4.5 Å deep.[203] GMs bind to DnaNs mainly via hydrophobic interactions and via three direct hydrogen bond interactions and one hydrogen bond interaction via a bridging water molecule (Figure 3-18). Thereby the cyclic part of GMs occupies subsite 1 and the linear part of GMs occupies subsite 2 of the mycobacterial sliding clamps. The reason for the different affinities of the binding of GMs to the *E. coli* and the mycobacterial sliding clamps remains somewhat elusive, as preliminary crystal structures of the *E. coli* sliding clamp with bound GM (resolved by Dr. Peer Lukat, data not shown) revealed no obvious differences in the binding mode of GMs to the *E. coli* sliding clamp compared to the *M. smegmatis* and *M. tuberculosis* sliding clamps. For comparison, the amino acids shaping the binding pocket of the sliding clamps of *M. tuberculosis* (which binds GMs with high affinity in the picomolar range) and of *E. coli* (which binds GMs with an affinity in the high nanomolar range) are shown Table 4-2, together with the amino acids shaping the binding pocket of the conventional sliding clamp of *S. caelicus* (which also bind GMs with high affinity in the picomolar range) and of the second sliding clamp GriR of *S. caelicus* (which binds GMs with a kinetic profile comparable to that of the *E. coli* sliding clamp) (Figure 4-4). In *E. coli*, five conservative amino acid exchanges were observed in subsite 1 of the sliding clamp binding pocket compared to the *S. caelicus* DnaN and *M. tuberculosis* DnaN, but only one of the conservative amino acid exchanges also occurs in GriR of *S. caelicus*. The according amino acid P_{351} in the *M. tuberculosis* DnaN (see Table 4-2) is not involved in direct contacts to GM. However, it was described that the side chains of some amino acids in the *E. coli* sliding clamp binding pocket (residues M_{362}, S_{346} and R_{365}) undergo movements upon binding of a peptide ligand (although the general structures of the free or bound pockets were found to be similar as assessed by their C_α positions)[202], whereby one of these amino acids (S_{346} of the *E. coli* DnaN) corresponds to P_{351} of the *M. tuberculosis* DnaN (Table 4-2). In the unbound *E. coli* sliding clamp binding pocket, residue M_{362} was described to separate subsite 1 and subsite 2, whereby in the bound structure the residues M_{362}, S_{346} and R_{365} are shifted so that the two subsites are joined and a hydrophobic platform is extended between subsite 1 and 2.[183] The process of the binding site formation is not described in detail, but it was suggested that peptides could bind via a two step process, with an initial interaction in subsite 1 and subsequent binding to subsite 2.[183] Residue R_{399} of *M. tuberculosis* (corresponding to R_{365} of

E. coli) is invoved direct contacts to GM and adopts an altered conformation compared to that in the free *M. tuberculosis*. However, the conformational change is different to that described for the corresponding residue of *E. coli*. For the amino acids corresponding to M_{362} and S_{346} of *E. coli,* major conformational changes could not yet be detected in *M. tuberculosis*. However, the amino acid exchanges at this positions and possibly resulting minor conformational differences in the binding sites could contribute to the differences in the affinity of the binding of GM to the *E. coli* and the mycobacterial sliding clamps.

Table 4-2: Amino acids shaping the peptide binding pocket of *M. tuberculosis*, *S. caelicus*, *E. coli* and of GriR of *S. caelicus*. Hydrophobic residues are indicated in grey; basic residues are indicated in blue; neutral residues are not coloured; subscripts indicate amino acid positions.

Protein	Amino acids shaping subsite 2																Amino acids shaping subsite 1			
DnaN *E. coli*	R_{152}	Y_{154}	L_{155}	T_{172}	G_{174}	H_{175}	R_{176}	L_{177}	P_{242}	V_{247}	N_{320}	Y_{323}	V_{344}	S_{346}	V_{360}	V_{361}	M_{362}	P_{363}	M_{364}	R_{365}
DnaN *M. tub.*	L_{161}	M_{163}	L_{164}	T_{181}	R_{183}	F_{184}	R_{185}	L_{186}	P_{259}	L_{264}	N_{336}	Y_{339}	G_{350}	P_{351}	L_{394}	L_{395}	M_{396}	P_{397}	V_{398}	R_{399}
DnaN *S. caelicus*	L_{149}	V_{151}	L_{152}	T_{169}	R_{171}	Y_{172}	R_{173}	F_{174}	P_{245}	L_{250}	N_{322}	F_{325}	T_{346}	P_{347}	L_{368}	I_{369}	M_{370}	P_{371}	V_{372}	R_{373}
GriR *S. caelicus*	L_{149}	V_{151}	L_{152}	T_{169}	R_{171}	Y_{172}	R_{173}	F_{174}	P_{242}	L_{247}	N_{319}	F_{322}	N_{343}	K_{344}	L_{365}	V_{366}	M_{367}	P_{368}	V_{369}	R_{370}

The sliding clamp interacts with different subunits of the replicative DNA polymerase but also with other proteins involved in DNA replication and repair. Thereby the sliding clamp acts as a switch for its interaction partners during DNA replication and repair.[204] Most of the studies regarding sliding clamp interaction partners were performed in *E. coli*, therefore the identified sliding clamp interaction partners in *E. coli* are described in the following section. In *E. coli* the sliding clamp interacts with all five DNA polymerases (Pol I, II, III, VI and V).[205,206] Pol I exibits 3'-5'- and 5'-3' exonuclease proofreading activity and is involved in DNA replication, Okazaki fragment maturation and DNA repair. Pol II exibits 3'-5'-exonuclease proofreading activity and is involved in DNA replication as a backup DNA polymerase and in DNA repair and translesion synthesis (the replication of DNA sections containing unrepaired damage by polymerases that are capable of bypassing DNA lesions). Pol III is the main replicative polymerase, it exibits 3'-5' exonuclease proofreading activity and is involved in DNA replication and repair. Pol IV and Pol V are involved in tranlesion synthesis. In contrast to *E. coli*, *Streptomyces* and mycobacteria contain one Pol I, two Pol III (DnaE and DnaE2) and two Pol IV (DinB1 and DinB2) (and no Pol II and Pol V). *M. smegmatis* contains a third Pol IV (DinB3). In mycobacteria DnaE1 is the essential main replicative polymerase whereas DnaE2 is responsible for DNA damage induced mutagenesis and is involved in the SOS response. DnaE2 of *Streptomyces* is not involved in error-prone DNA repair and the function remains to be elucidated.[207] The main replicative DNA

polymerase of *E. coli* is composed of 10 subunits (α, β, ε, θ, τ, γ, δ, δ', χ, ψ) that are subassembled into three main parts, the polymerase core (composed of the α, ε, and θ subunits), the sliding clamp (β) and the clamp loader complex (composed of the γ, δ, δ', χ and ψ subunits).[208] Sliding clamps interact with the clamp loader subunit of Pol III, which can load clamps onto DNA and also remove them from the DNA, and direct them to sites of DNA synthesis initiation by specifically recognizing primer template junctions. The template ssDNA of the primed site also interacts with the sliding clamp by binding to the protein binding pocket of the clamp, which is assumed to induce ring closure or hold the clamp at the primed site during loading.[209] The dsDNA portion that goes through the clamp also makes contacts with the clamp (but not to the protein binding pocket of the clamp). Additionally, the sliding clamp interacts with the α subunit of Pol III, which is the catalytic center of the replicative polymerase.[210] The α subunit has two binding sites for the sliding clamp (an internal and an extreme C-terminal site) that are separated by a DNA binding domain. It is assumed that the two binding sites of the α subunit interact simultaneously with the two peptide binding sites of the DnaN dimer while the DNA binding domain interacts with double stranded DNA (Figure 4-5).[217,211] The internal DnaN binding site of the α subunit was shown to be critical in *E. coli*, as mutations in the internal binding site eliminated detectable binding of the α subunit to the sliding clamp and abolished DNA replication by the resulting polymerase *in vivo*, whereby mutations in or removal of the C-terminal binding site retained near wildtype polymerase function. In agreement with these findings, a *M. tuberculosis* DnaE1 derived peptide containing the internal DnaN binding site was reported to show higher affinity to the *M. tuberculosis* DnaN than the peptide containing the C-terminal binding site.[169]

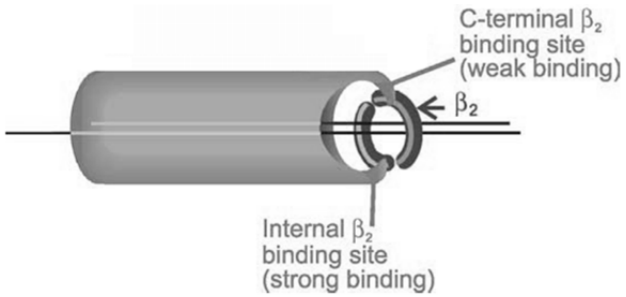

Figure 4-5: Schematic representation of the assumed association of the DNA polymerase III α subunit and the sliding clamp. The α subunit is associated with the peptide binding sites of the sliding clamp via an internal and a C-terminal binding site (modified from reference 211).

Furthermore, the *E. coli* sliding clamp interacts with the DNA ligase, with MutS and MutL, and with Hda.[212,213,214] However, for mycobacteria (and other Actinobacteria) no homologs of the mismatch repair system (such as MutS and MutL) and of Hda were detected.[215,216] DNA ligases seal nicks between synthesized fragments during lagging strand synthesis or during mismatch repair and the sliding clamp may serve in targeting DNA ligases to the site of action.[212] The proteins MutS and MutL are involved in DNA mismatch repair (MMR), where DNA damage generated by replicative errors during DNA synthesis is corrected by removal of DNA segments by the combined action of helicase and nucleases and re-synthesis of the resulting gap by DNA polymerases.[213] MutS directly recognizes and binds DNA mismatches and recruits MutL, which initiates the MMR system. MutL thereby only interacts with the sliding clamp in the presence of ssDNA. The role of the sliding clamp in the MMR process remains unclear, clamps may target the MMR machinery to the site of action. The regulatory factor Hda (homologous to DnaA) is required for the regulatory inactivation of DnaA (RIDA) and is thus involved in regulation of replication initiation.[214] The ATP-bound form of the DnaA protein is responsible for the initiation of replication, and RIDA, which requires the activity of Hda and the sliding clamp, stimulates the conversion of ATP-DnaA into the initiation incompetent ADP-DnaA and prevents excess initiation of replication. All proteins described so far that interact with the sliding clamp bind to a hydrophobic binding pocket between domains II and III of a sliding clamp monomer (and in some cases to additional sites of the clamp).

Proteins that interact with the sliding clamp typically bind to the sliding clamp binding pocket via a conserved five- or six residue binding site. For *E. coli* the variants of the binding motifs QL[S/D]LF and QLxLx[L/F] were shown to be responsible for binding to the sliding clamp.[217] For example, for the Pol III δ subunit the QAMSLF sequence[218], for the Pol III α subunit the internal QADMF sequence[219] and the C-terminal QVELEF sequence[220], for Hda the QL(S/P)LPL sequence[221], for Pol II the QLGLF sequence[209] and for Pol IV the QLDLGL sequence[222] were identified as DnaN binding sites. For *M. tuberculosis* a peptide derived from Pol III δ subunit that contains the LSPSLF motif (corresponding to the QAMSLF residues of the *E. coli* δ subunit) and a peptide derived from the Pol III α that contains the internal QFDLF sequence (corresponding to the QADMF residues of the *E. coli* α subunit) were reported to interact with the *M. tuberculosis* sliding clamp (with a K_D of 50 and 16 µM for the δ and the α derived peptide, respectively, as measured by SPR).[169] The C-terminus of the *M.*

tuberculosis Pol III α subunit does not contain a motif with amino acid similarities to the corresponding *E. coli* motif (QVELEFD) and was reported to show low binding affinity to the *M. tuberculosis* DnaN in SPR measurements. Peptides containing DnaN binding motifs of different interaction partners of the *E. coli* DnaN were shown to have different binding affinities to the *E. coli* DnaN, which indicates a hierarchy for the binding of proteins to sliding clamps.[217] For example the Hda binding motif sequence binds with higher affinity to DnaN than that of the Pol III δ subunit and binding motifs of the polymerases involved in translesion synthesis show stronger affinities to DnaN than that of the Pol III α subunit.[217] Consistent with these findings, the translesion polymerase Pol IV was shown to replace stalled Pol III and overproduction of Pol IV was shown to inhibit Pol III in *E coli*.[223,224] Additionally, the inhibitor RU7 that binds to the peptide binding site of the *E. coli* sliding clamp, was shown to differentially affect the activity of Pol II, III and IV (Pol IV was at least 50-fold less inhibited than Pol III, and Pol III is inhibited more strongly than Pol II) and the binding motifs of Pol II, III and IV were shown to differentially interact with the peptide binding site of the *E. coli* clamp in crystal structures.[209] Regarding the C-terminal sequence motif $Q_1V_2E_3L_4E_5F_6$ of Pol III residues Q_1, V_2 and E_3 occupy subsite 2 and residues L_6, E_7 and F_8 occupy subsite 1, whereby L_6 and E_7 are buried deep into this site. The sequence motif $Q_1L_2G_3L_4F_5$ of Pol II forms similar contacts in subsite 2 whereby in subsite 1 residue L_4 appears to be more efficiently buried and establishes additional hydrophobic contacts compared to the corresponding residue in the C-terminal Pol III motif. The Pol IV sequence motif QLDLGL binds similarly to subsite 2 but in subsite 1 the E_5 residue of the Pol III motif forms two interactions that are lacking in Pol IV peptide (however, Pol IV is known to form additional contacts to DnaN outside the peptide binding site). Binding of enzymes to the sliding clamp thus appears to be regulated by different affinities of the respective binding motif to the sliding clamp but also by additional factors. For example, the interaction of the clamp loader with the sliding clamp necessitates conformational changes of the clamp loader δ subunit which depend on ATP binding and hydrolysis. The interaction of the Pol III α subunit with the sliding clamp is assumed depend on the affinity of the τ subunit to the α subunit, which increases in the presence of dsDNA and may then compete with the interaction of the sliding clamp to α.[225]

GM is composed of the 10 amino acids $V_1P_2T_3L_4P_5L_6V_7P_8L_9G_{10}$ (V_1 is acetylated, methylated amino acids are italicized) (Figure 1-6) and superposition of the crystal structure of the

mycobacterial DnaN with bound GM, with the internal Pol III α (DnaE1) peptide that contains the DnaN binding motif, shows that GM mimicks the conformation of the internal DnaE1 peptide bound to DnaN (Figure 4-6). GM does not show sequence similarities to the identified DnaN binding motifs LSPSLF and QFDLF of the α and δ subunit of the DNA polymerase III of *M. tuberculosis*. However, for DnaE2 the putative DnaN binding motif sequence RPGML (observed e.g. in mycobacteria and nocardia) or QLPLx (observed e.g. in streptomycetes) was suggested by bioinformatics analyses[116,226], whereby the latter motif resembles the LPL motif present in GM. The *M. tuberculosis* DnaN was reported not to interact with DnaE2 but with the accessory factor ImuB, which in turn interacts with DnaE2.[227] ImuB is a protein that retains structural characteristics of Y-family polymerases but lacks polymerase activity. Lack of the interaction between DnaN and ImuB reduced mutagenesis induction and DNA damage tolerance. The DnaN binding motif QLPLWG was verified in the *M. tuberculosis* ImuB, which was found to be highly conserved among mycobacterial ImuBs,[227] and resembles the LPL motif present in GM.

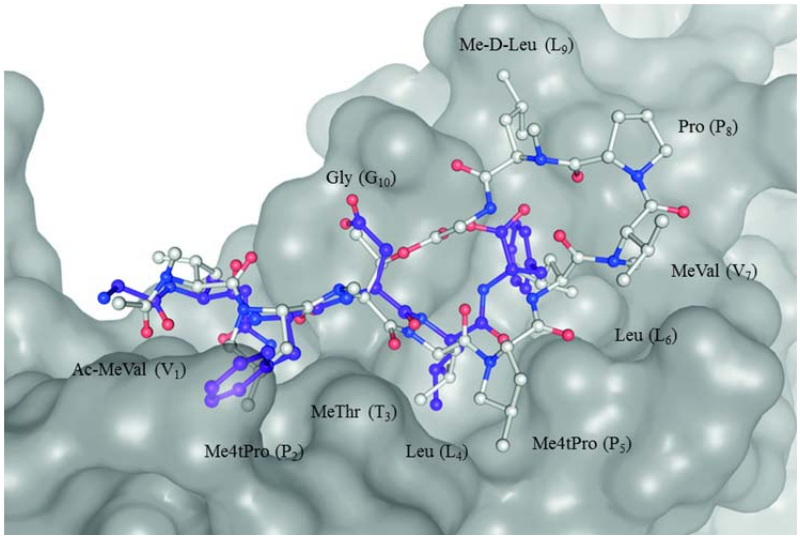

Figure 4-6: Binding of GM and the internal *M. smegmatis* DnaE1 peptide to the sliding clamp. Superposition of *M. smegmatis* DnaN (shown as surface) in complex with GM (white, amino acids are indicated) with the internal DnaN binding motif of the mycobacterial DnaE1 (GQFDLF, purple) comprising the residues 948 – 953 (*M. smegmatis*)/945 – 950 (*M. tuberculosis*). (The peptide has been modelled based on the C-terminal DnaN binding motif (GQLGLF) from DNA polymerase II bound to the *E. coli* β-clamp, PDB: 3D1E[203]) (modified from reference 154).

To examine if binding of GMs to the peptide binding site of the sliding clamp affects binding of the replicative DNA polymerase in mycobacteria, binding of a *M. smegmatis* DnaE1 derived peptide that contains the internal sliding clamp binding motif (with the sequence

KAEAMGQFDLFG, the binding motif is underlined) to the *M. smegmatis* DnaN was monitored by SPR in the presence and in the absence of GM (Figure 3-19). As a result, the binding of the internal DnaE1 peptide to the sliding clamp with bound GM was significantly reduced compared to the binding to the pure sliding clamp. This indicates an impaired binding of the main replicative DNA polymerase in the presence of GM and implicates impaired DNA replication. Considering other known interaction partners of the sliding clamp (such as other DNA polymerases and DNA ligase) treatement with GM most probably also affects DNA repair.

The inhibition of binding of DnaE1 to the sliding clamp presumably results in a decreased processivity and therefore in inefficient DNA replication. As inefficient replication should result in DNA damage (DNA strand breaks), the induction of the SOS response upon GM exposure was analyzed in *M. smegmatis*. The SOS response is a global stress response system in bacteria that is activated by DNA damage and results in direct genetic changes that increase the chances to survive mutagenic consequences of DNA damage.[228] The main regulators of the SOS response in bacteria are *recA* and *lexA*. RecA is a bacterial recombinase that recognizes and binds regions of single-stranded DNA that arise directly upon exposure to DNA damaging agents or indirectly by stalled DNA replication. The complex of RecA and single-stranded DNA stimulates the self-cleavage of the LexA repressor and results in the derepression of SOS genes. These genes encode enzymes involved in DNA repair and recombination or DNA synthesis past lesions, such as DNA polymerases II, IV and V of *E. coli* and in actinobacteria additionally DnaE2, which are able to replicate damaged DNA and restart stalled replication forks. Pol IV, Pol V and DnaE2 are low fidelity polymerases and increased levels of these polymerases lead to an increase in the mutation rate. Indeed, exposure to GM resulted in elevated expression levels of *recA* and *lexA* in *M. smegmatis,* which indicated the induction of the SOS response (Table 3-9, Figure 3-20). Additionally, an increased expression level of *dnaE2* and *dnaB* was observed upon GM exposure in *M. smegmatis*. DnaE2 was previously reported to be upregulated upon DNA damage in *M. tuberculosis.*[116] DnaB is a replicative helicase which is also induced by DNA damage in *M. tuberculosis*.[229,230] As the sliding clamp is involved in polymerase switching[205], inhibition of polymerase binding to the sliding clamp by GM may also affect the course of the SOS response after derepression of the SOS response genes. Prevention of the SOS response induction was shown to potentiate killing by quinolone antibiotics[231] and the SOS response

may be involved in survival of pathogens in macrophages[232] so that an impaired SOS response may also contribute to the killing of mycobacteria by GMs *in vitro* and *in vivo*.

In the recent years few other inhibitors that bind to the peptide binding site of bacterial sliding clamps or that inhibit dimerization of the sliding clamp were described, but none of these is used therapeutically yet. These inhibitors are small molecules or short peptide chains with low activity on whole cells. For example, the antibacterial properties of the nonsteroidal antiinflammatory drugs (NSAIDs) carprofen, bromfenac and vedaprofen were found to be based on binding to the bacterial sliding clamp.[233] Crystal structures showed that all three NSAIDs bind to subsite 1 of the protein binding site of the *E. coli* sliding clamp, thereby burying a hydrophobic moiety into the deep pocket of subsite 1 and positioning aromatic rings in the shallower region. The antibacterial activity of these compounds was in the range of 40 to > 1000 µg/mL in MIC assays against *S. aureus* and *E. coli*. Furthermore, two cyclic peptides (with the sequences VFLCGC and SQGLFK) were found to inhibit the *S. aureus* sliding clamp by interfering with dimerization of the sliding clamp.[234] These peptides inhibited DNA replication, induced SOS response and led to cell death. The MIC was about 50 µg/mL for *S. aureus* cells. Another example is the synthetic small molecule RU7, which was described to bind to the *E. coli* sliding clamp and inhibit DNA synthesis *in vitro*.[203] The crystal structure showed that RU7 binds to subsite 1 of the protein binding site of the *E. coli* sliding clamp. RU7 did not show antibacterial activity against *E. coli* or *M. smegmatis* cells (own results, MICs for RU7 on *E. coli* DH10B and *M. smegmatis* mc^2155 were > 64 µg/mL). The potency of GMs on mycobacteria thus presumably results from the high affinity to the mycobacterial sliding clamp together with the ability to traverse the cell wall. In addition, other sliding clamp inhibitors were reported to bind only to subsite 1 of the peptide binding pocket whereas GMs occupy both subsites of the binding pocket, similar as reported for peptides derived from the *E. coli* polymerases II, III, and IV that contain the DnaN binding motifs.[203]

Further efforts to elucidate the subtle differences of the binding of peptide ligands to the sliding clamp binding pockets of different microorganisms and to elucidate possible differences in the dynamic sliding clamp binding site formation in Gram-positive and Gram-negative microorganisms, could guide the design of sliding clamp inhibitors that either show an improved affinity for certain organisms or affect a broader spectrum of microorganisms. The general consensus sequence QLDLGL (derived from *E. coli* DNA Pol IV) was already

shown to bind to the sliding clamps of different organisms (*E. coli*, *P. aeruginosa*, *B. subtilis*, *M. tuberculosis*) with similar affinity (with a only 3-fold variation of the K_D of around 10^{-6} M^{-1} as determined by SPR)[183] and could be used as a lead structure for the design of broad spectrum sliding clamp inhibitors. On the other hand, thermodynamic analyses showed that designed peptides with optimized affinity for the *E. coli* sliding clamp efficiently interact with the sliding clamp of the Gram-negative organism *P. aeruginosa* but show poor or no binding to the sliding clamps of the Gram-positive organisms *B. subtilis*, *S. aureus and M. tuberculosis*.[183] For this analysis the QLDLGL peptide was optimized for the tight binding to the *E. coli* DnaN by stepwise introduction of chemical substitutions and the binding affinities to different sliding clamps were characterized.[202] A similar analysis of peptides that are optimized for the tight binding to the sliding clamp of a Gram-positive organism could reveal the structural key differences between ligands that show a high affinity for Gram-positive or Gram-negativ organisms and guide the design of (broad and narrow spectrum) sliding clamp inhibitors.

Since the sliding clamp is a novel antibiotic target, sliding clamp inhibitors provide the opportunity to treat infections caused by resistant pathogens due to the lack of a pre-existing resistance. In addition, for the treatment of TB, sliding clamp inhibitors mean the possibility to add a novel mechanism of action to a multiple drug therapy and to design novel combination regimens. The treatment of infections using the sliding clamp as a target is full of potential as the sliding clamp is conserved across bacterial species but shows low sequence similarity to the human sliding clamp analog. This provides the additional option for the design of sliding clamp inhibitors for a broader spectrum of bacteria. At least one copy of the sliding clamp is essential for bacteria, which explains link between sliding clamp inhibition and the antibacterial effect. Furthermore, the sliding clamp is considered to be one of the most trafficked proteins in the cell and acts as a central switch for numerous binding partners during replication and repair, so that high affinity sliding clamp inhibitors likely affect quite a number of processes in the bacterial cell (such as DNA replication and DNA replication initiation, DNA repair, and SOS response) which all might contribute to the antibacterial effect.

4.3 GRISELIMYCIN RESISTANCE MECHANISM IN MYCOBACTERIA

For the investigation of the development of resistance against GMs in mycobacteria, GM resistant *M. smegmatis* mc^2155 mutants were generated *in vitro* by exposure to increasing concentrations of GM in five sequential steps (2.5, 5, 10, 20 and 40 µg/mL GM). CGM resistant *M. tuberculosis* were obtained *in vivo* from nude mice after 4 weeks of CGM monotherapy (100 mg/kg, once daily). In mice without a functional immune system once daily monotherapy cannot inhibit bacterial replication when drug levels fall below the therapeutic concentration, as also previously observed for INH.[235]

Susceptibility testing of a GM resistant *M. smegmatis* mutant against a panel of antibiotics with different mechanisms of action and different resistance mechanisms (Table 3-10) revealed a lack of cross-resistance between GM and other tested antibiotics, which indicated that GM induces a different resistance mechanism. Additionally, CGM resistant *M. tuberculosis* showed no cross-resistance to IHN, RIF, MFX and STM. Similarly, *M. tuberculosis* strains with resistance against first- or second-line anti-TB drugs showed a similar MIC against CGM as the according *M. tuberculosis* wildtype strain (Table 3-11, Table 3-5). This lack of a pre-existing resistance to GM constitutes an advantage for a possible TB therapy with GMs.

The *in silico* genome analysis revealed that GM resistant *M. smegmatis* mutants contained a mutation in the *dnaN* promoter region (Table 3-12), an amplification of a chromosomal segment (Table 3-12, Table 3-13, Figure 3-22) that contains the *dnaN* gene (and which was confirmed by Southern blot, Figure 3-23), and several inconsistent mutations (Table 3-14, Table 3-15). CGM resistant *M. tuberculosis* only contained an amplification of a chromosomal segment that contained the *dnaN* gene (Table 3-17, Figure 3-25). These observations indicate that resistance against GMs in mycobacteria is mediated by amplification of the molecular target DnaN. The self-resistance mechanism in the GM producer *S. caelicus* is similar, whereby in this strain the molecular target is not only duplicated but also modified.

The first mutant steps of all GM resistant *M. smegmatis* mutants contained a G > A transition mutation in the *dnaN* promoter region 115 bp upstream of the *dnaN* gene (Table 3-12). However, this promoter mutation was not consistently maintained in all steps of all mutants but complemented or replaced by the amplification of a chromosomal segment in the course

of the exposure to increasing concentrations GM. The *dnaN* gene is regulated by two different promoters[237] ($P1_{dnaN}$ or $P2_{dnaN}$), and the mutation in GM resistant mutants is located in the Pribnow box (also called -10 region) of $P2_{dnaN}$. The -10 and -35 promoter elements are recognized by sigma factors which in turn bind to the RNA polymerase and thereby regulate the transcription of the respective gene[236], so that this promoter mutation was assumed to mediate resistance by overexpression of *dnaN*. Since the -35 region of the *M. smegmatis* $P2_{dnaN}$ was reported to show an overlap with a DnaA binding site (a so-called DnaA box) of the *ori* region, $P2_{dnaN}$ was assumed to be also be regulated by DnaA[237] and the amplification of *dnaA* (which is also located on the amplicon in GM resistant *M. smegmatis* mutants) may have an additional effect on the *dnaN* expression level. The promoter mutation indeed led to an increase in the *dnaN* expression level in a mutant containing only the *dnaN* promoter mutation but not the amplification of the *dnaN* containing chromosomal segment (Table 3-16, Figure 3-24). The *dnaN* expression level was further increased in a mutant containing the promoter mutation as well as an amplification of the *dnaN* containing chromosomal segment. Since GM mutants, which contained an amplification of *dnaN*, showed a higher GM resistance (in terms of GM insensitivity) compared to mutants containing only a *dnaN* promoter mutation (Table 3-12), the increase of the *dnaN* expression level by the promoter mutation apparently confers low level resistance to GM whereby the amplification of a chromosomal segment containing the *dnaN* gene further increases the *dnaN* expression level and confers high level resistance to GM. In accordance with these results, the resistance to GM increased also with increasing numbers of amplicons (Table 3-12).

The amplicons observed in GM resistant *M. smegmatis* mutants varied in size (ranging from about 9 to about 28 kb) and copy number (ranging from 3 to 49 copies) and occurrence of the amplicons was observed in different steps of different mutants (Table 3-12, Table 3-13, Figure 3-22, Figure 3-23). In some mutant selection steps a mix of amplicons with different sizes was observed. However, all amplicons included the genes *dnaA*, *dnaN, recF*, *gnd* and a hypothetical protein (MSMEG_0004), and additionally the *ori* region and the *dnaN* promoter region, which are located in between *dnaA* and *dnaN*.[237] Several mutants include an amplification of *gyrA* and/or *gyrB*, which might have to be considered in combination treatments with fluoroquinolones. Additional *ori* regions that equal the chromosomal *ori* were previously shown to be compatible in mycobacteria, since a stable maintenance of plasmids with chromosomal *ori* regions were reported for *M. smegmatis* and *M. tuberculosis*, although

these plasmids were maintained at a low copy number.[238,239] The genes *gnd* (encoding the 6-phosphogluconate dehydrogenase), *recF* (encoding the recombination factor F) and *dnaA* (encoding the chromosomal replication initiation protein) are located directly adjacent to *dnaN* (Figure 3-22) and are possibly amplified randomly whereby resistance to GM may necessitate only the amplification of *dnaN*, as overexpression of only *griR* was found to mediate GM resistance in sensitive *Streptomyces* (Table 3-1). However, the DnaA protein is responsible for the initation of the replication, and overexpression of DnaA was previously reported to lead to overinitiation of replication.[240] The amplification of the *dnaA* gene in GM resistant *M. smegmatis* mutants thus may promote repeated replication initiation and a repeated replication of the directly adjacent *dnaN* and *dnaA* genes and a random number of further genes, which could explain the different sizes of the different amplicons in independent mutants. Gene duplication events were described to arise via RecA-dependent mechanisms, such as homologous recombination between direct repeat sequences or mechanisms based on the rolling circle replication at homologous or microhomologous sites (whereby a double strand break allows single-strand invasion followed by replication) (Figure 4-7).[241] However, homology regions (of 1 – 13 bp) flanking the different amplicons in GM resistant *M. smegmatis* mutants, which may serve as recombination sites, were found in only 7 of the 10 amplicons. Thus, the other three GM resistant *M. smegmatis* mutants may contain microhomologous sites which were not yet detected, or the initial duplication event may occur via RecA-independent processes that are capable of random end-joining in the absence of repetitive sequences (such as strand slippage during DNA replication, pairing of single stranded regions of sister chromosomes after passage of the replication fork or ligation of DNA ends via DNA gyrase).[242] The higher-level amplifications in GM resistant *M. smegmatis* mutants may then occur via homologous regions generated by the initial duplication, which would explain the occurrence of amplicons of the same size in stepwise mutants. Chromosomal gene amplifications that lead to antibiotic resistance were previously described in several cases, for example kanamycin resistance in *S. kanamyceticus* mutants (which were optimized for kanamycin production) was reported to be mediated by 2 - 36 copies of a 145 kb amplicon that contains the entire kanamycin biosynthetic gene cluster, whereby the kanamycin production increased with increasing amplicon number.[243]

The three CGM resistant *M. tuberculosis* mutants similarly contained an amplified chromosomal segment that contained the genes *dnaN*, *recF*, *gyrB* and *gyrA*, and additionally

the *ori* region but only a fraction of the *dnaA* gene (Table 3-17, Figure 3-25). None of the three CGM resistant *M. tuberculosis* mutants contained a mutation in the *dnaN* promotor region. In addition, in none of the CGM resistant *M. tuberculosis* mutants homology regions flanking the amplicons could be observed. Replication initiation is regulated by the accessibility of the *ori* to DnaA (by sequestration of the *ori* by SeqA proteins) or by the modulation of the DnaA protein activity or protein level but also by other regulatory factors. For example the mycobacterial IciA (inhibitor of chromosomal initiation) protein was reported to inhibit DnaA mediated open complex formation by binding to specific sequences in the *ori* region.[244] An excess of such specific binding sequences (as present in GM resistant *M. smegmatis* mutants or CGM resistant *M. tuberculosis* mutants due to an initial duplication or the high-level amplification of the *ori* containing chromosomal segment) above such inhibitory factors might also promote overinitiation of replication.

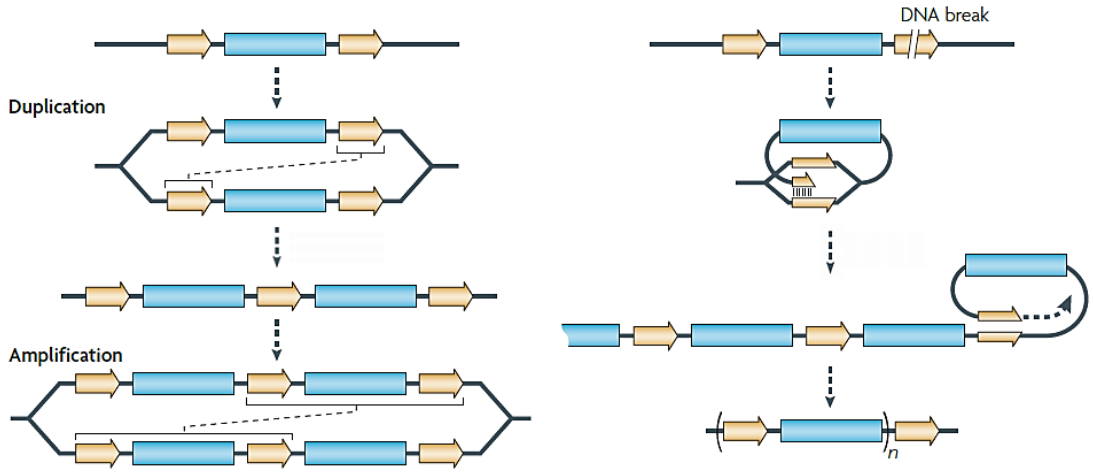

Figure 4-7: Proposed mechanisms of gene duplication and amplification. Left image: Duplication via homologous recombination. Right image: Gene duplication via rolling circle replication (whereby a double strand break allows single-strand invasion followed by replication). After a duplication is formed, higher level amplification can arise via recombination between the tandem repeat generated by the initial duplication (modified from reference 241).

In addition, GM resistant *M. smegmatis* exhibited an elongated cellular morphology (Figure 3-21), which has been also previously observed in GM exposed *M. tuberculosis*.[245] Elongated cells were also reported for *E. coli* mutants with inactivated *hda*[246] and *E. coli* and *B. subtilis* mutants which overexpress *dnaA*[247,248], so that the cell elongation appears to be related to excess of free DnaA, but the precise causation remains unclear.

A number of inconsistent mutations were also observed in GM resistant *M. smegmatis* mutants (Table 3-14, Table 3-15). Overall 0 to 8 mutations emerged in each step during mutant selection. For comparison, among the five *M. smegmatis* parental strains (i.e. GM_0 in Table 3-14) no inconsistent mutations were observed as expected. Most of the 48 inconsistent mutations are present in only one of the five independent GM resistant mutants, except for two mutations (mutations 25 and 28) which are present in two of the mutants, and for three of the mutations (mutations 7, 8, and 9) which affect same gene. As almost all of the 48 observed inconsistent mutations occurred in only one of the five independent mutants, they appear to emerge randomly upon exposure to GM rather than as a contribution to GM resistance. The inconsistent mutations might be a result of the induction of the low fidelity polymerase DnaE2 (Figure 3-20). The error rate (i.e. the probability of the occurrence of a mutation per basepair per generation) of mycobacterial DnaE2 was not yet determined, but deletion of the error-prone DnaE2 was reported to reduce the mutation frequency of *M. smegmatis in vitro* and of *M. tuberculosis in vitro* and *in vivo*.[116] The *M. smegmatis* wildtype was reported to show a mutation rate of about 4×10^{-10} and about 10^{-3} mutations per genome per generation. Thereby the replicative polymerase DnaE1 appears to be responsible for the low error rate, as *M. smegmatis* mutants containing a DnaE1 with inactivated 3'-5' exonuclease (proofreading) activity showed an increased mutation rate of about 10^{-6} and about 7 - 11 mutations per genome per generation.[249] Notably, *M. smegmatis* mutants with proofreading defective DnaE1 polymerases were reported to show a severe growth defect, which is assumed to depend on the large increase in the mutation rate and on DNA replication stalling due to the inability of DnaE1 to extend from mismatched bases.[249] However, CGM resistant *M. tuberculosis* mutants obtained *in vivo* did not contain single point mutations. This may be due to the emergence of *M. tuberculosis* persister cells *in vivo*, as an estimated 10-fold lower mutation rate was reported for *M. tuberculosis* during latent infections.[250]

To investigate if resistance presents an obstacle for a therapeutic use of GM, GM resistance was further characterized regarding resistance frequency, resistance reversibility and induced fitness costs. It turned out that resistance to GM in *M. smegmatis* occurred only at a low frequency of 5×10^{-10} (at 10 µg/mL GM) and that no spontaneous resistant mutants could be observed at concentrations higher than 10 µg/mL GM. If the low resistance frequency *in vitro* translates to a low resistance frequency of *M. tuberculosis in vivo* this would be a preferable attribute of GMs. In addition, GM resistance was accompanied by a considerable fitness loss,

whereby the growth of *M. smegmatis* mutants decreased (regarding growth rate and cell density) with increasing resistance (Figure 3-26). For some mutants the growth was so retarded that determination of MIC values was not possible (Table 3-12). The overexpression of *dnaA*, *dnaN* and *recF* was reported to lead to a decreased viability of *E. coli* and may thus be also responsible for the decreased fitness of GM resistant *M. smegmatis* mutants.[247] The fitness loss may also partly result from the increased number of possibly unfavorable single point mutations (Table 3-14). Furthermore, GM resistance was reversible, as the GM susceptibility increased for *M. smegmatis* mutants grown without GM (i.e. mutant $1.GM_{40\rightarrow0}$ and mutant $9.GM_{40\rightarrow0}$, Table 3-12). Additionally, growth was less retarded for a mutant grown without GM (Figure 3-26). Genome sequence comparison of the mutants grown without GM with their parental mutant strains revealed that the basis of the reversibility of the resistance was a decrease in the amplicon copy number. For one of the mutants grown in the absence of GM ($9.GM_{40\rightarrow0}$) no change in the inconsistent mutations was observed compared to the parental mutant strain ($9.GM_{40}$), whereby the other mutant grown in the absence of GM ($1.GM_{40\rightarrow0}$) contained two additional single point mutations and one single point mutation was restored to the original sequence (Table 3-14, Table 3-15). This might indicate that the error prone DnaE2 polymerase is still elevated in GM resistant mutants grown in the absence of GM due to remaining GM resistance modifications (such as amplification of *dnaA* and the *ori* region which may lead to overinitiation of replication and by this to stalled replisomes or collision of replication forks and by this to SOS response induction).

5 SUMMARY AND CONCLUSION

GM was first isolated and characterized in the 1960s but was neglected after rifampicin became available for TB therapy. Recently, GM was rediscovered in a search for neglected antibiotics with high antituberculosis potential and the studies on GM were reinitiated.

Examination of the GM biosynthesis gene cluster of the GM producing strain *Streptomyces caelicus* revealed that the cluster contained a gene that encodes for an additional sliding clamp homolog (GriR), which was found to be the GM self-resistance determinant. It was observed that GMs directly bind to the conventional sliding clamp (DnaN) of *S. caelicus* with high affinity. GMs also bind to the additional homolog GriR of *S. caelicus* but with lower affinity and with a faster dissociation from the protein. GriR thus apparently confers self-resistance by binding GMs with lower affinity and for a shorter period, which presumably does not completely inhibit the interaction of GriR with other binding partners.

GMs are narrow-spectrum agents that exhibit potent bactericidal activity on drug-resistant *M. tuberculosis in vitro* and *in vivo*. CGM is active on intracellular mycobacteria in murine macrophages and is to a certain extent also active on nonreplicating mycobacteria *in vivo*. GMs were found to bind to the peptide binding site of mycobacterial sliding clamps and to affect binding of the replicative polymerase and are assumed to affect also the binding of other sliding clamp interaction partners. In accordance with these observations, exposure to GM leads to DNA damage in mycobacteria. Sliding clamps confer processivity to DNA polymerases and act as switch for enyzmes and other factors during DNA replication and repair, whereby all proteins that were described to interact with the sliding clamp bind to the peptide binding site. GMs thus exert their activity by inhibiting DNA replication and most probably also DNA repair.

GM resistance in mycobacteria was found to be mediated by target amplification. However, resistance to GM in *M. smegmatis* occurred only at a low frequency. GM resistance was accompanied by a considerable fitness loss and the growth retardation of GM resistant *M. smegmatis* mutants increased with increasing resistance. Furthermore, GM resistance was reversible, as *M. smegmatis* mutants grown without GM showed an increased GM susceptibility together with a decreased target amplification and a less retarded growth.

The molecular target of GMs, the sliding clamp, is a novel mycobacterial target, which is essential for viability and which does not share significant sequence homology with the eukaryotic sliding clamp equivalent (PCNA). The activity, the novel mechanism of action and the lack of a pre-existing resistance make GMs promising antituberculosis lead structures. Current antituberculosis drug classes mostly inhibit cell wall synthesis or protein translation. GMs inhibit DNA synthesis, whereby only the class of fluorquinolones also inhibits DNA synthesis but using a completely different mechanism compared to GMs. GMs therefore provide the opportunity to inhibit an additional cellular pathway during combination therapy to improve treatment efficacy. *In vivo* studies in mouse models of TB already revealed that administration of CGM in combination with first-line antituberculosis drugs resulted in a shortened treatement period compared to the TB standard regimen. In addition, the lack of cytochrome (CYP) P450 enzyme induction or inhibition, which suggests limited potential for drug-drug interactions and suitability for the treatment of HIV positive tuberculosis, and the optimized pharmacokinetic profile of CGM, which suggests suitability for once-daily oral dosing, point out the translational potential of GMs.

6 SUPPORTING INFORMATION

Table 6-1: X-ray data collection and refinement statistics for DnaN-GM and DnaN-CGM complexes. The RCSB Protein Data Bank ID for each dataset is in bold.[154]

	M. smegmatis DnaN + GM **5AH2**	*M. smegmatis* DnaN + CGM **5AH4**	*M. tuberculosis* DnaN + GM **5AGU**	*M. tuberculosis* DnaN + CGM **5AGV**
Data collection				
Space group	$P2_1$	C2	$P6_1$	$P2_1$
Cell dimensions				
a, *b*, *c* (Å)	80.2, 125.9, 94.9	151.9, 96.1, 92.3	87.5, 87.5, 199.3	72.9, 89.8, 81.9
α, β, γ (°)	90.0, 104.42, 90.0	90.0, 124.4, 90.0	90.0, 90.0, 120.0	90.0, 95.1, 90.0
Resolution (Å)	125.867 – 2.129 (2.136 – 2.129)	76.270 – 2.313 (2.320 – 2.313)	199.296 – 2.173 (2.180 – 2.173)	40.800 – 1.930 (1.937 – 1.930)
R_{merge} (%)	10.6 (93.1)	6.7 (86.0)	20.3 (162.4)	9.7 (81.9)
R_{pim} (%)	4.4 (38.1)	2.8 (34.2)	4.6 (36.5)	4.0 (34.4)
$I/\sigma I$	13.6 (2.1)	19.5 (2.2)	13.2 (2.1)	13.7 (2.2)
Completeness (%)	100 (100)	99.9 (100)	100 (100)	100 (99.9)
Redundancy	6.9 (6.9)	7.0 (7.2)	20.8 (20.7)	6.8 (6.6)
$CC_{1/2}$ (%)	99.7 (63.7)	90.4 (77.9)	99.9 (69.9)	99.8 (66.2)
DnaN molecules per asymmetric unit	4	2	2	2
Refinement				
Resolution (Å)	2.129	2.313	2.173	1.930
No. reflections	102003	47824	45371	78969
R_{work}/R_{free} (%)	18.20/23.14	17.29/22.33	18.38/22.67	16.88/20.95
Protein residues				
total/built	1668/1581	834/786	812/747	812/775
truncated at C_β	49	35	11	13
No. atoms				
Protein	11183	5625	5600	6078
Ligand/ion	318	171	172	218
Water	770	194	357	975
B-factors (Å^2)				
Protein	43.13	63.79	42.54	33.01
Ligand/ion	40.02	44.00	31.35	31.10
Water	43.38	51.88	47.75	44.34
R.m.s deviations				
Bond lengths (Å)	0.008	0.009	0.008	0.007
Bond angles (°)	1.21	1.17	1.27	1.13
Ramachandran Plot				
Favored (%)	97.1	96.3	97.9	98.3
Allowed (%)	2.5	3.6	2.1	1.7
Outliers (%)	0.3	0.2	0.0	0.0

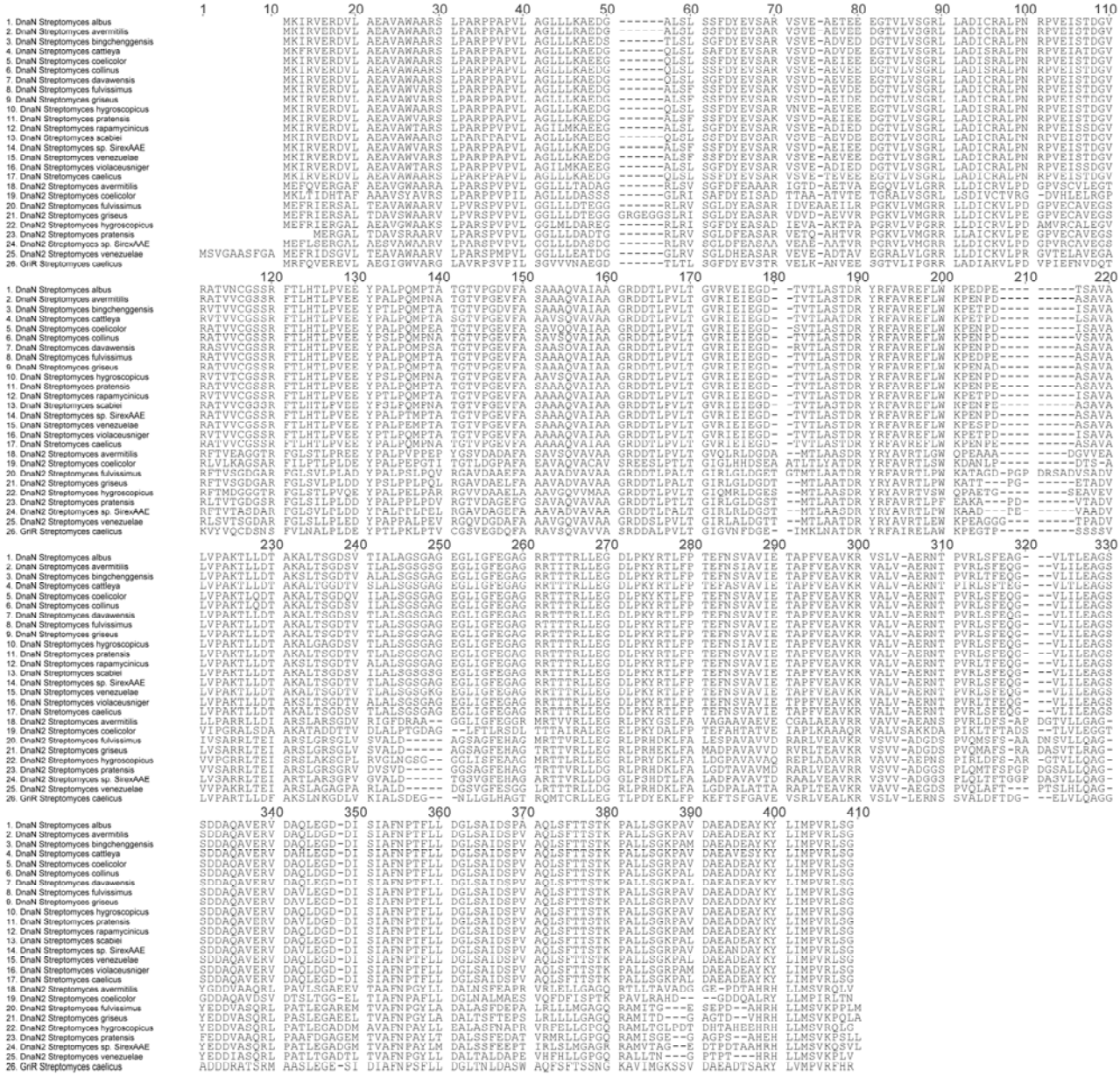

Figure 6-1: Alignment (generated using the clustalW plugin in the geneious software) of the amino acid sequences of DnaN1 and DnaN2 of *Streptomyces* strains with available genome sequences including DnaN and GriR of *S. caelicus*. GeneInfo Identifier (gi) numbers of the sequences used in this analysis are as follows: DnaN *S. coelicolor A3(2)*, 21222286; DnaN *S. griseus*, 182437494; DnaN *S. albus*, 478689546; DnaN *S. avermitilis*, 29830860; DnaN *S. bingchenggensis*, 374988140; DnaN *S. cattelya*, 386356756; DnaN *S. collinus Tu*, 529226638; DnaN *S. davawensis JCM*, 471324000; DnaN *S. fulvissimus*, 488611034; DnaN *S. hygroscopicus TL01*, 474983487; DnaN *S. pratensis*, 357412382; DnaN *S. rapamycinicus*, 557687913; DnaN *S. scabiei*, 290959003; DnaN2 *S. coelicolor* A3(2), 695227561; DnaN2 *S. griseus*, 182437190; DnaN2 *S. hygroscopicus* TL01, 474984464; DnaN2 *S. pratensis*, 357412572; DnaN2 *S. sp. SirexAAE*, 345000616; DnaN2 *S. venezuelae*, 408680935.

	DnaN *S. albus*	DnaN *S. avermitilis*	DnaN *S. bingchengge*	DnaN *S. cattleya*	DnaN *S. coelicolor*	DnaN *S. collinus*	DnaN *S. davawensis*	DnaN *S. fulvissimus*	DnaN *S. griseus*	DnaN *S. hygroscopicu*	DnaN *S. pratensis*	DnaN *S. rapamycinicu*	DnaN *S. scabiei*	DnaN *S. sp. SirexAA*	DnaN *S. venezuelae*	DnaN *S. violaceusnige*	DnaN *S. caelicus*	DnaN2 *S. avermitilis*	DnaN2 *S. coelicolor*	DnaN2 *S. fulvissimus*	DnaN2 *S. griseus*	DnaN2 *S. hygroscopicu*	DnaN2 *S. pratensis*	DnaN2 *S. sp. SirexAA*	DnaN2 *S. venezuelae*	GriR *S. caelicus*
DnaN *S. albus*		94.9	93.1	90.4	93.4	93.4	94.4	94.1	93.9	93.1	94.1	91.5	94.7	93.9	94.7	91	95.5	48.7	46.1	45.8	43.2	46.5	42.7	45.4	46.5	52.7
DnaN *S. avermitilis*	94.9		94.4	91	94.9	96.5	96.5	95.5	96	96.3	96.3	93.6	97.1	96	97.1	93.1	97.3	47.6	46.3	45	42.7	45.9	42.2	44.1	45.9	51.6
DnaN *S. bingchenggens*	93.1	94.4		91.2	93.1	93.9	94.4	93.4	93.6	92.8	93.4	97.1	94.1	93.6	94.9	96.5	94.4	48.2	46.8	45.3	43.4	46.7	42.7	44.9	46.5	53.5
DnaN *S. cattleya*	90.4	91	91.2		91.5	91.8	92.3	91.2	91.5	92.3	90.7	90.2	91.5	91.2	91.2	89.6	92	48.4	47.4	45.8	44.7	47.8	42.2	45.4	47.8	53.5
DnaN *S. coelicolor*	93.4	94.9	93.1	91.5		96.3	95.5	93.6	94.7	94.7	94.4	92.6	95.7	94.7	94.4	92.6	95.5	48.2	46.1	45.3	42.7	46.7	42	44.4	46.2	51.3
DnaN *S. collinus*	93.4	96.5	93.9	91.8	96.3		96.3	94.1	94.7	96.5	94.9	92.8	96.8	94.7	95.5	92.3	96.5	47.6	46.3	45	42.9	45.7	42.2	44.1	45.7	51.6
DnaN *S. davawensis*	94.4	96.5	94.4	92.3	95.5	96.3		94.9	95.5	95.5	95.2	92.8	96.8	95.5	96.3	92.3	97.6	48.7	46.1	44.8	43.2	46.5	42	44.1	46.5	52.1
DnaN *S. fulvissimus*	94.1	95.5	93.4	91.2	93.6	94.1	94.9		98.4	92.8	98.7	92.3	95.2	97.9	96.8	92.3	95.5	47.6	46.8	44.2	42.7	45.7	41.4	44.1	44.9	51.3
DnaN *S. griseus*	93.9	96	93.6	91.5	94.7	94.7	95.5	98.4		93.4	98.7	93.1	95.2	98.9	97.1	93.1	95.5	48.4	46.6	45.3	42.9	45.9	42	44.1	45.4	51.3
DnaN *S. hygroscopicus*	93.1	96.3	92.8	92.3	94.7	96.5	95.5	92.8	93.4		93.6	92.3	95.5	93.4	94.1	91.8	96.3	47.6	46.3	45	43.2	45.9	42	44.1	46.5	52.4
DnaN *S. pratensis*	94.1	96.3	93.4	90.7	94.4	94.9	95.2	98.7	98.7	93.6		93.4	94.9	98.7	96.8	93.4	95.7	47.9	46.6	44.5	42.4	45.7	42	43.9	45.1	51.1
DnaN *S. rapamycinicus*	91.5	93.6	97.1	90.2	92.6	92.8	92.8	92.3	93.1	92.3	93.4		93.1	93.1	93.9	99.5	93.4	47.1	45.5	45	42.9	46.5	42.2	44.1	45.7	52.4
DnaN *S. scabiei*	94.7	97.1	94.1	91.5	95.7	96.8	96.8	95.2	95.2	95.5	94.9	93.1		94.7	96.3	92.6	98.1	47.9	46.1	45	43.4	46.5	42	44.1	45.7	51.3
DnaN *S. sp. SirexAAE*	93.9	96	93.6	91.2	94.7	94.7	95.5	97.9	98.9	93.4	98.7	93.1	94.7		97.3	93.1	95.5	47.9	46.3	45.3	42.9	45.9	42	44.1	45.4	51.3
DnaN *S. venezuelae*	94.7	97.1	94.9	91.2	94.4	95.5	96.3	96.8	97.1	94.1	96.8	93.9	96.3	97.3		93.4	96.8	47.6	46.6	45.3	42.9	46.5	42	44.4	45.7	51.9
DnaN *S. violaceusniger*	91	93.1	96.5	89.6	92.6	92.3	92.3	92.3	93.1	91.8	93.4	99.5	92.6	93.1	93.4		92.8	47.1	45.3	44.8	42.9	46.5	42	43.9	45.4	52.1
DnaN *S. caelicus*	95.5	97.3	94.4	92	95.5	96.5	97.6	95.5	95.5	96.3	95.7	93.4	98.1	95.5	96.8	92.8		47.6	46.3	45.3	43.2	46.5	41.7	44.6	46.2	51.3
DnaN2 *S. avermitilis*	48.7	47.6	48.2	48.4	48.2	47.6	48.7	47.6	48.4	47.6	47.9	47.1	47.9	47.9	47.6	47.1	47.6		39.3	59.4	58.7	66.3	58.8	61.6	58.2	41.3
DnaN2 *S. coelicolor*	46.1	46.3	46.8	47.4	46.1	46.3	46.1	46.8	46.6	46.3	46.6	45.5	46.1	46.3	46.6	45.3	46.3	39.3		35.5	35.9	39.2	35.8	37	40.5	38.8
DnaN2 *S. fulvissimus*	45.8	45	45.3	45.8	45.3	45	44.8	44.2	45.3	45	44.5	45	45	45.3	45.3	44.8	45.3	59.4	35.5		83.2	62.3	74.3	75.5	65.8	41.4
DnaN2 *S. griseus*	43.2	42.7	43.4	44.7	42.7	42.9	43.2	42.7	42.9	43.2	42.4	42.9	43.4	42.9	42.9	42.9	43.2	58.7	35.9	83.2		59.2	74.3	73.6	64.7	40.6
DnaN2 *S. hygroscopicus*	46.5	45.9	46.7	47.8	46.7	45.7	46.5	45.7	45.9	45.9	45.7	46.5	46.5	45.9	46.5	46.5	46.5	66.3	39.2	62.3	59.2		59	63.4	60.3	39.6
DnaN2 *S. pratensis*	42.7	42.2	42.7	42.2	42	42.2	42	41.4	42	42	42	42.2	42	42	42	42	41.7	58.8	35.8	74.3	74.3	59		75.9	63.7	37.4
DnaN2 *S. sp. SirexAAE*	45.4	44.1	44.9	45.4	44.4	44.1	44.1	44.1	44.1	44.1	43.9	44.1	44.1	44.1	44.4	43.9	44.6	61.6	37	75.5	73.6	63.4	75.9		66.9	38.8
DnaN2 *S. venezuelae*	46.5	45.9	46.5	47.8	46.2	45.7	46.5	44.9	45.4	46.5	45.1	45.7	45.7	45.4	45.7	45.4	46.2	58.2	40.5	65.8	64.7	60.3	63.7	66.9		40.9
GriR *S. caelicus*	52.7	51.6	53.5	53.5	51.3	51.6	52.1	51.3	51.3	52.4	51.1	52.4	51.3	51.3	51.9	52.1	51.3	41.3	38.8	41.4	40.6	39.6	37.4	38.8	40.9	

Table 6-2: Similarity matrix (generated using the geneious software) based on the alignment (Figure 6-1) of amino acid sequences of DnaN1 and DnaN2 of *Streptomyces* strains with available genome sequences including DnaN and GriR of *S. caelicus*. The similarity matrix shows the percentage of amino acid identities (distances) between the different sequences. GeneInfo Identifier (gi) numbers of the sequences used in this analysis are as follows: DnaN *S. coelicolor A3(2)*, 21222286; DnaN *S. griseus*, 182437494; DnaN *S. albus*, 478689546; DnaN *S. avermitilis*, 29830860; DnaN *S. bingchenggensis*, 374988140; DnaN *S. cattelya*, 386356756; DnaN *S. collinus Tu*, 529226638; DnaN *S. davawensis JCM*, 471324000; DnaN *S. fulvissimus*, 488611034; DnaN *S. hygroscopicus TL01*, 474983487; DnaN *S. pratensis*, 357412382; DnaN *S. rapamycinicus*, 557687913; DnaN *S. scabiei*, 290959003; DnaN2 *S. coelicolor* A3(2), 695227561; DnaN2 *S. griseus*, 182437190; DnaN2 *S. hygroscopicus* TL01, 474984464; DnaN2 *S. pratensis*, 357412572; DnaN2 *S. sp. SirexAAE*, 345000616; DnaN2 *S. venezuelae*, 408680935.

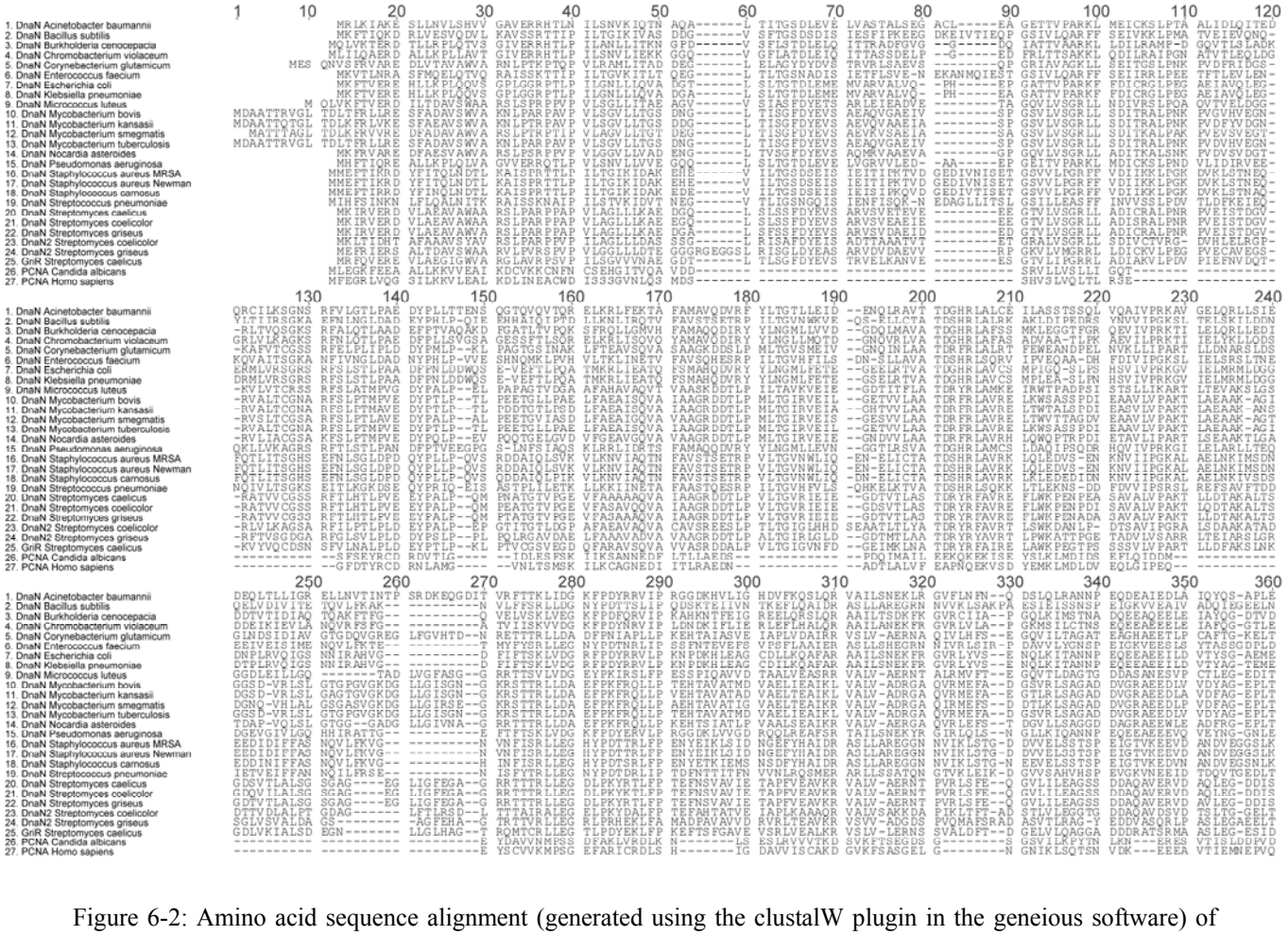

Figure 6-2: Amino acid sequence alignment (generated using the clustalW plugin in the geneious software) of amino acid of sliding clamps of various microorganisms. GeneInfo Identifier (gi) numbers of the included DnaN amino acid sequences are as follows: *A. baumannii*, 213987621; *B. subtilis*, 16077070; *B. cenocepacia*, gi 206558824; *C. violaceum*, 34495457; *C. glutamicum*, 21322767; *E. faecium*, 389867185; *E. coli* DH10B, 169891038; *K. pneumonia*, 238897211; *M. luteus*, 239837780; *M. bovis* BCG, 224988385; *M. kansasii*, 240172092; *M. smegmatis* mc^{2}155, 118169404; *M. tuberculosis* H37Rv, 15607144; *N. asteroides* NBRC 15531, 549076545; *P. aeruginosa* PAO1, 9945820; *S. aureus* MRSA, 49240384; *S. aureus* Newman, 151220214; *S. carnosus*, 222422562; *S. pneumoniae*, 116077515; *S. coelicolor* A3(2), 21219691; *S. griseus*, 182437190; *H. sapiens* PCNA, 49456555; *C. albicans* PCNA, 723213130.

	DnaN *A. baumannii*	DnaN *B. subtilis*	DnaN *B. cenocepacia*	DnaN *C. violaceum*	DnaN *C. glutamicum*	DnaN *E. faecium*	DnaN *E. coli*	DnaN *K. pneumonia*	DnaN *M. luteus*	DnaN *M. bovis*	DnaN *M. kansasii*	DnaN *M. smegmatis*	DnaN *M. tuberculosi*	DnaN *N. asteroides*	DnaN *P. aeruginosa*	DnaN *S. aureus*	DnaN *S. aureus*	DnaN *S. carnosus*	DnaN *S. pneumonia*	DnaN *S. caelicus*	DnaN *S. coelicolor*	DnaN *S. griseus*	DnaN2 *S. coelicolor*	DnaN2 *S. griseus*	GriR *S. caelicus*	PCNA *C. albicans*	PCNA *H. sapiens*
DnaN *A. baumannii*		25,7	37,4	38,5	20,2	23,5	44,2	44,2	21,2	23,3	23,2	23,2	23,3	21,4	46,3	24	24	23,5	21,9	22,9	22,4	23,2	19,9	19,4	22,2	6,8	8,6
DnaN *B. subtilis*	25,7		24,9	24,6	22,6	48,8	25,2	24,9	21,6	22,9	23,3	22,8	22,9	21,8	24,4	54,2	54,2	54,5	40,5	21,6	21,3	21,8	20,1	20,1	21,2	6,3	6,8
DnaN *B. cenocepacia*	37,4	24,9		53,2	20,1	22,6	42,2	42,7	21,4	20,5	20,1	21,1	20,5	18,6	43,8	22,5	22,5	23	21,2	24	23,5	24,8	20,8	19,3	21	9,7	10
DnaN *C. violaceum*	38,5	24,6	53,2		21,6	21,8	41,5	41,7	20,1	21,2	21,6	21,1	21,2	20,6	44,3	25,4	25,4	24,6	20,7	22,9	23,2	23,4	22,3	17,4	20,9	7,2	8,8
DnaN *C. glutamicum*	20,2	22,6	20,1	21,6		22,1	21,1	21,4	41,4	48,1	48,7	50	48,4	51,9	23,4	21,3	21,3	20,3	20,8	42,7	42,2	42,2	32,8	35,2	38,6	8,7	7,7
DnaN *E. faecium*	23,5	48,8	22,6	21,8	22,1		24,7	24,5	18,6	21,5	21,4	23,1	21,5	21,6	23,2	42,7	42,7	43,7	47,7	17,8	18,3	18,1	21,6	17,3	19,2	7,9	8,2
DnaN *E. coli*	44,2	25,2	42,2	41,5	21,1	24,7		96,2	23,5	23,5	24,2	24,2	23,5	24,4	55,6	25,3	25,3	24,7	20,8	24,2	23,4	24,2	21	21	22,5	7,6	8,6
DnaN *K. pneumoniae*	44,2	24,9	42,7	41,7	21,4	24,5	96,2		23,8	23,5	24,4	24,4	23,5	24,2	55,3	26,1	26,1	25,5	21,6	24,2	23,4	24,5	21,3	21,3	21,7	7	8,9
DnaN *M. luteus*	21,2	21,6	21,4	20,1	41,4	18,6	23,5	23,8		43,7	43,7	42,2	43,7	45,1	25,1	22,4	22,4	22,4	18,3	51,6	51,3	50,5	39,6	41,6	42,1	9,1	9,1
DnaN *M. bovis*	23,3	22,9	20,5	21,2	48,1	21,5	23,5	23,5	43,7		86,3	76,8	99,8	65,2	25,5	21,4	21,4	22,2	22,7	48,5	48,7	49	38,1	42,1	38,5	8,9	10,7
DnaN *M. kansasii*	23,2	23,3	20,1	21,6	48,7	21,4	24,2	24,4	43,7	86,3		79,1	86,6	67	25,7	21,3	21,3	22,3	22,8	49,4	49,4	49,9	38,9	39,7	40,4	9	11,5
DnaN *M. smegmatis*	23,2	22,8	21,1	21,1	50	23,1	24,2	24,4	42,2	76,8	79,1		76,8	68,8	26,2	22,1	22,1	21,8	23,8	48,1	48,8	49,1	39,9	41,2	39,8	7,7	10,3
DnaN *M. tuberculosis*	23,3	22,9	20,5	21,2	48,4	21,5	23,5	23,5	43,7	99,8	86,6	76,8		65,5	25,5	21,4	21,4	22,2	22,9	48,5	48,7	49	38,1	42,1	38,5	8,9	10,7
DnaN *N. asteroides*	21,4	21,8	18,6	20,6	51,9	21,6	24,4	24,2	45,1	65,2	67	68,8	65,5		24,2	23,1	23,1	22,9	19,2	49,9	50,6	50,1	39,6	39,4	42,6	8	8,2
DnaN *P. aeruginosa*	46,3	24,4	43,8	44,3	23,4	23,2	55,6	55,3	25,1	25,5	25,7	26,2	25,5	24,2		23,7	23,7	23,2	22,6	24,7	24,5	24,7	22,8	23,4	24,1	7,3	9,5
DnaN *S. aureus MRSA*	24	54,2	22,5	25,4	21,3	42,7	25,3	26,1	22,4	21,4	21,3	22,1	21,4	23,1	23,7		100	89,2	39,6	23,9	23,2	23,4	24,2	19,6	21	7,3	8,4
DnaN *S. aureus Newman*	24	54,2	22,5	25,4	21,3	42,7	25,3	26,1	22,4	21,4	21,3	22,1	21,4	23,1	23,7	100		89,2	39,6	23,9	23,2	23,4	24,2	19,6	21	7,3	8,4
DnaN *S. carnosus*	23,5	54,5	23	24,6	20,3	43,7	24,7	25,5	22,4	22,2	22,3	21,8	22,2	22,9	23,2	89,2	89,2		38,9	24,4	24,2	24,4	22,4	19,1	21,7	8,9	8,9
DnaN *S. pneumoniae*	21,9	40,5	21,2	20,7	20,8	47,7	20,8	21,6	18,3	22,7	22,8	23,8	22,9	19,2	22,6	39,6	39,6	38,9		18,1	18,3	18,1	21,3	15,5	18,2	7,6	9,5
DnaN *S. caelicus*	22,9	21,6	24	22,9	42,7	17,8	24,2	24,2	51,6	48,5	49,4	48,1	48,5	49,9	24,7	23,9	23,9	24,4	18,1		95,5	95,5	46,3	44,2	51,3	8,7	9,8
DnaN *S. coelicolor*	22,4	21,3	23,5	23,2	42,2	18,3	23,4	23,4	51,3	48,7	49,4	48,8	48,7	50,6	24,5	23,2	23,2	24,2	18,3	95,5		94,7	46,1	43,4	51,3	9	9,5
DnaN *S. ariseus*	23,2	21,8	24,8	23,4	42,2	18,1	24,2	24,5	50,5	49	49,9	49,1	49	50,1	24,7	23,4	23,4	24,4	18,1	95,5	94,7		46,6	43,6	51,3	8,7	9,5
DnaN2 *S. coelicolor*	19,9	20,1	20,8	22,3	32,8	21,6	21	21,3	39,6	38,1	38,9	39,9	38,1	39,6	22,8	24,2	24,2	22,4	21,3	46,3	46,1	46,6		38	38,9	7,8	10,4
DnaN2 *S. ariseus*	19,4	20,1	19,3	17,4	35,2	17,3	21	21,3	41,6	42,1	39,7	41,2	42,1	39,4	23,4	19,6	19,6	19,1	15,5	44,2	43,4	43,6	38		41,9	8,7	8,7
GriR *S. caelicus*	22,2	21,2	21	20,9	38,6	19,2	22,5	21,7	42,1	38,5	40,4	39,8	38,5	42,6	24,1	21	21	21,7	18,2	51,3	51,3	51,3	38,9	41,9		8,3	7,7
PCNA *C. albicans*	6,8	6,3	9,7	7,2	8,7	7,9	7,6	7	9,1	8,9	9	7,7	8,9	8	7,3	7,3	7,3	8,9	7,6	8,7	9	8,7	7,8	8,7	8,3		41,7
PCNA *H. sapiens*	8,6	6,8	10	8,8	7,7	8,2	8,6	8,9	9,1	10,7	11,5	10,3	10,7	8,2	9,5	8,4	8,4	8,9	9,5	9,8	9,5	9,5	10,4	8,7	7,7	41,7	

Table 6-3: Similarity matrix (generated using the geneious software) based on the alignment (Figure 6-2) of DnaN sequences of various organisms. The similarity matrix shows the percentage of amino acid identities (distances). GeneInfo Identifier (gi) numbers sequences are as follows: *A. baumannii*, 213987621; *B. subtilis*, 16077070; *B. cenocepacia*, gi 206558824; *C. violaceum*, 34495457; *C. glutamicum*, 21322767; *E. faecium*, 389867185; *E. coli* DH10B, 169891038; *K. pneumonia*, 238897211; *M. luteus*, 239837780; *M. bovis* BCG, 224988385; *M. kansasii*, 240172092; *M. smegmatis* mc^2155, 118169404; *M. tuberculosis* H37Rv, 15607144; *N. asteroides* NBRC 15531, 549076545; *P. aeruginosa* PAO1, 9945820; *S. aureus* MRSA, 49240384; *S. aureus* Newman, 151220214; *S. carnosus*, 222422562; *S. pneumoniae*, 116077515; *S. coelicolor* A3(2), 21219691; *S. griseus*, 182437190; *H. sapiens* PCNA, 49456555; *C. albicans* PCNA, 723213130.

	DnaN *E. coli*	DnaN *A. baumannii*	DnaN *B. cenocepacia*	DnaN *C. violaceum*	DnaN *K. pneumonia*	DnaN *P. aeruginosa*	DnaN *S. aureus*	DnaN *E. faecium*	DnaN *S. pneumonia*	DnaN *B. subtilis*	DnaN *S. coelicolor*	DnaN2 *S. coelicolor*	DnaN *S. griseus*	DnaN *S. caelicus*	GriR *S. caelicus*	DnaN2 *S. griseus*	DnaN *M. luteus*	DnaN *N. asteroides*	DnaN *C. glutamicum*	DnaN *M. tuberculosi*	DnaN *M. smegmatis*
DnaN *E. coli*		95	95	90	100	95	55	55	60	50	40	40	40	40	45	35	55	50	50	50	50
DnaN *A. baumannii*	95		95	90	95	100	55	55	55	50	40	40	40	40	50	35	55	50	50	50	50
DnaN *B. cenocepacia*	95	95		95	95	95	55	55	55	50	40	40	40	40	45	35	55	55	55	50	55
DnaN *C. violaceum*	90	90	95		90	90	55	55	55	50	40	40	40	40	45	35	55	55	55	50	55
DnaN *K. pneumoniae*	100	95	95	90		95	55	55	60	50	40	40	40	40	45	35	55	50	50	50	50
DnaN *P. aeruginosa*	95	100	95	90	95		55	55	55	50	40	40	40	40	50	35	55	50	50	50	50
DnaN *S. aureus Newman*	55	55	55	55	55	55		80	80	85	60	55	60	60	50	40	60	60	60	60	60
DnaN *E. faecium*	55	55	55	55	55	55	80		95	85	60	50	60	60	50	45	70	65	65	65	65
DnaN *S. pneumoniae*	60	55	55	55	60	55	80	95		85	60	50	60	60	50	45	70	65	65	65	65
DnaN *B. subtilis*	50	50	50	50	50	50	85	85	85		55	45	55	55	45	40	65	60	60	60	60
DnaN *S. coelicolor*	40	40	40	40	40	40	60	60	60	55		85	100	100	85	60	75	70	70	70	70
DnaN2 *S. coelicolor*	40	40	40	40	40	40	55	50	50	45	85		85	85	75	60	70	70	70	70	70
DnaN *S. griseus*	40	40	40	40	40	40	60	60	60	55	100	85		100	85	60	75	70	70	70	70
DnaN *S. caelicus*	40	40	40	40	40	40	60	60	60	55	100	85	100		85	60	75	70	70	70	70
GriR *S. caelicus*	45	50	45	45	45	50	50	50	50	45	85	75	85	85		60	75	65	65	65	65
DnaN2 *S. griseus*	35	35	35	35	35	35	40	45	45	40	60	60	60	60	60		65	65	65	70	65
DnaN *M. luteus*	55	55	55	55	55	55	60	70	70	65	75	70	75	75	75	65		80	80	80	80
DnaN *N. asteroides*	50	50	55	55	50	50	60	65	65	60	70	70	70	70	65	65	80		100	95	100
DnaN *C. glutamicum*	50	50	55	55	50	50	60	65	65	60	70	70	70	70	65	65	80	100		95	100
DnaN *M. tuberculosis*	50	50	50	50	50	50	60	65	65	60	70	70	70	70	65	70	80	95	95		95
DnaN *M. smegmatis*	50	50	55	55	50	50	60	65	65	60	70	70	70	70	65	65	80	100	100	95	

Table 6-4: Similarity matrix (generated using the geneious software) based on the alignment (Table 3-6) of the binding pockets of sliding clamps of various microorganisms. The similarity matrix shows the percentage of amino acid identities (distances) between the different sequences. GeneInfo Identifier (gi) numbers of the included DnaN amino acid sequences are as follows: *A. baumannii*, 213987621; *B. subtilis*, 16077070; *B. cenocepacia*, gi 206558824; *C. violaceum*, 34495457; *C. glutamicum*, 21322767; *E. faecium*, 389867185; *E. coli* DH10B, 169891038; *K. pneumonia*, 238897211; *M. luteus*, 239837780; *M. smegmatis* mc^2155, 118169404; *M. tuberculosis* H37Rv, 15607144; *N. asteroides* NBRC 15531, 549076545; *P. aeruginosa* PAO1, 9945820; 49240384; *S. aureus* Newman, 151220214; *S. carnosus*, 222422562; *S. pneumoniae*, 116077515; *S. coelicolor* A3(2), 21219691; *S. griseus*, 182437190;

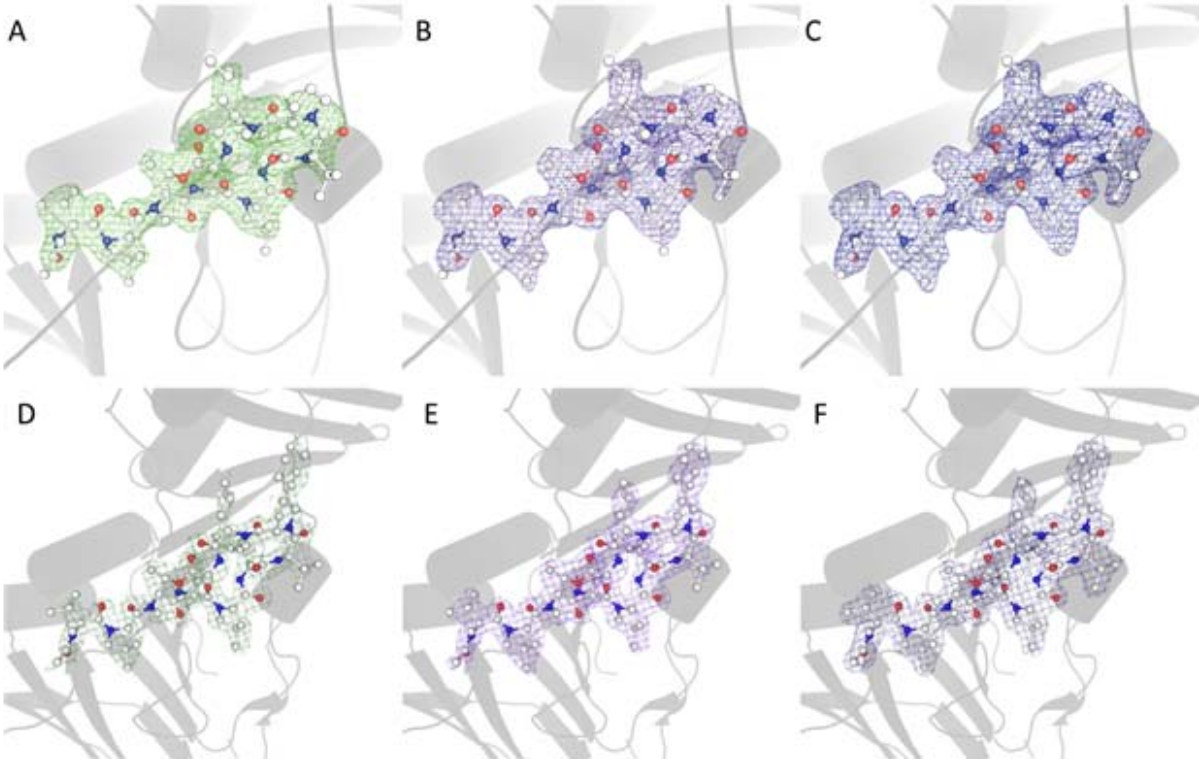

Figure 6-3: Electron density for GM in the *M. smegmatis* DnaN crystal structure and or CGM in the *M. tuberculosis* crystal structure. A, mF_o-DF_c difference density map for GM (green), contoured at σ = +3. B, $2mF_o$-DF_c map with GM omitted (purple), contoured at σ = +1. C, $2mF_o$-DF_c map (blue) refined with the model including GM, contoured at σ = +1. D, mF_o-DF_c difference density map for CGM (green), contoured at σ = +2. E, 2mFo-DFc map with CGM omitted (purple), contoured at σ = +1. F, 2mFo-DFc map (blue) refined with the model including CGM, contoured at σ = +1. To avoid model bias, new molecular replacements were carried out using the finalized models excluding the ligands and followed by refinement. The models containing GM/CGM were then superimposed with the resulting electron density maps.[154]

7 APPENDIX

ABBREVIATIONS

GM	Griselimycin
MGM	Methylgriselimycin
CGM	Cyclohexylgriselimycin
MIC	Minimal inhibitory concentration
CFU	Colony forming unit
TB	Tuberculosis
SPR	Surface plasmon resonance
K_D	Equilibrium dissociation constant
kd	Dissociation rate constant
ka	Dissociation rate constant
$t_{½}$	Dissociative half-life
ITC	Isothermal titration calorimetry
ΔG	Gibbs free energy change
ΔH	Enthalpy change
ΔS	Entropy change
PCNA	Proliferating cell nuclear antigen
CFU	Colony forming unit
Log D	Logarithm of the distribution coefficient
Pol	DNA polymerase
ssDNA	Single stranded DNA
ds DNA	Double stranded DNA
bp	Basepair
kb	Kilobasepairs
Mb	Megabasepairs

ORIGINAL PUBLICATION AND CONFERENCE CONTRIBUTIONS

Original publication

Parts of this thesis are published in the following publication:

*Kling, A., *Lukat, P., Almeida, D. V, Bauer, A., Fontaine, E., Sordello, S., Zaburannyi, N., Herrmann, J., Wenzel, S. C., König, C., Ammerman, N. C., Barrio, M. B., Borchers, K., Bordon-Pallier, F., Brönstrup, M., Courtemanche, G., Gerlitz, M., Geslin, M., Hammann, P., Heinz, D. W., Hoffmann, H., Klieber, S., Kohlmann, M., Kurz, M., Lair, C., Matter, H., Nuermberger, E., Tyagi, S., Fraisse, L., Grosset, J. H., Lagrange, S., Müller, R. (2015). **Targeting DnaN for tuberculosis therapy using novel griselimycins.** *Science*, *348* (6239), 1106–1112. (* these authors contributed equally.)

Conference contributions

Kling, A., Lukat, P., Zaburannyi, N., Herrmann, J., Wenzel, S. C., Bauer, A., Fontaine, E, Brönstrup, M., Fraisse, L., Grosset, J. H., Lagrange, S., Müller, R. (October 1st-2nd, 2015): Oral presentation – **Deciphering the mechanism of action and the resistance mechanism of griselimycins.** International workshop: *Biacore User Days 2015*; Berlin, Germany.

Kling, A., Lukat, P., Zaburannyi, N., Herrmann, J., Wenzel, S. C., Bauer, A., Fontaine, E, Brönstrup, M., Fraisse, L., Lagrange, S., Müller, R. (September 6th–9th, 2015): Poster presentation – **Griselimycins: Streptomyces-derived leads with potent antituberculosis activity that target the sliding clamp.** International conference: *2nd European conference on Natural Products;* Frankfurt a.M., Germany.

Kling, A., Lukat, P., Almeida, D. V, Bauer, A., Fontaine, E., Sordello, S., Zaburannyi, N., Herrmann, J., Wenzel, S. C., König, C., Ammerman, N. C., Barrio, M. B., Borchers, K., Bordon-Pallier, F., Brönstrup, M., Courtemanche, G., Gerlitz, M., Geslin, M., Hammann, P., Heinz, D. W., Hoffmann, H., Klieber, S., Kohlmann, M., Kurz, M., Lair, C., Matter, H., Nuermberger, E., Tyagi, S., Fraisse, L., Grosset, J. H., Lagrange, S., Müller, R. (July 2nd, 2015): Oral presentation – **Griselimycins: novel antituberculosis leads that target the sliding clamp.** International symposium: *5th international HIPS Symposium*, Saarbrücken, Germany.

Kling, A., Herrmann J. and Müller R. (January 21st, 2013): Poster presentation – **Screening for compounds that target staphylococcal adherence to host cells.** International seminar: *8th Status Seminar Chemical Biology*; Frankfurt a.M., Germany.

AUTHOR'S CONTRIBUTION TO THE WORK PRESENTED IN THIS THESIS

Examination of the griselimycin biosynthetic cluster and overexpression of *griR* was performed by Dr. Silke Wenzel. *In silico* analyses were performed by Dr. Nestor Zaburannyi, except for the homology analyses of DnaNs which were performed by the author. Determination of MICs, genotoxicity and resistance frequency were performed by Dr. Jennifer Herrmann, except for the MIC determinations of GM resistant *M. smegmatis* which were performed by the author. Cloning of *E. coli dnaN* was performed by Dr. Peer Lukat and Claudia Wylegalla, cloning of all other *dnaN* genes was performed by the author. Expression and purification of DnaN proteins was performed by Dr. Peer Lukat, except for the *M. smegmatis* DnaN which was expressed and purified by the author. Crystallographic and modeling experiments and were performed by Dr. Peer Lukat. Synthesis, purification and chemical analyses of griselimycins were performed at the Sanofi-Aventis LGCR/Chemistry (Frankfurt a. M., Germany). *In vitro* experiments with *M. tuberculosis* were performed at the Sanofi-Aventis Infectious Disease Therapeutic Strategic Unit (Toulouse, France and Frankfurt a. M., Germany). Mouse infection experiments were performed by the group of Prof. Dr. Jacques Grosset at the Johns Hopkins University School of Medicine (Baltimore, Maryland). All other experiments presented in this thesis were planned, performed and evaluated by the author under the supervision of Prof. Dr. Rolf Müller at the Helmholtz Institute of Pharmaceutical Research Saarland/ HIPS (Saarbrücken, Germany).

DANKSAGUNG

Bei Prof. Dr. Rolf Müller möchte ich mich herzlich für die Aufnahme in seine Arbeitsgruppe und die Überlassung des spannenden Themas und für die hervorragende Betreuung bedanken.

Prof. Dr. Manfred Schmitt danke ich sehr für die hilfreichen Diskussionen während der Treffen des Promotionskomitees und für die Übernahme des Zweitgutachtens.

Besonders bedanken möchte ich mich bei Dr. Peer Lukat für die ständige Diskussionsbereitschaft und die gute Zusammenarbeit. Dr. Jennifer Herrmann danke ich für sämtliche Ratschläge und Diskussionen. Dr. Nestor Zaburannyi danke ich für seine hilfreichen *in silico* Analysen und die Ideen und Diskussionen dazu. Dr. Silke Wenzel danke ich für ihre Unterstützung bei molekularbiologischen Fragen aller Art. Dr. Kevin Sours danke ich für die interessanten Diskussionen zum Griselimycin. PD Dr. Joachim Wink danke ich für die hilfreichen Informationen über den „historischen" Hintergrund von Griselimycin.

Allen Kooperationspartnern von der Arbeitsgruppe von Prof. Dr. Jacques Grosset und von Sanofi-Aventis, die am Griselimycin Projekt mitgewirkt haben, möchte ich für die gute Zusammenarbeit danken.

Allen Mitgliedern der Arbeitsgruppe danke ich für die Hilfsbereitschaft und Kollegialität, insbesondere Fabienne Hennessen, Viktoria Schmitt, Sonja Burkart, Dr. Katja Gemperlein und Dr. Stefan Müller. Bei Viktoria Schmitt und Fabienne Hennessen möchte ich mich besonders für die nette Arbeitsatmosphäre bei uns im ehemaligen 1.OG bedanken.

Ganz besonders möchte ich mich bei meinem Mann, meinen Eltern und meiner restlichen Familie und meinen Freunden aus der Heimat für ihre Unterstützung bedanken. Dankeschön.

BIBLIOGRAPHY

[1] Coscolla, M., Lewin, A., Metzger, S., Maetz-Rennsing, K., Calvignac-Spencer, S., Nitsche, A., Dabrowski, P. W., Radonic, A., Niemann, S., Parkhill, J., Couacy-Hymann, E., Feldman, J., Comas, I., Boesch, C., Gagneux, S., Leendertz, F. H. (2013). Novel Mycobacterium tuberculosis complex isolate from a wild chimpanzee. *Emerging Infectious Diseases*, *19*(6), 969–976.

[2] Gutierrez, M. C., G., Brisse, S., Brosch, R., Fabre, M., Omaïs, B., Marmiesse, M., Supply, P., Vincent, V. (2005). Ancient origin and gene mosaicism of the progenitor of Mycobacterium tuberculosis. *PLoS Pathogens*, *1*(1), 0055–0061.

[3] Falkinham, J. O. (1996). Epidemiology of Infection by Nontuberculous Mycobacteria. *Clinical Microbiology Reviews*, *9*(2), 177–215.

[4] Centers for Disease Control and Prevention. Core curriculum on Tuberculosis: What the clinician should know. Sixth Edition 2013

[5] Kaufmann, S. H. E. (2001). How can immunology contribute to the control of tuberculosis? *Nature Reviews. Immunology*, *1*(1), 20-30.

[6] Kaufmann, S. H. E. (2002). Protection against tuberculosis: cytokines, T cells, and macrophages. *Ann Rheum Dis*, *61*, 54–58.

[7] Daniel, T. M. (2006). The history of tuberculosis. *Respiratory Medicine*, *100*(11), 1862–1870.

[8] Mitchison, D., Davies, G. (2012). The chemotherapy of tuberculosis: past, present and future. *Int J Tuberc Lung Dis*., *16*(6), 724–732.

[9] Rook, G., Dheda, K., Zumla, A. (2005). Immune responses to tuberculosis in developing countries: implications for new vaccines, *Nature Reviews 5*, 661–667.

[10] WHO. Global tuberculosis report 2014. *World Health Organization*, Geneva; 2014

[11] Galagan, J. E. (2014). Genomic insights into tuberculosis. *Nature Reviews. Genetics*, *15*(5), 307–20.

[12] Zumla, A., Nahid, P., Cole, S. T. (2013). Advances in the development of new tuberculosis drugs and treatment regimens. *Nature Reviews. Drug Discovery*, *12*(5), 388–404.

[13] Erondu, N., Ginsberg, A. (2011). Issues and Challenges in the Development of Novel Tuberculosis Drug Regimens. *Antituberculosis Chemotherapy. Prog Respir Res. Basel, Karger*, *40*,118-127.

[14] Upton, A. M., Cho, S., Yang, T. J., Kim, Y., Wang, Y., Lu, Y., Wang, B., Xu, J., Mdluli, K, Ma, Z., Franzblau, S. G. (2015). In Vitro and In Vivo Activities of the Nitroimidazole

TBA-354 against Mycobacterium tuberculosis. *Antimicrobial Agents and Chemotherapy*, *59*(1), 136–144.

[15] Barbachyn, M. R., Hutchinson, D. K., Brickner, S. J., Cynamon, M. H., Kilburn, J. O., Klemens, S. P., Glickman, S. E., Grega, K.C., Hendges, S. K., Toops, D. S., Ford, C. W., Zurenko, G. E. (1996). Identification of a novel oxazolidinone (U-100480) with potent antimycobacterial activity. *Journal of Medicinal Chemistry*, *39*(3), 680–685.

[16] Tahlan, K., Wilson, R., Kastrinsky, D. B., Arora, K., Nair, V., Fischer, E., Barnes, S. W., Walker, J. R., Alland, D., Barry, C. E., Boshoff, H. I. (2012). SQ109 targets MmpL3, a membrane transporter of trehalose monomycolate involved in mycolic acid donation to the cell wall core of *Mycobacterium tuberculosis*. *Antimicrobial Agents and Chemotherapy*, *56*(4), 1797–1809.

[17] Conte, J. E., Golden, J. A., Mcquitty, M., Kipps, J., Lin, E. T., Zurlinden, E. (2000). Single-dose intrapulmonary pharmacokinetics of rifapentine in normal subjects. *Antimicrobial Agents and Chemotherapy*, *44*(4), 985–990.

[18] Andries, K., Verhasselt, P., Guillemont, J., Göhlmann, H. W. H., Neefs, J., Winkler, H., Van Gestel, J., Timmerman, P., Zhu, M., Lee, E., Williams, P., Chaffoy, D., Huitric, E., Hoffner, S., Cambau, E., Truffot-Pernot, C., Lounis, N., Jarlier, V. (2005). A Diarylquinoline Drug Active on the ATP Synthase of Mycobacterium tuberculosis. *Science*, *307*, 223–227.

[19] Matsumoto, M., Hashizume, H., Tomishige, T., Kawasaki, M., Tsubouchi, H., Sasaki, H., Shimokawa, Y., Komatsu, M. (2006). OPC-67683, a nitro-dihydro-imidazooxazole derivative with promising action against tuberculosis in vitro and in mice. *PLoS Medicine*, *3*(11), 2131–2144.

[20] Tasneen, R., Li, S. Y., Peloquin, C. A., Taylor, D., Williams, K. N., Andries, K., Mdluli, K. E., Nuermberger, E. L. (2011). Sterilizing activity of novel TMC207- and PA-824-containing regimens in a murine model of tuberculosis. *Antimicrobial Agents and Chemotherapy*, *55*(12), 5485–5492.

[21] Dawson, R., Diacon, A. H., Everitt, D., van Niekerk, C., Donald, P. R., Burger, D., A., Schall, R., Spigelman, M., Conradie, A., Eisenach, K., Venter, A., Ive, P., Page-Shipp, L., Variava, E., Reither, K., Ntinginya, N. E., Pym, A., von Groote-Bidlingmaie, C. M. (2015). Efficiency and safety of the combination of moxifloxacin, pretomanid (PA-824), and pyrazinamide during the first 8 weeks of antituberculosis treatment: a phase 2b, open-label, partly randomised trial in patients with drug-susceptible or drug-resistant pul. *The Lancet*, *385*(9979), 1738–1747.

[22] Roy, A, Eisenhut, M., Harris, R. J., Rodrigues, L. C., Sridhar, S., Habermann, S., Snell, Mangtani, P., Adetifa, I., Lalvani, A. L., Abubakar, I. (2014). Effect of BCG vaccination against Mycobacterium tuberculosis infection in children: systematic review and meta-analysis. *BMJ (Clinical Research Ed.)*, *349*, 1-11.

[23] Montagnani, C., Chiappini, E., Galli, L., de Martino, M. (2014). Vaccine against tuberculosis: what´s new?. *BMC Infectious diseases, 14* (Suppl 1): S2.

[24] Zhang, Y. (2004). Persistent and dormant tubercle bacilli and latent tuberculosis. *Frontiers in Bioscience 9*, 1136-1156.

[25] Dartois, V. (2014). The path of anti-tuberculosis drugs: from blood to lesions to mycobacterial cells. *Nature Reviews. Microbiology*, *12*, 159–167.

[26] Jia, J., Zhu, F., Ma, X., Cao, Z. W., Li, Y. X., Chen, Y., Z. (2009). Mechanism of drug combinations: interaction and network perspectives. *Nature Reviews drug discovery 8*, 111-128.

[27] Bala, S., Khanna, R., Dadhwal, M., Prabagaran, S. R., Shivaji, S., Cullum, J., Lal, R. (2004). Reclassification of *Amycolatopsis mediterranei* DSM 46095 as *Amycolatopsis rifamycinica* sp. nov. *International Journal of Systematic and Evolutionary Microbiology*, *54*(4), 1145–1149.

[28] Wehrli, W. (1983). Rifampin: mechanisms of action and resistance. *Reviews of Infectious Diseases*, *5 Suppl 3*, S407–11.

[29] Feklistov, A., Mekler, V., Jiang, Q., Westblade, L. F., Irschik, H., Jansen, R., Mustaev A., Darst, S. E., Ebright, R. H. (2008). Rifamycins do not function by allosteric modulation of binding of Mg2+ to the RNA polymerase active center. *Proceedings of the National Academy of Sciences of the United States of America*, *105*(39), 14820–14825.

[30] Global Alliance for TB Drug Development (2008). Handbook of anti-tuberculosis agents. *Tuberculosis*, *88*(2), 85–170. Elsevier, Robertson, B. D., Brennan, P. J., Young, D. B. (Eds.).

[31] Sarathy, J., Dartois, V., Dick, T., Gengenbacher, M. (2013). Reduced drug uptake in phenotypically resistant nutrient-starved nonreplicating Mycobacterium tuberculosis. *Antimicrobial Agents and Chemotherapy*, *57*(4), 1648–1653.

[32] Mor, N., Simon, B., Mezo, N., Heifets, L. (1995). Comparison of activities of rifapentine and rifampin against Mycobacterium tuberculosis residing in human macrophages. *Antimicrobial Agents and Chemotherapy*, *39*(9), 2073–2077.

[33] Binda, G., Domenichini, E., Gottardi, A., Orlandi, B., Ortelli, E., Pacini, B., Fowst, G. (1971). Rifampicin , a general review. *Arzneitmittelforschung*, *21*(12), 1907–1977.

[34] Banerjee, A., Dubnau, E., Annaik, Q., Balasubramanian, V., Urn, K. S., Wilson, T., Collins, D., de Lisle, G., William, E. J. (1994). inhA, a gene encoding a target for isoniazid and ethionamide in Mycobacterium tuberculosis. *Science*, *263*, 227–230.

[35] Timmins, G. S., Deretic, V. (2006). Mechanisms of action of isoniazid. *Molecular Microbiology*, *62*(5), 1220–1227.

[36] Kolyva, A. S., Karakousis, P. C. (2012). Old and New TB Drugs : Mechanisms of Action and Resistance. *Understanding Tuberculosis - New Approaches to Fighting Against Drug Resistance*, Cardona P.-J. (Ed.), InTech.

[37] Brennan, P. J., Rooney, S. A., Winder, F. G. (1970). The lipids of Mycobacterium tuberculosis BCG: fractionation, composition, turnover and the effects of isoniazid. *Irish Journal of Medical Science*, *3*(8), 371–390.

[38] Gangadharam, P R J, Harold, F, M, Schaefer, W, B. (1963). Selective Inhibition of Nucleic Acid Synthesis in Mycobacterium tuberculosis by Isoniazid. *Nature Publishing Group*, *198*(4881), 712–714.

[39] Bekierkunst, A. (1966). Nicotinamide-adenine dinucleotide in tubercle bacilli exposed to isoniazid. *Science*, *152*(721), 525–526.

[40] Rastogi, N., Labrousse, V., Goh, K. S. (1996). In vitro activities of fourteen antimicrobial agents against drug susceptible and resistant clinical isolates of Mycobacterium tuberculosis and comparative intracellular activities against the virulent H37Rv strain in human macrophages. *Current Microbiology*, *33*(3), 167–175.

[41] Konno K., Feldman F. M., McDermott W. (1967). Pyrazinamide susceptibility and amidase activity of tubercle bacilli. *American Review of Respiratory Disease*, 95,461-469.

[42] Zimhony, O., Cox, J. S., Welch, J. T., Vilcheze, C., Jacobs, W.R. (2000). Pyrazinamide inhibits the eukaryotic- like fatty acid synthetase I (FASI) of Mycobacterium tuberculosis. *Nat Med.,* 6, 1043–1047.

[43] Boshoff, H. I., Mizrahi, V., Barry, C. E. (2002). Effects of pyrazinamide on fatty acid synthesis by whole mycobacterial cells and purified fatty acid synthase I. *J Bacteriol.*, 184 (8), 2167–2172.

[44] Shi, W., Zhang, X., Jiang, X., Yuan, H., Lee, J. S., Barry, C. E., Whang, H., Zhang, W., Zhang, Y. (2011). Pyrazinamide inhibits trans-translation in Mycobacterium tuberculosis. *Science (New York, N.Y.)*, *333*(6049), 1630–1632.

[45] Shakya, N., Garg, G., Agrawal, B., Kumar, R. (2012). Chemotherapeutic interventions against tuberculosis. *Pharmaceuticals*, *5*(7), 690–718.

[46] Heifets, L., Higgins, M., Simon, B. (2000). Pyrazinamide is not active against Mycobacterium tuberculosis residing in cultured human monocyte-derived macrophages. *International Journal of Tuberculosis and Lung Disease*, *4*(6), 491–495.

[47] Zhang, Y., Shi, W., Zhang, W., Mitchison, D. (2013). Mechanisms of Pyrazinamide Action and Resistance. *Microbiol Spectr.*, *4*(4), 1–12.

[48] Zhang, Y., Mitchison, D. (2003). The curious characteristics of pyrazinamide: A review. *International Journal of Tuberculosis and Lung Disease*, *7*(1), 6–21.

[49] Belanger, A. E., Besra, G. S., Ford, M. E., Mikusová, K., Belisle, J. T., Brennan, P. J., Inamine, J. M. (1996). The embAB genes of Mycobacterium avium encode an arabinosyl transferase involved in cell wall arabinan biosynthesis that is the target for the antimycobacterial drug ethambutol. *Proceedings of the National Academy of Sciences of the United States of America*, *93*(21), 11919–11924.

[50] Sacksteder, K. A., Protopopova, M., Barry, C. E., Andries, K., Nacy, C. A. (2012). Discovery and development of SQ109: a new antitubercular drug with a novel mechanism of action. *Future Microbiol.*, *7*(7), 823–837.

[51] Siegenthaler, W., Bonetti, A., Luthy, R. (1986). Aminoglycoside Antibiotics in Infectious Diseases. *The American Journal of Medicine*, *80*, 2–14.

[52] Kohanski, M. A, Dwyer, D. J., Collins, J. J. (2010). How antibiotics kill bacteria: from targets to networks. *Nature Reviews. Microbiology*, *8*(6), 423–435.

[53] Allison, K. R., Brynildsen, M. P., Collins, J. J. (2011). Metabolite-enabled eradication of bacterial persisters by aminoglycosides. *Nature*, *473*(7346), 216–220.

[54] Maurin, M., Raoult, D. (2001). Use of Aminoglycosides in Treatment of Infections Due to Intracellular Bacteria MINIREVIEW Use of Aminoglycosides in Treatment of Infections Due to Intracellular Bacteria. *Antimicrobial Agents and Chemotherapy*, *45*(11), 2977–2986.

[55] Herr, E. B., Haney, M. E., Pittenger, G. E., Higgens, C. E. (1960). Isolation and characterization of a new peptide antibiotic. *Proceedings Indiana Academiy of Sciences. 69*, 134.

[56] Caltrider, P. G. (1967). Viomycin. *Mechanism of Action, 1*, 677-689 Gottlieb D. (Ed.), Springer.

[57] Akbergenov, R., Shcherbakov, D., Matt, T., Duscha, S., Meyer, M., Wilson, D. N., Böttger, E. C. (2011). Molecular basis for the selectivity of antituberculosis compounds capreomycin and viomycin. *Antimicrobial Agents and Chemotherapy*, *55*(10), 4712–4717.

[58] Heifets, L., Simon, J., & Pham, V. (2005). Capreomycin is active against nonreplicating M. tuberculosis. *Annals of Clinical Microbiology and Antimicrobials*, *4*, 6.

[59] Achan, J., Talisuna, A. O., Erhart, A., Yeka, A., Tibenderana, J. K., Baliraine, F. N., Rosenthal, P. J., D'Alessandro, U. (2011). Quinine, an old anti-malarial drug in a modern world: role in the treatment of malaria. *Malaria Journal*, *10*(1), 144.

[60] Andersson, M. I., MacGowan, A. P. (2003). Development of the quinolones. *The Journal of Antimicrobial Chemotherapy*, *51 Suppl 1*, 1–11.

[61] Gordon, S., Eiglmeier, K., Garnier, T., Brosch, R., Parkhill, J., Barrell, B., Cole, S. T., Hewinson, R. G. (2001) Genomics of Mycobacterium bovis. *Tuberculosis 81*(1-2), 157 163.

[62] Mustaev, A., Malik, M., Zhao, X., Kurepina, N., Luan, G., Oppegard, L. M., Hiasa, H., Marks, K. E., Kerns, R. J., Berger, J. M., Drlica, K. (2014). Fluoroquinolone-gyrase-DNA complexes two modes of drug binding. *Journal of Biological Chemistry*, *289*(18), 12300–12312.

[63] Mdluli, K., Ma, Z. (2007). Mycobacterium tuberculosis DNA gyrase as a target for drug discovery. *Infectious Disorders Drug Targets*, *7*(2), 159–168.

[64] Shandil, R. K., Jayaram, R., Kaur, P., Gaonkar, S., Suresh, B. L., Mahesh, B. N. Jayashree, R., Nandi, V., Bharath, S., Balasubramanian, V. (2007). Moxifloxacin, ofloxacin, sparfloxacin, and ciprofloxacin against Mycobacterium tuberculosis: Evaluation of in vitro and pharmacodynamic indices that best predict in vivo efficacy. *Antimicrobial Agents and Chemotherapy*, *51*(2), 576–582.

[65] Sato, K., Tomioka, H., Sano, C., Shimizu, T., Sano, K., Ogasawara, K., Cai, S., Kamei, T. (2003). Comparative antimicrobial activities of gatifloxacin, sitafloxacin and levofloxacin against Mycobacterium tuberculosis replicating within Mono Mac 6 human macrophage an A-549 type II alveolar cell lines. *Journal of Antimicrobial Chemotherapy*, *52*(2), 199–203.

[66] Wachtel-Galor, S., Benzie, I. F. F. (2011) Herbal Medicine: An Introduction to Ist History, Usage, Regulation, Current Trends and Research Needs. *Herbal Medicine: Biomolecular and Cinical Aspects.* Chapter 1. Wachtel-Galor, S., Benzie, I. F. F. (Eds.), CRC Press.

[67] Zheng, J., Rubin, E. J., Bifani, P., Mathys, V., Lim, V., Au, M., Jichan, J., Jiyoun, N., Dick, T., Walker, J. R., Pethe, K., Camacho, L. R. (2013). *Para*-aminosalicylic acid is a prodrug targeting dihydrofolate reductase in mycobacterium tuberculosis. *Journal of Biological Chemistry*, *288*(32), 23447–23456.

[68] Zheng, J., Rubin, E. J., Bifani, P., Mathys, V., Lim, V., Au, M., Jang, J., Nam, J., Dick, T., Walker, J. R., Pethe, K., Camacho, L. R. (2013). *Para*-aminosalicylic acid is a prodrug targeting dihydrofolate reductase in mycobacterium tuberculosis. *Journal of Biological Chemistry*, *288*(32), 23447–23456.

[69] MacKaness, G. B., Smith, N. (1953). The bactericidal action of isoniazid, streptomycin and terramycin on extracellular and intracellular tubercle bacilli. *Am Rev Tuberc 67* (3),322-340.

[70] Otten, H. (). Cycloserine (CS) and Terizidone (TZ). *Anti-tuberculosis drugs.* Chaper 8, 158-166. Bartmann, K. (Ed.), Springer.

[71] Di Perri, G., Bonora, S. (2004). Which agents should we use for the treatment of multidrug-resistant Mycobacterium tuberculosis*? J Antimicrob Chemother* 54, 593 602.

[72] Vannelli, T. A., Dykman, A., Ortiz De Montellano, P. R. (2002). The antituberculosis drug ethionamide is activated by a flavoprotein monooxygenase. *Journal of Biological Chemistry*, *277*(15), 12824–12829.

[73] Brossier, F., Veziris, N., Truffot-Pernot, C., Jarlier, V., & Sougakoff, W. (2011). Molecular investigation of resistance to the antituberculous drug ethionamide in multidrug-resistant clinical isolates of Mycobacterium tuberculosis. *Antimicrobial Agents and Chemotherapy*, *55*(1), 355–360.

[74] Quian, L., Ortiz de Montellano, P. R. (2006). Oxidative Activation of Thiacetazone by the Mycobacterium tuberculosis Flavin Monooxygenase EtaA and Human FMO1 and FMO3. *Chem Res Toxicol.*, *19*(3), 443–449.

[75] Grzegorzewicz, A. E., Korduláková, J., Jones, V., Born, S. E. M., Belardinelli, J. M., Vaquié, A., Gundi, V. A. K. B., Madacki, J., Slama, N., Laval, F., Vaubourgeix, J., Crew, R. M., Gicquel, B., Daffe, M., Morbidoni, H. R., Brennan, P. J., Quemard, A., McNeil, M., Jackson, M. (2012). A common mechanism of inhibition of the Mycobacterium tuberculosis mycolic acid biosynthetic pathway by isoxyl and thiacetazone. *Journal of Biological Chemistry*, *287*(46), 38434–38441.

[76] Alahari, A., Trivelli, X., Guérardel, Y., Dover, L. G., Besra, G. S., Sacchettini, J. C., Reynolds, R. C., Coxon, G. D., Kremer, L. (2007). Thiacetazone, an antitubercular drug that inhibits cyclopropanation of cell wall mycolic acids in mycobacteria. *PLoS ONE*, *2*(12).

[77] Gopal, P., Dick, T. (2015). The new tuberculosis drug Perchlozone® shows cross-resistance with thiacetazone. *International Journal of Antimicrobial Agents*, *45*(4), 430–433.

[78] Heifets, L. B., Lindholm-Levy, P. J., Flory, M. (1991) Thiacetazone: in vitro activity against Mycobacterium avium and M. tuberculosis. *Tubercle 71 (4),* 287-291.

[79] Cho, S. H., Warit, S., Wan, B., Hwang, C. H., Pauli, G. F., Franzblau, S. G. (2007). Low-oxygen-recovery assay for high-throughput screening of compounds against nonreplicating Mycobacterium tuberculosis. *Antimicrobial Agents and Chemotherapy*, *51*(4), 1380–1385.

[80] Shaw, K. J., Barbachyn, M. R. (2011). The oxazolidinones: Past, present, and future. *Annals of the New York Academy of Sciences*, *1241*(1), 48–70.

[81] Balasubramanian, V., Solapure, S., Iyer, H., Ghosh, A., Sharma, S., Kaur, P., Deepthi, R., Subbulakshmi, V., Ramya, V., Ramachandran, V., Balganesh, M., Wright, L., Melnick, D., Butler, S. L., Sambandamurthy, V. K. (2014). Bactericidal activity and mechanism of action of AZD5847, a novel oxazolidinone for treatment of tuberculosis. *Antimicrobial Agents and Chemotherapy*, *58*(1), 495–502.

[82] Wilson, D. N., Schluenzen, F., Harms, J. M., Starosta, A. L., Connell, S. R., Fucini, P. (2008). The oxazolidinone antibiotics perturb the ribosomal peptidyl-transferase center and effect tRNA positioning. *Proceedings of the National Academy of Sciences of the United States of America*, *105*(36), 13339–13344.

[83] Wilson, D. N. (2014). Ribosome-targeting antibiotics and mechanisms of bacterial resistance. *Nature Reviews. Microbiology*, *12*(1), 35–48.

[84] Myungsun, L., Lee, J., Carroll, M. W., Choi, H., Min, S., Song, T., Via, Laura E., Goldfeder, L. C., Kang, E., Jin, B., Park, H., Kwak, H., Kim, H., Jeon, H., Jeong, I., Joh, J. S., Chen, R. Y., Olivier, K. N., Shaw, P. A., Follmann, D., Song, S. D., Lee, J., Lee, D.,

Kim, C. T., Dartois, V., Park, S., Cho, S., Barry, C. E. (2012). Linezolid for Treatment of Chronic Extensively Drug-Resistant Tuberculosis. *N Engl J Med.*, *267*(16), 109–113.

[85] Mukherjee, T., Boshoff, H. (2011). Nitroimidazoles for the treatment of TB: past, present and future. *Future Medicinal Chemistry*, *3*(11), 1427–1454.

[86] Marriner, G. A., Nayyar, A., Uh, E., Wong, S. Y., Mukherjee, T., Via, L. E., Carroll, M., Edwards, R. L., Gruber, T. D., Choi, I., Lee, J., Arora, K., England, K., D., Boshoff, H. I. M., Barry, C. E. Paslay, J., Morin, J., & Harrison, R. (2011). The medicinal chemistry of tuberculosis chemotherapy. *Topics in Medicinal Chemistry*, *4,* 47-124.

[87] Stover, C. K., Warrener, P., VanDevanter, D. R., Sherman, D. R., Arain, T. M., Langhorne, M. H., Anderson, S. W., Towell, A. J., Yuan, Y., McMurray, D. N., Kreisweith, B. N., Barry, C. E., Baker, W. R. (2000). A small-molecule nitroimidazopyran drug candidate for the treatment of tuberculosis. *Nature*, *405*(6789), 962–966.

[88] Reddy, V. M., O'Sullivan, J. F., Gangadharam, P. R. J. (1999). Antimycobacterial activities of riminophenazines. *Journal of Antimicrobial Chemotherapy*, *43*(5), 615–623.

[89] Yano, T., Kassovska-Bratinova, S., Shin Teh, J., Winkler, J., Sullivan, K., Isaacs, A., Schechter, N. M., Rubin, H. (2011). Reduction of clofazimine by mycobacterial type 2 NADH: Quinone Oxidoreductase: A pathway for the generation of bactericidal levels of reactive oxygen species. *Journal of Biological Chemistry*, *286*(12), 10276–10287.

[90] Cholo, M. C., Steel, H. C., Fourie, P. B., Germishuizen, W. A., Anderson, R. (2012). Clofazimine: Current status and future prospects. *Journal of Antimicrobial Chemotherapy*, *67*(2), 290–298.

[91] Lu, Y., Zheng, M., Wang, B., Fu, L., Zhao, W., Li, P., … Ma, Z. (2011). Clofazimine analogs with efficacy against experimental tuberculosis and reduced potential for accumulation. *Antimicrobial Agents and Chemotherapy*, *55*(11), 5185–5193.

[92] Haagsma, A. C., Podasca, I., Koul, A., Andries, K., Guillemont, J., Lill, H., Bald, D. (2011). Probing the interaction of the diarylquinoline TMC207 with its target mycobacterial ATP synthase. *PLoS ONE*, *6*(8), 1–7.

[93] Dhillon, J., Andries, K., Phillips, P. P. J., Mitchison, D. a. (2010). Bactericidal activity of the diarylquinoline TMC207 against Mycobacterium tuberculosis outside and within cells. *Tuberculosis*, *90*(5), 301–305.

[94] Bandyopadhyay, A., Das, D. K., Mandal, S. K. (1993). Erythromycin production by *Streptomyces erythreus* entrapped in calcium alginate beads. *Biotechnology letters*, 15 (10), 1003-1006.

[95] Zuckerman, J. M. (2004). Macrolides and ketolides: azithromycin, clarithromycin, telithromycin. *Infectious Disease Clinics of North America*, *18*(3), 621–649.

[96] Sato, K., Tomioka, H., Akaki, T., Kawahara, S. (2000). Antimicrobial activities of levofloxacin, clarithromycin, and KRM-1648 against Mycobacterium tuberculosis and

Mycobacterium avium complex replicating within Mono Mac 6 human macrophage and A-549 type II alveolar cell lines. *International Journal of Antimicrobial Agents*, *16*(1), 25–29.

[97] Phunpruch, S., Warit, S., Suksamran, R., Billamas, P., Jaitrong, S., Palittapongarnpim, P., Prammananan, T. (2013). A role for 16S rRNA dimethyltransferase (ksgA) in intrinsic clarithromycin resistance in Mycobacterium tuberculosis. *International Journal of Antimicrobial Agents*, *41*(6), 548–551.

[98] Cho, S. H., Warit, S., Wan, B., Hwang, C. H., Pauli, G. F., Franzblau, S. G. (2007). Low-oxygen-recovery assay for high-throughput screening of compounds against nonreplicating Mycobacterium tuberculosis. *Antimicrobial Agents and Chemotherapy*, *51*(4), 1380–1385.

[99] Papp-Wallace, K. M., Endimiani, A., Taracila, M. A., Bonomo, R. a. (2011). Carbapenems: Past, present, and future. *Antimicrobial Agents and Chemotherapy*, *55*(11), 4943–4960.

[100] Handsfield, H. H., Clark, H., Wallace, J. F., Holmes, K. K., Turck, M. (1973). Amoxicillin, a new penicillin antibiotic. *Antimicrobial Agents and Chemotherapy*, *3*(2), 262–265.

[101] Drawz, S. M., Bonomo, R. A. (2010). Three decades of β-lactamase inhibitors. *Clinical Microbiology Reviews*, *23*, 160–201.

[102] Kahan, F. M., Kropp, H., Sundelof, J. G., Birnbaum, J. (1983). Thienamycin : development of imipenem-cilastatin. *Journal of Antimicrobial Chemotherapy*, *12,* Suppl. D, 1–35.

[103] Solapure, S., Dinesh, N., Shandil, R., Ramachandran, V., Sharma, S., Bhattacharjee, D., Ganguly, S., Reddy, J., Ahuja, V., Panduga, V., Parab, M., Vishwas, K. G., Kumar, N., Balganesh, M., Balasubramanian, V. (2013). In vitro and in vivo efficacy of β-lactams against replicating and slowly growing/nonreplicating mycobacterium tuberculosis. *Antimicrobial Agents and Chemotherapy*, *57*(6), 2506–2510.

[104] Chambers, H. F., Moreau, D., Yajko, D., Miick, C., Wagner, C., Hackbarth, C., Kocagöz, S., Rosenberg, E., Hadley, W. K., Nikaido, H. (1995). Can penicillins and other beta-lactam antibiotics be used to treat tuberculosis? *Antimicrobial Agents and Chemotherapy*, *39*(12), 2620–2624.

[105] England, K., Boshoff, H. I. M., Arora, K., Weiner, D., Dayao, E., Schimel, D., Via, L. E., Barry, C. E. (2012). Meropenem-clavulanic acid shows activity against Mycobacterium tuberculosis in vivo. *Antimicrobial Agents and Chemotherapy*, *56*(6), 3384–3387.

[106] D'Costa, V. M., King, C. E., Kalan, L., Morar, M., Sung, W. W. L., Schwarz, C., Froese, D., Zazula, G., Calmels, F., Debruyne, R., Golding, B., Poinar, H. N., Wright, G. D. (2011). Antibiotic resistance is ancient. *Nature*, *477*(7365), 457–461.

[107] Wright, G. D., Poinar, H. (2012). Antibiotic resistance is ancient: Implications for drug discovery. *Trends in Microbiology*, *20*(4), 157–159.

[108] Laxminarayan, R., Duse, A., Wattal, C., Zaidi, A. K. M., Wertheim, H. F. L., Sumpradit, N., Vlieghe, E., Hara, G. L., Gould, I. M., Goossens, H., Greko, C., So, A. D., Bigdeli, M., Tomson, G., Woodhouse, W., Ombaka, E., Peralta, A. Q., Qamar, F. N., Mir, F., Kariuki, S., Bhutta, Z. A., Coates, A., Bergstrom, R., Wright, G. D., Brown, E. D., Cars, O. (2013). Antibiotic resistance-the need for global solutions. *The Lancet Infectious Diseases*, *13*(12), 1057–1098.

[109] Blair, J. M. A., Webber, M. A., Baylay, A. J., Ogbolu, D. O., Piddock, L. J. V. (2015). Molecular mechanisms of antibiotic resistance. *Nature*, *13*, 42–51.

[110] Da Silva, P. E. A., Palomino, J. C. (2011). Molecular basis and mechanisms of drug resistance in Mycobacterium tuberculosis: Classical and new drugs. *Journal of Antimicrobial Chemotherapy*, *66*(7), 1417–1430.

[111] Sacchettini, J. C., Rubin, E. J., Freundlich, J. S. (2008). Drugs versus bugs: in pursuit of the persistent predator Mycobacterium tuberculosis. *Nature Reviews. Microbiology*, *6*(1), 41–52.

[112] Mitchison, D. A., Jindani, A., Davies, G. R., Sirgel, F. (2007). Isoniazid activity is terminated by bacterial persistence. *The Journal of Infectious Diseases*, *195*(12), 1870–1873.

[113] Louw, G. E., Warren, R. M., Gey Van Pittius, N. C., McEvoy, C. R. E., Van Helden, P. D., Victor, T. C. (2009). A balancing act: Efflux/influx in mycobacterial drug resistance. *Antimicrobial Agents and Chemotherapy*, *53*(8), 3181–3189.

[114] Cirz, R.T., Chin J. K., Andes D. R., de Crécy- Lagard, V., Craig W. A., Romesberg, F. E. (2005) Inhibition of mutation and combating the evolution of antibiotic resistance. *PLOS Biol.* 3(6):e176.

[115] Nachega, J. B., Chaisson, R. E. (2003). Tuberculosis drug resistance: a global threat. *Clinical Infectious Diseases : An Official Publication of the Infectious Diseases Society of America*, *36*(Suppl 1), S24–S30.

[116] Boshoff, H. I. M., Reed, M. B., Barry, C. E., Mizrahi, V. (2003). DnaE2 polymerase contributes to *in vivo* survival and the emergence of drug resistance in *Mycobacterium tuberculosis*. *Cell*, *113*, 183–193.

[117] Mather, R., Karenchak, L. M., Romanowski, E. G., Kowalski, R. P. (2002). Fourth generation fluoroquinolones: New weapons in the arsenal of ophthalmic antibiotics. *American Journal of Ophthalmology*, *133*(4), 463–466.

[118] Munck, C., Gumpert, H. K., Wallin, A. I. N., Wang, H. H., Sommer, M. O. A. (2014). Prediction of resistance development against drug combinations by collateral responses to component drugs. *Science Transl. Med.*, *156*.

[119] Lázár, V., Pal Singh, G., Spohn, R., Nagy, I., Horváth, B., Hrtyan, M., Busa-Fekete, R., Bogos, B., Mehi, O., Csörgö, B., Posfai, G., Fekete, G., Szappanos, B., Kegl, B., Papp,

B., Pál, C. (2013). Bacterial evolution of antibiotic hypersensitivity. *Molecular Systems Biology*, *9* (700), 1-12.

[120] Köser, C. U., Javid, B., Liddell, K., Ellington, M. J., Feuerriegel, S., Niemann, S., Brown, N. M., Burman, W. J., Abubakar, I., Ismail, N. A., Moore, D., Peacock, S. J., Török, M. E. (2015). Drug-resistance mechanisms and tuberculosis drugs. *The Lancet*, 385 (9965), 305-307.

[121] Huitric, E., Werngren, J., Juréen, P., Hoffner, S. (2006). Resistance levels and rpoB gene mutations among in vitro-selected rifampin-resistant Mycobacterium tuberculosis mutants. *Antimicrobial Agents and Chemotherapy*, *50*(8), 2860–2862.

[122] Koch, A., Mizrahi, V., & Warner, D. F. (2014). The impact of drug resistance on Mycobacterium tuberculosis physiology: what can we learn from rifampicin? *Emerging Microbes & Infections*, *3*(3), e17.

[123] Musser, J. M. (1995). Antimicrobial agent resistance in mycobacteria : molecular genetic insights . Antimicrobial Agent Resistance in Mycobacteria : Molecular Genetic Insights, *8*(4), 496–514.

[124] David, H. L. (1970). Probability distribution of drug-resistant mutants in unselected populations of Mycobacterium tuberculosis. *Applied Microbiology*, *20*(5), 810–814.

[125] Stoffels, K., Mathys, V., Fauville-Dufaux, M., Wintjens, R., Bifania, P. (2012). Systematic analysis of pyrazinamide-resistant spontaneous mutants and clinical isolates of Mycobacterium tuberculosis. *Antimicrobial Agents and Chemotherapy*, *56*(10), 5186–5193.

[126] Safi, H., Lingaraju, S., Amin, A., Kim, S. (2013). of high-level ethambutol-resistant tuberculosis through interacting mutations in decaprenylphosphoryl-D-arabinose biosynthetic and utilization pathway genes. *Nature 45*(10), 1190–1197.

[127] Sowajassatakul, A., Prammananan, T., Chaiprasert, A., Phunpruch, S. (2014). Molecular characterization of amikacin, kanamycin and capreomycin resistance in M/XDR-TB strains isolated in Thailand. *BMC Microbiology*, *14*(1), 165.

[128] Raivio, T. L. (2014) Everything old is new again. An update on current research on the Cpx envelope stress response. *Science 1843 (8),* 1529-1541.

[129] Okamoto, S., Tamaru, A., Nakajima, C., Nishimura, K., Tanaka, Y., Tokuyama, S., Suzuki, Y., Ochi, K. (2007). Loss of a conserved 7-methylguanosine modification in 16S rRNA confers low-level streptomycin resistance in bacteria. *Molecular Microbiology*, *63*(4), 1096–1106.

[130] Maus, C. E., Plikaytis, B. B., Thomas, M., Shinnick, T. M. (2005). Mutation of tlyA Confers Capreomycin Resistance in *Mycobacterium tuberculosis Antimicrobial agents and chemotherapy 49*(2), 571–577.

[131] Malik, S., Willby, M., Sikes, D., Tsodikov, O. V., Posey, J. E. (2012). New insights into fluoroquinolone resistance in *Mycobacterium tuberculosis*: Functional genetic analysis of gyrA and gyrB mutations. *PLoS ONE*, *7*(6).

[132] Alangaden, G. J., Manavathu, E. K., Vakulenko, S. B. (1995). Characterization of fluoroquinolone-resistant mutant strains of *Mycobacterium tuberculosis* selected in the laboratory and isolated from patients. *Antimicrobial agents and chemotherapy 39*(8), 1700–1703.

[133] Rengarajan, J., Sassetti, C. M., Naroditskaya, V., Sloutsky, A., Bloom, B. R., Rubin, E. J. (2004). The folate pathway is a target for resistance to the drug *para*-aminosalicylic acid (PAS) in mycobacteria. *Molecular Microbiology*, *53*(1), 275–282.

[134] Zhao, F., Wang, X. De, Erber, L. N., Luo, M., Guo, A. Z., Yang, S. S., Gu, J., Turman, B. J., Gao, Y., Li, D., Cui, Z., Zhang, Z., Bi, L., Baughn, A., Zhang, X., Deng, J. Y. (2014). Binding pocket alterations in dihydrofolate synthase confer resistance to *para*-aminosalicylic acid in clinical isolates of Mycobacterium tuberculosis. *Antimicrobial Agents and Chemotherapy*, *58*(3), 1479–1487.

[135] Feng, Z., Barletta, G. R.(2003). Roles of *Mycobacterium smegmatis* D -Alanine : D -Alanine Ligase and D -Alanine Racemase in the Mechanisms of Action of and Resistance to the Peptidoglycan Inhibitor D -Cycloserine. *Society*, *47*(1), 283–291.

[136] Brossier, F., Veziris, N., Truffot-Pernot, C., Jarlier, V., Sougakoff, W. (2011). Molecular investigation of resistance to the antituberculous drug ethionamide in multidrug-resistant clinical isolates of *Mycobacterium tuberculosis*. *Antimicrobial Agents and Chemotherapy*, *55*(1), 355–360.

[137] Vilchèze, C., Av-Gay, Y., Attarian, R., Liu, Z., Hazbón, M. H., Colangeli, R., Chen, B., Liu, W., Alland, D., Sacchettini, J. C., Jacobs, W. R. (2008). Mycothiol biosynthesis is essential for ethionamide susceptibility in *Mycobacterium tuberculosis*. *Molecular Microbiology*, *69*(5), 1316–1329.

[138] Belardinelli, J. M., Morbidoni, H. R. (2012). Mutations in the essential FAS II β-hydroxyacyl ACP dehydratase complex confer resistance to thiacetazone in *Mycobacterium tuberculosis* and *Mycobacterium kansasii*. *Molecular Microbiology*, *86*(3), 568–579.

[139] Hillemann, D., Rüsch-Gerdes, S., Richter, E. (2008). In vitro-selected linezolid-resistant Mycobacterium tuberculosis mutants. *Antimicrobial Agents and Chemotherapy*, *52*(2), 800–801.

[140] Cellitti, S. E., Shaffer, J., Jones, D. H., Mukherjee, T., Gurumurthy, M., Bursulaya, B., Boshoff, H. I., Choi, I., Nayyar, A., Lee, Y. S., Cherian, J., Niyomrattankit, P., Dick, T., Manjunatha, U. H., Carry, C. E., Spraggons, G., Geierstanger, B. H. (2012). Structure of Ddn, the deazaflavin-dependent nitroreductase from Mycobacterium tuberculosis involved in bioreductive activation of PA-824. *Structure*, *20*(1), 101–112.

[141] Manjunatha, U. H., Boshoff, H., Dowd, C. S., Zhang, L., Albert, T. J., Norton, J. E., Daniels, L., Dick, T., Pang, S. S, Barry, C. E. (2006). Identification of a nitroimidazo-oxazine-specific protein involved in PA-824 resistance in Mycobacterium tuberculosis. *Proceedings of the National Academy of Sciences of the United States of America*, *103*(2), 431–436.

[142] Andries, K., Verhasselt, P., Guillemont, J., Goehlmann, H. W. H., Neefs, J.-M., Winkler, H., Van Gestel J., Timmerman, P., Zhu, M., Lee, Ennis, Wiliams, P., de Chaffoy, D., Huitric, E., Hoffner, S., Cambau, E., Truffot-Pernot, C., Lounis, N., Jarlier, V. (2005). A Diarylquinoline Drug Active on the ATP Synthase of Mycobacterium tuberculosis. *Science*, *307*, 223–227.

[143] Hartkoorn, R. C., Uplekar, S., Cole, S. T. (2014). Cross-resistance between clofazimine and bedaquiline through upregulation of mmpl5 in mycobacterium tuberculosis. *Antimicrobial Agents and Chemotherapy*, *58*(5), 2979–2981.

[144] Andini, N., Nash, K. a. (2006). Intrinsic macrolide resistance of the Mycobacterium tuberculosis complex is inducible. *Antimicrobial Agents and Chemotherapy*, *50*(7), 2560–2562.

[145] Lun, S., David Miranda, Kubler, A., Guo, H., Maiga, M. C., Winglee, K., Pelly, S., Bishaia, W. R. (2014). Synthetic Lethality Reveals Mechanisms of Mycobacterium tuberculosis Resistance to β-Lactams. *mBio*, *5*(5), e01767–14. doi:10.1128/mBio.01767-14

[146] Wang, F., Cassidy, C., Sacchettini, J. C. (2006). Crystal structure and activity studies of the Mycobacterium tuberculosis β-lactamase reveal its critical role in resistance to β-lactam antibiotics. *Antimicrobial Agents and Chemotherapy*, *50*(8), 2762–2771.

[147] Broenstrup, M., Koenig, C., Toti, L., Wink, J., Leuschner, W., Gassenhuber, J., Müller, R., Wenzel, S., Binz, T., Volz, C. (2014). Gene cluster for biosynthesis of griselimycin and methylgriselimycin. United States Patent US2014/0295457 A1.

[148] Cung, M. T., Vitoux, B., Demange, P., Marraud, M. (1991). 2D-NMR Conformational Analysis of Griselimycin, an antituberculous cyclodepsipeptide. *Molecular conformation and biological interactions,* Indian academy of sciences, Bangalore, Balaram, P., Ramaseshan, S. (Eds.).

[149] Anonymous (1962). New antibiotic product, its preparation and compositions containing it. GB Patent 966,124.

[150] Mancy, D., Ninet, L., Preudhomme, J. (1968). Antibiotic for treating tuberculosis and method of producing same. US Patent 3365362.

[151] Terlain, B., Thomas, J. P. (1971). Structure of griselimycin, polypeptide antibiotic extracted from Streptomyces cultures. *Bull, soc. Chim. Fr.* 3, 2349-2365.

[152] F. Bénazet et al., in Antibiotics – Advances in Research, Production and Clinical Use: Proceedings of the Congress on Antibiotics held in Prague, 15-19 June, 1964, M. Herold, Z. Gabriel, Eds. (Butterworths, London, 1966), pp. 262–264.

[153] H. Noufflard-Guy-Loé, S. Berteaux, Experimental antituberculous action of a new antibiotic: RP 11,072. *Rev. Tuberc. Pneumol. (Paris) 29*, 301–326 (1965).

[154] Kling, A., Lukat, P., Almeida, D. V, Bauer, A., Fontaine, E., Sordello, S., Zaburannyi, N., Herrmann, J., Wenzel, S. C., König, C., Ammerman, N. C., Barrio, M. B., Borchers, K., Bordon-Pallier, F., Brönstrup, M., Courtemanche, G., Gerlitz, M., Geslin, M., Hammann, P., Heinz, D. W., Hoffmann, H., Klieber, S., Kohlmann, M., Kurz, M., Lair, C., Matter, H., Nuermberger, E., Tyagi, S., Fraisse, L., Grosset, J. H., Lagrange, S., Müller, R. (2015). Targeting DnaN for tuberculosis therapy using novel griselimycins. *Science*, *348*(6239), 1106–1112.

[155] Duthie E. S. (1952). Variation in the antigenic composition of staphylococcal coagulase. *J. Gen. Microbiol.* 7, 320–326.

[156] Kieser, T., Bibb, M. J., Buttner, M. J., Chater, K. F., Hopwood, D. A. (2000). Practical Streptomyces Genetics (Johns Innes Foundation, Norwich, UK).

[157] Doumith, M., Weingarten, P., Wehmeier, U. F., Salah-Bey, K., Benhamou, B., Capdevila, C., Michel, J. M., Piepersberg, W., Raynal, M. C. (2000). Analysis of genes involved in 6-deoxyhexose biosynthesis and transfer in Saccharopolyspora erythraea. *Mol. Gen. Genet. 264,* 477– 485.

[158] Böddinghaus, B., Rogall, T., Flohr, T., Blöcker, H., Böttger, E. C. (1990): Detection and identification of mycobacteria by amplification of rRNA. *J. Clin. Microbiol. 28*, 1751–1759.

[159] Studier, F. W. (2005). Protein production by auto-induction in high density shaking cultures. *Protein Expr. Purif. 41*, 207–234.

[160] Gasteiger, E., Gattiker, A., Hoogland, C., Ivanyi, I., Appel, R. D., Bairoch, A.(2003). ExPASy: The proteomics server for in-depth protein knowledge and analysis. *Nucleic Acids Res. 31*, 3784–3788.

[161] Andrews, J. M. (2001). Determination of minimum inhibitory concentrations. J. Antimicrob. Chemother. 48 (suppl. 1), 5–16.

[162] Vonrhein, C., Flensburg, C., Keller, P. Sharff, A., Smart, O., Paciorek, W., Womack, T. Bricogne, G (2011). Data processing and analysis with the autoPROC toolbox. *Acta Crystallogr. D 67*, 293–302.

[163] Kabsch, W. (2010). XDS. *Acta Crystallogr. D 66,* 125–132.

[164] Evans, P. (2006). Scaling and assessment of data quality. *Acta Crystallogr. D 62*, 72–82.

[165] Evans, P. R., Murshudov, G. N. (2013). How good are my data and what is the resolution? *Acta Crystallogr. D 69*, 1204–1214.

[166] Karplus, P. A., Diederichs, K. (2012). Linking crystallographic model and data quality. *Science 336*, 1030–1033.

[167] McCoy, A. J., Grosse-Kunstleve, R. W., Adams, P. D., Winn, M. D., Storoni, L. C., Read, R. J. (2007). Phaser crystallographic software. *J. Appl. Cryst. 40*, 658–674.

[168] Adams, P. D., Afonine, P. V., Bunkóczi, G., Chen, V. B., Davis, I. W., Echols, N., Headd, J. J., Hung, L. W., Kapral, G. J., Grosse-Kunstleve, R. W., McCoy, A. J., Moriarty, N. W., Oeffner, R., Read, R. J., Richardson, D. C., Richardson, J. S., Terwilliger, T. C., Zwart, P. H. (2010). PHENIX: A comprehensive Python-based system for macromolecular structure solution. *Acta Crystallogr. D 66,* 213–221.

[169] Gui, W. J., Lin, S. Q., Chen, Y. Y., Zhang, X. E., Bi, L. J., Jiang, T. (2011). Crystal structure of DNA polymerase III β sliding clamp from Mycobacterium tuberculosis. *Biochem. Biophys. Res. Commun. 405*, 272–277.

[170] P. Emsley, B. Lohkamp, W. G. Scott, K. Cowtan, Features and development of Coot. Acta Crystallogr. D 66, 486–501.

[171] Afonine, P. V., Grosse-Kunstleve, R. W., Echols, N., Headd, J. J., Moriarty, N. W., Mustyakimov, M., Terwilliger, T. C., Urzhumtsev, A., Zwart, P. H., Adams P. D. (2010). Towards automated crystallographic structure refinement with phenix.refine. *Acta Crystallogr. D* 68, 352–367 (2012).

[172] Baker, N. A., Sept, D., Joseph, S., Holst, M. J., McCammon, J. A. (2001). Electrostatics of nanosystems: Application to microtubules and the ribosome. *Proc. Natl. Acad. Sci. U.S.A. 98,* 10037–10041.

[173] Laskowski, R. A., Swindells, M. B. (2011). LigPlot+: Multiple ligand-protein interaction diagrams for drug discovery. *J. Chem. Inf. Model. 51*, 2778–2786.

[174] Kearse, M., Moir, R., Wilson, A., Stones-Havas, S., Cheung, M., Sturrock, S., Buxton, S., Cooper, A., Markowitz, S., Duran, C., Thierer, T., Ashton, B., Meintjes, P., Drummond, A. (2012): Geneious Basic: An integrated and extendable desktop software platform for the organization and analysis of sequence data. *Bioinformatics 28,* 1647–1649.

[175] McKenna, A., Hanna, M., Banks, E., Sivachenko, A., Cibulskis, K., Kernytsky, A., Garimella, K., Altshuler, D., Gabriel, S., Daly, M., DePristo, M. A. (2010): The Genome Analysis Toolkit: A MapReduce framework for analyzing next-generation DNA sequencing data. *Genome Res. 20*, 1297–1303.

[176] Darling, A. C., Mau, B., Blattner, F. R., Perna, N. T. (2004): Mauve: Multiple alignment of conserved genomic sequence with rearrangements. *Genome Res. 14*, 1394–1403.

[177] Altschul, S. F., Gish, W., Miller, W., Myers, E. W., Lipman, D. J. (1990): Basic local alignment search tool. *J. Mol. Biol. 215*, 403–410.

[178] Medema, M. H., Blin, K., Cimermancic, P., De Jager, V., Zakrzewski, P., Fischbach, M. A., Weber, T., Takano, E., Breitling, R. (2011). AntiSMASH: Rapid identification, annotation and analysis of secondary metabolite biosynthesis gene clusters in bacterial and fungal genome sequences. *Nucleic Acids Research*, *39*(SUPPL. 2), 339–346.

[179] Huelsenbeck, J. P., Ronquist, F. (2001): MRBAYES: Bayesian inference of phylogenetic trees. *Bioinformatics 17*, 754–755.

[180] L. Collins, S. G. Franzblau, Microplate alamar blue assay versus BACTEC 460 system for high-throughput screening of compounds against *Mycobacterium tuberculosis* and Mycobacterium avium. *Antimicrob. Agents Chemother. 41,* 1004–1009 (1997).

[181] Mosmann, T. (1983): Rapid Colorimetric Assay for Cellular Growth and Survival: Application to Proliferation and Cytotoxicity Assays, *J. Immunol. Meth.,* vol. 65, pp. 55-63.

[182] Southern, E. (2006). Southern blotting. Nat. Protoc. 1, 518–525.

[183] Wolff, P., Amal, I., Olieric, V., Chaloin, O., Gygli, G., Ennifar, E., Lorber, B., Guichard, G., Wagner, J., Dejaegere, Burnouf, D. Y. (2014). Differential Modes of Peptide Binding onto Replicative Sliding Clamps from Various Bacterial Origins. *J. Med. Chem. 57*, 7565-7576.

[184] Burnouf, D. Y., Olieric, V., Wagner, J., Fujii, S., Reinbolt, J., Fuchs, R. P. P., Dumas, P. (2004). Structural and Biochemical Analysis of Sliding Clamp/Ligand Interactions Suggest a Competition between Replicative and Translesion DNA Polymerases. *Journal of Molecular Biology*, *335*, 1187–1197.

[185] Hedglin, M., Kumar, R., Benkovic, S. J. (2013). Replication clamps and clamp loaders. *Cold Spring Harbor Perspectives in Biology*, *5*(4), 1–19.

[186] Kong, X. P., Onrust, R., O'Donnell, M., Kuriyan, J. (1992). Three-dimensional structure of the beta subunit of E. coli DNA polymerase III holoenzyme: a sliding DNA clamp. *Cell*, *69*(3), 425–437.

[187] Neuwald, A. F. (2003). Evolutionary clues to DNA polymerase III β clamp structural mechanisms. *Nucleic Acids Research*, *31*(15), 4503–4516.

[188] Tanner, N. a, Tolun, G., Loparo, J. J., Jergic, S., Griffith, J. D., Dixon, N. E., van Oijen, A. M. (2011). E. coli DNA replication in the absence of free β clamps. *The EMBO Journal*, *30*(9), 1830–1840.

[189] Yang, H., Miller, J. H. (2012). Deletion of dnaN1 generates a mutator phenotype in Bacillus anthracis. *DNA Repair (Amst)*, *7*(3), 507–514.

[190] Parumasivam, T., Naveen Kumar, H. S., Ibrahim, P., Sadikun, A., Mohamad, S. (2013). Anti-tuberculosis activity of lipophilic isoniazid derivatives and their interactions with first-line anti-tuberculosis drugs. *Journal of Pharmacy Research*, *7*(4), 313–317.

[191] Haemers, A., Leysen, D. C., Bollaert, W., Zhang, M., Pattyn, S. R. (1990). Influence of N Substitution on Antimycobacterial Activity of Ciprofloxacin, *34*(3), 496–497.

[192] Kawakami, K., Namba, K., Tanaka, M., Matsuhashi, N., Product, N., Co, D. P. (2000). Antimycobacterial Activities of Novel Levofloxacin Analogues, *44*(8), 2126–2129.

[193] Liu, X., Testa, B., Fahr, A. (2011). Lipophilicity and its relationship with passive drug permeation. *Pharmaceutical Research*, *28*(5), 962–977.

[194] Kieser, K. J., Rubin, E. J. (2014). How sisters grow apart: mycobacterial growth and division. *Nature Reviews. Microbiology*, *12*(8), 550–562.

[195] Rastogi, N., Goh, K. S. (1990). Action of 1-isonicotinyl-2-palmitoyl hydrazine against the Mycobacterium avium complex and enhancement of its activity by *m*-fluorophenylalanine. *Antimicrobial Agents and Chemotherapy*, *34*(11), 2061–2064.

[196] Danilchanka, O., Pavlenok, M., Niederweis, M. (2008). Role of porins for uptake of antibiotics by *Mycobacterium smegmatis*. *Antimicrobial Agents and Chemotherapy*, *52*(9), 3127–34.

[197] Jarlier, V. Nikaido, H. (1994): Mycobacterial cell wall: structure and role in natural resistance to antibiotics. *FEMS Microbiol. Lett. 123*:11-118.

[198] Brennan, P., Nikaido, H. (1995). The envelope of mycobacteria. *Annu. Rev. Biochem, 64*:29-63.

[199] National Committee for Clinical Laboratory Standards. Methods for determining bactericidal activity of anti-microbial agents; tentative guidelines M26-T. Villanova, Pennsylvania: NCCLS, 1992.

[200] Kong, X. P., Onrust, R., O'Donnell, M., Kuriyan, J. (1992). Three-dimensional structure of the beta subunit of E. coli DNA polymerase III holoenzyme: a sliding DNA clamp. *Cell, 69,* 425-427.

[201] Gui, W.-J., Lin, S.-Q., Chen, Y.-Y., Zhang, X.-E., Bi, L.-J., Jiang, T. (2011). Crystal structure of DNA polymerase III β sliding clamp from Mycobacterium tuberculosis. *Biochemical and Biophysical Research Communications*, *405*(2), 272–7.

[202] Wolff, P., Oliéric, V., Briand, J. P., Chaloin, O., Dejaegere, A., Dumas, P., Ennifar, E., Guichard, G., Wagner, J., Burnour, D. Y. (2011). Structure-Based Design of Short Peptide Ligands Binding onto the E. coli Processivity Ring. *Journal of Medicinal Chemistry*, *54*(13), 4627–4637.

[203] Georgescu, R. E., Yurieva, O., Kim, S.-S., Kuriyan, J., Kong, X.-P., O'Donnell, M. (2008). Structure of a small-molecule inhibitor of a DNA polymerase sliding clamp. *Proceedings of the National Academy of Sciences of the United States of America*, *105*(32), 11116–21.

[204] Sutton, M. D. (2010). Coordinating DNA polymerase traffic during high and low fidelity synthesis. *Biochimica et Biophysica Acta*, *1804*(5), 1167–1179.

[205] Indiani, C., McInerney, P., Georgescu, R., Goodman, M. F., O'Donnell, M. (2005). A sliding-clamp toolbelt binds high- and low-fidelity DNA polymerases simultaneously. *Molecular Cell*, *19*(6), 805–815.

[206] Fijalkowska, I. J., Schaaper, R. M., Jonczyk, P. (2012). DNA replication fidelity in Escherichia coli: A multi-DNA polymerase affair. *FEMS Microbiology Reviews*, *36*(6), 1105–1121.

[207] Tsai, H. H., Shu, H. W., Yang, C. C., Chen, C. W. (2012). Translesion-synthesis DNA polymerases participate in replication of the telomeres in Streptomyces. *Nucleic Acids Research*, *40*(3), 1118–1130.

[208] Toste Rêgo, A., Holding, A. N., Kent, H., Lamers, M. H. (2013). Architecture of the Pol III-clamp-exonuclease complex reveals key roles of the exonuclease subunit in processive DNA synthesis and repair. *The EMBO Journal*, *32*(9), 1334–43.

[209] Georgescu, R. E., Kim, S. S., Yurieva, O., Kuriyan, J., Kong, X. P., O'Donnell, M. (2008). Structure of a Sliding Clamp on DNA. *Cell*, *132*(1), 43–54.

[210] Gefter, M.L., Hirota, Y., Kornberg, T., Wechsler, J.A., Barnoux, C. (1971) Analysis of DNA polymerases II and 3 in mutants of Escherichia coli thermosensitive for DNA synthesis. *Proc Natl Acad Sci USA 68*: 3150–3153.

[211] Dohrmann, P. R., McHenry, C. S. (2005). A bipartite polymerase-processivity factor interaction: Only the internal β binding site of the α subunit is required for processive replication by the DNA polymerase III holoenzyme. *Journal of Molecular Biology*, *350*(2), 228–239.

[212] López de Saro, F. J., O'Donnell, M. (2001). Interaction of the beta sliding clamp with MutS, ligase, and DNA polymerase I. *Proceedings of the National Academy of Sciences of the United States of America*, *98*(15), 8376–8380.

[213] López De Saro, F. J., Marinus, M. G., Modrich, P., O'Donnell, M. (2006). The β sliding clamp binds to multiple sites within MutL and MutS. *Journal of Biological Chemistry*, *281*(20), 14340–14349.

[214] Fernandez-Fernandez, C., Grosse, K., Sourjik, V., Collier, J. (2013). The β-sliding clamp directs the localization of HdaA to the replisome in Caulobacter crescentus. *Microbiology (United Kingdom)*, *159*(PART11), 2237–2248.

[215] Mizrahi, V., Andersen, S. J. (1998). DNA repair in Mycobacterium tuberculosis. What have we learnt from the genome sequence? *Molecular Microbiology*, *29*(1998), 1331–1339.

[216] Cole, S. T., Brosch, R., Parkhill, J., Garnier, T., Churcher, C., Harris, D., Gordon, S. V., Eiglmeier, K., Barry, C. E., Tekaia, F., Badcock, K., Basham, D., Brown, D.,

Chillingworth, T., Connor, R., Davies, R., Devlin, K., Feltwell, R., Gentles, S., Hamlin, N., Holroyd, S., Hornsby, T., Jagels, K., Krogh, A., McLean, J., Moule, S., Murphy, L., Olever, K., Osborne, J., Quail, M. A., Rajandream, M.-A., Rogers, J., Rutter, S., Seeger, K., Skelton, J., Squares, R., Squares, S., Sulston, J. E., Taylor, K., Whitehead, S., Barrell, B. G. (1998). Deciphering the biology of Mycobacterium tuberculosis from the complete genome sequence. *Nature*, *393*(6685), 537–544.

[217] Wijffels, G., Dalrymple, B. P., Prosselkov, P., Kongsuwan, K., Epa, V. C., Lilley, P. E., Jergie, S., Buchardt, J., Brown, S. E., Alewood, P. F., Jennings, P. A., Dixon, N. E. (2004). Inhibition of protein interactions with the beta 2 sliding clamp of Escherichia coli DNA polymerase III by peptides from beta 2-binding proteins. *Biochemistry*, *43*(19), 5661–71.

[218] Jeruzalmi, D., Yurieva, O., Zhao, Y., Young, M., Stewart, J., Hingorani, M., O'Donnell, M, Kuriyan, J. (2001): Mechanism of processivity clamp opening by the delta subunit wrench of the clamp loader complex of E. coli DNA polymerase III, Cell 106 (2001) 417–428.

[219] Dalrymple, B.P., Kongsuwan, K., Wijffels, G., Dixon, N.E., Jennings, P.A. (2001): A universal protein-protein interaction motif in the eubacterial DNA replication and repair systems, *Proc. Natl. Acad. Sci. USA 98*, 11627– 11632.

[220] Lopez de Saro, F.J., Georgescu, R.E., O'Donnell, M. (2003): A peptide switch regulates DNA polymerase processivity, Proc. Natl. Acad. Sci. USA 100 14689– 14694.

[221] Kurz, M., Dalrymple, B., Wijffels, G., Kongsuwan, K. (2004): Interaction of the sliding clamp β-subunit and Hda, a DnaA-related protein. *J. Bacteriol. 186*, 11, 3508-3515.

[222] Bunting, K. A., Roe, S. M., Pearl, L. H. (2003): Structural basis for recruitment of trnslesion DNA polymerase Pol IV/DinB to the beta-clamp. *EMBO J. 22 (21)*, 5883-5892.

[223] Furukohri, A., Goodman, M. F., Maki, H. (2008). A dynamic polymerase exchange with Escherichia coli DNA polymerase IV replacing DNA polymerase III on the sliding clamp. *Journal of Biological Chemistry*, *283*(17), 11260–11269.

[224] Uchida, K., Furukohri, A., Shinozaki, Y., Mori, T., Ogawara, D., Kanaya, S., Nohmi, T., Maki, H., Akiyama, M. (2008). Overproduction of Escherichia coli DNA polymerase DinB (Pol IV) inhibits replication fork progression and is lethal. *Molecular Microbiology*, *70*(3), 608–622.

[225] López de Saro, F. J. (2009). Regulation of interactions with sliding clamps during DNA replication and repair. *Current Genomics*, *10*(3), 206–215.

[226] Timinskas, K., Balvočiūtė, M., Timinskas, A., Venclovas, Č. (2014). Comprehensive analysis of DNA polymerase III α subunits and their homologs in bacterial genomes. *Nucleic Acids Research*, *42*(3), 1393–413.

[227] Warner, D. F., Ndwandwe, D. E., Abrahams, G. L., Kana, B. D., Machowski, E. E., Venclovas, C., Mizrahi, V. (2010). Essential roles for *imuA'*- and *imuB*-encoded accessory factors in DnaE2-dependent mutagenesis in *Mycobacterium tuberculosis*. *PNAS*, *107*(29), 13093–13098.

[228] Foster, P. L. (2007). Stress-induced mutagenesis in bacteria. *Crit Rev Biochem Mol Biol.*, *42*(5), 373–397.

[229] Brooks, P. C., Movahedzadeh, F., Davis, E. O. (2001). Identification of some DNA damage-inducible genes of Mycobacterium tuberculosis: Apparent lack of correlation with LexA binding. *Journal of Bacteriology*, *183*(15), 4459–4467.

[230] Kleinsteuber, S., Quinones, A. (1995) Expression of the dnaB gene of Escherichia coli is inducible by replication- blocking DNA damage in a recA-independent manner. *Mol Gen Genet 248:* 695–702.

[231] Kohanski, M. A., Dwyer, D. J., Hayete, B., Lawrence, C. A., Collins, J. J. (2007). A Common Mechanism of Cellular Death Induced by Bactericidal Antibiotics. *Cell*, *130*(5), 797–810.

[232] Flannagan, R. S., Cosío, G., Grinstein, S. (2009). Antimicrobial mechanisms of phagocytes and bacterial evasion strategies. *Nature Reviews. Microbiology*, *7*(5), 355–366.

[233] Yin, Z., Wang, Y., Whittell, L. R., Jergic, S., Liu, M., Harry, E., Dixon, N. E., Kelso, M., J., Beck, J. L., Oakley, A. J. (2014). DNA Replication Is the Target for the Antibacterial Effects of Nonsteroidal Anti-Inflammatory Drugs. *Chemistry & Biology*, 1–7.

[234] Kjelstrup, S., Hansen, P. M. P., Thomsen, L. E., Hansen, P. R., Løbner-Olesen, A. (2013). Cyclic peptide inhibitors of the β-sliding clamp in Staphylococcus aureus. *PloS One*, *8*(9).

[235] Grosset, J. Ji, B. (1998). Mycobacteria, *Volume II Chemotherapy*, P. R. J. Gangadharam, P. A. Jenkins, Eds. (Chapman and Hall, New York), 51–97.

[236] Thakur, K. G., Joshi, A. M., Gopal, B. (2007). Structural and biophysical studies on two promoter recognition domains of the extra-cytoplasmic function σ factor σ^C from *Mycobacterium tuberculosis*. *Journal of Biological Chemistry*, *282*(7), 4711–4718.

[237] Salazar, L. (2003). Transcription analysis of the dnaA gene and oriC region of the chromosome of Mycobacterium smegmatis and Mycobacterium bovis BCG, and its regulation by the DnaA protein. *Microbiology*, *149*(3), 773–784.

[238] Qin, M. H., Madiraju, M. V, Zachariah, S., Rajagopalan, M. (1997). Characterization of the *oriC* region of *Mycobacterium smegmatis*. *Journal of Bacteriology*, *179*(20), 6311–6317.

[239] Qin, M. H., Madiraju, M. V, Rajagopalan, M. (1999). Characterization of the functional replication origin of *Mycobacterium tuberculosis*. *Gene*, *233*(1-2), 121–30.

[240] Atlung, T., Løbner-Olesen, A., Hansen, F. G. (1987). Overproduction of DnaA protein stimulates initiation of chromosome and minichromosome replication in Escherichia coli. *Molecular and General Genetics : MGG*, *206*(1), 51–9.

[241] Sandegren, L., Andersson, D. I. (2009). Bacterial gene amplification: implications for the evolution of antibiotic resistance. *Nature Reviews. Microbiology*, *7*(8), 578–588.

[242] Andersson, D. I., Hughes, D. (2009). Gene Amplification and Adaptive Evolution in Bacteria. *Annual Review of Genetics*, *43*(1), 167–195.

[243] Yanai, K., Murakami, T., Bibb, M. (2006). Amplification of the entire kanamycin biosynthetic gene cluster during empirical strain improvement of Streptomyces kanamyceticus. *Proceedings of the National Academy of Sciences of the United States of America*, *103*(25), 9661–9666.

[244] Hatfull, G. F., Jacobs, W. R., Eds. (2014) Molecular Genetics of Mycobactera, *American Society for Microbiology Press* (Herndorn, USA).

[245] Noufflard-Guy-Loé, H., Berteaux, S. (1965). Experimental antituberculous action of a new antibiotic: RP11,072. Rev. Tuberc. Pneumol. (Paris) 29, 301–326.

[246] Fujimitsu, K., Su'etsugu, M., Yamaguchi, Y., Mazda, K., Fu, N., Kawakami, H., Katayama, T. (2008). Modes of overinitiation, dnaA gene expression, and inhibition of cell division in a novel cold-sensitive *hda* mutant of *Escherichia coli*. *Journal of Bacteriology*, *190*(15), 5368–5381.

[247] Grigorian, A. V, Lustig, R. B., Guzmán, E. C., Mahaffy, J. M., Zyskind, J. W., & Guzma, E. C. (2003). Escherichia coli Cells with Increased Levels of DnaA and Deficient in Recombinational Repair Have Decreased Viability Escherichia coli Cells with Increased Levels of DnaA and Deficient in Recombinational Repair Have Decreased Viability, *185*(2), 630–644.

[248] Ogura, Y., Imai, Y., Ogasawara, N., Moriya, S. (2001). Autoregulation of the *dnaA-dnaN* operon and effects of DnaA protein levels on replication initiation in *Bacillus subtilis*. *Journal of Bacteriology*, *183*(13), 3833–3841.

[249] Rock, J. M., Lang, U. F., Chase, M. R., Ford, C. B., Gerrick, E. R., Gawande, R., Coscolla, M., Gagneux, S., Fortune, S. M., Lamers, M. H. (2015). DNA replication fidelity in *Mycobacterium tuberculosis* is mediated by an ancestral prokaryotic proofreader. *Nature Genetics*, *47*(6), 677–681.

[250] Colangeli, R., Arcus, V. L., Cursons, R. T., Ruthe, A., Karalus, N., Coley, K., Manning, S. D., Kim, S., Marchiano, Alland, D. (2014). Whole genome sequencing of *Mycobacterium tuberculosis* reveals slow growth and low mutation rates during latent infections in humans. *PLoS ONE*, *9*(3), 1–9.